

DISSERTATION

LOPHODERMELLA NEEDLE CAST PATHOSYSTEM: THE PHYLOGENETIC
RELATIONSHIPS, HOST-MYCOBIOTA INTERACTIONS, AND MOLECULAR
DIAGNOSIS OF *LOPHODERMELLA* PATHOGENS ON *PINUS*

Submitted by

Jessa Pude Ata

Department of Agricultural Biology

In partial fulfillment of the requirements

For the Degree of Doctor of Philosophy

Colorado State University

Fort Collins, Colorado

Spring 2022

Doctoral Committee:

Advisor: Jane E. Stewart

Zaid Abdo

Mee-Sook Kim

Stephen J. Mondo

Andrew P. Norton

Copyright by Jessa Pude Ata 2022

All Rights Reserved

ABSTRACT

LOPHODERMELLA NEEDLE CAST PATHOSYSTEM: THE PHYLOGENETIC RELATIONSHIPS, HOST-MYCOBIOTA INTERACTIONS, AND MOLECULAR DIAGNOSIS OF *LOPHODERMELLA* PATHOGENS ON *PINUS*

The impact of needle diseases in conifer stands has increased worldwide due to regional variations of warmer and wetter climates that spur the activity of needle pathogens. Heavy needle cast infection results in loss of growth among pine stands which can lead to losses in biomass production and decline in ecosystem goods and services. Despite this threat, a well-informed disease management strategy is lacking due to limited research on many needle pathogens that remain to have unclear taxonomy, uncharacterized fungal biology, and unknown trophic lifestyles and interactions. Thus, this research applied molecular tools to understand conifer needle pathosystems, particularly *Lophodermella* needle casts that have caused epidemics on *Pinus contorta* stands in Colorado, USA. Specifically, this research aims to analyze the phylogeny of *Lophodermella* species using molecular data and identify shared derived characters for taxa delimitation; investigate the interaction of the mycobiota and the *P. contorta* host in healthy versus diseased states; and develop molecular tools for the rapid diagnosis of *Lophodermella* needle cast.

To achieve these objectives, this research is divided into five chapters. The first chapter gives an overview of the emerging needle diseases worldwide and the needle cast epidemics on *P. contorta* in Colorado caused by *Lophodermella concolor* and *L. montivaga*. It discusses current knowledge on the *Lophodermella* pathogens and management strategies for needle diseases. The second chapter highlights the relationship of *Lophodermella* species from North America (*L.*

arcuata, *L. concolor* and *L. montivaga*) and Europe (*L. sulcigena* and *L. conjuncta*), and their potential synapomorphic characters. It also revealed a newly identified, genetically unique rhytismataceous species on *Pinus flexilis* that is morphologically similar to *L. arcuata*. The third chapter discusses the adverse impact of the diseases to needle mycobiota and the defense strategies of the *P. contorta* host. It further shows, for the first time, the endophytic lifestyle of *Lophodermella* pathogens on *P. contorta*. The fourth chapter details the efficiency of the PCR-based markers developed from multi-copy and single-copy gene regions to identify and detect *L. concolor* and *L. montivaga* on *P. contorta*, and *L. arcuata* and *Bifusella linearis* on *P. flexilis*. And lastly, the fifth chapter summarizes the important results of this research and discusses their potential implications on the management of emerging needle diseases. My dissertation closes with recommendations on future research that will address further questions of needle diseases caused by *Lophodermella* species and other pathogens.

ACKNOWLEDGEMENTS

My journey to doctorate degree would have never been possible without the efforts of my academic advisor Dr. Jane Stewart, Drs. Ned Klopfenstein and Mee-Sook Kim who I first met in the Philippines years back, and my best friend Dr. Jorge Ibarra Caballero.

My gratitude and respect also go to my graduate committee members Drs. Zaid Abdo, Mee-Sook Kim, Stephen Mondo, and Andrew Norton for keeping me on track with my academic and research goals. Their advice and expertise in research and mentoring have been my guide and aspiration.

I am also grateful to the USDA Forest Service Forest Health Protection especially the researchers who helped me with my study: Kelly Burns, Suzanne Marchetti and Dr. James Worrall, for without them my research would have never been funded and productive. I also want to thank our collaborators, Drs. Isabel Munck and Ludwig Beenken, who helped improve our phylogenetic investigation on *Lophodermella* pathogens. I also would like to acknowledge the 1000 Fungal Genomes project through the US Department of Energy Joint Genome Institute for allowing us access to unpublished genomes data which deepened our analysis on mycobiota-host tree interactions and marker development.

My graduate school experience was brighter and warmer because of the supportive peers, colleagues, donors, and professors in the Department of Agricultural Biology. Led by Dr. Amy Charkowski, this department is indeed an epitome of an inclusive and nurturing environment for graduate students and researchers. This department, along with all my students, also gave me the opportunity to teach with a broader perspective in creating a safe and brave space for learning.

I am also thankful to my home department and university, the Department of Forest Biological Sciences of the University of the Philippines Los Baños, for allowing me to embark on this journey of professional and personal growth.

Lastly, I would like to thank my family and friends for their constant support. Despite life's chaos, in them, I have found peace and inspiration.

To all of them, I am forever indebted.

Daghang Salamat! (Thank you very much!)

TABLE OF CONTENTS

ABSTRACT.....	ii
ACKNOWLEDGEMENTS.....	iv
LIST OF TABLES.....	viii
LIST OF FIGURES.....	x
Chapter 1: Lophodermella Needle Cast as an Emerging Forest Disease.....	1
Climate Change increases Needle Disease Risks.....	1
Lophodermella Needle Cast Pathogens.....	3
Mycobiome Interaction in a Lophodermella Needle Cast Pathosystem.....	7
Needle Disease Monitoring and Assessment.....	9
References.....	11
Chapter 2: Molecular Characterization and Phylogenetic Analyses of Five <i>Lophodermella</i> Needle Pathogens (Rhytismataceae) on <i>Pinus</i> Species in the USA and Europe.....	21
Introduction.....	21
Methodology.....	24
Sampling and Morphology.....	24
DNA Extraction and Sequencing.....	24
Character Mapping.....	35
Results.....	36
Molecular and Phylogenetic Analyses.....	36
Morphology and Phylogeny of <i>Lophodermella</i> on <i>P. flexilis</i>	37
Shared Characteristics of <i>Lophodermella</i> Clade.....	38
Discussion.....	42
Molecular and Phylogenetic Analyses of <i>Lophodermella</i>	42
Phylogeny of <i>Lophodermella</i> sp. from <i>P. flexilis</i>	46
Morphological and Lifestyle Traits of the <i>Lophodermella</i> Clade.....	46
References.....	49
Chapter 3: Community and Transcriptome Foliar Mycobiota Transitions in Response to Pathogenic Conifer Needle Interactions.....	56
Introduction.....	56
Methodology.....	58
Sample Collection and Preparation.....	58
Metabarcoding and Metatranscriptome Sequencing.....	61
Metabarcoding Analysis.....	62
Metatranscriptome Analysis.....	64
Results.....	66
Mycobiome Sequences, Composition and Diversity.....	66
Metatranscriptome Assembly.....	68
Metatranscriptome Differential Gene Expression.....	72
Functional Annotation of Fungal Transcripts.....	75
Functional Annotation of Plant Transcripts.....	82
Functional Annotation of Other Transcripts.....	83
Discussion.....	85

Mycobiome Composition and Diversity	86
Fungal Gene Expression in the Lophodermella Needle Cast Pathosystem	87
Plant Interactions in the Lophodermella Needle Cast Pathosystem	88
Characterization of Other Transcripts.....	90
<i>Lophodermella</i> as Latent Pathogens in <i>P. contorta</i> Needles	91
References.....	93
Chapter 4: Development of PCR-based Markers for the Identification and Detection of Lophodermella Needle Cast Pathogens on <i>Pinus contorta</i> and <i>P. flexilis</i>	111
Introduction.....	111
Methodology	114
Sample Collection and DNA Extraction.....	114
Primer Development and Assay from ITS Region	118
Primer Development and Assay from Genomic Data.....	118
<i>In silico</i> and <i>In vitro</i> Primer Testing.....	121
Detection of <i>Lophodermella</i> Pathogens on Environmental Samples	121
Results.....	127
Identification of Needle Pathogens and Non-Target Species	127
Primer Specificity	127
Primer Sensitivity.....	129
Discussion	130
Pathogen Identification and Detection using Specific ITS and RH_2175 Primers.....	131
Genome Sequences of Related Species to Search for Markers	133
Detection of <i>Lophodermella concolor</i> on <i>P. flexilis</i>	134
Detection of <i>B. linearis</i> on Environmental Samples.....	134
Challenges in using Primers for Accurate Latent Pathogen Identification and Detection	135
References.....	137
Chapter 5: Summary and Conclusions.....	145
Research Synthesis.....	145
Research Outlook.....	149
References.....	153
Appendices.....	157

LIST OF TABLES

Chapter 2: Molecular Characterization and Phylogenetic Analyses of Five *Lophodermella* Needle Pathogens (Rhytismataceae) on *Pinus* Species in the USA and Europe

Table 2.1. Collection information, GenBank accession and genotype numbers for each <i>Lophodermella</i> species and <i>Lophophacidium dooksii</i> for the three loci, namely: internal transcribed spacer region 1, 5.8S ribosomal RNA and internal transcribed spacer region 2 (ITS), large ribosomal subunit (LSU) and translation elongation factor (TEF1- α).....	25
Table 2.2. Characteristics of <i>Lophodermella</i> species and <i>Lophophacidium dooksii</i> based on published descriptions.....	29
Table 2.3. Character and character states used for phylogenetic reconstructions of <i>Lophodermella</i> species.....	40

Chapter 3: Community and Transcriptome Foliar Mycobiota Transitions in response to Pathogenic Conifer Needle Interactions

Table 3.1. Asymptomatic and symptomatic needle samples from <i>Pinus contorta</i> individual trees that were infected with <i>Lophodermella</i> needle cast pathogens in various sites in Gunnison National Forest, Colorado, USA	59
Table 3.2. Diversity measures among asymptomatic and symptomatic <i>Pinus contorta</i> needles collected from Gunnison National Forest, Colorado, USA.....	69
Table 3.3. Metabarcoding and metatranscriptome profile of <i>Pinus contorta</i> needle samples	71

Chapter 4: Development of PCR-based Markers for the Identification and Detection of *Lophodermella* Needle Cast Pathogens on *Pinus contorta* and *P. flexilis*

Table 4.1. PCR amplification using specific primers designed from the internal transcribed spacer (ITS) and gene cluster 2175 on <i>Lophodermella</i> spp. and <i>Bifusella linearis</i> (Rhytismataceae) samples collected from <i>Pinus</i> stands in Colorado (CO) and in Maine (ME), USA.....	115
Table 4.2. Non-target species used in the study to test specificity of primers for <i>Lophodermella concolor</i> and <i>L. montivaga</i> on <i>Pinus contorta</i> , and <i>Bifusella linearis</i> and <i>L. arcuata</i> on <i>P. flexilis</i>	116

Table 4.3. Primers developed for *Lophodermella concolor*, *L. montivaga* and *Bifusella linearis* and their parameters for direct and nested PCR amplification.....119

Table 4.4. Amplification using primers designed for *Lophodermella concolor* (LC) and *L. montivaga* (LM) on *Pinus contorta*, and *Bifusella linearis* (BL) and *L. arcuata* (LA) on *P. flexilis* on non-target species122

Table 4.5. Amplification using primers designed for *Lophodermella concolor* (LC) and *L. montivaga* (LM) on *Pinus contorta*, and *Bifusella linearis* (BL) and *L. arcuata* (LA) on *P. flexilis* on *P. contorta* needles asymptomatic and symptomatic of *L. concolor* and *L. montivaga* and asymptomatic *P. flexilis* needles124

LIST OF FIGURES

Chapter 1: Lophodermella Needle Cast as an Emerging Forest Disease

- Figure 1.1. *Pinus contorta* tree in Gunnison National Forest, Colorado, USA (A) showing symptoms of Lophodermella needle cast with signs of *Lophodermella concolor* (B) and *L. montivaga* (C)4

Chapter 2: Molecular Characterization and Phylogenetic Analyses of Five *Lophodermella* Needle Pathogens (Rhytismataceae) on *Pinus* Species in the USA and Europe

- Figure 2.1. Ascomata of *Lophodermella concolor* (a) and *L. montivaga* (b) on *Pinus contorta* from Gunnison National Forest, Colorado, USA; *Lophodermella* sp. (c) and *Lophodermella arcuata* (d) on *P. flexilis* from Rocky Mountain National Park, Colorado, USA; *Lophophacidium dooksii* on *P. strobus* from Massabesic, Maine, USA (e); and *L. conjuncta* (f) and *L. sulcigena* (g) on *P. mugo* from Austria and Switzerland.....28

- Figure 2.2. Maximum likelihood phylogeny depicting phylogenetic relationships of *Lophodermella* species within Rhytismataceae based on three gene regions including the internal transcribed spacer (ITS), large ribosomal subunit (LSU) and translation elongation factor 1-alpha (TEF1 α)38

- Figure 2.3. Morphological characters of *Lophodermella* sp. on *Pinus flexilis* collected from Rocky Mountain National Park, Colorado, USA39

- Figure 2.4. Morphological characters mapped onto Bayesian ITS phylogenetic tree with the parsimony ancestral reconstruction method using Mesquite v.3.6 with retention indices ≥ 0.50 , ascomata position (a) and ascospore shape (b)41

- Figure 2.5. Morphological characters mapped onto Bayesian ITS phylogenetic tree with the parsimony ancestral reconstruction method using Mesquite v.3.6, fusion of ascomata (a) and number of needles of pine host (b)43

Chapter 3: Community and Transcriptome Foliar Mycobiota Transitions in response to Pathogenic Conifer Needle Interactions

- Figure 3.1. Relative abundance of fungal taxa (removing OTUs assigned as unclassified fungi) within the mycobiome across *Pinus contorta* needles that were asymptomatic and symptomatic of *Lophodermella concolor* and *L. montivaga* identified through metabarcoding67

Figure 3.2. Principal coordinate analysis (PCoA) based on relative abundance of fungal operational taxonomic units (OTUs) showing fungal community structure on <i>Pinus contorta</i> needles that are symptomatic or symptomatic of <i>Lophodermella concolor</i> and <i>L. montivaga</i>	70
Figure 3.3. Heatmap of the differentially expressed transcripts (isoforms) in <i>Pinus contorta</i> asymptomatic (ASYM) and symptomatic (SYM) of <i>Lophodermella concolor</i> (LC) and <i>L. montivaga</i> (LM) based on counts per million (CPM) reads	73
Figure 3.4. Abundance of the 25 most active fungal families within the mycobiome across <i>Pinus contorta</i> needles asymptomatic (ASYM) and symptomatic (SYM) of <i>Lophodermella concolor</i> (LC) and <i>L. montivaga</i> (LM) identified from the metatranscriptome using the concatenated NCBI nr-JGI MycoCosm databases	75
Figure 3.5. Number of fungal enzymes that degrade proteins and various substrates that were differentially expressed between (A) <i>Pinus contorta</i> needles symptomatic and asymptomatic of <i>Lophodermella concolor</i> (LC_ASYM vs. LC_SYM) and <i>L. montivaga</i> (LM_ASYM vs. LM_SYM), and (B) between symptomatic needles of <i>L. concolor</i> and <i>L. montivaga</i> (LC_SYM vs. LM_SYM) inferred from dbCAN2 and PFAM.....	77
Figure 3.6. PHI-base hits of fungal transcripts between (A) <i>Pinus contorta</i> needles symptomatic and asymptomatic of <i>Lophodermella concolor</i> (LC_ASYM vs. LC_SYM) and <i>L. montivaga</i> (LM_ASYM vs. LM_SYM), and (B) between symptomatic needles of <i>L. concolor</i> and <i>L. montivaga</i> (LC_SYM vs. LM_SYM).....	78
Figure 3.7. Number of fungal transcripts involved in the production of secondary metabolites, environmental adaptation, and membrane transport between (A) <i>Pinus contorta</i> needles symptomatic and asymptomatic of <i>Lophodermella concolor</i> (LC_ASYM vs. LC_SYM) and <i>L. montivaga</i> (LM_ASYM vs. LM_SYM), and (B) between symptomatic needles of <i>L. concolor</i> and <i>L. montivaga</i> (LC_SYM vs. LM_SYM) inferred from KEGG	80
Figure 3.8. Gene ontologies of fungal DE transcripts between (A) <i>Pinus contorta</i> needles symptomatic and asymptomatic of <i>Lophodermella concolor</i> (LC_ASYM vs. LC_SYM) and <i>L. montivaga</i> (LM_ASYM vs. LM_SYM), and (B) between symptomatic needles of <i>L. concolor</i> and <i>L. montivaga</i> (LC_SYM vs. LM_SYM) inferred from OrthoVenn2	81
Figure 3.9. Gene ontologies of plant DE transcripts between (A) <i>Pinus contorta</i> needles symptomatic and asymptomatic of <i>Lophodermella concolor</i> (LC_ASYM vs. LC_SYM) and <i>L. montivaga</i> (LM_ASYM vs. LM_SYM), and (B) between symptomatic needles of <i>L. concolor</i> and <i>L. montivaga</i> (LC_SYM vs. LM_SYM) inferred from OrthoVenn2	84

Chapter 4: Development of PCR-based Markers for the Identification and Detection of Lophodermella Needle Cast Pathogens on *Pinus contorta* and *P. flexilis*

Figure 4.1. Needles of *Pinus contorta* that were asymptomatic and symptomatic of either *L. concolor* and *L. montivaga* (A), and asymptomatic needles of *P. flexilis* (B).....123

CHAPTER 1: LOPHODERMELLA NEEDLE CAST AS AN EMERGING FOREST DISEASE

Lophodermella needle cast is an emerging conifer needle disease that has increasing frequency as a result of more warm rain events. This disease is caused by *Lophodermella* pathogens, a group of understudied species with limited molecular research that could elucidate phylogenetic relationships, fungal lifestyles, and interactions with host and microbial communities. Scant information about these pathogens could lead to difficulty in formulating efficient strategies to manage emerging needle diseases and in addressing the threat that they might pose in changing environments. Here, I review the current knowledge and challenges on the taxonomy, interactions within its ecological niche, and tools for identification and detection of *Lophodermella* species. I also discuss the diverse opportunities for *Lophodermella* research with the surge of molecular technologies.

Climate Change increases Needle Disease Risks

Climate change is among the major drivers of emerging diseases of forest trees which are defined as those that have newly appeared or have increased incidence and/or geographic reach (Anderson et al., 2004; Ghelardini et al., 2016). Depending on the type of pathogen and pathogen pressure, environmental changes, like drought, have the potential to impact disease severity in forest ecosystems. The risk of plant diseases caused by fungal pathogens are likely to increase due to their increasing reproductive rate with increasing temperatures (Garrett et al., 2006; Juroszek et al., 2020). While not exempt from the negative effects of rapid environmental shifts, pathogens have the capacity to rapidly evolve and adapt to these environmental changes owing to their shorter life cycles compared to their host plants (Garrett et al., 2006). Apart from the direct effects to pathogens, increasing temperatures can also impact host physiology negatively and increase vector

actively enhancing disease risk (Canto et al., 2009; Desprez-Loustau et al., 2007). Climate change could also trigger pathogen migration via host-mediated or host independent dispersal mechanisms which further increases the risk of invasive pathogens in new highly susceptible hosts (Chakraborty, 2013; La Porta et al., 2008). Simulations of the effect of warming climates on forest pathogens in Europe showed that climate change would be favorable to some foliar and shoot, and root pathogens limited by winter temperature but may have a negative effect to others (Desprez-Loustau et al., 2007).

Needle pathogens are increasingly becoming emergent pathogens, due to frequent warm rain events that are becoming more prevalent due to climate change. Besides the intensified occurrence of native needle pathogens worldwide, cryptic and introduced pathogens are also emerging that further enhanced potential damage to conifer forests (Barnes et al., 2008; Mullett et al., 2018; Piškur et al., 2013). This could result in considerable losses of ecosystem goods and services such as wood volume, landscape value and recreational uses (EFSA Panel on Plant Health, 2013). For example, reduced growth and consequent financial losses were observed in *P. sylvestris* stands after a 17-year period of severe Lophodermium needle cast (Jansons et al., 2020). Similarly, needle cast caused by *Cyclaneusma minus* was projected to significantly reduce the total volume and, subsequently, the revenue for every 10% increase in the number of infected *P. radiata* trees (van der Pas et al., 1984). White pine needle damage further predisposes stressed *Pinus strobus* to other diseases which then increases the threat of a white pine needle decline (Wyka et al., 2018).

As needle pathogens sporulate and infect at high temperature and moisture, climate change models predicted with high certainty an increased impact of needle diseases in pine stands (Sturrock et al., 2011). However, such prediction models may vary depending on regional climatic factors. For example, a decrease in summer rainfall would negatively affect European needle

pathogens such as *Mycosphaerella pini* (Desprez-Loustau et al., 2007), while predicted increasing temperature and precipitation levels in the Pacific Northwest of USA would likely increase Swiss needle cast severity caused by *Nothophaeocryptopus gaeumannii* (Stone et al., 2008). Nonetheless, the growing number of reports on emerging needle diseases spreading across new geographic regions pose concern for forest disease management and phytosanitary protocols. While drier summers may limit needle pathogen activity, severe annual infection during warmer winters also threatens long-term host survival and productivity (Mullett & Brown, 2018; Piškur et al., 2013). Establishment and spread of introduced needle pathogen propagules are likely especially in many areas exhibiting favorable conditions for disease development (EFSA Panel on Plant Health, 2013).

Despite these threats, the ecology and pathogenicity of many needle pathogens are still poorly understood. Among them are the *Lophodermella* needle cast pathogens whose taxonomic issues and unique trophic lifestyles further complicate areas of research and disease management. Thus, while classical techniques remain useful, molecular tools can provide unique opportunities to gain deeper insights into the evolutionary history, host interactions and disease mechanisms of these understudied pathogens.

Lophodermella Needle Cast Pathogens

Lophodermella needle cast is caused by *Lophodermella* Höhn. species within Rhytismataceae (Order Rhytismatales, Class Leotiomycetes, Phylum Ascomycota). Disease symptoms include needle discoloration and defoliation, branch kill and crown dieback (Figure 1.1; Rocky Mountain Region, Forest Health Protection, 2010; Worrall et al., 2012). In symptomatic needles, these pathogens are characterized by their subhypodermal ascomata, clavate ascospores

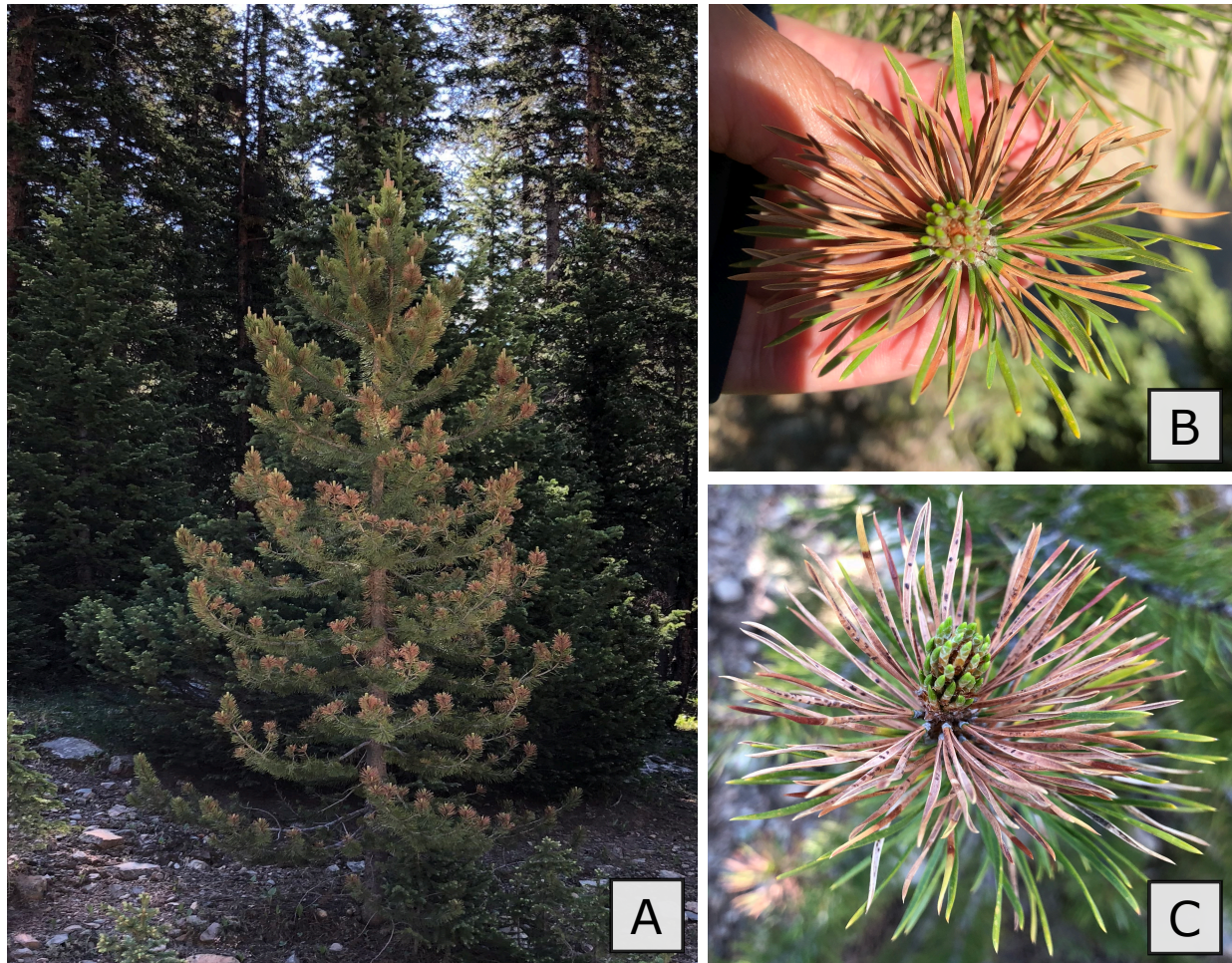


Figure 1.1. *Pinus contorta* tree in Gunnison National Forest, Colorado, USA (A) showing symptoms of *Lophodermella* needle cast with signs of *Lophodermella concolor* (B) and *L. montivaga* (C).

surrounded by mucilaginous sheath, and wider asci than a closely related genus *Lophodermium* (Darker, 1967). Although there were no records of nursery infections, the disease can occur in both seedlings and mature trees in natural stands (Millar, 1984). The disease is common in *Pinus* species in North America but has also been reported in pine stands in Europe and Asia. In addition to their limited geographic distribution, *Lophodermella* pathogens have a narrow host range. Based on the occurrence of fruiting bodies, some *Lophodermella* species occur on a single pine species whereas others are restricted to a group of pine species with a specific number of needles (Millar, 1984).

This includes *L. sulcigena* and *L. conjuncta* on two-needle pines of subsection *Pinus* in Europe and *L. concolor* on two-needle pines of subgenus *Pinus* in western North America (Gernandt et al., 2005; Millar, 1984). Despite sharing host species within a geographic range, there are no records of coexistence and interaction of *Lophodermella* pathogens in infected needles.

While a few *Lophodermella* species were more aggressive than others, most identified infections have been found to be either benign or restricted in small patches (Darker, 1967; Minter & Millar, 1993). However, when severely infected, pine stands can experience significant loss in growth and, consequently, yield (Jalkanen, 1985; Worrall et al., 2012). Past studies have found that outbreaks in their native ranges can occur intermittently over several years, such was the case of *L. concolor* on *P. contorta* stands in Northern America (Darker, 1932), and *L. sulcigena* in Europe (Jalkanen, 1985). Recently, *Lophodermella* needle cast is among the many needle diseases that have been reported as increasing in severity. In 2008-2011, two *Lophodermella* needle cast epidemics caused by *L. concolor* and *L. montivaga* were observed on *P. contorta* stands along the Rocky Mountain Region, USA (Worrall et al., 2012). Similarly, two-needle pines in Canada were heavily infected with *L. concolor* (Forest Management Branch, 2019; Melnick, 2016), while *L. sulcigena* severely infected *P. mugo* in the European alps in 2019 (Beenken, 2019). Current management for heavily infected stands include silvicultural approaches (i.e., even-aged management, low stand density and resistant genotypes) and fungicide use (Worrall et al., 2012; Ying & Hunt, 1987).

As recent incidence of these emerging needle diseases reaches an alarming rate, correct identification of these pathogens is important to diagnose needle diseases rapidly and accurately. However, relying only on morphological characteristics, identification of *Lophodermella* species is challenging due to similarities in symptomology, variability of morphometric features across

developmental stages and mounting media, secondary fungal invasion and lack of ideally mature specimens (Worrall et al., 2012). Description of mycelial characters on culture media are also absent due to the ephemeral growth of *Lophodermella* ascospores (Darker, 1932). Also, since only two of the nine described *Lophodermella* species were reported to reproduce asexually (Millar, 1984), features that could further discriminate at the species level are thus limited. Fungal identification via host specialization may also falter as cryptic pathogen occurrence, albeit unknown among *Lophodermella* species, could confound host diversity (Slippers & Wingfield, 2007). These issues have led to inaccurate reports of disease incidence in the past (Millar, 1984) and confusion in species taxonomic classification (e.g., Laflamme et al., 2015).

Molecular characterization could help improve species delineation and identification of *Lophodermella* species. Genetic data can also provide valuable information regarding pathogenicity and disease spread that are not necessarily inferred from morphological attributes (Crous et al., 2016). However, recent searches have identified that only a single *Lophodermella* species had the most basic genetic information available in public databases despite the explosion of genetic information and databases of fungal species. Thus, polymorphisms in a specific gene region among *Lophodermella* species cannot be determined. While commonly used ribosomal and house-keeping loci (e.g., internal transcribed spacer, translation elongation factor 1-alpha, etc.) have been successful in differentiating species within genera (e.g., Hermosa et al., 2000), the genome data of some fungal species provided in-depth distinction between species in terms of genome structure and evolutionary divergence (e.g. Kubicek et al., 2019). Hence, exploring the *Lophodermella* genomes could not only reveal genomic architecture distinct across species, but more importantly, elucidate evolution and specialization of species.

Mycobiome Interactions in a *Lophodermella* Needle Cast Pathosystem

Endophytes modify disease impacts on hosts in a variety of mechanisms. In a broad sense, endophytes are microorganisms that thrive asymptotically in a healthy plant tissue for a prolonged period (Stone et al., 2004). This definition, however, excludes those that have either obvious mutualistic or parasitic associations with their hosts such as mycorrhizae and nitrogen-fixing bacteria and pathogens with no known latent stage, respectively (Stergiopoulos & Gordon, 2014). It is hypothesized that the wide endophytic diversity comes with a vast set of ecologically important functions (Terhonen et al., 2019). Improving host plant fitness and survival amid stressors, particularly insects and pathogens, is perhaps the most studied ecological role of endophytes. However, this mutualistic (and even commensal) relationship is only part of a continuum of interactions between hosts and microbes (Schulz & Boyle, 2005; Stergiopoulos & Gordon, 2014). Endophytic lifestyles and functions can change with varying environmental conditions, host type and/or microbe-microbe interactions, which may be harmful to the hosts. Some endophytes have also been documented as latent pathogens that produce symptoms when hosts are subject to environmental stress (Sieber, 2007), while others enable and/or facilitate pathogen activity resulting to severe disease damage (Busby et al., 2016; Martí et al., 2020; Ridout & Newcombe, 2015).

Characterizing the mycobiome in a pathosystem can provide clues on the interactions between pathogens and other endophytes. This is particularly relevant as more evidence shifts our view of disease development from the classical “one-microbe-one disease” to a more complex system that involves co-infection of a concert of microbial organisms interacting with their environment known as the pathobiome (Feau & Hamelin, 2017; Koskella et al., 2017). Next

generation sequencing can help reveal changes in the pathobiome when subject to different selective forces such as those environmental factors changing due to climate change. These discoveries could have a variety of applications particularly in disease management and industry (Gibson et al., 2011; Grigoriev et al., 2011). For example, fungal endophytes that are significantly associated with absence of infection may be applied to control emerging forest diseases that are highly dependent on fungicide use (Griffiths et al., 2020). Interestingly, the identification of core microbiomes in healthy and diseased tissues could also lead to a unique customized therapeutic approach to treat plant diseases (Gopal et al., 2013). Meanwhile, enzymatic ability of the pathobiome to degrade lignocellulose may be harnessed as tools for an efficient biomass breakdown in biofuel production (Corrêa et al., 2014; Feldbrügge et al., 2013).

In *Lophodermella* needle cast, basic information on the interactions between pathogens and fungal endophytes are scant, although colonizers and pathogen inhibitors had been identified. Secondary colonization by *Lophodermium* species and *Leptostroma* were noted on needles infected with *Lophodermella* species (Millar, 1984). Interestingly, fungal species such as *Hendersonia pinicola*, *H. acicola*, and *Lophodermium seditosum* were recorded to restrict symptom development or suppress occurrence of *L. concolor* (Millar, 1984) and *L. sulcigena* (Jalkanen, 1985; Jalkanen & Laakso, 1986). It is not clear, however, whether these fungal species thrive as part of the host microbiome. Apart from beneficial fungal endophytic communities, the endophytic lifestyle of pathogens (e.g., *Lophodermium*, *Rhizosphaera*, and *Cyclaneusma*) have been explored through isolation from asymptomatic needles (Stone et al., 2004). But as needles senesce or inciting factors occur, the balance between fungal virulence and host defense is lost and thus results to needle disease (Schulz & Boyle, 2005; Sieber, 2007). While currently unknown, the ability of *Lophodermella* species to be latent pathogens could impact disease management in

natural stands and plantations, and quarantine measures in areas where hosts would be vulnerable to stresses.

Needle Disease Monitoring and Assessment

Pathogen identification and detection are crucial in disease diagnosis, monitoring, risk assessments, and quarantine measures. The widespread occurrence and severity of emerging forest diseases also prompt the need for further understanding of their origins and patterns of spread. Additionally, as international trade continues to boom and accelerate forest disease spread, accurate pathogen identification, which could be addressed by adapting molecular technologies, are crucial in phytosanitary systems (Crous et al., 2016). While slow traditional methods (i.e., isolation of pathogens in culture media) are useful, molecular techniques had evolved towards accelerated and reliable plant diagnostics (López et al., 2003; Luchi et al., 2020; Pandey et al., 2015). The specificity of these markers allows for discrimination of closely related species at various taxonomic levels that are difficult to morphologically classify (Capote et al., 2012). Further, sensitive molecular diagnostic tools detect the introduction of and track invasive plant pathogens even at low incidence or in symptomless planting materials (e.g., Lamarche et al., 2015; Mishra et al., 2013; Walter et al., 2016). These culture-free techniques are also an efficient mechanism for the early detection of obligate or fastidious pathogens (e.g., Bergeron et al., 2019; Mougou-Hamdane et al., 2010). While development of such tools is still limited by factors such as cost and availability of molecular data (Raja et al., 2017), its application in plant diagnosis and protection is undeniably promising.

Given the difficulty in identifying and isolating *Lophodermella* pathogens, the utilization of molecular tools will fast track needle disease surveys. While microsatellite and qPCR markers for needle pathogen identification on symptomatic needles are now available, these are limited to

only a few needle pathogens such as *Dothistroma septosporum*, *D. pini*, and *Lecanosticta acicola* (Barnes et al., 2008; Schneider et al., 2019; Siziba et al., 2016). Interestingly, PCR-based methods can also detect latent pathogens (e.g., *L. acicola* and *Pestalotiopsis neglecta*) in asymptomatic *P. thunbergii* needles which suggests the utility of molecular markers not only as tools for rapid diagnosis but also for monitoring of potential pathogens in pine needles (Kihara et al., 2015). Thus far, however, no tools have yet been developed to assist in identifying and monitoring *Lophodermella* pathogens for potential needle cast epidemics except for the needle trace method that detected retroactively such phenomenon (Jalkanen et al., 1994). Gene-based tools can greatly improve the efficiency and speed in correctly identifying morphologically similar *Lophodermella* pathogens. Further, it can monitor shifts in host range and spread of known and cryptic *Lophodermella* species.

My research fills in the gaps in our understanding of understudied and emerging needle pathosystems, particularly the *Lophodermella* needle cast. It will make use of molecular tools to address basic and applied fungal pathology questions about *Lophodermella* species. I specifically focus on three research themes which are discussed in respective chapters: (a) molecular characterization and phylogeny of five *Lophodermella* species within Rhytismataceae (Chapter 2), (b) mycobiome characterization in symptomatic and asymptomatic *P. contorta* needles using next generation sequencing (Chapter 3), and (c) development of molecular markers for rapid identification and detection of *Lophodermella* pathogens (Chapter 4). Finally, synthesis of results and implications for forest disease management will be discussed in Chapter 5.

References

- Anderson, P. K., Cunningham, A. A., Patel, N. G., Morales, F. J., Epstein, P. R., & Daszak, P. (2004). Emerging infectious diseases of plants: Pathogen pollution, climate change and agrotechnology drivers. *Trends in Ecology & Evolution*, *19*(10), 535–544. <https://doi.org/10.1016/j.tree.2004.07.021>
- Barnes, I., Cortinas, M. N., Wingfield, M. J., & Wingfield, B. D. (2008). Microsatellite markers for the red band needle blight pathogen, *Dothistroma septosporum*. *Molecular Ecology Resources*, *8*(5), 1026–1029. <https://doi.org/10.1111/j.1755-0998.2008.02142.x>
- Beenken, L. (2019). Lophodermella-Nadelschütte. In *Queloz V, Forster B, Beenken L, Stroheker S, Odermatt O, Hölling D, Meyer JB, Dubach V. Waldschutzüberblick 2018* (Vol. 79, pp. 1–33). <https://www.wsl.ch/de/publikationen/waldschutzueberblick-2018.html>
- Bergeron, M.-J., Feau, N., Stewart, D., Tanguay, P., & Hamelin, R. C. (2019). Genome-enhanced detection and identification of fungal pathogens responsible for pine and poplar rust diseases. *PLOS ONE*, *14*(2), e0210952. <https://doi.org/10.1371/journal.pone.0210952>
- Busby, P. E., Ridout, M., & Newcombe, G. (2016). Fungal endophytes: Modifiers of plant disease. *Plant Molecular Biology*, *90*(6), 645–655. <https://doi.org/10.1007/s11103-015-0412-0>
- Canto, T., Aranda, M. A., & Fereres, A. (2009). Climate change effects on physiology and population processes of hosts and vectors that influence the spread of hemipteran-borne plant viruses. *Global Change Biology*, *15*(8), 1884–1894. <https://doi.org/10.1111/j.1365-2486.2008.01820.x>

- Capote, N., Mara, A., Aguado, A., & Snchez-Torres, P. (2012). Molecular Tools for Detection of Plant Pathogenic Fungi and Fungicide Resistance. In C. J. Cumagun (Ed.), *Plant Pathology*. InTech. <https://doi.org/10.5772/38011>
- Chakraborty, S. (2013). Migrate or evolve: Options for plant pathogens under climate change. *Global Change Biology*, *19*(7), 1985–2000. <https://doi.org/10.1111/gcb.12205>
- Corrêa, R. C. G., Rhoden, S. A., Mota, T. R., Azevedo, J. L., Pamphile, J. A., de Souza, C. G. M., Polizeli, M. de L. T. de M., Bracht, A., & Peralta, R. M. (2014). Endophytic fungi: Expanding the arsenal of industrial enzyme producers. *Journal of Industrial Microbiology & Biotechnology*, *41*(10), 1467–1478. <https://doi.org/10.1007/s10295-014-1496-2>
- Crous, P. W., Groenewald, J. Z., Slippers, B., & Wingfield, M. J. (2016). Global food and fibre security threatened by current inefficiencies in fungal identification. *Philosophical Transactions of the Royal Society B: Biological Sciences*, *371*(1709), 20160024. <https://doi.org/10.1098/rstb.2016.0024>
- Darker, G. (1932). *The Hypodermataceae of Conifers* (Vol. 1). Contributions from the Arnold Arboretum of Harvard University.
- Darker, G. (1967). A revision of the genera of the Hypodermataceae. *Canadian Journal of Botany*, *45*, 1399–1444.
- Desprez-Loustau, M.-L., Robin, C., Reynaud, G., Déqué, M., Badeau, V., Piou, D., Husson, C., & Marçais, B. (2007). Simulating the effects of a climate-change scenario on the geographical range and activity of forest-pathogenic fungi. *Canadian Journal of Plant Pathology*, *29*(2), 101–120. <https://doi.org/10.1080/07060660709507447>

- EFSA Panel on Plant Health. (2013). Scientific Opinion on the risk to plant health posed by *Dothistroma septosporum* (Dorog.) M. Morelet (*Mycosphaerella pini* E. Rostrup, syn. *Scirrhia pini*) and *Dothistroma pini* Hulbary to the EU territory with the identification and evaluation of risk reduction options. *EFSA Journal*, 2013; 11(1):3026.
<https://doi.org/10.2903/j.efsa.2013.3026>
- Feau, N., & Hamelin, R. C. (2017). Say hello to my little friends: How microbiota can modulate tree health. *New Phytologist*, 215(2), 508–510. <https://doi.org/10.1111/nph.14649>
- Feldbrügge, M., Kellner, R., & Schipper, K. (2013). The biotechnological use and potential of plant pathogenic smut fungi. *Applied Microbiology and Biotechnology*, 97(8), 3253–3265. <https://doi.org/10.1007/s00253-013-4777-1>
- Forest Management Branch. (2019). *2018 Yukon Forest Health Report*. Energy, Mines and Resources, Government of Yukon.
- Garrett, K. A., Dendy, S. P., Frank, E. E., Rouse, M. N., & Travers, S. E. (2006). Climate Change Effects on Plant Disease: Genomes to Ecosystems. *Annual Review of Phytopathology*, 44(1), 489–509.
<https://doi.org/10.1146/annurev.phyto.44.070505.143420>
- Gernandt, D. S., Gaeda López, G., Ortiz García, S., & Liston, A. (2005). Phylogeny and Classification of *Pinus*. *Taxon*, 54(1), 29–42.
- Ghelardini, L., Pepori, A. L., Luchi, N., Capretti, P., & Santini, A. (2016). Drivers of emerging fungal diseases of forest trees. *Forest Ecology and Management*, 381, 235–246.
<https://doi.org/10.1016/j.foreco.2016.09.032>

- Gibson, D. M., King, B. C., Hayes, M. L., & Bergstrom, G. C. (2011). Plant pathogens as a source of diverse enzymes for lignocellulose digestion. *Current Opinion in Microbiology*, *14*(3), 264–270. <https://doi.org/10.1016/j.mib.2011.04.002>
- Gopal, M., Gupta, A., & Thomas, G. V. (2013). Bespoke microbiome therapy to manage plant diseases. *Frontiers in Microbiology*, *4*. <https://doi.org/10.3389/fmicb.2013.00355>
- Griffiths, S. M., Galambao, M., Rowntree, J., Goodhead, I., Hall, J., O'Brien, D., Atkinson, N., & Antwis, R. E. (2020). Complex associations between cross-kingdom microbial endophytes and host genotype in ash dieback disease dynamics. *Journal of Ecology*, *108*(1), 291–309. <https://doi.org/10.1111/1365-2745.13302>
- Grigoriev, I. V., Cullen, D., Goodwin, S. B., Hibbett, D., Jeffries, T. W., Kubicek, C. P., Kuske, C., Magnuson, J. K., Martin, F., Spatafora, J. W., Tsang, A., & Baker, S. E. (2011). Fueling the future with fungal genomics. *Mycology*, *2*(3), 192–209. <https://doi.org/10.1080/21501203.2011.584577>
- Hermosa, M. R., Grondona, I., Iturriaga, E. A., Diaz-Minguez, J. M., Castro, C., Monte, E., & Garcia-Acha, I. (2000). Molecular Characterization and Identification of Biocontrol Isolates of *Trichoderma* spp. *Applied and Environmental Microbiology*, *66*(5), 1890–1898. <https://doi.org/10.1128/AEM.66.5.1890-1898.2000>
- Jalkanen, R., Aalto, T., & Kurkela, T. (1994). The use of needle-trace method (NTM) in retrospectively detecting *Lophodermella* needle-cast epidemic. *Forest Pathology*, *24*(6–7), 376–385. <https://doi.org/10.1111/j.1439-0329.1994.tb00831.x>
- Jalkanen, Risto. (1985). The occurrence and importance of *Lophodermella sulcigena* and *Hendersonia acicola* on Scots pine in Finland. *Karstenia*, *25*(2), 53–61. <https://doi.org/10.29203/ka.1985.237>

- Jalkanen, Risto, & Laakso, R. (1986). *Hendersonia acicola* in an epidemic caused by *Lophodermella sulcigena* with special reference to biological control. *Karstenia*, 26(2), 49–56. <https://doi.org/10.29203/ka.1986.244>
- Jansons, Ā., Zeltiņš, P., Donis, J., & Neimane, U. (2020). Long-Term Effect of *Lophodermium* Needle Cast on The Growth of Scots Pine and Implications for Financial Outcomes. *Forests*, 11(7), 718. <https://doi.org/10.3390/f11070718>
- Juroszek, P., Racca, P., Link, S., Farhumand, J., & Kleinhenz, B. (2020). Overview on the review articles published during the past 30 years relating to the potential climate change effects on plant pathogens and crop disease risks. *Plant Pathology*, 69(2), 179–193. <https://doi.org/10.1111/ppa.13119>
- Kihara, J., Ueno, M., & Arase, S. (2015). PCR-Mediated Detection of Endophytic and Phytopathogenic Fungi from Needles of the Japanese Black Pine, <i>Pinus thunbergii</i>. *Open Journal of Forestry*, 05(04), 431–442. <https://doi.org/10.4236/ojf.2015.54037>
- Koskella, B., Meaden, S., Crowther, W. J., Leimu, R., & Metcalf, C. J. E. (2017). A signature of tree health? Shifts in the microbiome and the ecological drivers of horse chestnut bleeding canker disease. *New Phytologist*, 215(2), 737–746. <https://doi.org/10.1111/nph.14560>
- Kubicek, C. P., Steindorff, A. S., Chenthamara, K., Manganiello, G., Henrissat, B., Zhang, J., Cai, F., Kopchinskiy, A. G., Kubicek, E. M., Kuo, A., Baroncelli, R., Sarrocco, S., Noronha, E. F., Vannacci, G., Shen, Q., Grigoriev, I. V., & Druzhinina, I. S. (2019). Evolution and comparative genomics of the most common *Trichoderma* species. *BMC Genomics*, 20(1), 485. <https://doi.org/10.1186/s12864-019-5680-7>

- La Porta, N., Capretti, P., Thomsen, I. M., Kasanen, R., Hietala, A. M., & Von Weissenberg, K. (2008). Forest pathogens with higher damage potential due to climate change in Europe. *Canadian Journal of Plant Pathology*, *30*(2), 177–195. <https://doi.org/10.1080/07060661.2008.10540534>
- Laflamme, G., Broders, K., Côté, C., Munck, I., Iriarte, G., & Innes, L. (2015). Priority of *Lophophacidium* over *Canavirgella*: Taxonomic status of *Lophophacidium dooksii* and *Canavirgella banfieldii*, causal agents of a white pine needle disease. *Mycologia*, *107*(4), 745–753. <https://doi.org/10.3852/14-096>
- Lamarche, J., Potvin, A., Pelletier, G., Stewart, D., Feau, N., Alayon, D. I. O., Dale, A. L., Coelho, A., Uzunovic, A., Bilodeau, G. J., Brière, S. C., Hamelin, R. C., & Tanguay, P. (2015). Molecular Detection of 10 of the Most Unwanted Alien Forest Pathogens in Canada Using Real-Time PCR. *PLOS ONE*, *10*(8), e0134265. <https://doi.org/10.1371/journal.pone.0134265>
- López, M. M., Bertolini, E., Olmos, A., Caruso, P., Gorris, M. T., Llop, P., Penyalver, R., & Cambra, M. (2003). Innovative tools for detection of plant pathogenic viruses and bacteria. *International Microbiology*, *6*(4), 233–243. <https://doi.org/10.1007/s10123-003-0143-y>
- Luchi, N., Ioos, R., & Santini, A. (2020). Fast and reliable molecular methods to detect fungal pathogens in woody plants. *Applied Microbiology and Biotechnology*, *104*(6), 2453–2468. <https://doi.org/10.1007/s00253-020-10395-4>
- Martí, J. M., Arias-Giraldo, L. F., Díaz-Villanueva, W., Arnau, V., Rodríguez-Franco, A., & Garay, C. P. (2020). Metatranscriptomic dynamics after *Verticillium dahliae* infection

- and root damage in *Olea europaea*. *BMC Plant Biology*, 20(1), 79.
<https://doi.org/10.1186/s12870-019-2185-0>
- Melnick, P. (2016). A Good Year for Pine Needle Cast. *Bugs and Diseases*, 27(3), 1–2.
- Millar, C. S. (1984). Lophodermella species on pines. In: *Recent Research on Conifer Needle Diseases*. Eds. Glenn W. Peterson. USDA Forest Service, General Technical Report GTR-WO 50., 45–55.
- Minter, D. W., & Millar, C. S. (1993). IMI Descriptions of Fungi and Bacteria. *Mycopathologia*, 121(1), 53–56.
- Mishra, R. K., Pandey, B. K., Muthukumar, M., Pathak, N., & Zeeshan, M. (2013). Detection of Fusarium wilt pathogens of *Psidium guajava* L. in soil using culture independent PCR (ciPCR). *Saudi Journal of Biological Sciences*, 20(1), 51–56.
<https://doi.org/10.1016/j.sjbs.2012.10.007>
- Mougou-Hamdane, A., Giresse, X., Dutech, C., & Desprez-Loustau, M.-L. (2010). Spatial distribution of lineages of oak powdery mildew fungi in France, using quick molecular detection methods. *Annals of Forest Science*, 67(2), 212–212.
<https://doi.org/10.1051/forest/2009105>
- Mullett, M. S., & Brown, A. V. (2018). Effect of dothistroma needle blight on needle and shoot lengths. *Forest Pathology*, 48(1), e12382. <https://doi.org/10.1111/efp.12382>
- Pandey, P., Pandey, N. S., Shamim, Md., Srivastava, D., Dwivedi, D. K., Awasthi, L. P., & Singh, K. N. (2015). Molecular Tools and Techniques for Detection and Diagnosis of Plant Pathogens. In L. P. Awasthi (Ed.), *Recent Advances in the Diagnosis and Management of Plant Diseases* (pp. 253–271). Springer India.
https://doi.org/10.1007/978-81-322-2571-3_19

- Piškur, B., Hauptman, T., & Jurc, D. (2013). Dothistroma Needle Blight in Slovenia is caused by two cryptic species: *Dothistroma pini* and *Dothistroma septosporum*. *Forest Pathology*, 43(6), 518–521. <https://doi.org/10.1111/efp.12059>
- Raja, H. A., Miller, A. N., Pearce, C. J., & Oberlies, N. H. (2017). Fungal Identification Using Molecular Tools: A Primer for the Natural Products Research Community. *Journal of Natural Products*, 80(3), 756–770. <https://doi.org/10.1021/acs.jnatprod.6b01085>
- Ridout, M., & Newcombe, G. (2015). The frequency of modification of Dothistroma pine needle blight severity by fungi within the native range. *Forest Ecology and Management*, 337, 153–160. <https://doi.org/10.1016/j.foreco.2014.11.010>
- Rocky Mountain Region, Forest Health Protection. (2010). *Field guide to diseases & insects of the Rocky Mountain Region* (Gen. Tech. Rep. RMRS-GTR-241). Department of Agriculture, Forest Service, Rocky Mountain Research Station.
- Schneider, S., Jung, E., Queloz, V., Meyer, J. B., & Rigling, D. (2019). Detection of pine needle diseases caused by *Dothistroma septosporum*, *Dothistroma pini* and *Lecanosticta acicola* using different methodologies. *Forest Pathology*, e12495. <https://doi.org/10.1111/efp.12495>
- Schulz, B., & Boyle, C. (2005). The endophytic continuum. *Mycological Research*, 109(6), 661–686. <https://doi.org/10.1017/S095375620500273X>
- Sieber, T. N. (2007). Endophytic fungi in forest trees: Are they mutualists? *Fungal Biology Reviews*, 21(2–3), 75–89. <https://doi.org/10.1016/j.fbr.2007.05.004>
- Siziba, V. I., Wingfield, M. J., Sadiković, D., Mullett, M. S., Piškur, B., & Barnes, I. (2016). Development of microsatellite markers for the pine needle blight pathogen, *Dothistroma pini*. *Forest Pathology*, 46(5), 497–506. <https://doi.org/10.1111/efp.12282>

- Slippers, B., & Wingfield, M. J. (2007). Botryosphaeriaceae as endophytes and latent pathogens of woody plants: Diversity, ecology and impact. *Fungal Biology Reviews*, 21(2–3), 90–106. <https://doi.org/10.1016/j.fbr.2007.06.002>
- Stergiopoulos, I., & Gordon, T. R. (2014). Cryptic fungal infections: The hidden agenda of plant pathogens. *Frontiers in Plant Science*, 5. <https://doi.org/10.3389/fpls.2014.00506>
- Stone, J. K., Coop, L. B., & Manter, D. K. (2008). Predicting effects of climate change on Swiss needle cast disease severity in Pacific Northwest forests. *Canadian Journal of Plant Pathology*, 30(2), 169–176. <https://doi.org/10.1080/07060661.2008.10540533>
- Stone, J. K., Polishook, J. D., & White, J. F. (2004). ENDOPHYTIC FUNGI. In *Biodiversity of Fungi* (pp. 241–270). Elsevier. <https://doi.org/10.1016/B978-012509551-8/50015-5>
- Sturrock, R. N., Frankel, S. J., Brown, A. V., Hennon, P. E., Kliejunas, J. T., Lewis, K. J., Worrall, J. J., & Woods, A. J. (2011). Climate change and forest diseases: Climate change and forest diseases. *Plant Pathology*, 60(1), 133–149. <https://doi.org/10.1111/j.1365-3059.2010.02406.x>
- Terhonen, E., Blumenstein, K., Kovalchuk, A., & Asiegbu, F. O. (2019). Forest Tree Microbiomes and Associated Fungal Endophytes: Functional Roles and Impact on Forest Health. *Forests*, 10(1), 42. <https://doi.org/10.3390/f10010042>
- van der Pas, J. B., Slater-Hayes, J. D., Gadgil, P. D., & Bulman, L. (1984). Cylaneusma (Naemacyclus) needle-cast of pinus radiata in New Zealand. *New Zealand Journal of Forestry Science*, 14(2), 197–209.
- Walter, S., Ali, S., Kemen, E., Nazari, K., Bahri, B. A., Enjalbert, J., Hansen, J. G., Brown, J. K. M., Sicheritz-Pontén, T., Jones, J., Vallavieille-Pope, C., Hovmøller, M. S., & Justesen, A. F. (2016). Molecular markers for tracking the origin and worldwide distribution of

invasive strains of *Puccinia striiformis*. *Ecology and Evolution*, 6(9), 2790–2804.

<https://doi.org/10.1002/ece3.2069>

Worrall, J. J., Marchetti, S. B., & Mask, R. A. (2012). An Epidemic of Needle Cast on Lodgepole Pine in Colorado. In *Biological Evaluation R2-12-01* (p. 16). USDA Forest Service, Rocky Mountain Region, Forest Health Protection.

Wyka, S. A., Munck, I. A., Brazee, N. J., & Broders, K. D. (2018). Response of eastern white pine and associated foliar, blister rust, canker and root rot pathogens to climate change. *Forest Ecology and Management*, 423, 18–26.

<https://doi.org/10.1016/j.foreco.2018.03.011>

Ying, C. C., & Hunt, R. S. (1987). Stability of resistance among *Pinus contorta* provenances to *Lophodermella concolor* needle cast. *Canadian Journal of Forest Research*, 17(12), 1596–1601. <https://doi.org/10.1139/x87-244>

CHAPTER 2: MOLECULAR CHARACTERIZATION AND PHYLOGENETIC ANALYSES
OF FIVE *LOPHODERMELLA* NEEDLE PATHOGENS (RHYTISMATACEAE) ON *PINUS*
SPECIES IN THE USA AND EUROPE¹

Introduction

Conifer needle diseases are becoming increasingly prevalent due to several factors such as climate change and introduction to new hosts (Brodde et al., 2019; Lee et al., 2017; Woods et al., 2005; Wyka et al., 2017). Native needle pathogens emerge as they move into novel geographic areas while others are increasing in incidence due to faster sporulation enhanced by warmer and wetter conditions (Barnes et al., 2014; Gray et al., 2013; Rodas et al., 2016; Welsh et al., 2014). Recent examples of needle diseases with enhanced severity include Dothistroma needle blight (Woods, 2014), Swiss needle cast and Cedar leaf blight (Gray et al., 2013), and white pine needle damage (Broders et al., 2015; Wyka et al., 2018).

In the western region of USA, an increasing prevalence of native *Lophodermella* needle pathogens, which may be attributed to climate change, were observed (Worrall et al., 2012) in *Pinus contorta* and *P. flexilis*. These two pine hosts are naturally dominant and ecologically important species along the Rocky Mountain Region (Lotan & Critchfield, 1990; Schoettle, 2004). Two needle cast epidemics caused by *L. concolor* and *L. montivaga* were recorded on *P. contorta* (Worrall et al., 2012) while increased frequency of *L. arcuata* infection was observed in patches of limber pine (*P. flexilis*) stands. Meanwhile, in Europe, heavy infection of *L. sulcigena* and *L.*

¹ Published as: Ata, J. P., Burns, K. S., Marchetti, S., Munck, I. A., Beenken, L., Worrall, J. J., & Stewart, J. E. (2021). Molecular characterization and phylogenetic analyses of *Lophodermella* needle pathogens (Rhytismataceae) on *Pinus* species in the USA and Europe. *PeerJ*, 9, e11435. <https://doi.org/10.7717/peerj.11435>

conjuncta on European mountain pine (*P. mugo*) along the Swiss Alps were recorded in 2018 (Beenken, 2019). Despite increasing incidence, there are no wide scale assessments on the impact of *Lophodermella* pathogens in natural pine stands amidst climate change. Past surveys reported short outbreaks or minor incidence of *Lophodermella* species such as *L. cerina* in southern USA, *L. morbida* in the western USA, *L. maureri* in Mexico, and *L. orientalis* in Asia (Czabator et al., 1971; Darker, 1932; Minter, 1988b, 1993) but there are no recent surveys nor reports about their increasing incidence in these regions.

Thus far, only nine species belong to *Lophodermella* genus, including *L. arcuata*, *L. cerina*, *L. concolor*, *L. maureri*, *L. montivaga* and *L. morbida* in North America, *L. conjuncta* and *L. sulcigena* in Europe, and *L. orientalis* in Asia (Robert et al., 2005). *Lophodermella* species (Rhytismataceae) are distinguished by their subhypodermal ascomata, clavate ascospores surrounded by mucilaginous sheath, and wider asci than the closely related genus *Lophodermium* (Darker, 1967). While morphometric descriptions are clear in the literature, identification and differentiation among these *Lophodermella* species is challenging. This may be attributed to similarities in early symptoms of the disease, highly variable morphometric features at different developmental stages and mounting medium, secondary fungal invasion, and lack of ideally mature specimens (Worrall et al., 2012). Based on morphological characteristics, there have been doubts on disease reports of *L. sulcigena* on *P. radiata*, *P. halepensis* and *P. contorta* while other diseases still need verification, such as the occurrence of *L. montivaga* on *P. monticola* and *P. flexilis* (Millar, 1984).

Molecular characterization could help resolve classification of species closely related to *Lophodermella* such as the case of *Lophophacidium dooksii* on needles of five-needle *Pinus strobus*. In 1984, the newly described *L. dooksii* was classified under Phacidiaceae due to the lack

of morphological characteristics distinctive of Rhytismataceae (Corlett & Shoemaker, 1984). However, recent internal transcribed spacer (ITS) phylogenetic studies and morphology suggest *Lophophacidium dooksii* is closely related to *L. arcuata* (Ekanayaka, 2019; Laflamme et al., 2015). Following the phylogenetic evidence, Ekanayaka (2019) reclassified *L. dooksii* to Rhytismataceae, but the phylogenetic relationship of *L. dooksii* and *L. arcuata* with other *Lophodermella* species is still unclear.

The lack of molecular information on *Lophodermella* spp. makes it difficult to resolve intra- and interspecific phylogenetic relationships. Currently, out of the nine known *Lophodermella* species, only the ITS sequence of *L. arcuata* represents the genus in fungal genetic databases (i.e., NCBI-nr, UNITE, DNA Data Bank of Japan). As emerging pathogens, molecular studies on *Lophodermella* are important for pathogen identification. These will elucidate phylogenetic relationship of *Lophodermella* with other rhytismataceous species. These will also aid in assessing the diversity and impact of emerging or invasive disease threats in conifer forest and will provide insights on fungal biology and evolution of traits. This study aims to fill this gap by analyzing the three-loci phylogeny of *Lophodermella* species that cause emerging needle cast diseases in western USA and Europe which include *L. arcuata*, *L. concolor*, *L. conjuncta*, *L. montivaga*, and *L. sulcigena*. We test monophyly of this genus by including other genera within Rhytismataceae and by using molecular phylogenies to guide the identification of shared and unique traits among *Lophodermella* species for genus and species delineation.

Methodology

Sampling and Morphology

Sampling was conducted in known geographic distributions of *L. arcuata*, *L. concolor*, *L. montivaga* and *L. dooksii* in the USA. Similarly, *L. sulcigena* and *L. concolor* samples were

collected from their known distributions in Europe. Needles from 32 *P. contorta* trees from natural stands infected with *L. montivaga* and/or *L. concolor* were collected in June and August 2018 across 12 sites within Gunnison National Forest, Colorado, USA (Table 2.1). *Lophodermella arcuata* on *P. flexilis* stands were collected from Rocky Mountain National Park, Colorado, USA in June 2018 and July 2019 while the eastern white pine (*P. strobus*) needles symptomatic of *L. dooksii* were collected from natural stands in Maine, USA in May 2019. Meanwhile, needles of the *P. mugo* infected with *L. sulcigena* and *L. conjuncta* were collected in the Swiss and Austrian Alps in 2018 (Table 2.1). The needles were placed into separate paper bags and stored at 4°C until DNA extraction.

Morphology of the fungal pathogens from randomly selected fresh symptomatic needles was characterized for fungal identification (Fig 2.1). Midsections of ascomata were cut using a razor blade and mounted in 3% potassium hydroxide (KOH). Measurements of fruiting structures were taken from mounted materials. Observations were made using both dissecting and compound microscopes. Morphological traits common among species based on published descriptions were compared (Table 2.2; Corlett & Shoemaker, 1984; Darker, 1932; Millar & Minter, 1966, 1978; Minter & Millar, 1993; Worrall et al., 2012).

DNA Extraction and Sequencing

Cultures from single-spore isolations of *L. montivaga*, *L. concolor* and *L. arcuata* were attempted but did not yield pure cultures, as these are thought to be potentially obligate fungi. Similar to previous observations (Darker, 1967), most mature spores isolated did not germinate and development of germ tubes in a few spores became arrested. Therefore, to be able to extract adequate amounts of quality DNA, fruiting bodies from three to five symptomatic needles from each tree were used for DNA extraction. DNA was extracted using CTAB method with slight

Table 2.1. Collection information, GenBank accession and genotype numbers for each *Lophodermella* species and *Lophophacidium dooksii* for the three loci, namely: internal transcribed spacer region 1, 5.8S ribosomal RNA and internal transcribed spacer region 2 (ITS), large ribosomal subunit (LSU) and translation elongation factor (TEF1- α).

Sample ID	Location	Host	Collection Date	Collectors	GenBank Accession Number; (Genotype)		
					ITS	LSU	TEF1- α
<i>Lophodermella concolor</i> (Dearn.) Darker							
CS6C	CS, GNF, CO, USA	<i>Pinus contorta</i>	12 June 2018	JE Stewart, JP Ata, KS Burns, SB Marchetti, JJ Worrall	MN937619; (1)	MN937581; (1)	MN937651; (1)
CS9C	CS, GNF, CO, USA	<i>P. contorta</i>	12 June 2018	"	MN937612; (1)	MN937579; (1)	MN937650; (1)
FS6C	FS, GNF, CO, USA	<i>P. contorta</i>	12 June 2018	"	MN937618; (1)	MN937582; (1)	MN937647; (1)
FS8C	FS, GNF, CO, USA	<i>P. contorta</i>	12 June 2018	"	MN937610; (2)	MN937580; (1)	MN937653; (1)
LP7C	LP, GNF, CO, USA	<i>P. contorta</i>	12 June 2018	"	MN937621; (1)	MN937588; (3)	MN937654; (1)
LV7C	LV, GNF, CO, USA	<i>P. contorta</i>	14 June 2018	"	MN937620; (1)	MN937575; (1)	MN937657; (1)
LV8C	LV, GNF, CO, USA	<i>P. contorta</i>	12 June 2018	"	MN937615; (1)	MN937576; (2)	MN937655; (1)
PT2C	PT, GNF, CO, USA	<i>P. contorta</i>	14 June 2018	"	MN937616; (1)	MN937577; (1)	MN937646; (1)
PT3C	PT, GNF, CO, USA	<i>P. contorta</i>	14 June 2018	"	MN937614; (1)	MN937583; (1)	MN937652; (1)
SR3C	SR, GNF, CO, USA	<i>P. contorta</i>	13 June 2018	"	MN937617; (1)	MN937578; (1)	MN937649; (1)
SR6C	SR, GNF, CO, USA	<i>P. contorta</i>	13 June 2018	"	MN937613; (1)	MN937584; (1)	MN937648; (1)
OJ11C	OJ, GNF, CO, USA	<i>P. contorta</i>	13 June 2018	"	MN937611; (1)	MN937574; (1)	MN937656; (1)

<i>Lophodermella montivaga</i> Petrak							
CU1M	CU, GNF, CO, USA	<i>P. contorta</i>	14 June 2018	"	MN937633; (1)	MN937586; (1)	MN937669; (1)
LVP2M	LV, GNF, CO, USA	<i>P. contorta</i>	14 June 2018	"	MN937634; (1)	MT906358; (1)	-
LVP3M	LV, GNF, CO, USA	<i>P. contorta</i>	14 June 2018	"	MN937635; (1)	MN937598; (1)	MN937672; (1)
NC2M	NC, GNF, CO, USA	<i>P. contorta</i>	14 June 2018	"	MN937625; (1)	MN937592; (1)	MN937667; (1)
NC6M	NC, GNF, CO, USA	<i>P. contorta</i>	14 June 2018	"	MN937626; (1)	MN937601; (1)	MN937674; (1)
NC8M	NC, GNF, CO, USA	<i>P. contorta</i>	14 June 2018	"	MN937627; (1)	MN937593; (1)	MN937671; (1)
NC9M	NC, GNF, CO, USA	<i>Pinus contorta</i>	14 June 2018	"	MN937636; (1)	-	MN937668; (1)
NC10M	NC, GNF, CO, USA	<i>P. contorta</i>	14 June 2018	"	MN937637; (1)	-	MT919224; (1)
OJ3M	OJ, GNF, CO, USA	<i>P. contorta</i>	13 June 2018	"	MN937641; (1)	-	MT919226; (1)
PT6M	PT, GNF, CO, USA	<i>P. contorta</i>	14 June 2018	"	MN937640; (2)	MN937594; (1)	MN937661; (1)
PT8M	PT, GNF, CO, USA	<i>P. contorta</i>	14 June 2018	"	MN937628; (1)	MN937602; (1)	MN937660; (1)
PT9M	PT, GNF, CO, USA	<i>P. contorta</i>	14 June 2018	"	MN937642; (1)	MN937587; (1)	-
PT10M	PT, GNF, CO, USA	<i>P. contorta</i>	14 June 2018	"	MN937622; (1)	MN937591; (1)	MN937670; (1)
PT11M	PT, GNF, CO, USA	<i>P. contorta</i>	14 June 2018	"	MN937630; (1)	MN937595; (1)	MN937663; (1)
SR9M	SR, GNF, CO, USA	<i>P. contorta</i>	13 June 2018	"	MN937643; (3)	-	MN937659; (1)
TC1M	TC, GNF, CO, USA	<i>P. contorta</i>	14 June 2018	"	MN937631; (1)	MN937596; (1)	-

TC3M	TC, GNF, CO, USA	<i>P. contorta</i>	14 June 2018	"	MN937632; (1)	MN937597; (1)	MN937666; (1)
TC9M	TC, GNF, CO, USA	<i>P. contorta</i>	14 June 2018	"	MN937629; (1)	MN937599; (1)	MN937673; (1)
TL8M	TL, GNF, CO, USA	<i>P. contorta</i>	21 August 2018	SB Marchetti	MN937638; (1)	MN937600; (1)	MN937662; (1)
TL9M	TL, GNF, CO, USA	<i>P. contorta</i>	21 August 2018	SB Marchetti	MN937639; (2)	-	MT919225; (1)
<i>Lophodermella</i> sp.							
RMNP_01	RMNP, CO, USA	<i>Pinus flexilis</i>	05 July 2018	KS Burns	MN937645	MN937590	MN937665
<i>Lophodermella arcuata</i> (Darker) Darker							
RMNP_LU1	RMNP, CO, USA	<i>P. flexilis</i>	24 July 2019	KS Burns	MN937644; (1)	MN937585; (1)	MN937658; (1)
RMNP_LU16	RMNP, CO, USA	<i>P. flexilis</i>	24 July 2019	KS Burns	MT906333; (1)	MT906359; (1)	MT919227; (2)
<i>Lophophacidium dooksii</i> Corlett and Shoemaker							
MB5	Massabesic Experimental Forest, ME, USA	<i>Pinus strobus</i>	03 May 2019	IA Munck, JE Stewart, JP Ata, A Bergdahl, W Searles	MN937623	MN937589	MN937664
<i>Lophodermella sulcigena</i> (Rostr.) Höhn.							
PH18_0656	Canton Ticino, Passo del Lucomagno, SW	<i>Pinus mugo</i>	10 July 2018	G Moretti	MN937624	MN937604	MN937675
<i>Lophodermella conjuncta</i> (Darker) Darker							
PH18_0655	Canton Grisons, Lenzerheide, SW	<i>P. mugo</i>	18 April 2018	M Vanoni	MN937607; (1)	MN937605; (1)	MN937677; (1)
PHP19_0986	Canton Bern, Kandersteg,	<i>P. mugo</i>	18 June 2018	J Meyer, L Beenken	MN937609; (2)	MN937606; (1)	MN937676; (1)

	Oeschi-Forest, CH						
PHP19_0987	Tyrol, Scharnitz, Karwendel Valley, AT	<i>P. mugo</i>	11 June 2018	T Cech, L. Beenken	MN937608; (3)	MN937603; (1)	MN937678; (1)
Location: CS - Cold Springs Campground, CU – Cumberland, FS – Fisherman Trail, LP – Lodgepole Campground, LV – Lakeview Campground, NC – North Cumberland, OJ – Oh Be Joyful, PT – Pitkin, SR – Slate River, TC – Tincup, TL – Taylor Park, GNF – Gunnison National Forest, RMNP – Rocky Mountain National Park, CO – Colorado, ME – Maine, USA – United States of America, CH – Switzerland, AT - Austria							

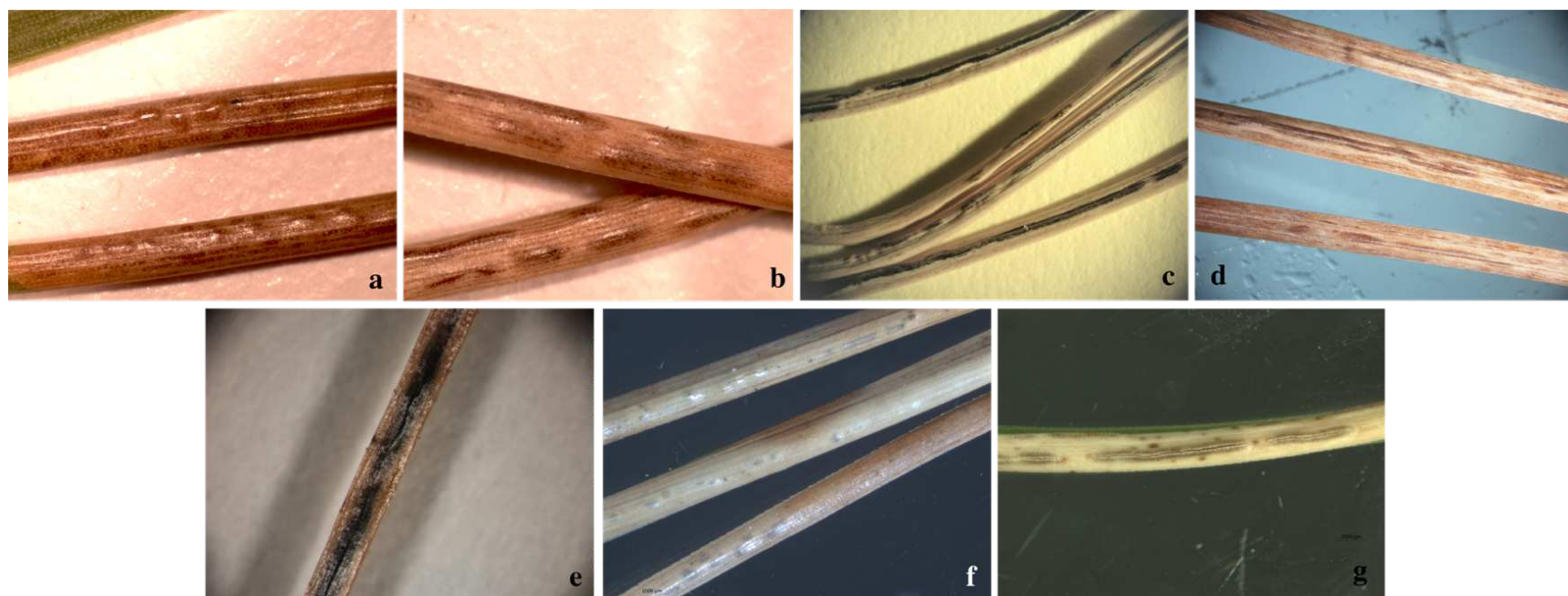


Figure 2.1. Ascomata of *Lophodermella concolor* (a) and *L. montivaga* (b) on *Pinus contorta* from Gunnison National Forest, Colorado, USA; *Lophodermella* sp. (c) and *Lophodermella arcuata* (d) on *P. flexilis* from Rocky Mountain National Park, Colorado, USA; *Lophophacidium dooksii* on *P. strobus* from Massabesic, Maine, USA (e); and *L. conjuncta* (f) and *L. sulcigena* (g) on *P. mugo* from Austria and Switzerland.

Table 2.2. Characteristics of *Lophodermella* species and *Lophophacidium dooksii* based on published descriptions

Features	<i>Lophodermella concolor</i> (Dearn.) Darker	<i>Lophodermella montivaga</i> Petrak	<i>Lophodermella arcuata</i> (Darker) Darker	<i>Lophodermella sulcigena</i> (Rostr.) Höhn.	<i>Lophodermella conjuncta</i> (Darker) Darker
<i>Ascomata (hysterothecia)</i>					
Size (mm)	0.4-0.8 × 0.28-0.44	0.75-8 × 0.28-0.4	0.38-3.13 × 0.25-0.45	2-20 × 0.30-0.45	0.50-4.0 × 0.20-0.30
Depth (µm)	200-280	220-250	210-260	200-250	140-180
Opening	longitudinal split along stomata	longitudinal split	Longitudinal split along stomata	longitudinal split	longitudinal split
<i>Paraphyses</i>					
Size (µm)	About as long as the asci	Up to 150 × ca 1	120-135 × 0.5-1	100– 120 × 1	135-150 × 1.0-2.0
Gelatinous sheath/ Mucous coat	Present	Present	Present	Present	Absent
Septation	Present	Present	Inconspicuous	Present	Present
<i>Asci</i>					
Size (µm)	120-225 × 15-17	120-160 × 12-15	110-160 × 14-20	110-140 × 13-15	(100)110–160 × 15–16
Opening mechanism	No obvious pre-formed apical apparatus (small apical hole or split after spores are released)	No obvious pre-formed apical apparatus (small apical hole or split after spores are released)	No obvious pre-formed opening mechanism (small apical hole or split after spores are released)	No obvious pre-formed apical apparatus	No obvious pre-formed apical apparatus
Number of spores	8	8	8	4–8	8

<i>Ascospore</i>					
Size (µm)	45-60 × (4) 6-8	40-50 × 3-4	40-50-(95) × 4-6	27-40 (65) × 4-5 (6)	(65) 75-90 (100) × 2.5-3.5
Mucilaginous/ gelatinous sheath	Present	Present	Present	Present	Present
Hosts (number of needles)	<i>Pinus banksiana</i> (2), <i>P. contorta</i> (2), <i>P.</i> <i>contorta</i> var. <i>murrayana</i> (2), <i>P.</i> <i>sylvestris</i> (2)	<i>Pinus attenuata</i> (3), <i>P. contorta</i> (2), <i>P. sylvestris</i> (2), <i>P.</i> <i>ponderosa</i> (3), <i>P.</i> <i>radiata</i> (3), <i>P.</i> <i>flexilis</i> (5), <i>P.</i> <i>monticola</i> (5)	<i>Pinus albicaulis</i> (5), <i>P. flexilis</i> (5), <i>P. lambertiana</i> (5), <i>P. monticola</i> (5)	<i>Pinus sylvestris</i> (2), <i>P. mugo</i> (2), <i>P. nigra</i> var. <i>maritima</i> (2)	<i>Pinus mugo</i> (2), <i>P.</i> <i>nigra</i> var. <i>Maritima</i> (2), <i>P.</i> <i>sylvestris</i> (2).
<i>Distribution</i>	Western USA, Canada	Western USA	Western USA	Europe	Europe
<i>Conidiomata</i>	Not observed	Not observed	Not observed	Unknown	Unknown
<i>References</i>	Darker 1932, Millar 1984, Minter and Millar 1993b, Funk 1985, Worrall et al. 2012	Darker 1932, Millar 1984, Minter and Millar 1993c, Worrall et al. 2012	Darker 1932, Minter and Millar 1993a	Darker 1932, Millar 1984, Millar and Minter 1978, Beenken 2019	Darker 1932, Millar 1984, Millar and Minter 1966, Beenken 2019

Table 2.2 (cont'd). Characteristics of *Lophodermella* species and *Lophophacidium dooksii* based on published descriptions

Features	<i>Lophodermella cerina</i> (Darker) Darker	<i>Lophodermella maureri</i> Minter and Cibrián	<i>Lophodermella morbida</i> Staley and Bynum	<i>Lophodermella orientalis</i> Minter and Ivory	<i>Lophophacidium dooksii</i> Corlett & Shoemaker
<i>Ascomata (hysterothecia)</i>					
Size (mm)	0.6-2.75 × 0.3-0.63	300-2500 × 250-550	1-6 (22)	0.5-2 × 0.4-0.8	(4.5-) 13-22 × 0.28-0.4
Depth (µm)	ca 280	--	350-370	--	180-280
Opening	longitudinal split along stomata	Longitudinal split	--	longitudinal split along stomata	Vertical row of cells
<i>Paraphyses</i>					
Size (µm)	180-200 × 1-3	2.5-3.5 (width)	120-140 × 2-3.5	2-3 (width)	(80-) 90-120 × 1.5-2.0
Gelatinous sheath/Mucous coat	Present (inconspicuous)	Present	--	Present	Present
Septation	Present	Present	Present	Present	Present
<i>Asci</i>					
Size (µm)	160-225 × 17-21	55-80 × 8-13	95-162	110-150 × 14-18	(70-) 85-110 (-120) × 14-18 (-20)
Opening mechanism	No obvious pre-formed apical apparatus (small apical hole or split after spores are released)	Opening by a large apical hole	--	No obvious pre-formed apical apparatus (small apical hole or split after spores are released)	Unitunicate
Number of spores	8	8	8	8	8
<i>Ascospore</i>					
Size (µm)	68-78 × 3-3.5	30-50 × 2.5-3.5	23-53 × 2.5-3.5	30-65 × 2.5-3.5	22-32 × 6-7.5

Mucilaginous/gelatinous sheath	Present	Present	Present	Present	Lacking
Hosts (number of needles)	<i>Pinus contorta</i> (2), <i>P. elliotii</i> var. <i>elliotii</i> (3), <i>P. ponderosa</i> (3), <i>P. taeda</i> (3), <i>P. sylvestris</i> (2)	<i>Pinus ayacahuite</i> (5)	<i>Pinus ponderosa</i> (3), <i>P. attenuata</i> (3)	<i>Pinus kesiya</i> (3, sometimes 2 or 4)	<i>Pinus strobus</i> (5)
Distribution	Western USA	Mexico	Western USA	Asia	Canada, USA
Conidiomata	Not observed (present in <i>P. contorta</i>)	Not observed	Present	Only fresh collected specimens	Not reported
References	Darker 1932, Millar 1984, Minter and Millar 1993d	Minter 1988b	Staley and Bynum 1972	Minter 1993	Corlett and Shoemaker 1984, Merrill et al. 1996

modifications in tissue grinding (Cubero et al., 1999). To prepare the samples, hysterothecia were cut into 1 mm long pieces and placed in 2 mL centrifuge tubes with one 5 mm glass bead and two 2.3 mm metal beads. To grind the samples, the tubes were submerged in liquid nitrogen before grinding using FastPrep (MP Biomedicals) for 30 seconds at speed 4 or 5. This previous process was repeated three times prior to the CTAB DNA extraction procedure developed by Cubero et al. (1999). DNA quantification and nucleic acid purity assessment were conducted using NanoDrop 1000 Spectrophotometer (Thermo Scientific). Meanwhile, the DNA extraction of *L. sulcigena* and *L. conjuncta* samples was performed in Europe. Single fruiting bodies (ca. 3-4 mm long pieces) each were prepared out of dry pine needles. DNA was extracted from the lyophilized and ground fruit bodies using the KingFisher/Flex Purification System (ThermoFisher Scientific) according to the manufacturer's protocol and the chemicals for automated DNA extraction from fungal samples with Kingfisher 96/Flex supplied by LGC Genomics GmbH (Berlin).

DNA was amplified at the following loci: internal transcribed spacer region 1, 5.8S ribosomal RNA and internal transcribed spacer region 2 (ITS), large subunit ribosomal nucleic acid (LSU), and translation elongation factor (TEF1 α). Primers used include ITS1 and ITS4 (White et al., 1990), LROR and LR5 or LR6 (Vilgalys & Hester, 1990), and EF1-983F and EFgr (Rehner, 2001). The ITS locus was amplified at optimal annealing temperatures between 50 – 55 °C with 30 cycles while TEF1 α and LSU were amplified at 56°C annealing temperature with 35 cycles and other cycle parameters following Tanney & Seifert (2017). Amplification of each locus was performed in a 25- μ L PCR reaction mixture of 1 \times standard Taq reaction buffer, 0.2 mM of each dNTP, 0.4 μ M of forward and reverse primer set, 0.625 units Taq polymerase, and 40 ng template DNA. For ITS amplification, the cycle parameters included initial denaturation at 94 °C

for 2 mins, followed by 30 cycles of denaturation at 94 °C for 40 s, optimal annealing temperature for 40 s, extension at 72 °C for 1 min, and final extension at 72 °C for 5 mins.

PCR products were purified using ExoSAP-IT (Affymetrix™). All purified amplicons were sent to Eurofins Genomics LLC for sequencing. Additionally, cloning of PCR products for each locus was performed on at least three randomly selected *L. concolor* and *L. montivaga* samples using pGEM® T-Easy Vector Systems (Promega) to confirm that sequenced amplicon was of single species. Three to seven clones were sequenced for each locus per sample and found to be 99.81 to 100% identical to the sequence of its corresponding original PCR product. Sequences were compared to NCBI sequence database using Nucleotide Basic Local Assignment Search Tool (BLASTn) for fungal identification and were accessioned in NCBI GenBank (Table 1). Sequence data were trimmed and manually checked using Geneious version R9.0.5 (Biomatters, Auckland, New Zealand) and subsequently aligned using MUSCLE (Edgar, 2004). Consensus tree of the concatenated dataset was stored in TreeBase (Submission ID 26836). Polymorphic sites were determined using DnaSP (Rozas et al., 2003).

Phylogenetic analyses for each locus were constructed using Bayesian inference (MrBayes; Huelsenbeck & Ronquist, 2001) and maximum likelihood methods (PhyML; Guindon et al., 2010) as modules in Geneious v. R9.0.5. Optimal substitution models for each dataset generated using DT-ModSel (Minin et al. 2003) were as follows: *SYM + G* for ITS, *TrNef + G* for TEF1 α , *TrN + I + G* for LSU, and *SYM + I + G* for the concatenated dataset. For models of evolution that are not available in either MrBayes or PhyML modules, the next best complex models were applied. Bayesian tree was analyzed by running Markov Chain Monte Carlo (MCMC) for up to 1,100,000 generations with four heated chains. Maximum likelihood tree was analyzed using 1000 bootstraps. Bayesian and maximum likelihood trees were generated with support thresholds of

80% with a 20% burn-in and 50%, respectively. The phylogenies were rooted to *Chalara* spp. (*Chalara* sp. MFLU 18-1812 and *Chalara* sp. MFLU 15-3167) following Ekanayaka (2019)

To evaluate the congruence of the three loci dataset, partition homogeneity test was conducted using PAUP version 4.0a (Barker & Lutzoni, 2002). This resulted in a p-value = 0.99, indicating congruence among the ITS, LSU and TEF1 α datasets. Tree topologies from individual loci were also compared using the reciprocal 70% bootstrap approach (Mason-Gamer and Kellogg 1996). Similarly, results also revealed no significant incongruence between the three datasets. Thus, the three loci dataset was combined using Sequence Matrix (Vaidya et al., 2011). The alignment and consensus tree of the concatenated dataset were stored in TreeBase (Submission ID 26836). Published sequences of known related species in GenBank database were included in the phylogenetic analysis (Supplementary Table 1). The rhytismataceous species were selected based on similarity to *Lophodermella* sequences and availability in NCBI database.

Character Mapping

Morphological characters were selected based on the presence in literature and their use for taxonomic classification of Rhytismataceae. Characters were coded based on published descriptions (Supplementary Table 4; Darker, 1932, 1967; *Fungi of Great Britain and Ireland*, 2019; Minter, 1988a; Minter & Millar, 1993a, 1993c, 1993b; Robert et al., 2005; Tanney & Seifert, 2017) and then mapped on the Bayesian ITS dataset phylogeny which had a more comprehensive set of Rhytismataceae species in well-supported clades. To assess distinct morphological characters among *Lophodermella* species, key characters were selected based on Darker (1932) and Hunt & Ziller (1978). These were then mapped on a separate Bayesian ITS phylogeny (GTR+I+G model) that was limited to *Lophodermella* species and two outgroups (*Elytroderma deformans* and *Chalara* sp.). All morphological characters were coded as unordered and mapped

with parsimony ancestral trace reconstruction using Mesquite v.3.6 (Maddison & Maddison, 2018).

Results

Molecular and Phylogenetic Analyses

PCR amplification produced a single band for each sample per locus. Chromatograms for forward and reverse sequences did not show multiple peaks at base calls, indicating uniform amplicons. Amplicons of the ITS, TEF1 α and LSU yielded products that ranged from 347 to 543, 678 to 811 and 790 to 1077 base pairs, respectively. Of the 40 samples of *Lophodermella* species and *L. dooksii* at the ITS, a total of nine genotypes were found with 83 polymorphic (segregating) sites and 64 parsimony informative sites were observed. At the TEF1 α , the 37 samples of *Lophodermella* species and *L. dooksii* had eight genotypes, and 77 of the 105 polymorphic sites were considered informative. Sequences of the 35 *Lophodermella* species and *L. dooksii* samples at the LSU resulted in nine genotypes with 106 total polymorphic sites and 62 parsimony informative sites. BLAST results of sequences are presented in Supplementary Table 2.

Several *Lophodermella* species and *L. dooksii* clustered in a well-supported clade (hereinafter referred to as the LOD clade) at the ITS, LSU and TEF1 α phylogenies. This clade composed of genotypes of *L. montivaga*, *L. concolor*, *L. arcuata*, *L. sulcigena*, *Lophodermella* sp. and *L. dooksii* in the ITS phylogeny was well-supported in the Bayesian phylogeny with a 0.96 posterior probability (PP), excluding *L. conjuncta* (Supplementary Figure 1). Similarly, for the LSU phylogeny, both Bayesian and ML phylogenies produced the same well-supported clade (1.0 PP and 97.9 bootstrap support (BS); Supplementary Figure 2). *Lophodermella conjuncta* remained distinct from the clade representing all other *Lophodermella* species at the LSU phylogeny. At the TEF1 α region, LOD clade had high support at 1.0 PP and 94.4 BS, (Supplementary Figure 3), but

did not include both *L. concolor* and *L. conjuncta*. Similar to the ITS and LSU phylogenies, the concatenated phylogeny showed all *Lophodermella* species, except *L. conjuncta*, that were sampled in this study, as well as *L. dooksii*, belonged to a well-supported clade with 0.99 PP and 75.5 BS support values (Figure 2.2). Distance matrix is shown in Supplementary Table 3.

Morphology and Phylogeny of Lophodermella on P. flexilis

Based on the phylogenetic analyses, two separate *Lophodermella* species were collected from *P. flexilis* in the Rocky Mountain Region. Using the concatenated dataset, *L. arcuata* from Rocky Mountain National Park (RMNP_LU1 and RMNP_LU16) clustered with *L. arcuata* AY465518.1 from NCBI GenBank with 1.0 PP and 100 BS, whereas RMNP_01 clustered with *Lophophacidium dooksii* samples with 0.98 PP (Figure 2.2). Similarly, RMNP_01 and *L. dooksii* (MB5) were found into a cluster with 0.98 PP and 89.9 BS, and 0.96 PP and 71.2 BS at the ITS (Supplementary Figure 1) and TEF1 α (Supplementary Figure 3) trees respectively, indicating that RMNP_01 may represent a new species, distinct from *L. arcuata*. Morphologically, sample RMNP_01 had subhypodermal hysterothecia measuring 0.48 – 0.6 × 0.16 – 0.168 mm and were tanned at mesophyll and hypodermis. Asci were broadly saccate measuring 96 – 130 × 12 – 14 μ m. Ascospores were clavate, measuring 58 – 76 μ m long and 3.8 – 4 μ m wide. Ascospores were also covered with mucilaginous sheath (10 μ m wide, Figure 2.3). These fit the morphometric traits of *L. arcuata* (Table 2.2). Further, both *Lophodermella* sp. and *L. arcuata* were found on *P. flexilis* in similar geographic location.

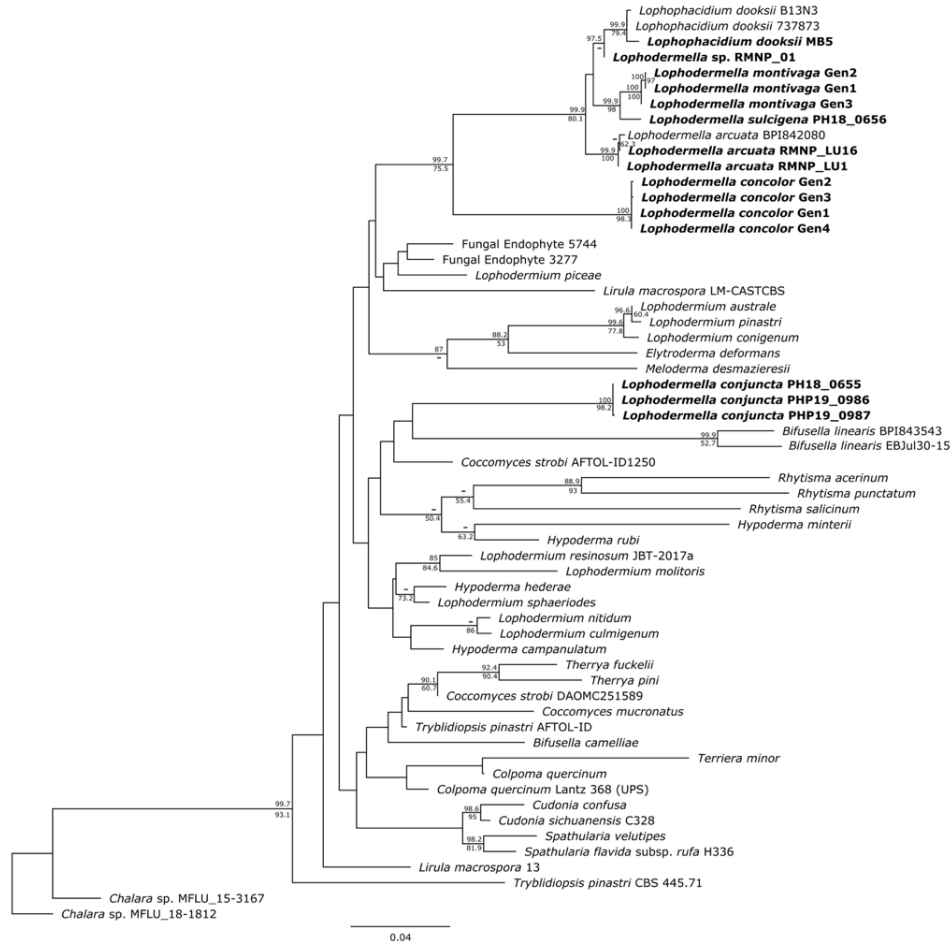


Figure 2.2. Maximum likelihood phylogeny depicting phylogenetic relationships of *Lophodermella* species within Rhytismataceae based on three gene regions including the internal transcribed spacer (ITS), large ribosomal subunit (LSU) and translation elongation factor 1-alpha ($TEF1\alpha$). Bayesian posterior probabilities (PP) greater than 0.80 and bootstrap (BS) support values from maximum likelihood analysis greater than 50 are shown above and below node, respectively. Species in bold are samples derived from this study. Numbers correspond to genotypes after concatenation.

Shared Characteristics of Lophodermella Clade

Five traits were used in this study due to the unavailability of morphological data or unclear morphological distinctions of other species within Rhytismataceae (Table 2.3, Supplementary Table 4). The first four morphological characteristics included were those described by Darker (1967) as key characteristics of species within *Lophodermella*. These included ascomata shape and

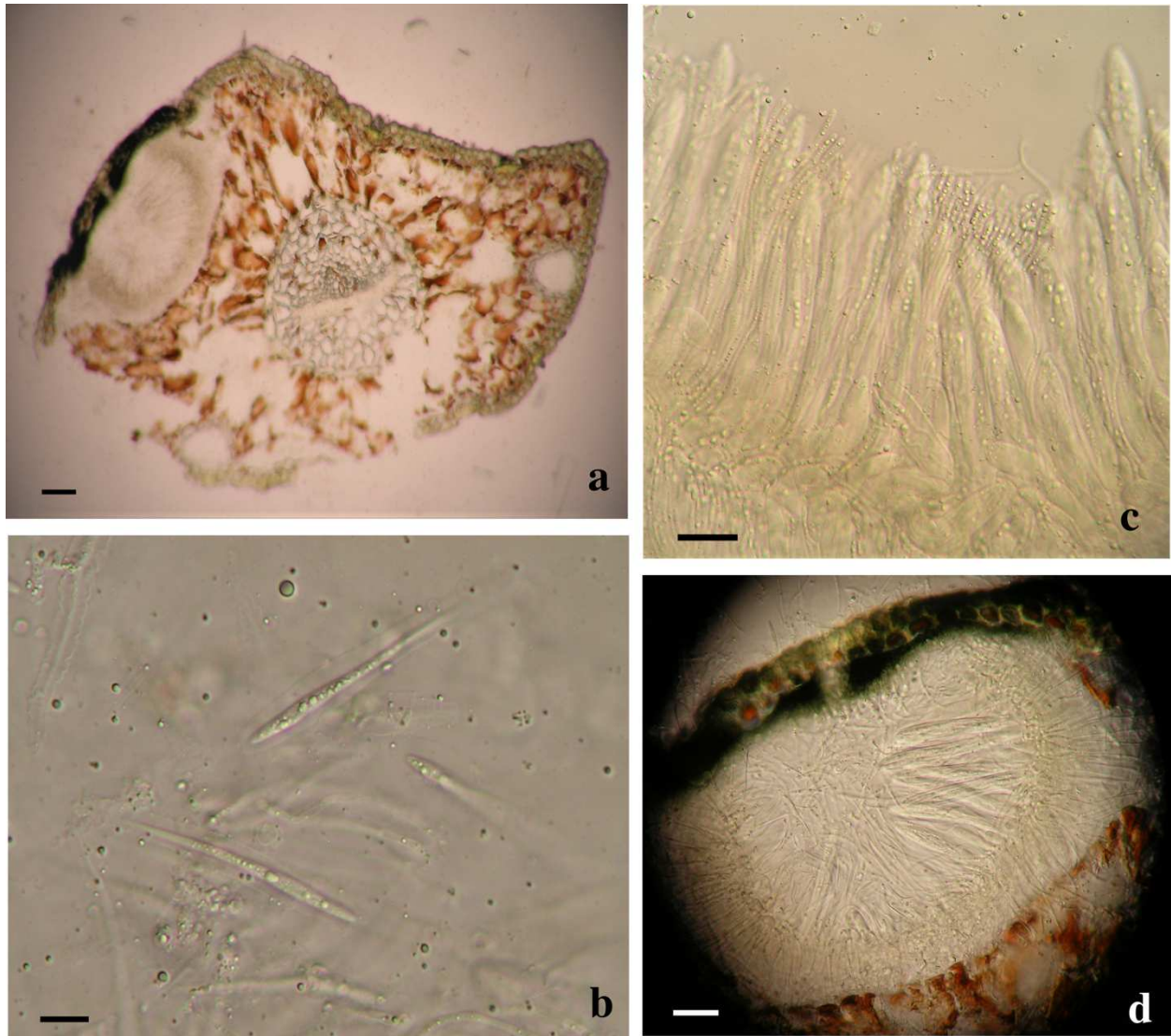


Figure 2.3. Morphological characters of *Lophodermella* sp. on *Pinus flexilis* collected from Rocky Mountain National Park, Colorado, USA. Subhypodermal hysterothecia with tanned mesophyll and hypodermis (a, d), clavate ascospores with gelatinous sheath (b) and broadly saccate asci (c). Size bars a, c and d 20 μ m; b 10 μ m.

position, asci shape and ascospore shape. Host was included as an ecological trait. The only character conserved within the LOD clade composed of the five *Lophodermella* species and *L. dooksii* was subhypodermal ascomata position in a median transverse section (Figure 2.4). All of the *Lophodermella* species sampled in this study occur on pine hosts. The shape of ascomata or

hysterothecia, asci and ascospores differed within the LOD clade. *Lophodermella* hysterothecia were mostly elliptical and elongated while hysterothecia of *Lophophacidium dooksii* were linear. *Lophodermella* had clavate ascospores while ascospores of *L. dooksii* were fusiform to oval. All species in the clade, except *L. concolor*, had broadly saccate to clavate asci. To measure homoplasy and fit of characters, individual consistency (CI) and retention indices (RI) were measured. While all morphological characters obtained an $RI \geq 0.50$, only ascomata position and ascospore shape had $CI \geq 0.50$, which may imply synapomorphy of the two characters (Figure 2.4).

Table 2.3. Character and character states used for phylogenetic reconstructions of *Lophodermella* species.

<i>A. Characters to assess genus delineation</i>		
No.	Character	Character States
1	Ascomata: Shape	0 non-linear or -elliptical, 1 mostly linear, nervisequious, dark brown to black, 2 mostly elliptical to elongate, concolorous to black
2	Ascomata: Position on substrate/host tissue (median transverse section)	0 external/superficial, 1 subcuticular, 2 intraepidermal, 3 subepidermal, 4 subhypodermal
3	Asci: Shape	0 more or less broadly saccate to clavate, 1 narrowly clavate or cylindrical
4	Ascospores: Shape	0 acicular, 1 filiform, 2 clavate, 3 cylindrical, 4 fusiform to oval, 5 rod-shaped, 6 double spindle-shaped, 7 ellipsoid to fusoid
5	Ecological character: Host	0 non-pine, 1 pine
<i>B. Characters to assess species delineation</i>		
1	Ascomata: length	0 hysterothecia ≥ 1 mm, 1 hysterothecia short
2	Ascomata: color	0 brown, 1 concolorous
3	Ascomata: fusion	0 not fused, 1 fused
4	Ascospores: shape, size	0 short (23-60 μ m) clavate, 1 elongate clavate (68-90 μ m), 2 fusiform to oval, 3 cylindrical, 4 ellipsoid to fusoid
5	Asci: number of spores	4 four-spored, 8 eight-spored
6	Host: number of pine needles	2 two-needle pine, 3 three-needle pine, 5 five-needle pine

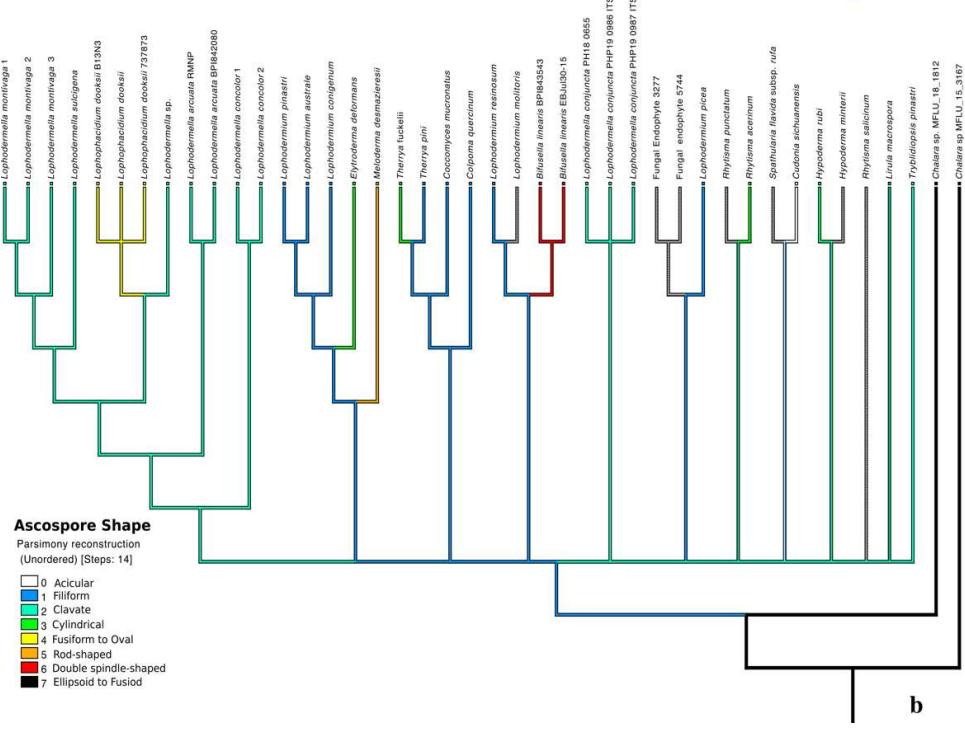
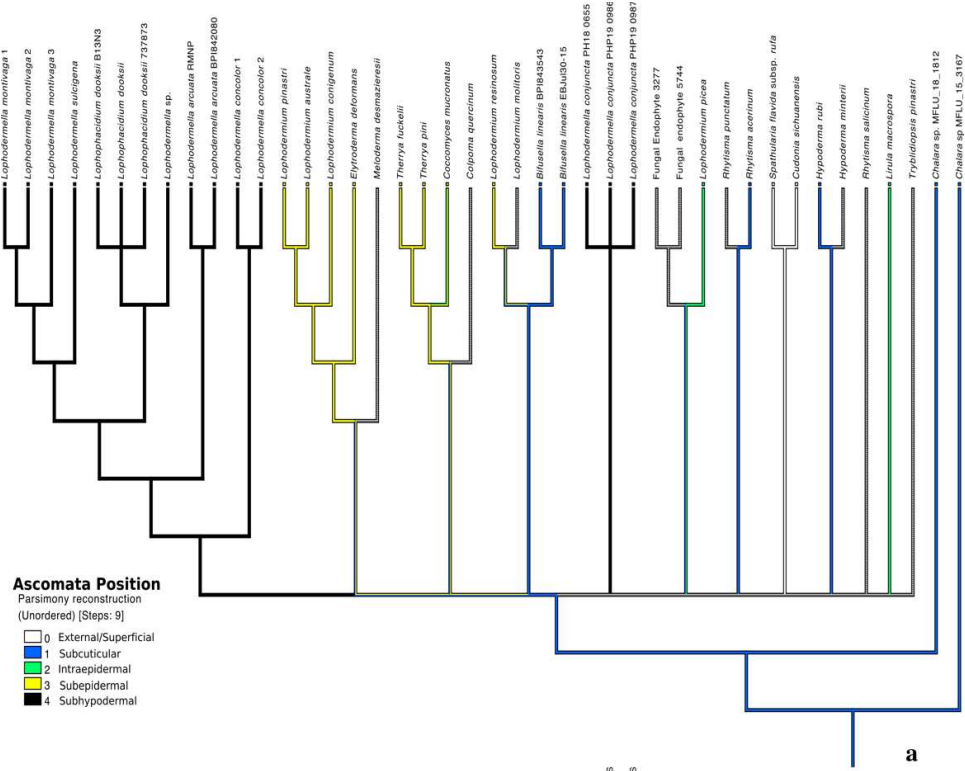


Figure 2.4. Morphological characters mapped onto Bayesian ITS phylogenetic tree with the parsimony ancestral reconstruction method using Mesquite v.3.6 with retention indices ≥ 0.50 , ascomata position (a) and ascospore shape (b).

Distinct characters were observed across *Lophodermella* species, which may be useful for species identification and delineation (Figure 2.5, Supplementary Table 5). Short and concolorous hysterothecia were distinct in *L. concolor* while elongated clavate ascospore and fused hysterothecia were distinct in *L. conjuncta*. The fusiform to oval ascospore was unique to *L. dooksi*. Meanwhile, *L. montivaga*, *Lophodermella* sp. (RMNP_01) and *L. sulcigena* only differed at their host occurrence. Hysterothecia of *L. arcuata* was reported to be concolorous when dry as opposed to that of *Lophodermella* sp. (RMNP_01) which remains dark brown. All of the six characters for species delineation generated a mean CI and RI of 0.95 and 0.92, respectively.

Discussion

This study revealed a well-supported clade consisting of several *Lophodermella* species including *L. montivaga*, *L. concolor*, *L. arcuata*, *L. sulcigena*, and *Lophodermella* sp. within Rhytismataceae. *Lophodermella conjuncta*, however, was consistently placed outside of this clade. In all phylogenies, *Lophophacidium dooksii* consistently clustered within the LOD clade. Despite highly similar morphological characteristics, this study showed that *Lophodermella* pathogens are molecularly distinct from each other and may represent more genetic diversity than previously thought. This study also identified shared characteristics within the LOD clade and explored on morphological characters that could be useful in taxon classification.

Molecular and Phylogenetic Analyses of Lophodermella

A concatenated dataset of the three loci clearly separated *L. montivaga* and *L. concolor* that both infect *P. contorta* and distinguished the *Lophodermella* species from other closely related fungi. *Lophodermella montivaga*, *L. concolor*, *L. arcuata*, *L. sulcigena*, *Lophodermella* sp. and *Lophophacidium dooksii* formed the LOD clade, which were distinct from species within the genera *Lophodermium* (Ortiz-García et al., 2003) and *Spathularia-Cudonia* (Ge et al., 2014).

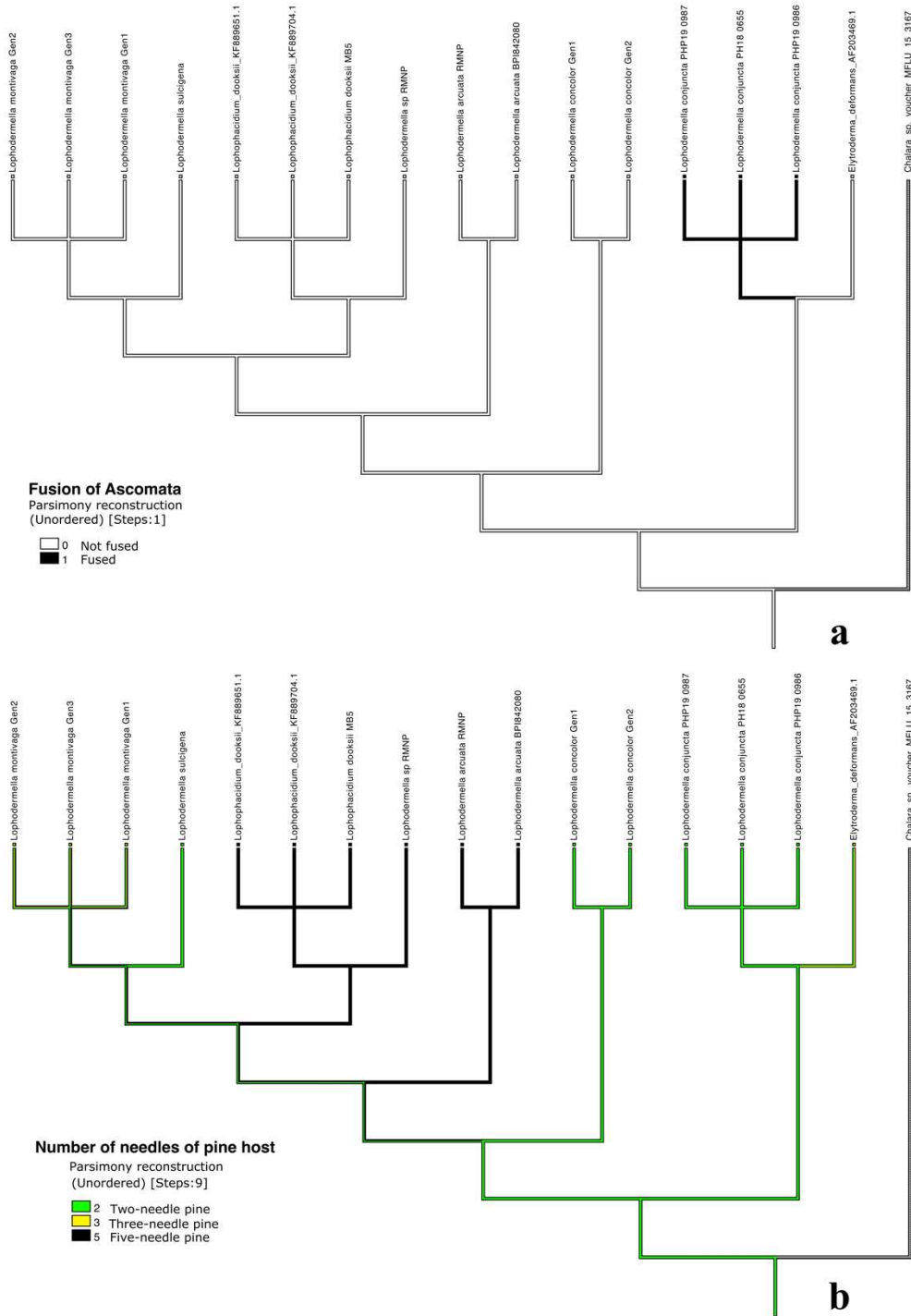


Figure 2.5. Morphological characters mapped onto Bayesian ITS phylogenetic tree with the parsimony ancestral reconstruction method using Mesquite v.3.6, fusion of ascomata (a) and number of needles of pine host (b).

However, in the TEF1 α phylogeny, *L. concolor* was excluded from the LOD clade, but was placed in the clade at the LSU and ITS phylogenies. This could be attributed to a fewer number of sequenced Rhytismataceae species resulting in low phylogenetic resolution or other genetic loci may best represent the species phylogeny. While additional sequences at each locus would likely improve phylogenetic resolution, whole-genome sequencing would provide greater advantage in phylogenetic reconstruction as well as gain deeper evolutionary perspectives on rhytismataceous needle pathogens.

Exclusion of *L. conjuncta* in the LOD clade may suggest polyphyly of the genus. This is the first report of the potential polyphyly of *Lophodermella* within Rhytismataceae. Polyphyletic genera are commonly observed within Rhytismatales partly due to the use of distinctive yet non-synapomorphic characters for generic-level classification (Lantz et al., 2011). *Lophodermium* is an example of a polyphyletic genus that appears in the radiate, bilateral and *Picea*-associated clades (2011). Reorganization of *Lophodermium* was not possible due to the wide diversity of species in the group (Darker, 1967). Monophyletic genera also exist within Rhytismataceae that includes *Cudonia* and *Terriera* (Lantz et al., 2011). However, this present study does not disregard potential changes in the phylogenetic arrangement and polyphyly as more *Lophodermella* species will be genetically investigated. Increased sampling of species within the two genera provided further evidence of *Cudonia* as a monophyletic genus but suggested that *Spathularia* was polyphyletic (Ge et al., 2014). It may also be possible that *L. conjuncta* belong to a separate genus that shares close morphological and phylogenetic relationship with *Lophodermella*. Thus, further investigation of other *Lophodermella* species which so far have no available sequence data still needs to be conducted to confirm these phylogenetic arrangements.

The present study supported a close relationship of *L. montivaga* and *L. sulcigena* compared to the other species within the LOD clade. Darker (1932) speculated that *L. sulcigena* from Europe may be identical to *L. montivaga* due to morphological similarities. Despite the overlapping morphological distinctions between the two species, this present study provided molecular evidence that *L. montivaga* and *L. sulcigena* are two distinct species. Another previous speculation was the possibility that *L. arcuata* is a variety of either *L. montivaga* or *L. sulcigena* owing to its resemblance to both species and its limited occurrence (Darker, 1932). However, symptom and ascocarp development in both species were different and thus were maintained as two different species (Millar, 1984). Genetic evidence gave support that *L. arcuata* is distinct from *L. sulcigena* and *L. montivaga*.

Consistent nesting of *Lophophacidium dooksii* in a *Lophodermella* clade was observed in all phylogenies, which concurs with a previous molecular study (Laflamme et al., 2015). Results herein showed that *L. dooksii* is more closely related to *Lophodermella* sp. (from *P. flexilis*) than to *L. montivaga* and *L. arcuata*, and provides more evidence for the transfer of the species from Phacidiaceae to Rhytismataceae as proposed by Ekanayaka (2019). We did not attempt to reclassify the taxon to *Lophodermella* since we did not have large sample size and type specimen to conduct further validations. Interestingly, *L. dooksii* was synonymous to *Canavirgella banfieldii*, a species classified under Rhytismataceae, but the former taxonomic name was given priority due to its earlier publication (Laflamme et al., 2015). In other studies, use of multiple loci supported the placement of *Cudonia* and *Spathularia* from Geoglossaceae to Rhytismataceae (Ge et al., 2014; Gernandt et al., 2001; Lantz et al., 2011), which these results also support (Supplementary Figures 1-3).

Phylogeny of Lophodermella sp. from P. flexilis

Individual phylogenies in this study could not confirm the species identity of the *Lophodermella* sp. from *P. flexilis* collected at RMNP as it did not cluster together with *L. arcuata* samples. Aside from morphometric features, initial examination identified RMNP_01 sample as *L. arcuata* due to its occurrence on *P. flexilis* in Colorado. Minter & Millar (1993a) considered host preference and geographic distribution as criteria for identification of *L. arcuata* due to the consistent reports on this species being the only member of the genus occurring on five-needle pines in North America. However, genetic data suggests *Lophodermella* sp. may represent a separate species distinct from *L. arcuata*. Since needle samples with this potentially new species were only collected from one tree, we did not attempt to formally name the species but temporarily named at the genus level as *Lophodermella*. Further investigation needs to be conducted to differentiate this species with other *Lophodermella* species described in literature and to define the population diversity of *L. arcuata*. Further, results from this study also suggest that undescribed cryptic *Lophodermella* species exist on pine hosts.

Morphological and Lifestyle Traits of the Lophodermella Clade

Classification of Rhytismataceae genera has been challenged by the limited morphological features for characterization. Darker (1967) revised the genera within the previous Hypodermataceae based on the characteristics of their ascomata or hysterothecia, asci, and pycnidia or a combination of these characters. Spore shape, septation and color were secondary characters to delimit the genera (Darker, 1967). Further, Lantz et al. (2011) described ascomata and spores as unreliable characters for genus delimitation in Rhytismatales but found that a combination with other traits was potentially useful. This study showed that, at the genus level, subhypodermal ascomata and ascospore shape may be used as diagnostic characters for

delimitation of genus *Lophodermella*. This is congruent to the dichotomous key produced by Darker (1967) to delimit this genus. Despite its inclusion in the LOD clade, *Lophophacidium dooksii* did not have clavate ascospores but rather had ascospores with fusiform to oval shape. Interestingly, aside from subhypodermal hysterothecia, all species within the LOD clade produced a tanned hypodermis. Furthermore, despite low consistency, the strong retention of asci shape may also suggest its role in taxa distinction.

Within *Lophodermella* genus, morphometric traits such as size of ascospores and hysterothecia are still used as distinctive characters. This study showed that a combination of morphological and ecological characters may be used to distinguish *Lophodermella* species, particularly ascospore and hysterothecia length, hysterothecia color, and the number of needles on pine host. However, these characters may also become problematic in practice. For example, while ascospore size was identified as a reliable criterion, measurements of spores varied depending on the freshness of specimen and thus cannot easily be used for identification of *Lophodermella* species (Millar, 1984). Further, concolorous hysterothecia as key character may be misleading as some species can also produce conspicuous hysterothecia (Millar, 1984).

Difficulty in obtaining pure cultures of *L. montivaga*, *L. concolor* and *L. dooksii* can also potentially limit further characterization of other traits such as physiology and pathogenicity. Similar to other studies, we were not able to grow in culture the *Lophodermella* species sampled in this study, suggesting an obligate lifestyle. Use of agar cultures including pine extract agar did not yield successful cultures of *Lophodermella* (Millar, 1984). Some studies also described *L. dooksii* and *Bifusella linearis* as obligate fungal pathogens after unsuccessful attempts of obtaining cultures or only obtaining short-lived cultures (Broders et al., 2015; Merrill et al., 1996). In contrast, previous studies were able to isolate pure cultures of *L. sulcigena* on malt agar (Jalkanen,

1985; Kowalski & Krygier, 1996). Similarly, a number of studies documented several *Lophodermium* species (e.g., Deckert et al., 2001; Wilson et al., 1994) growing in 2% malt extract agar. *Elytroderma deformans* needed an acidic pine decoction agar substrate or an addition of pine needle extracts to significantly grow in culture (Laurent, 1962; Legge, 1967). Consequently, while environmental DNA may be available, the absence of pure cultures of many *Lophodermella* species limit further molecular research that require a high pure DNA concentration.

Most *Lophodermella* species appear to be either specific to a single host species distributed in a certain geographic region (i.e., *L. maureri* on *P. ayacahuite* in Mexico and *L. orientalis* on *P. kesiya* in Asia) or to a group of host species within a *Pinus* classification with similar number of needles (i.e., *L. sulcigena* and *L. conjuncta* on two-needle pines of subsection *Pinus* in Europe, and *L. concolor* on two-needle pines of subgenus *Pinus* in western North America; Gernandt et al., 2005; Millar, 1984). Furthermore, *L. arcuata* and *L. maureri* are the only two *Lophodermella* species on five-needle pines of subsection *Strobus* while *L. morbida* only occurs exclusively on three-needle pines under section *Trifoliae*. In contrast, *L. cerina* was reported to have a broader host range occurring on two- to three-needle *Pinus* species in sections *Trifoliae* and *Pinus* (subgenus *Pinus*; Gernandt et al., 2005; Millar, 1984). *Lophodermella montivaga* was also documented on two- to five-needle *Haploxyton* and *Diploxyton* pines. In this study, genetic information was used to verify the association of *Lophodermella* species with a known host. It allowed us to identify additional species on *P. flexilis* that would have otherwise been classified as *L. arcuata* based on its morphology and host association. Thus, it can serve as a tool to assess the extent of these fungal species across different hosts in different geographic regions.

References

- Barker, F. K., & Lutzoni, F. M. (2002). The Utility of the Incongruence Length Difference Test. *Systematic Biology*, 51(4), 625–637. <https://doi.org/10.1080/10635150290102302>
- Barnes, I., Wingfield, M. J., Carbone, I., Kirisits, T., & Wingfield, B. D. (2014). Population structure and diversity of an invasive pine needle pathogen reflects anthropogenic activity. *Ecology and Evolution*, 4(18), 3642–3661. <https://doi.org/10.1002/ece3.1200>
- Beenken, L. (2019). Lophodermella-Nadelschütte. In *Queloz V, Forster B, Beenken L, Stroheker S, Odermatt O, Hölling D, Meyer JB, Dubach V. Waldschutzüberblick 2018* (Vol. 79, pp. 1–33). <https://www.wsl.ch/de/publikationen/waldschutzueberblick-2018.html>
- Brodde, L., Adamson, K., Julio Camarero, J., Castaño, C., Drenkhan, R., Lehtijärvi, A., Luchi, N., Migliorini, D., Sánchez-Miranda, Á., Stenlid, J., Özdağ, Ş., & Oliva, J. (2019). Diplodia Tip Blight on Its Way to the North: Drivers of Disease Emergence in Northern Europe. *Frontiers in Plant Science*, 9, 1818. <https://doi.org/10.3389/fpls.2018.01818>
- Broders, K., Munck, I., Wyka, S., Iriarte, G., & Beaudoin, E. (2015). Characterization of Fungal Pathogens Associated with White Pine Needle Damage (WPND) in Northeastern North America. *Forests*, 6(12), 4088–4104. <https://doi.org/10.3390/f6114088>
- Corlett, M., & Shoemaker, R. A. (1984). Lophophacidium dooksii n.sp., a phacidiaceous fungus on needles of white pine. *Canadian Journal of Botany*, 62, 1836–1840.
- Cubero, O. F., Crespo, A., Fatehi, J., & Bridge, P. D. (1999). DNA extraction and PCR amplification method suitable for fresh, herbarium-stored, lichenized, and other fungi. *Plant Systematics and Evolution*, 216(3–4), 243–249. <https://doi.org/10.1007/BF01084401>

- Czabator, F. J., Staley, J. M., & Snow, G. A. (1971). Extensive southern pine needle blight during 1970-1971, and associated fungi. *Plant Disease Reporter*, 55, 764–766.
- Darker, G. (1932). *The Hypodermataceae of Conifers* (Vol. 1). Contributions from the Arnold Arboretum of Harvard University.
- Darker, G. (1967). A revision of the genera of the Hypodermataceae. *Canadian Journal of Botany*, 45, 1399–1444.
- Deckert, R. J., Melville, L. H., & Peterson, R. L. (2001). Structural features of a Lophodermium endophyte during the cryptic life-cycle phase in the foliage of *Pinus strobus*. *Mycological Research*, 105(8), 991–997.
- Edgar, R. C. (2004). MUSCLE: Multiple sequence alignment with high accuracy and high throughput. *Nucleic Acids Research*, 32(5), 1792–1797.
<https://doi.org/10.1093/nar/gkh340>
- Ekanayaka, A. (2019). Preliminary classification of Leotiomycetes. *Mycosphere*, 10(1), 310–489. <https://doi.org/10.5943/mycosphere/10/1/7>
- Fungi of Great Britain and Ireland*. (2019). <https://fungi.myspecies.info>
- Ge, Z.-W., Yang, Z. L., Pfister, D. H., Carbone, M., Bau, T., & Smith, M. E. (2014). Multigene Molecular Phylogeny and Biogeographic Diversification of the Earth Tongue Fungi in the Genera *Cudonia* and *Spathularia* (Rhytismatales, Ascomycota). *PLoS ONE*, 9(8), e103457. <https://doi.org/10.1371/journal.pone.0103457>
- Gernandt, D. S., Gaeda López, G., Ortiz García, S., & Liston, A. (2005). Phylogeny and Classification of *Pinus*. *Taxon*, 54(1), 29–42.
- Gernandt, D. S., Platt, J. L., Stone, J. K., Spatafora, J. W., Holst-Jensen, A., Hamelin, R. C., & Kohn, L. M. (2001). Phylogenetics of Helotiales and Rhytismatales Based on Partial

- Small Subunit Nuclear Ribosomal DNA Sequences. *Mycologia*, 93(5), 915.
<https://doi.org/10.2307/3761757>
- Gray, L. K., Russell, J. H., Yanchuk, A. D., & Hawkins, B. J. (2013). Predicting the risk of cedar leaf blight (*Didymascella thujina*) in British Columbia under future climate change. *Agricultural and Forest Meteorology*, 180, 152–163.
<https://doi.org/10.1016/j.agrformet.2013.04.023>
- Guindon, S., Dufayard, J.-F., Lefort, V., Anisimova, M., Hordijk, W., & Gascuel, O. (2010). New Algorithms and Methods to Estimate Maximum-Likelihood Phylogenies: Assessing the Performance of PhyML 3.0. *Systematic Biology*, 59(3), 307–321.
<https://doi.org/10.1093/sysbio/syq010>
- Huelsenbeck, J. P., & Ronquist, F. (2001). MRBAYES: Bayesian inference of phylogenetic trees. *Bioinformatics*, 17(8), 754–755. <https://doi.org/10.1093/bioinformatics/17.8.754>
- Hunt, R. S., & Ziller, W. G. (1978). Host-genus keys to the Hypodermataceae of conifer leaves. *Mycotaxon*, 6(3), 481–496.
- Jalkanen, R. (1985). The occurrence and importance of *Lophodermella sulcigena* and *Hendersonia acicola* on Scots pine in Finland. *Karstenia*, 25(2), 53–61.
<https://doi.org/10.29203/ka.1985.237>
- Kowalski, T., & Krygier, J. (1996). *Mycological study on symptomless and diseased needles in pine stand attacked by Lophodermella sulcigena (Rostr.) V. Höhn. 11*, 159–168.
- Laflamme, G., Broders, K., Côté, C., Munck, I., Iriarte, G., & Innes, L. (2015). Priority of *Lophophacidium* over *Canavirgella*: Taxonomic status of *Lophophacidium dooksii* and *Canavirgella banfieldii*, causal agents of a white pine needle disease. *Mycologia*, 107(4), 745–753. <https://doi.org/10.3852/14-096>

- Lantz, H., Johnston, P. R., Park, D., & Minter, D. W. (2011). Molecular phylogeny reveals a core clade of Rhytismatales. *Mycologia*, *103*(1), 57–74. <https://doi.org/10.3852/10-060>
- Laurent, T. H. (1962). *Studies of the developmental morphology and life history of Elytroderma deformans* [Master of Science, University of Montana].
<https://scholarworks.umt.edu/etd/6778>
- Lee, E. H., Beedlow, P. A., Waschmann, R. S., Tingey, D. T., Cline, S., Bollman, M., Wickham, C., & Carlile, C. (2017). Regional patterns of increasing Swiss needle cast impacts on Douglas-fir growth with warming temperatures. *Ecology and Evolution*, *7*(24), 11167–11196. <https://doi.org/10.1002/ece3.3573>
- Legge, T. W. (1967). *Partial characterization of Elytroderma deformans* [Master of Science, University of Montana]. <https://scholarworks.umt.edu/etd/3181>
- Lotan, J. E., & Critchfield, W. B. (1990). *Pinus contorta* Dougl. Ex Loud. In *In: R.M. Burns and B.H. Honkala (technical coordinators). Silvics of North America. USDA Agriculture Handbook No. 654* (Vol. 1, pp. 302–315).
- Maddison, W. P., & Maddison, D. R. (2018). *Mesquite: A modular system for evolutionary analysis*. (Version 3.51) [Computer software]. <http://mesquiteproject.org>
- Merrill, W., Wenner, N. G., & Dreisbach, T. A. (1996). *Canavirgella banfieldii* gen. And sp. Nov.: A needle-cast fungus on pine. *Canadian Journal of Botany*, *74*, 1476–1481.
- Millar, C. S. (1984). *Lophodermella* species on pines. In: *Recent Research on Conifer Needle Diseases*. Eds. Glenn W. Peterson. USDA Forest Service, General Technical Report GTR-WO 50., 45–55.
- Millar, C. S., & Minter, D. W. (1966). *Lophodermella conjuncta*. *CMI Descriptions of Pathogenic Fungi and Bacteria*, *66*(658).

- Millar, C. S., & Minter, D. W. (1978). *Lophodermella sulcigena*. *CMI Descriptions of Pathogenic Fungi and Bacteria*, 57(562).
- Minter, D. W. (1988a). CMI Descriptions of Pathogenic Fungi and Bacteria no. 942. *Colpoma quercinum*. *Mycopathologia*, 102(1), 53–54.
- Minter, D. W. (1988b). CMI descriptions of pathogenic fungi and bacteria no. 945. *Lophodermella maureri*. *Mycopathologia*, 102(1), 59–60.
- Minter, D. W. (1993). IMI descriptions of fungi and bacteria no. 1148. *Lophodermella orientalis*. *Mycopathologia*, 121(1), 57–58.
- Minter, D. W., & Millar, C. S. (1993a). IMI Descriptions of Fungi and Bacteria. *Lophodermella arcuata*. *Mycopathologia*, 121(1), 49–50.
- Minter, D. W., & Millar, C. S. (1993b). IMI Descriptions of Fungi and Bacteria. *Lophodermella montivaga*. *Mycopathologia*, 121(1), 55–56.
- Minter, D. W., & Millar, C. S. (1993c). IMI Descriptions of Fungi and Bacteria. No. 1146. *Lophodermella concolor*. *Mycopathologia*, 121(1), 53–54.
- Ortiz-García, S., Gernandt, D. S., Stone, J. K., Johnston, P. R., Chapela, I. H., Salas-Lizana, R., & Alvarez-Buylla, E. R. (2003). Phylogenetics of *Lophodermium* from pine. *Mycologia*, 95(5), 846–859. <https://doi.org/10.1080/15572536.2004.11833044>
- Rehner, S. A. (2001). *EF1-alpha primers*. USDA, ARS, PSI Insect Biocontrol Laboratory. <http://www.aftol.org/pdfs/EF1primer.pdf>
- Robert, V., Stegehuis, G., & Stalpers, J. (2005). *The MycoBank engine and related databases*. <https://www.mycobank.org>

- Rodas, C. A., Wingfield, M. J., Granados, G. M., & Barnes, I. (2016). Dothistroma needle blight: An emerging epidemic caused by *Dothistroma septosporum* in Colombia. *Plant Pathology*, 65(1), 53–63. <https://doi.org/10.1111/ppa.12389>
- Rozas, J., Sanchez-DelBarrio, J. C., Messeguer, X., & Rozas, R. (2003). DnaSP, DNA polymorphism analyses by the coalescent and other methods. *Bioinformatics*, 19(18), 2496–2497. <https://doi.org/10.1093/bioinformatics/btg359>
- Schoettle, A. W. (2004). Ecological roles of five-needle pine in Colorado: Potential consequences of their loss. In *Breeding and genetic resources of five needle pines: Growth, adaptability and pest resistance*. Sniezko, R.A., Samman, S., Schlarbaum, S.E. and Howard, B. eds. IUFRO Working Party 2.02.15. Proceedings RMRS-P-32. (pp. 124–135). U.S. Department of Agriculture, Forest Service, Rocky Mountain Station.
- Tanney, J. B., & Seifert, K. A. (2017). *Lophodermium resinosum* sp. Nov. From red pine (*Pinus resinosa*) in Eastern Canada. *Botany*, 95(8), 773–784. <https://doi.org/10.1139/cjb-2017-0012>
- Vaidya, G., Lohman, D. J., & Meier, R. (2011). SequenceMatrix: Concatenation software for the fast assembly of multi-gene datasets with character set and codon information. *Cladistics*, 27(2), 171–180. <https://doi.org/10.1111/j.1096-0031.2010.00329.x>
- Vilgalys, R., & Hester, M. (1990). Rapid genetic identification and mapping of enzymatically amplified ribosomal DNA from several *Cryptococcus* species. *Journal of Bacteriology*, 172(8), 4238–4246. <https://doi.org/10.1128/jb.172.8.4238-4246.1990>
- Welsh, C., Lewis, K. J., & Woods, A. J. (2014). Regional outbreak dynamics of *Dothistroma* needle blight linked to weather patterns in British Columbia, Canada. *Canadian Journal of Forest Research*, 44(3), 212–219. <https://doi.org/10.1139/cjfr-2013-0387>

- White, T. J., Bruns, T., Lee, S., & Taylor, J. (1990). Amplification and direct sequencing of fungal ribosomal RNA genes for phylogenetics. In *PCR Protocols: A Guide to Methods and Applications*. Edited by: Innis MA, Gelfand DH, Sninsky JJ, White TJ (pp. 315–322). Academic Press Inc.
- Wilson, R., Wheatcroft, R., Miller, J. D., & Whitney, N. J. (1994). Genetic diversity among natural populations of endophytic *Lophodermium pinastri* from *Pinus resinosa*. *Mycological Research*, 98(7), 740–744. [https://doi.org/10.1016/S0953-7562\(09\)81047-2](https://doi.org/10.1016/S0953-7562(09)81047-2)
- Woods, A., Coates, K. D., & Hamann, A. (2005). Is an Unprecedented Dothistroma Needle Blight Epidemic Related to Climate Change? *BioScience*, 55(9), 761. [https://doi.org/10.1641/0006-3568\(2005\)055\[0761:IAUDNB\]2.0.CO;2](https://doi.org/10.1641/0006-3568(2005)055[0761:IAUDNB]2.0.CO;2)
- Woods, A. J. (2014). Warmer and wetter might not be better. *Journal of Forest Science*, 60(No. 11), 484–486. <https://doi.org/10.17221/18/2014-JFS>
- Worrall, J. J., Marchetti, S. B., & Mask, R. A. (2012). An Epidemic of Needle Cast on Lodgepole Pine in Colorado. In *Biological Evaluation R2-12-01* (p. 16). USDA Forest Service, Rocky Mountain Region, Forest Health Protection.
- Wyka, S. A., Munck, I. A., Brazee, N. J., & Broders, K. D. (2018). Response of eastern white pine and associated foliar, blister rust, canker and root rot pathogens to climate change. *Forest Ecology and Management*, 423, 18–26. <https://doi.org/10.1016/j.foreco.2018.03.011>
- Wyka, S. A., Smith, C., Munck, I. A., Rock, B. N., Ziniti, B. L., & Broders, K. (2017). Emergence of white pine needle damage in the northeastern United States is associated with changes in pathogen pressure in response to climate change. *Global Change Biology*, 23(1), 394–405. <https://doi.org/10.1111/gcb.13359>

CHAPTER 3: COMMUNITY AND TRANSCRIPTOME FOLIAR MYCOBIOTA TRANSITIONS IN RESPONSE TO PATHOGENIC CONIFER NEEDLE INTERACTIONS

Introduction

Endophytes are microorganisms that colonize plant tissues without causing symptoms and are known to play a vital role in plant health. The wide species diversity of endophytes has been associated with a suite of diverse, but often unknown or poorly understood, ecological functions (Rodriguez et al., 2009). In many host-endophyte interactions, their symbiosis with host plants provides beneficial effects on host plant fitness and survival amid stressors, particularly insects and pathogens (Terhonen et al., 2019). Directly or indirectly, effects against insects and pathogens occur through improving plant physiology, hyperparasitism, production of secondary metabolites, etc. (Gao et al., 2010; Jia et al., 2020). On the other hand, endophytes can also be harmful latent pathogens that remain dormant until favorable environmental conditions occur or when hosts become weakened when under stress (Sieber, 2007; Slippers & Wingfield, 2007). Some fungal endophytes can also increase disease severity by enabling pathogen infections (Busby et al., 2016; Ridout & Newcombe, 2018). These relationships, however, are only part of a complex continuum of host-endophyte interactions that have a significant impact on forest ecosystem health.

These diverse ecological roles of the microbiota can trigger different plant responses to microbial infection and invasion. While similar initial defense responses could be elicited by both pathogenic and non-pathogenic endophytes, some symbiotic microbes have sophisticated systems recognized by the host plant which result in the downregulation of defense genes (Brader et al., 2017). Similarly, in a direct fungal-host interaction, Peters et al. (1998) demonstrated that unlike for endophytes, plants recognize pathogens via overproduction of host defense enzymes. These

differing host responses by the host plant to pathogenic and endophytic fungal infections could likely indicate plant evolutionary adaptations that emerged through pathogenic interactions (Krings et al., 2007).

Profiling the mycobiota in a pathosystem and their interaction with the host plant can improve our understanding of disease development and suppression. Shifts in the microbial diversity (Koskella et al., 2017; Kovalchuk et al., 2018) and the gene expressions of the microbiome and host in healthy versus diseased plant systems elucidate the structural and functional changes that drive disease development (Hayden et al., 2018; Martí et al., 2020). This is particularly relevant as our view of disease development shifts from the classical “one-microbe-one disease” to a more complex nature that involves coinfection of a concert of microbial organisms interacting with their environment or a pathobiome (Feau & Hamelin, 2017; Koskella et al., 2017; Stewart et al., 2021). Conversely, disease suppressive activities of endophytic microbial consortia have been continuously explored to reduce disease impacts (Carrión et al., 2019).

Lophodermella concolor (Dearn.) Darker and *L. montivaga* Petrak of Rhytismataceae are potentially obligate pathogens causing needle cast on *Pinus contorta* (Darker, 1932), which is naturally distributed along the western region of northern America. Disease symptoms on infected hosts include needle discoloration and defoliation which could negatively impact growth when severe (Darker, 1932). Recently, two epidemics caused by these two pathogens were recorded in Colorado, USA (Worrall et al., 2012). Though found on the same host and in the same sites in Colorado, their ecological interaction on an individual host has not been well-documented. It has been reported that, among the infected sites, all but one had only a single pathogen occurrence based on hysterothecia development, which may be due to unknown ecological differences

between the two species (Worrall et al. 2012) or ecological competition prevailed by the most dominant and/or aggressive pathogen (Abdullah et al., 2017). Additionally, little information is known about the interaction between these pathogens and other fungal endophytes in *P. contorta*. However, invasion of other fungi was reported to inhibit ascocarp development (Millar, 1984).

This study aims to understand the interaction of *L. concolor* and *L. montivaga*, with the needle mycobiota in *P. contorta*. Using next generation sequencing, I specifically examined the fungal endophytic community composition and gene expression in asymptomatic and symptomatic needles of *P. contorta* trees infected with *Lophodermella* pathogens. I also explored the differences in plant responses at asymptomatic and symptomatic states. I hypothesized that no significant variations will be observed across asymptomatic needles, but that mycobiota abundance and gene expression will differ significantly between symptomatic and asymptomatic needles, and needles that are symptomatic of either *L. concolor* or *L. montivaga*. These differences will be driven by pathogenicity-related mechanisms distinctly employed by the pathogens, providing a competitive advantage over other fungal endophytes in causing disease. The results of this study support such hypotheses and integrate the interaction among the fungal community and plant host in the transition from healthy to diseased state.

Methodology

Sample Collection and Preparation

Second-year asymptomatic and symptomatic needles of *P. contorta* were randomly collected at breast height (approx. 1.37 m) from 60 trees infected with either *L. concolor* or *L. montivaga* from nine sites in Gunnison National Forest in June 2018 and 2019 (Table 3.1). Symptomatic needles were brown or discolored with hysterothecia of either *L. concolor* or *L.*

Table 3.1. Asymptomatic and symptomatic needle samples from *Pinus contorta* individual trees that were infected with *Lophodermella* needle cast pathogens in various sites in Gunnison National Forest, Colorado, USA. Asterisk (*) indicates the 10 samples that have next generation RNA sequences. Cross (†) and double cross (††) indicate samples excluded from the metabarcoding or metatranscriptome analysis.

Site	Location	Tree	<i>Lophodermella concolor</i>		Tree	<i>Lophodermella montivaga</i>	
			Asymptomatic	Symptomatic		Asymptomatic	Symptomatic
Cold Spring Campground	N 38°46.059' W 106°38.665'	1	CS01-19CN†	CS01-19CP		---	---
		2	CS02-19CN	CS02-19CP		---	---
		3	CS02-18CN*	CS02-18CP*		---	---
Lakeview Campground	N 38°49.022' W 106°34.796'	1	LV01-19CN	LV01-19CP	1	LV02-18MN*	LV02-18MP*
		2	LV03-19CN	LV03-19CP	2	LV03-18MN*	LV03-18MP
		3	LV05-19CN	LV05-19CP		---	---
Lodgepole Campground	N 38°45.733' W 106°39.714'	1	LP01-19CN	LP01-19CP		---	---
		2	LP02-19CN	LP02-19CP		---	---
		3	LP04-19CN	LP04-19CP		---	---
		4	LP05-19CN	LP05-19CP		---	---
		5	LP06-19CN	LP06-19CP		---	---
Marshall Pass	N 38°23.289' W 106°14.5'	1	MP01-19CN	MP01-19CP		---	---
		2	MP02-19CN	MP02-19CP		---	---
		3	MP03-19CN	MP03-19CP		---	---
North Cumberland	N 38°23.289' W 106°14.5'	1	NC02-19CN	NC02-19CP	1	NC01-19MN†	NC01-19MP
		2	NC03-19CN	NC03-19CP	2	NC04-18MN	NC04-18MP††
		3	NC04-19CN	NC04-19CP	3	NC07-19MN	NC07-19MP
		4	NC11-19CN	NC11-19CP	4	NC11-19MN	NC11-19MP
		5	NC13-19CN	NC13-19CP	5	NC13-19MN	NC13-19MP
			---	---	6	NC15-19MN	NC15-19MP
Oh Be Joyful	N 38°54.840'	1	OBJ01-19CN	OBJ01-19CP	1	OBJ09-18MN	OBJ09-18MP
		2	OBJ09-18CN	OBJ09-18CP	2	OBJ12-19MN	OBJ12-19MP

	W 107°01.963'	3	OBJ10-19CN	OBJ10-19CP		---	---
Pitkin	N 38°37.850' W 106°28.314'	1	PT01-19CN	PT01-19CP	1	PT02-19MN	PT02-19MP
		2	PT07-19CN	PT07-19CP	2	PT08-18MN	PT08-18MP
		3	PT08-19CN	PT08-19CP		---	---
		4	PT10-19CN	PT10-19CP		---	---
		5	PT11-19CN	PT11-19CP		---	---
		6	PT13-19CN	PT13-19CP		---	---
		7	PT15-19CN	PT15-19CP		---	---
Slate River	N 38°54.186' W 107°01.065'	1	SR01-19CN	SR01-19CP	1	SR09-18MN*	SR09-18MP*
		2	SR04-19CN	SR04-19CP	2	SR1X-19MN	SR1X-19MP
		3	SR05-19CN	SR05-19CP		---	---
		4	SR10-19CN	SR10-19CP*		---	---
Tincup	N 38°45.053' W 106°28.245'	1	TC01-19CN*	TC01-19CP	1	TC01-19MN	TC01-19MP
		2	TC02-19CN	TC02-19CP	2	TC03-19MN	TC03-19MP
		3	TC03-19CN	TC03-19CP	3	TC09-18MN	TC09-18MP
		4	TC04-19CN	TC04-19CP		---	---
		5	TC05-19CN	TC05-19CP		---	---
		6	TC07-19CN	TC07-19CP		---	---
		7	TC08-19CN	TC08-19CP		---	---
		8	TC09-19CN	TC09-19CP		---	---
		9	TC10-19CN	TC10-19CP		---	---
		10	TC11-19CN	TC11-19CP		---	---

montivaga, while asymptomatic needles were green. From each tree, two to three needles from different fascicles were pooled together as either symptomatic (n=60) or asymptomatic (n=60) needle samples. To remove superficial contamination, needles were washed with 0.2% Tween solution and vortexed at minimum speed for 10 mins. Samples were then rinsed in 70% ethanol for one min and dried before storing in -20°C (Prihatini et al., 2015; Rajala et al., 2013).

To evaluate the effectiveness of removing contamination, a modified method from Rajala et al. (2013) was used where three symptomatic and three asymptomatic samples were placed in distilled water and vortexed at minimum speed for 10 mins. Four microliters of the rinse solution then served as template for PCR amplification. DNA was amplified using primers ITS1 and ITS4 (White et al., 1990) following methods by Ata et al. (2021). Amplification was observed in symptomatic needles but not in asymptomatic needle samples. Amplification in symptomatic needles was expected since many *L. concolor* and *L. montivaga* hysterothecia were mature by the time of collection and thus spores were likely easily dispersed in water during vortexing.

Metabarcoding and Metatranscriptome Sequencing

DNA and RNA were extracted from asymptomatic and symptomatic needles combined per tree using a combination of methods by Zeng et al. (2018) and Cubero et al. (1999) (Supplementary File 1). DNA from 60 asymptomatic and 60 symptomatic needle samples were sent to the Genomics Center of the University of Minnesota, Minneapolis, Minnesota, USA for ITS sequencing. Fungal communities were determined by sequencing the ITS2 region [ITS3: (GCATCGATGAAGAACGCAGC) and ITS4: (TCCTCCGCTTATTGATATGC)] and reads were generated using Illumina MiSeq. Selected RNA samples from 5 asymptomatic and 5 symptomatic needle samples were sent to Novogene Corporation, Inc. for library preparation and sequencing (Table 1). Oligo (dT) beads and Ribo-Zero kit were used to enrich eukaryotic mRNA

and remove rRNA, respectively. Raw reads from ITS and RNA sequencing were deposited to NCBI SRA database (BioProject ID Number PRJNA753461).

Metabarcoding Analysis

Quality of ITS reads were assessed using FastQC (v0.11.9; Andrews, 2010). Samples with ≤ 581 reads (NC01-19MN and CS01-19CN) were excluded from the subsequent analyses. Reads were trimmed using Trimmomatic (v. 0.36; Bolger et al., 2014) to retain only those with minimum length of 150 bp, and a threshold of 15 for end bases and average quality within a 5-base window. Further sequence processing was conducted using Mothur (v.1.40.5; Schloss et al., 2009) following the MiSeq standard operating procedure (accessed 04/2020) as well as protocols developed by Kozich et al. (2013). Contigs with a length ≥ 426 bp, and those containing ambiguous bases and homopolymers ≥ 8 bp were discarded. Sequences associated with chloroplast, mitochondria, archaea, and bacteria lineages were removed from the table of classified sequences. UCHIME (Edgar et al., 2011) was used to *de novo* identify and remove chimeric sequences. USEARCH, utilizing the dgc (distance-based greedy clustering) option, was used for clustering. Groups that were at least 97% similar were classified to belong to the same operational taxonomic unit (OTU). Sequences were assigned to their taxonomic units using Wang's Naïve Bayes classifier with a cutoff value of 80 (Wang et al., 2007) and utilizing Mothur UNITE+INSD dataset (v.04022020, Abarenkov et al., 2020) with additional *Lophodermella* ITS dataset.

The statistical program R (v3.5.0), with the *vegan* package (Oksanen et al., 2020) and software packages *metagenomeseq* (Paulson et al., 2013) and *phyloseq* (McMurdie & Holmes, 2013), were used to analyze the data from Mothur. OTUs with low number of counts (≤ 10) were first removed to decrease error rate. Sequence depth and rarefaction curves were then obtained, using *vegan*, to assess whether the depth of sequences was sufficient to provide reasonable

evaluation of the fungal diversity within samples. After merging OTUs that were similar at certain taxonomic ranks using the *phyloseq* package, the distribution of taxa with at least 1% proportion across treatments was assessed through bar plots.

To analyze the significance of the interaction between treatments on the alpha and beta diversity, only those samples in sites that have both *L. concolor* and *L. montivaga* were considered in the succeeding statistical analyses (Table 3.1). Alpha diversity measures (Shannon and inverse Simpson indices) were generated using the *estimate_richness* function in *phyloseq*. Rarified richness was obtained through *vegan*. Linear models were fitted for richness, and Shannon and inverse Simpson diversity indices. Inverse Simpson diversity index was log-transformed to fit model assumptions. The interaction between pathogen species (*L. concolor* and *L. montivaga*) and disease symptoms (asymptomatic and symptomatic) was included as a variable alongside site as covariate. The *lm* and *Anova* functions from the *car* package (Fox & Weisberg, 2019) were used to fit the model. The *emmeans* function from the *emmeans* package (Lenth et al., 2020) was used to perform pairwise comparisons.

To analyze differences in beta diversity, Principal Coordinates Analysis (PCoA) was performed using the *vegan* package where dissimilarity was calculated using Bray-Curtis distance. A constant was added using the Legendre and Anderson (1999) method to correct for negative eigenvalues. To determine the differential endophyte community composition using relative abundances of OTUs, permutational multivariate analysis of variance (PERMANOVA) was implemented using *adonis2* function also from *vegan*. Marginal effect of the interaction between pathogen species and disease symptoms was assessed for potential significant impact while site was used to constrain permutations.

To investigate further the taxonomic identities of OTUs assigned as ‘Fungi unclassified,’ assigned contigs were used to perform BLAST against the NCBI-nt database. As 96% of these contigs had BLAST hits to non-fungal lineages, a separate set of analyses was performed where contigs assigned as ‘Fungi unclassified’ and non-fungal lineages were removed from the table of classified sequences. Subsequent statistical analyses, including alpha and beta diversity analyses, were conducted as mentioned above using the newly derived data.

Metatranscriptome Analysis

Quality of forward and reverse RNA sequences was evaluated by Novogene and using FastQC (Andrews, 2010). Raw Illumina reads containing adapter contamination, > 10% uncertain nucleotides, and > 50% low quality nucleotides (Qscore \leq 5) among samples were removed by Novogene. No filtered reads across samples were further trimmed due to high quality Phred scores (> 30) during FastQC visual inspection. *De novo* metatranscriptome assembly was performed using the Trinity software (v2.11.0; Grabherr et al., 2011). To examine the representation of reads in the assembly, bowtie2 was used to capture and count the reads from individual samples that mapped back to the metatranscriptome assembly. TransRate (Smith-Unna et al., 2016) was also used to examine the quality of the *de novo* assembly. Transcript abundance was estimated using the RNA-Seq by Expectation Maximization (RSEM v1.3.3; Li & Dewey, 2011). Correlation analyses of biological replicates between and across treatments were performed using the Pearson correlation matrix to check for outlier samples. Due to the low sum of mapped fragments (< 5e+6) and correlation value (< 0.02), NC04-18MP was removed from the subsequent analyses.

Differential expression of transcripts was analyzed using edgeR (v3.32.1; Robinson et al., 2010). The count table of the Trinity transcript (isoform) abundance was filtered at counts per million (CPM) of 1 and transcripts must be present in at least 1 replicate. Significantly

differentially expressed (DE) transcripts were determined using the following parameters: 0.05 level of significance after using false discovery rate (FDR) for multiple testing, and a minimum fold change of 2. Data were normalized using trimmed mean of M values (TMM) and fitted in a generalized linear model with four contrast arguments: (1) *L. concolor* asymptomatic (LC_ASYM) vs. *L. concolor* symptomatic (LC_SYM), (2) *L. montivaga* asymptomatic (LM_ASYM) vs. *L. montivaga* symptomatic (LM_SYM), (3) *L. concolor* asymptomatic (LC_ASYM) vs. *L. montivaga* asymptomatic (LM_ASYM), and (4) *L. concolor* symptomatic (LC_SYM) vs. *L. montivaga* symptomatic (LM_SYM).

SortMeRNA was used to distinguish the non-coding regions (rRNA) among the DE transcripts (Kopylova et al., 2012). The longest open reading frames of coding regions were predicted using orfipy (Singh & Wurtele, 2021). The resulting protein products were then subject to MMseqs2 search (Steinegger & Söding, 2017) against the following databases to predict the taxonomy, protein domains, and proteins related to pathogen-host interactions: concatenated databases of NCBI nr (NCBI Resource Coordinators et al., 2018) and published genome sequences including those of Rhytismataceae species stored at JGI Mycocosm (Grigoriev et al., 2014), PfamA full 2021 (Mistry et al., 2021), and PHI-base 4.10 (Urban et al., 2019), respectively. Overall, only the annotated transcripts with an e-value < 1e-05 were considered. Transcripts with coverage and identity $\geq 50\%$ in the concatenated NCBI nr and JGI Mycocosm database and PHI-base were retained. This concatenated database was used to sort fungal and plant transcripts.

Effectors (with $\geq 95\%$ probability) and carbohydrate active enzymes (CAZymes) were predicted using EffectorP 2.0 (Sperschneider et al., 2018) and dbCAN2 (Zhang et al., 2018), respectively. Within dbCAN2, transcripts with hits in at least two of the three databases (HMMER, DIAMOND and Hotpep) were considered. Metabolic pathways of predicted proteins (FDR < 0.05)

were searched through BlastKOALA (Kanehisa et al., 2016) using the family_eukaryotes KEGG database with the ‘fungi’ or ‘plant’ taxonomy option (Kanehisa et al., 2021). Orthologous gene clusters among treatments and their gene ontology (GO) annotations were determined through OrthoVenn2 (Xu et al., 2019) with an e-value of $< 1e-2$ and inflation value of 1.5. Expressed plant receptor genes with $> 50\%$ identity were determined through PRGdb 3.0 (Osuna-Cruz et al., 2018). DeepLoc 1.0 (Almagro Armenteros et al., 2017) was used to predict secreted proteins.

Results

Mycobiome Sequences, Composition and Diversity

A total of 7,670,091 contigs were obtained from the DNA of 60 symptomatic and 58 asymptomatic needle samples obtained after screening and filtering. Of these, 705,680 were unique contigs which were then further reduced to 664,848 unique contigs with a total of 7,436,294 sequences after removing chimeras and non-fungal lineages. There were only 1,246 OTUs out of 11,691 with > 10 counts, representing a total of 7,279,077 contigs across all samples. Of these OTUs, the majority (80%) fell under Ascomycota while 18% remained unclassified. The OTUs classified as fungi represented 159 species, 206 genera, 142 families, 62 orders and 20 classes. However, of the 260,014 contigs assigned as unclassified fungi, only 2% remained as unclassified fungal lineage based on BLAST hits against NCBI database while a majority (96%) belonged to non-fungal lineages and 2% had no taxonomic assignments.

Of the fungal OTUs classified using UNITE database, *Lophodermella concolor* and *L. montivaga* dominated in their respective symptomatic needles by 67% and 96%, respectively (Figure 3.1) followed by unclassified Ascomycota with an average of 5%, *Sydowia polyspora* (4%) and unclassified *Cladosporium* (2%). While one *Lophodermella* pathogen dominated, a low

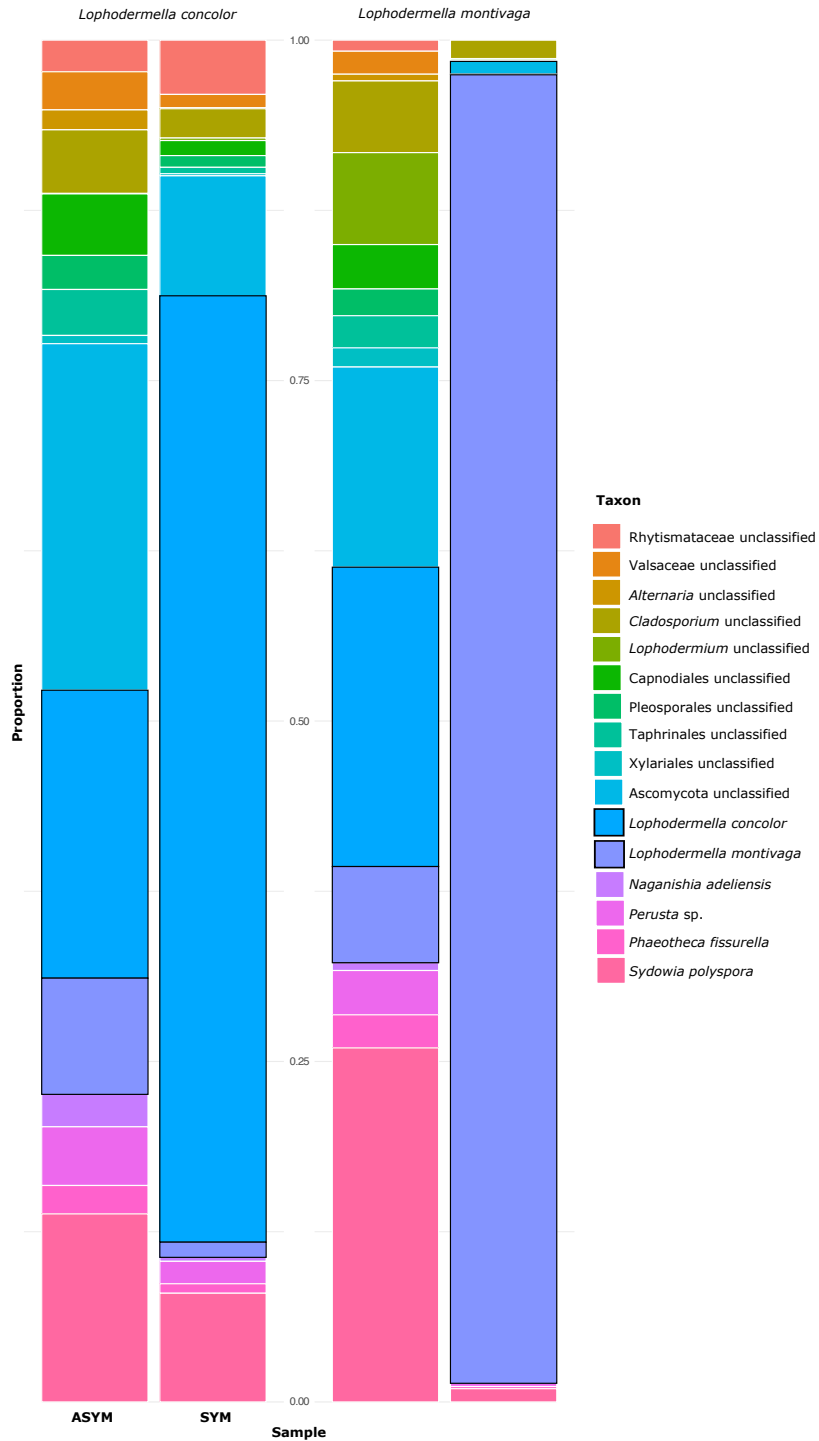


Figure 3.1. Relative abundance of fungal taxa (removing OTUs assigned as unclassified fungi) within the mycobiome across *Pinus contorta* needles that were asymptomatic and symptomatic of *Lophodermella concolor* and *L. montivaga* identified through metabarcoding.

proportion ($\leq 1\%$) of the other *Lophodermella* species was observed in symptomatic needles. Unclassified Ascomycota dominated among asymptomatic needles with an average of 18.1% followed by *S. polyspora* (18%) and unclassified *Cladosporium* (5%). Interestingly, *L. concolor* (19%) and *L. montivaga* (7%) were both present in asymptomatic needles albeit in low numbers relative to their symptomatic needle counterparts.

Results also showed that the pathogen species and disease symptoms, accounting for site variations, were significant predictors in both alpha and beta diversity (Supplementary Table 6). A significantly higher diversity was observed in asymptomatic needles compared to their symptomatic counterparts (Table 3.2), suggesting colonization of a variety of fungal species. While differences in diversity among asymptomatic needles was marginal (adjusted p-value > 0.05), the diversity between needles that were symptomatic of *L. concolor* and *L. montivaga* were profoundly different (adjusted p-value < 0.05). Meanwhile, 29% of the variability (PCoA1 = 16.02% and PCoA2 = 12.77%) was explained by pathogen and disease symptoms (Figure 3.2). Despite removing contigs that matched to ‘Fungi unclassified,’ diversity remained significantly different between asymptomatic needles vs. symptomatic needles, and between needles symptomatic of *L. concolor* and *L. montivaga* (Supplementary Table 7).

Metatranscriptome Assembly

The metatranscriptome libraries from the RNA of asymptomatic and symptomatic needle samples generated a total of 237,903,220 reads (Table 3.3). The assembly generated 2,079,387 transcript contigs with an average length of 552 bases. Fifty percent of the metatranscriptome sequence was covered by contigs with at least 765 bases (N50). More than 86% of the reads across all samples aligned back to the assembly (Table 3.3). Correlation assessment between samples

Table 3.2. Diversity measures among asymptomatic and symptomatic *Pinus contorta* needles collected from Gunnison National Forest, Colorado, USA

Needle Treatment	Species	Predicted means (se)	t-ratio	p-value
<i>Richness</i>				
Asymptomatic	<i>L. concolor</i>	66.78 (4.02)	-0.123	0.9025
	<i>L. montivaga</i>	67.62 (5.57)		
Symptomatic	<i>L. concolor</i>	35.94 (4.02)	3.842	0.0002
	<i>L. montivaga</i>	9.71 (5.57)		
<i>Shannon Index</i>				
Asymptomatic	<i>L. concolor</i>	2.13 (0.09)	-0.157	0.8756
	<i>L. montivaga</i>	2.16 (0.13)		
Symptomatic	<i>L. concolor</i>	1.20 (0.09)	5.799	< 0.0001
	<i>L. montivaga</i>	0.28 (0.13)		
<i>Inverse Simpson Index</i>				
Asymptomatic	<i>L. concolor</i>	0.68 (0.04)	-0.604	0.547
	<i>L. montivaga</i>	0.72 (0.05)		
Symptomatic	<i>L. concolor</i>	0.32 (0.04)	4.352	< 0.0001
	<i>L. montivaga</i>	0.06 (0.05)		

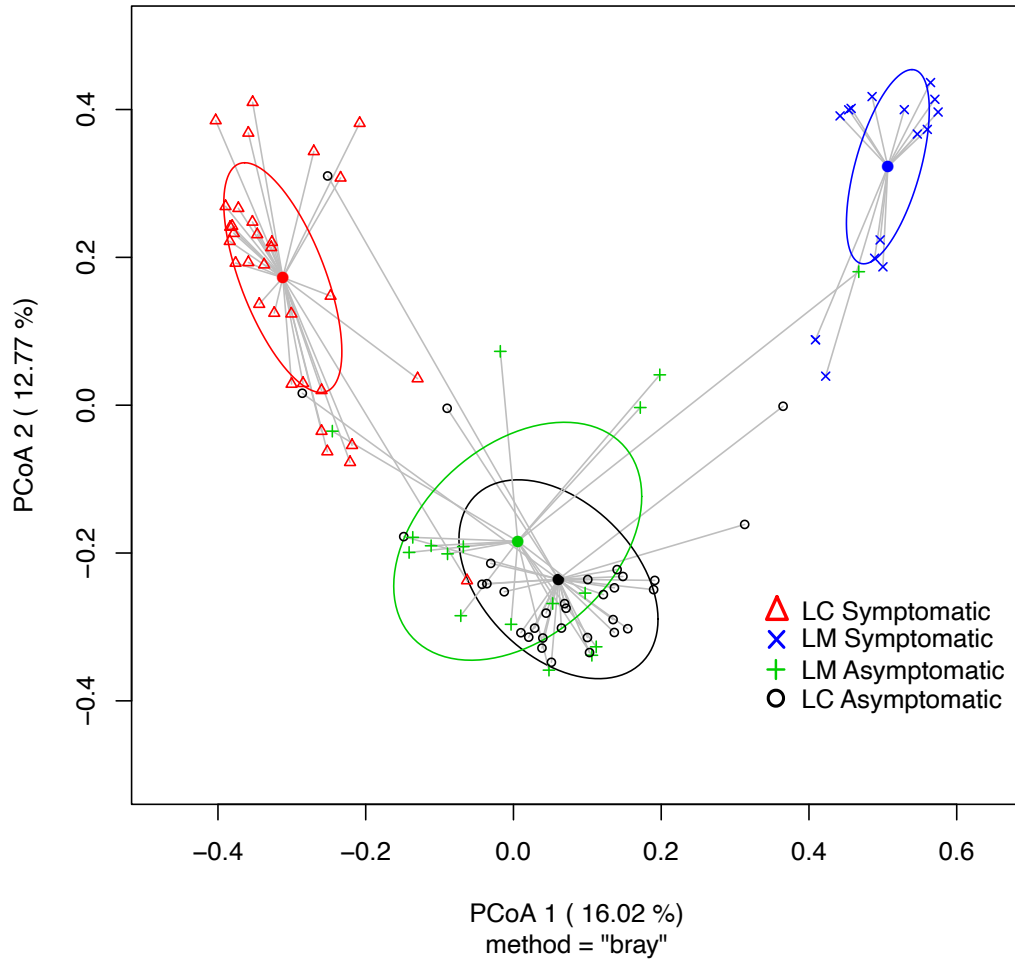


Figure 3.2. Principal coordinate analysis (PCoA) based on relative abundance of fungal operational taxonomic units (OTUs) showing fungal community structure on *Pinus contorta* needles that are symptomatic or symptomatic of *Lophodermella concolor* (LC) and *L. montivaga* (LM). Ellipses represent one standard deviation.

Table 3.3. Metabarcoding and metatranscriptome profile of *Pinus contorta* needle samples. Cross (†) represents samples excluded from the analyses. Proportions (%) of raw reads that aligned to the metatranscriptome assembly and the overall alignment rate are also shown.

Disease symptom	Sample	DNA contigs (metabarcoding)		Raw RNA reads	Paired reads that aligned concordantly to the assembly ≥ 1 time (%)	Overall rate (%) of alignment to the assembly
		<i>L. concolor</i>	<i>L. montivaga</i>			
Asymptomatic	CS02-18CN	1,014	173	21,337,962	78.82	93.4
	TC01-19CN	2,386	3,706	24,537,902	79.75	93.56
Symptomatic	CS02-18CP	26,149	84	20,416,050	66.61	87.89
	SR10-19CP	22,791	0	21,485,100	71.65	91.68
Asymptomatic	LV02-18MN	22,078	18,744	22,184,468	78.33	89.96
	LV03-18MN	522	4,785	25,400,132	73.79	86.48
	SR09-18MN	26,245	1,422	30,543,904	77.44	94.48
Symptomatic	LV02-18MP	0	20,353	20,609,968	79.88	92.06
	NC04-18MP†	3	63,789	24,456,808	77.26	92.70
	SR09-18MP	0	43,121	26,930,926	78.37	92.76

within treatments and Principal Component Analysis (Supplementary Figure 4) identified NC04-18MP sample as an outlier and thus was excluded from further analysis. The average Pearson correlation between samples within a treatment were 0.8 for LM_SYM (excluding NC04-18MP), 0.6 for LM_ASYM, 0.7 for LC_SYM and 0.7 for LC_ASYM. Notably, LC_ASYM and LM_ASYM samples were highly correlated than with their symptomatic counterpart. The 5 asymptomatic and 4 symptomatic samples, which contained a total of 510,575 fungal OTUs, had 10,505,207 transcripts (Supplementary Table 8).

Metatranscriptome Differential Gene Expression

Differential expression profiles were similar across LC_ASYM and LM_ASYM samples (Figure 3.3). In contrast, differential expression profiles between LC_SYM and LM_SYM were distinct from each other. A total of 85,798 transcripts were differentially expressed (DE) across all four comparisons: LC_ASYM_vs._LC_SYM, LM_ASYM_vs._LM_SYM, LC_ASYM_vs._LM_ASYM, and LC_SYM_vs._LM_ASYM. Collapsing identical transcripts produced a total of 51,363 transcripts with 93% (47,812) classified as non-rRNA.

The largest number of DE transcripts was observed in LC_SYM_vs._LM_SYM (38,439), followed by LM_ASYM_vs._LM_SYM (32,779) and LC_ASYM_vs._LC_SYM (14,562). Only 18 DE transcripts were found in the LC_ASYM_vs._LM_ASYM comparison. Greater expression of transcripts was observed in symptomatic needles compared to asymptomatic ones: 14,433 (99%) in LC_SYM vs. 129 (1%) in LC_ASYM, and 32462 (99%) in LM_SYM vs. 317 (1%) in LM_ASYM. Notably, of the 46,895 DE transcripts in needles symptomatic of *L. concolor* and *L. montivaga*, only 1.1% were shared between species. Similarly, needles asymptomatic of *L. concolor* and *L. montivaga* shared only 0.9% of the 446 DE transcripts. These may be attributed to possible sequence divergence that separated the orthologs into distinct transcripts. Orthovenn

analysis showed that symptomatic needles contained more transcripts that belong to unique protein clusters than in asymptomatic needles, with only 1% shared between them (Supplementary Figure

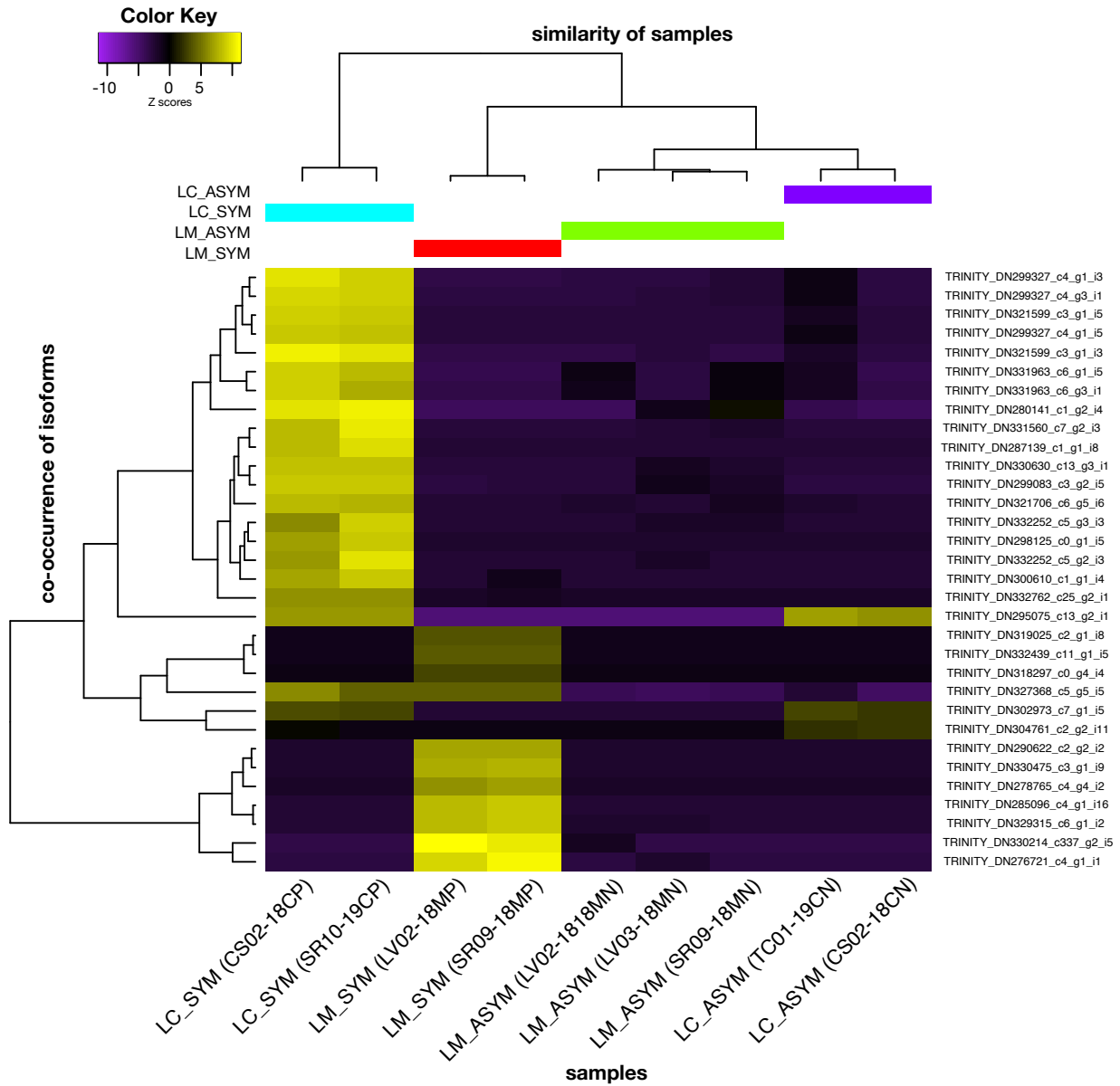


Figure 3.3. Heatmap of the differentially expressed transcripts (isoforms) in *Pinus contorta* needles asymptomatic (ASYM) and symptomatic (SYM) of *Lophodermella concolor* (LC) and *L. montivaga* (LM) based on counts per million (CPM) reads. Trinity transcripts shown are the top 10 differentially expressed features (p -value < 0.001 , fold change ≥ 2) within each of the four pairwise comparisons.

5). Nearly 98% of the total protein clusters in LC_ASYM_vs._LC_SYM (2,680) and LM_ASYM_vs._LM_SYM (5,679) were exclusive to symptomatic needles.

Of the 85,798 DE transcripts, only 39,807 had taxonomic annotations with 61% identified as fungi. Nearly 30% and 3% of these DE transcripts were identified as bacteria and plants, respectively (Supplementary Figure 6). The majority (98%) of the 24,289 fungal transcripts belonged to Ascomycota, followed by Basidiomycota (1.1%) and Mucoromycota (0.4%). None of the DE transcripts in LC_ASYM_vs._LM_ASYM were identified as fungi. Among the comparisons involving asymptomatic vs. symptomatic needles, no fungal taxa with > 10 DE transcripts were found in asymptomatic needles (Supplementary Table 9). However, fungal transcripts may still be present but were not significantly expressed. In symptomatic needles, many fungal DE transcripts (47% and 49% in LC_SYM and LM_SYM, respectively) were classified under Rhytismataceae (Figure 3.4). Since there are no available sequenced *Lophodermella* genomes, rhytismataceous transcripts could only be matched to other closely related genera (Supplementary Table 9).

Differentially expressed plant transcripts were more abundant in symptomatic needles than their asymptomatic counterparts (Supplementary Figure 6), with nearly twice the DE transcript count to that of asymptomatic needles. Out of the total 1,317 DE plant transcripts across all four comparisons, only 31% were classified as conifers. These conifer transcripts, dominated by *Picea sitchensis*, were more abundant in asymptomatic needles within comparisons LC_ASYM_vs._LC_SYM and LM_ASYM_vs._LM_SYM. In contrast, transcripts classified as non-conifers were generally abundant in symptomatic needles possibly due to the lack of genome annotation for *P. contorta* host.

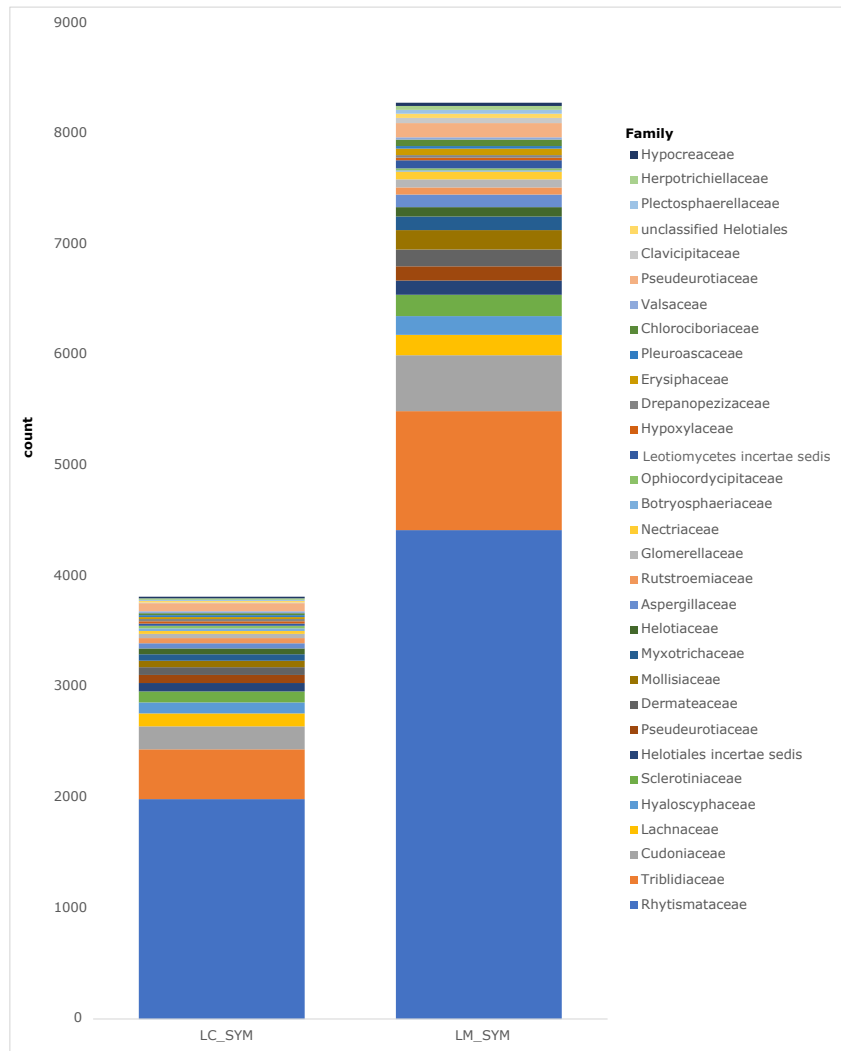


Figure 3.4. Abundance of the 25 most active fungal families within the mycobiome across *Pinus contorta* needles asymptomatic and symptomatic (SYM) of *Lophodermella concolor* (LC) and *L. montivaga* (LM) identified from the metatranscriptome using the concatenated NCBIInr-JGI Mycocosm databases.

Functional Annotation of Fungal Transcripts

To obtain insights into the metabolic activities of the mycobiome within healthy and diseased needles, DE fungal transcripts were compared in functional annotation databases: Pfam, PHI-base, EffectorP, dbCAN, KEGG, and Swiss-Prot and GO through Orthovenn. Roughly 80% of the total DE fungal transcripts across all three comparisons (LC_ASYM_vs._LC_SYM, LM_ASYM_vs._LM_SYM and LC_SYM_vs._LM_SYM) had annotations in at least one of the

databases, and many of these were greatly expressed in symptomatic needles (Figures 5-7). There were no DE transcripts identified as fungi in LC_ASYM_vs._LM_ASYM. In LC_SYM_vs._LM_SYM comparison, the functions of the DE transcripts in both treatments were generally similar despite a low proportion of shared transcripts, which may be influenced by sequence divergence between the two dominant *Lophodermella* pathogens.

The fungal community in symptomatic needles highly expressed carbohydrate-active and protein-degrading enzymes (Figure 3.5; Supplementary Table 10). Fungal proteases and peptidases commonly found in symptomatic needles included metallopeptidases, cysteine peptidases, and serine carboxypeptidase (Supplementary Table 10). While there was remarkable expression of enzymes involved in carbohydrate synthesis, other CAzymes that have been linked to lignin and carbohydrate degradation were also common in symptomatic needles. GHs were overrepresented in symptomatic needles (LC_SYM and LM_SYM). Between comparisons of LC_ASYM_vs._LC_SYM and LM_ASYM_vs._LM_SYM, a higher expression of CAzymes, proteases and peptidases was observed in LM_SYM than in LC_SYM. Similarly, lignin degrading enzymes (i.e., AAs 1, 2, 3 and 5) were more abundant in LM_SYM.

Genes related to pathogenicity were also expressed in symptomatic needles (Figure 3.6). In asymptomatic vs. symptomatic needle comparisons, more than 50% of the 604 and 1,235 PHI-base hits in *L. concolor* (64%) and *L. montivaga* (59%) symptomatic needles, respectively, were associated with pathogenicity, virulence, and/or chemical resistance. Of these, only 6 and 26 *L. concolor* and *L. montivaga* transcripts, respectively, were predicted as secreted proteins. Moreover, only 1 out of 5 and 1 out of 3 EffectorP-annotated DE transcripts were predicted as secreted effectors in *L. concolor* and *L. montivaga* symptomatic needles, respectively, using

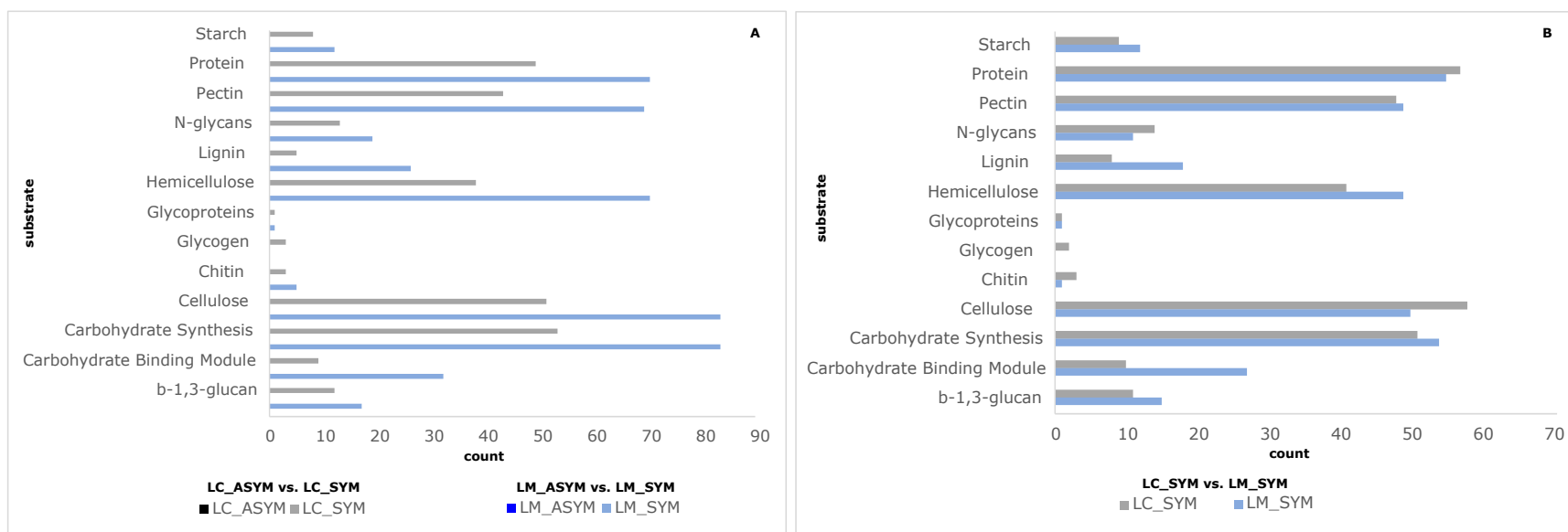


Figure 3.5. Number of fungal enzymes that degrade proteins and various substrates that were differentially expressed between (A) *Pinus contorta* needles symptomatic and asymptomatic of *Lophodermella concolor* (LC_ASYM vs. LC_SYM) and *L. montivaga* (LM_ASYM vs. LM_SYM), and (B) between symptomatic needles of *L. concolor* and *L. montivaga* (LC_SYM vs. LM_SYM) inferred from dbCAN2 and PFAM.

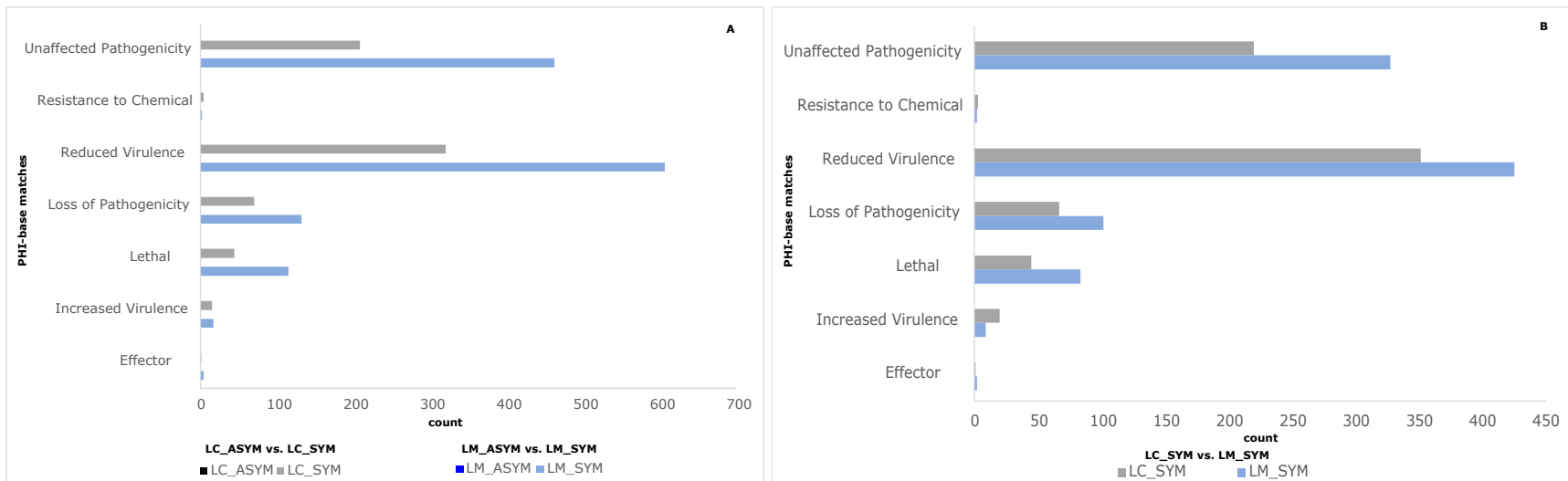


Figure 3.6. PHI-base hits of fungal transcripts between (A) *Pinus contorta* needles symptomatic and asymptomatic of *Lophodermella concolor* (LC_ASYM vs. LC_SYM) and *L. montivaga* (LM_ASYM vs. LM_SYM), and (B) between symptomatic needles of *L. concolor* and *L. montivaga* (LC_SYM vs. LM_SYM).

DeepLoc. In contrast, no significant DE transcripts in asymptomatic needles had hits to EffectorP nor PHI-base databases, suggesting no significant pathogenic activity in asymptomatic needles.

KEGG annotations of fungal transcripts also showed enhanced gene expression in symptomatic needles compared to asymptomatic ones. Genes involved in the synthesis of secondary metabolites were also highly expressed in symptomatic needles (Figure 3.7). Apart from terpenoids backbone synthesis (KO00900), other dominant proteins in symptomatic needles were involved in the synthesis of other secondary metabolites such as phenylpropanoid (KO00942), isoquinoline alkaloid (KO00950), tropane, piperidine and pyridine alkaloid (KO00960), and streptomycin (KO00521) (Supplementary Table 11). Interestingly, pathways in symptomatic needles also included membrane transport (KO02010 ABC transporters: LC_SYM=14, LM_SYM=31) and environmental adaptation (KO04626 Plant-pathogen interaction: LC_SYM=2, LM_SYM=1). A high expression of genes involved in xenobiotics biodegradation and metabolism were also observed in symptomatic needles.

More GO annotations were detected in symptomatic needles that were related to biological processes, molecular functions and cellular components observed (Figure 3.8). The only two fungal DE transcripts in LM_ASYM in comparison LM_ASYM_vs._LM_SYM were related to biological processes (i.e., xanthophyll cycle and transcription elongation). Interestingly, of the biological processes identified in symptomatic needles, processes such as protein and membrane transport, ubiquitin-dependent protein catabolic process, and pathogenesis were among the most common. Further, molecular functions common in symptomatic needles include oxidoreductase and metallopeptidase activities, and zinc and metal ion binding. Gene products or protein complexes in symptomatic needles were commonly observed in the cellular membrane.

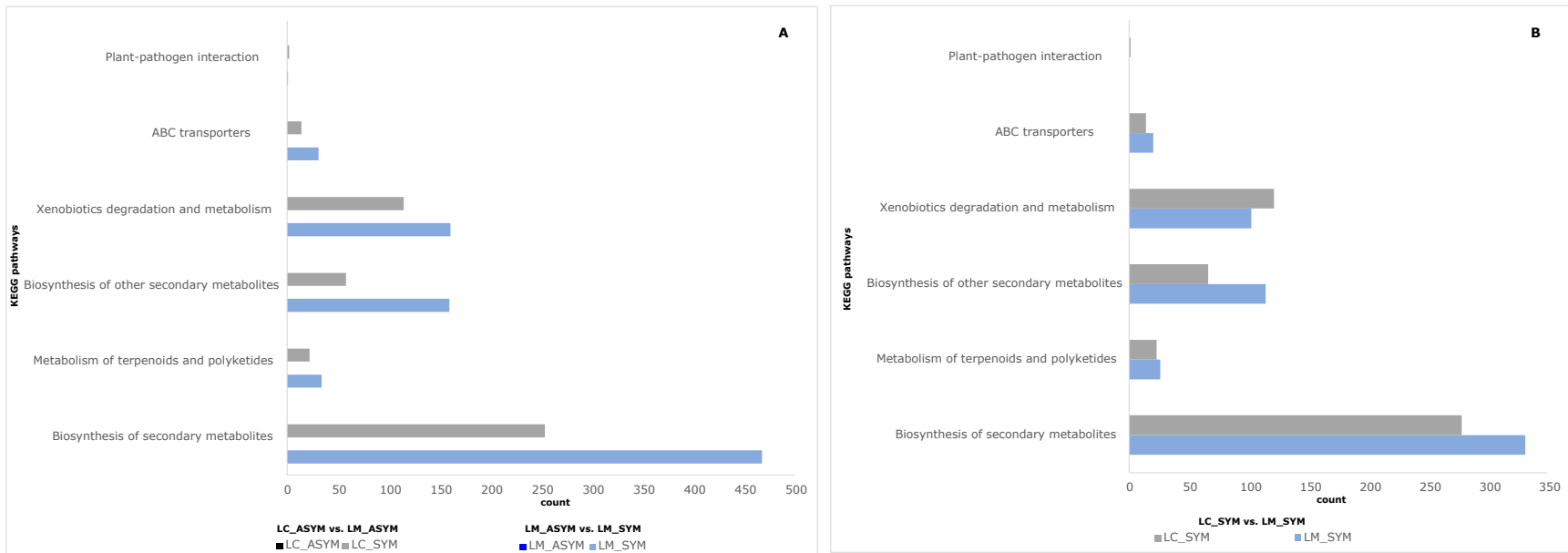


Figure 3.7. Number of fungal transcripts involved in the production of secondary metabolites, environmental adaptation, and membrane transport between (A) *Pinus contorta* needles symptomatic and asymptomatic of *Lophodermella concolor* (LC_ASYM vs. LC_SYM) and *L. montivaga* (LM_ASYM vs. LM_SYM), and (B) between symptomatic needles of *L. concolor* and *L. montivaga* (LC_SYM vs. LM_SYM) inferred from KEGG.

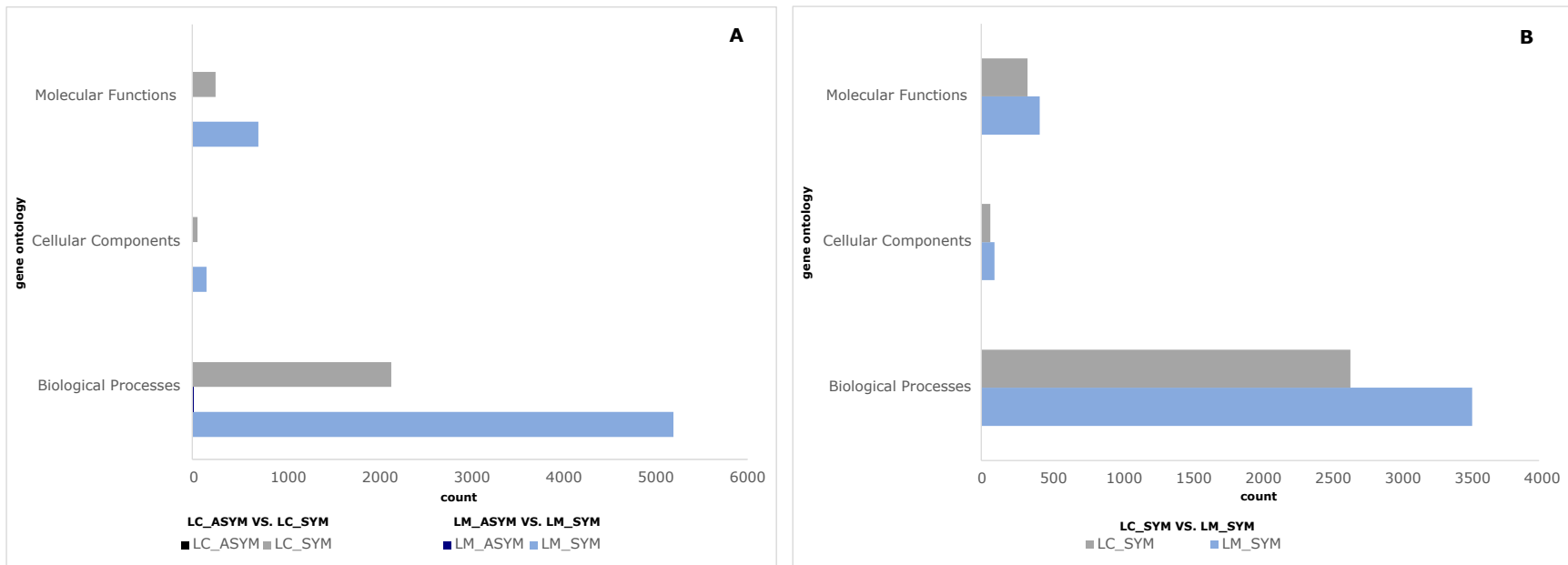


Figure 3.8. Gene ontologies of fungal DE transcripts between (A) *Pinus contorta* needles symptomatic and asymptomatic of *Lophodermella concolor* (LC_ASYM vs. LC_SYM) and *L. montivaga* (LM_ASYM vs. LM_SYM), and (B) between symptomatic needles of *L. concolor* and *L. montivaga* (LC_SYM vs. LM_SYM) inferred from Orthovenn2.

Functional Annotation of Plant Transcripts

For DE transcripts taxonomically annotated as plants, functional annotation was conducted using the following protein databases: Pfam, dbCAN, KEGG, PRGdb, NCBI, and Swiss-Prot and GO in Orthovenn. Seventy-eight percent of the total 1,317 plant transcripts across all four comparisons had annotations in at least one of the functional annotation databases, although a few (25 DE transcripts) were annotated as proteins with uncharacterized, unknown or hypothetical function.

DE plant transcripts in both asymptomatic and symptomatic needles mostly belonged to glycosyl hydrolase and glycosyltransferase families. However, only a small proportion of transcripts (3% in LC_ASYM vs. LC_SYM and 6% in LM_ASYM vs. LM_SYM) were annotated using dbCAN2. Interestingly, albeit in low numbers, protein-degrading enzymes such as metallopeptidases (peptidase family M20/M25/M40, M24 and M41) and serine peptidases (peptidase S26, serine aminopeptidase S33, X-Pro dipeptidyl-peptidase S15) were found in asymptomatic needles but not in symptomatic ones.

PRGdb annotation further showed higher expression of plant resistance genes in asymptomatic needles compared to symptomatic ones (Supplementary Table 12). Kinase (KIN) with transmembrane (TM) and kinase domains was the most dominant class in asymptomatic needles followed by receptor-like proteins (RLP) with TM and extra-cellular leucine-rich repeat (LRR) domains. Similarly, annotated through KEGG database, abundant proteins associated with the mitogen-activated protein kinase (MAPK) signaling pathway and plant hormone signal transduction were more abundant in asymptomatic needles. Phospholipase D signaling pathway was unique to asymptomatic needles.

In contrast, the DE transcripts associated with other pathways for signal transduction were slightly more abundant in symptomatic needles (Supplementary Table 8). About 37% of the DE transcripts in needles symptomatic of *L. concolor* (47 out of 127) and *L. monitvaga* (98 out of 265) were annotated through KEGG. However, of these, only 5 were common, which included ATP citrate lyase (ACL; K01648) and translation initiation factor 5A (eIF5A; K03262) that were exclusive to symptomatic needles, and serine/threonine-protein phosphatase 2A (PP2A; K04354) and cleavage and polyadenylation specificity factor (CPSF; K14404) which were abundant in symptomatic needles.

DE plant proteins in both asymptomatic and symptomatic needles were mostly related to biological processes, although GO annotated proteins were generally more abundant in symptomatic needles (Figure 3.9). Interestingly, in LC_SYM_vs._LM_SYM, plant proteins highly expressed in LC_SYM were related to response to stresses such as salt stress (11) and oxidative stress (4) whereas LM_SYM was mostly dominated by proteins related to pathogenesis (12) and transmembrane transport (9).

Functional Annotation of Other Transcripts

Despite the enrichment of eukaryotic organisms, bacterial transcripts were still recovered with a majority observed in symptomatic needles (LC_ASYM=2 and LC_SYM=2,0687 in LC_ASYM_vs._LC_SYM, and LM_ASYM=0 and LM_SYM=4,420 in LM_ASYM_vs._LM_SYM). Symptomatic needles contained an abundance of proteins (Supplementary Table 14) and enzymes for carbohydrate synthesis and degradation (Supplementary Figure 7). Interestingly, chitin-degrading enzymes (CE9 and GH125) were pronounced, though not the most abundant, among the bacterial transcripts in symptomatic

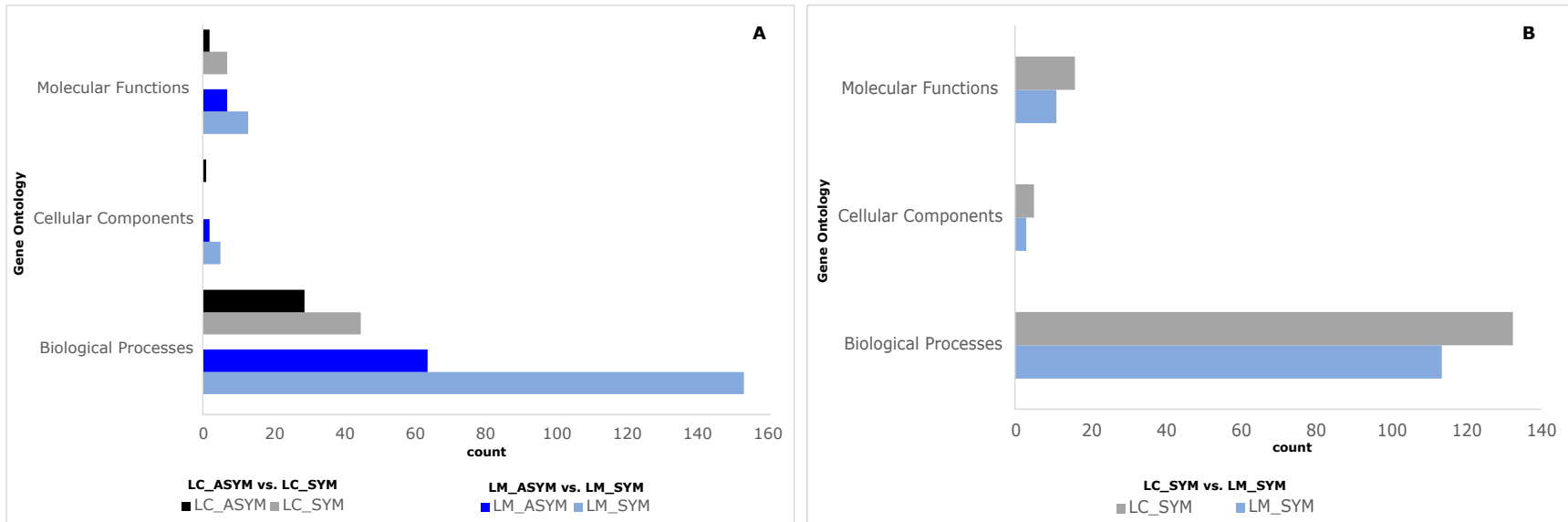


Figure 3.9. Gene ontologies of plant DE transcripts between (A) *Pinus contorta* needles symptomatic and asymptomatic of *Lophodermella concolor* (LC_ASYM vs. LC_SYM) and *L. montivaga* (LM_ASYM vs. LM_SYM), and (B) between symptomatic needles of *L. concolor* and *L. montivaga* (LC_SYM vs. LM_SYM) inferred from Orthovenn2.

needles. GO annotations also revealed high expression of genes involved in biological processes, particularly protein transport (GO:0015031) and pathogenesis (GO:0009405).

A large proportion (54%) of the metatranscriptome remained taxonomically unclassified and the majority was identified in symptomatic needles (Supplementary Figure 6). Of these, only 8% (3,676 out of 45,991) were functionally annotated using Pfam, PHI-base, EffectorP, dbCAN, and Swiss-Prot and GO through Orthovenn. Proteins associated with biological processes were abundant in symptomatic needles within comparisons LC_ASYM_vs._LC_SYM and LM_ASYM_vs._LM_SYM. In particular, ubiquitin-dependent protein catabolic process and protein transport were commonly abundant among symptomatic needles. LC_SYM was further dominated with proteins involved in pathogenesis and transcription while transposition and DNA integration were abundant in LM_SYM. Similarly, while only a few, CAzymes that degrade cellulose (AA9) and hemicellulose (GH16) were found in symptomatic needles while only GT1 for carbohydrate synthesis was observed in asymptomatic needles. Interestingly, extracellular effectors were predicted only among transcripts in symptomatic needles (LC_SYM=5, LM_SYM=7).

Discussion

This study explored the shifts in the interaction of fungal endophytes, *Lophodermella* pathogens, and *P. contorta* host in the *Lophodermella* needle cast pathosystem. The analyses revealed an adverse impact of the disease on the needle mycobiota, with a significant decrease of fungal diversity as the pathogenic mycobiota dominated by *Lophodermella* pathogens becomes highly active. It further showed an elicitation of diverse plant defense mechanisms that differed between healthy and diseased needles, and between *L. concolor* and *L. montivaga* dominated

mycobiota. This study also described for the first time the endophytic lifestyle of *L. concolor* and *L. montivaga*.

Mycobiome Composition and Diversity

This study showed that *P. contorta* needles host a diverse community of fungal species dominated by Ascomycetes, a group commonly abundant in conifer needle tissues (e.g., Oono et al., 2015; Würth et al., 2019). Similar to other studies, some fungal OTUs remain unclassified, which highlights the wide diversity of potentially novel endophytes with ecological roles that are yet to be identified (Arnold, 2007; Rodriguez et al., 2009). This study further identified that *L. concolor* and *L. montivaga* may be part of the ‘normal’ mycobiome of *P. contorta* needles as both are present in asymptomatic and symptomatic needles. The presence of pathogen in the absence of disease can occur in many pathosystems where potential pathogens are members of a healthy microbiome (Bass et al., 2019). Since this study only examined in *P. contorta* stands in Colorado, whether one or both *Lophodermella* pathogens are present in healthy needles of other *P. contorta* provenances, which have varying levels of needle cast resistance (Hunt et al., 1987), is still unknown. Alternatively, their existence in asymptomatic needles may not necessarily be part of the commensal microflora but instead are persistent infections due to their ability to evade the host immune response as endophytes (Monack et al., 2004). Susceptible hosts that are persistently infected then act as pathogen reservoirs.

Dysbiosis in the mycobiota, which is often the result of environmental disturbances (Bass et al., 2019; Pham & Lawley, 2014), is characterized as an overgrowth of pathogens, significant depletion of other taxa, loss of beneficial microbes or a combination of these (Petersen & Round, 2014). This is in contrast to a dense and diverse healthy microbiota under normal colonizing conditions (Liu et al., 2020). I found a highly diverse fungal community in asymptomatic needles,

which indicates a condition that allows many fungal species to colonize the needle tissue. However, at the symptomatic state, diversity was significantly reduced in the needle mycobiota with significant enrichment of *Lophodermella* pathogens. This dominance may be a manifestation of *Lophodermella* pathogens outcompeting other commensal species in the mycobiota for niche and/or other resources through various strategies (Jenior et al., 2018; Sorbara & Pamer, 2019), or a result of environmental changes favoring the growth of pathogens and symbionts over other endophytes (Pickard et al., 2017).

Fungal Gene Expressions in the Lophodermella Needle Cast Pathosystem

Plant pathogens upregulate an arsenal of pathogenicity-related genes that lead to disease emergence and increased severity until host mortality (O'Connell et al., 2012; Teixeira et al., 2014). This study showed a variety of pathogenicity-related genes (e.g., CAZymes, effectors, secondary metabolites and ABC transporters) that were highly expressed by the mycobiota, mostly Rhytismataceae, at the necrotrophic phase of the disease. These could largely be driven by *Lophodermella* pathogens as they dominate the mycobiota and colonize the needle tissue. In contrast, little to none of these genes were significantly expressed in asymptomatic needles, which could be an indication of low or absent pathogen activity. This could be part of the cryptic strategy of fungal endophytes after their initial host penetration to evade plant defense responses. Until needle senescence, latent needle pathogens exhibited either no additional growth or a slow continuous growth in intercellular spaces after initial infection (Deckert et al., 2002; Stone, 1987). Thus, the absence of disease in *P. contorta* could be a manifestation of *Lophodermella* pathogens evading host plant response through their marginal growth.

I found many plant cell wall degrading enzymes expressed in symptomatic needles which likely induced host necrosis and further facilitated pathogen growth. This is similar to previous

observations among hemibiotrophic foliar pathogens, where cell wall degradation via glycosyl hydrolases were significantly upregulated at the latter stage of disease (Yang et al., 2013; Ye et al., 2019). I also found effectors in symptomatic needles, which are likely necrotrophic effectors produced by hemibiotrophic or latent pathogens as they switch to the necrotrophic stage, and thus inducing host cell death (Vleeshouwers & Oliver, 2014). This possibly allowed *Lophodermella* pathogens access to more nutrients leading to sporulation on needles (Solomon, 2017). Metabolic pathways were also highly active in symptomatic needles, which could indicate abundance of toxins and other metabolites at the pathogenic necrotrophic state that potentially trigger plant hypersensitive response necessary for host invasion and produce reactive oxygen species that inhibit growth of biotrophs (Howlett, 2006). Transport and/or secretion of these metabolites may be facilitated by ABC transporters that were abundant in symptomatic needles, although ABC transporters may also be involved in host penetration, survival and virulence (Abou Ammar et al., 2013; Perlin et al., 2014; Zwiers et al., 2003).

Plant Interactions in the Lophodermella Needle Cast Pathosystem

Plant hosts have a wide ecological spectrum of interactions with the endophytic mycobiota. I observed an overexpression of host defense related genes, including KINs and RLPs, in asymptomatic needles suggesting the recognition of microbial infection by the plant host and thereby activating the first layer of plant inducible defense (Eaton et al., 2011; Tang et al., 2017) although RLPs could be involved in cell growth and development (Afzal et al., 2008) as part of the normal functioning of the plant host. Signaling pathways common in asymptomatic needles (e.g., MAPK and phospholipase D) could also be linked to plant hormone signaling and/or transduction with critical roles in plant growth and defense (Jagodzik et al., 2018; Zhao, 2015).

Albeit rare, protein-degrading enzymes were unique in asymptomatic needles compared to symptomatic needles which could indicate plant's response to improve tolerance against stressors. Some (e.g., prolyl aminopeptidases) can be rapidly over-induced when plants are subject to unfavorable environment (Sun et al., 2013; Szawłowska et al., 2012) and improve plant stress tolerance (Wang et al., 2015). I also found enzymes (e.g., M41) that could function as response to light stress resulting in photosystem repair (Nixon, 2004).

Plants are highly defensive and metabolically active as a response to the necrotrophic growth of hemibiotrophic pathogens (Yang et al., 2013). I found that symptomatic needles overly expressed a set of genes related to environmental stress, which may be triggered by the pathogenic activity of the mycobiota. Plants utilize glycoside hydrolases to degrade cell walls in response to stressors such as pathogen invasion and thereby inhibiting further fungal pathogen growth (Minic, 2008; Minic & Jouanin, 2006). The presence of these plant enzymes in symptomatic needles, although rare, could be part of host defense against further growth of *Lophodermella* pathogens. Similarly, enriched proteins in symptomatic needles that were involved in programmed cell death (CPFS, Bruggeman et al., 2014; eIF5A, Hopkins et al., 2008; ACL, Ruan et al., 2019), and stress signaling (PP2A; País et al., 2009) could likely be an attempt of *P. contorta* to defend itself against the pathogenic activity of the mycobiota. However, this plant defensive environment may only have eventually increased susceptibility and plant necrosis (Mahesh et al., 2012), and fungal pathogen growth and development (Shetty et al., 2007).

Despite highly similar functions of genes expressed by *L. concolor* and *L. montivaga* at the symptomatic phase, gene expression by the plant differed between *L. concolor* and *L. montivaga* symptomatic needles. This could indicate a set of unique and possibly uncharacterized strategies by each *Lophodermella* pathogen that elicit different responses in *P. contorta*, which could

influence important features (e.g., morphology and host specificity) unique to each species. Similar observations were noted in two *Phytophthora* pathogens of *Theobroma cacao* where the differences in genome structure and *in planta* transcriptome expression profiles presumably resulted in differences in host range (Ali et al., 2017).

Characterization of Other Transcripts

Metatranscriptome analyses in other pathosystems have shown a consortium of active microbes that drive disease development (Belibasakis & Manoil, 2021; Martí et al., 2020) and suppression (Hayden et al., 2018). The high expression of non-fungal genes mostly associated with protein and substrate breakdown in symptomatic needles could indicate a more complex interaction between disease players (i.e., endophytes, pathogen and host), and thus further investigation needs to be conducted. Interestingly, I found an overexpression of chitin-degrading enzymes at the symptomatic phase which could have likely reduced pathogen activity. Future studies should explore the potential of these beneficial bacterial communities as a strategy to control conifer foliage diseases.

I found an abundance of transcripts with unknown identities and functions, showing the existing limitations and challenges in our understanding about microbial community interactions (Kashyap et al., 2017; Martinez et al., 2017). Nonetheless, there is little doubt about the role CAZymes and effectors play in the necrosis observed in symptomatic needles. However, whether these were proteins employed by *Lophodermella* during pathogenesis or by another organism in the community remains unknown. Using sequenced genomes of *L. concolor* and *L. montivaga* as references in transcriptome assembly allow us to refine which transcripts belong to *Lophodermella* species within infected needle community. However, their inability to grow in culture media and lack of asexual reproductive structures present a challenge

in genome sequencing. Therefore, either metagenomic or single cell approaches may be necessary to effectively capture and assemble their genomes (Ahrendt et al., 2018).

Lophodermella as latent pathogens in P. contorta needles

Several needle pathogens were identified as latent pathogens through isolation from healthy needles of their conifer hosts (Magan & Smith, 1996; Stone et al., 2004). In contrast, until recently, there has been no documentation to suggest that endophytic species within the *Lophodermella* genus exist, possibly owing to their fastidious or likely obligate lifestyle. Previous observations pointed to *Lophodermella* species being active parasites (Darker, 1932; Millar, 1984) and survival throughout the next season is possible if infected needles are not shed (Kowalski & Krygier, 1996). This present study provided evidence of *L. concolor* and *L. montivaga* as likely latent needle pathogens in *P. contorta*. Despite their significant presence, I did not detect pathogenic activities in asymptomatic needles which suggests a period of dormancy for *Lophodermella* pathogens.

With the presence of *Lophodermella* spp. in healthy and diseased *P. contorta* needles, what triggers the lifestyle transition of these pathogens and symptom development remains a question. Nonetheless, it has been shown that environmental factors could favor further growth and/or activity of latent pathogens. The enhanced sporulation and infection of *Lophodermella* pathogens with warm moisture (Worrall et al., 2012) could exacerbate pathogen invasion resulting to an increase in relative abundance. This pathogen excess in host tissue then leads to an intensified disease incidence or severity (Bass et al., 2019; Ryan, 2013) and demonstrates an imbalance in an otherwise balanced system of antagonism between disease players that leads to disease development (Schulz & Boyle, 2005). Sieber (2007) further postulated that a rapid change in endophytic density due to adverse biotic and abiotic stresses, results to premature needle cast.

Alternatively, latency could be affected by processes involving physiological constraints and/or adaptation (Précigout et al., 2020) or a necessity to switch to necrotrophy for pathogen survival as H₂O₂ in plants accumulates (Shetty et al., 2007). Thus, more work needs to be done in understanding the transitional cues involved in the present pathosystem that would also incorporate environmental and anatomical factors at different life stages of the pathogens.

References

- Abarenkov, K., Zirk, A., Piirmann, T., Pöhönen, R., Ivanov, F., Nilsson, R. H., & Kõljalg, U. (2020). *Full mothur UNITE+INSD dataset 1* [Application/gzip]. UNITE Community. <https://doi.org/10.15156/BIO/786378>
- Abdullah, A. S., Moffat, C. S., Lopez-Ruiz, F. J., Gibberd, M. R., Hamblin, J., & Zerihun, A. (2017). Host–Multi-Pathogen Warfare: Pathogen Interactions in Co-infected Plants. *Frontiers in Plant Science*, 8, 1806. <https://doi.org/10.3389/fpls.2017.01806>
- Abou Ammar, G., Tryono, R., Döll, K., Karlovsky, P., Deising, H. B., & Wirsal, S. G. R. (2013). Identification of ABC Transporter Genes of *Fusarium graminearum* with Roles in Azole Tolerance and/or Virulence. *PLoS ONE*, 8(11), e79042. <https://doi.org/10.1371/journal.pone.0079042>
- Afzal, A. J., Wood, A. J., & Lightfoot, D. A. (2008). Plant Receptor-Like Serine Threonine Kinases: Roles in Signaling and Plant Defense. *Molecular Plant-Microbe Interactions*®, 21(5), 507–517. <https://doi.org/10.1094/MPMI-21-5-0507>
- Ahrendt, S. R., Quandt, C. A., Ciobanu, D., Clum, A., Salamov, A., Andreopoulos, B., Cheng, J.-F., Woyke, T., Pelin, A., Henrissat, B., Reynolds, N. K., Benny, G. L., Smith, M. E., James, T. Y., & Grigoriev, I. V. (2018). Leveraging single-cell genomics to expand the fungal tree of life. *Nature Microbiology*, 3(12), 1417–1428. <https://doi.org/10.1038/s41564-018-0261-0>
- Ali, S. S., Shao, J., Lary, D. J., Kronmiller, B. A., Shen, D., Strem, M. D., Amoako-Attah, I., Akrofi, A. Y., Begoude, B. A. D., ten Hoopen, G. M., Coulibaly, K., Kebe, B. I., Melnick, R. L., Gultinan, M. J., Tyler, B. M., Meinhardt, L. W., & Bailey, B. A. (2017). *Phytophthora megakarya* and *Phytophthora palmivora*, Closely Related Causal Agents of

- Cacao Black Pod Rot, Underwent Increases in Genome Sizes and Gene Numbers by Different Mechanisms. *Genome Biology and Evolution*, 9(3), 536–557.
<https://doi.org/10.1093/gbe/evx021>
- Almagro Armenteros, J. J., Sønderby, C. K., Sønderby, S. K., Nielsen, H., & Winther, O. (2017). DeepLoc: Prediction of protein subcellular localization using deep learning. *Bioinformatics*, 33(21), 3387–3395. <https://doi.org/10.1093/bioinformatics/btx431>
- Andrews, S. (2010). FastQC: a quality control tool for high throughput sequence data. *Available Online at: <Http://Www.Bioinformatics.Babraham.Ac.Uk/Projects/Fastqc>*.
- Arnold, A. E. (2007). Understanding the diversity of foliar endophytic fungi: Progress, challenges, and frontiers. *Fungal Biology Reviews*, 21(2–3), 51–66.
<https://doi.org/10.1016/j.fbr.2007.05.003>
- Ata, J. P., Burns, K. S., Marchetti, S., Munck, I. A., Beenken, L., Worrall, J. J., & Stewart, J. E. (2021). Molecular characterization and phylogenetic analyses of *Lophodermella* needle pathogens (Rhytismataceae) on *Pinus* species in the USA and Europe. *PeerJ*, 9, e11435.
<https://doi.org/10.7717/peerj.11435>
- Bass, D., Stentiford, G. D., Wang, H.-C., Koskella, B., & Tyler, C. R. (2019). The Pathobiome in Animal and Plant Diseases. *Trends in Ecology & Evolution*, 34(11), 996–1008.
<https://doi.org/10.1016/j.tree.2019.07.012>
- Belibasakis, G. N., & Manoil, D. (2021). Microbial Community-Driven Etiopathogenesis of Peri-Implantitis. *Journal of Dental Research*, 100(1), 21–28.
<https://doi.org/10.1177/0022034520949851>

- Bolger, A. M., Lohse, M., & Usadel, B. (2014). Trimmomatic: A flexible trimmer for Illumina sequence data. *Bioinformatics*, *30*(15), 2114–2120.
<https://doi.org/10.1093/bioinformatics/btu170>
- Brader, G., Compant, S., Vescio, K., Mitter, B., Trognitz, F., Ma, L.-J., & Sessitsch, A. (2017). Ecology and Genomic Insights into Plant-Pathogenic and Plant-Nonpathogenic Endophytes. *Annual Review of Phytopathology*, *55*(1), 61–83.
<https://doi.org/10.1146/annurev-phyto-080516-035641>
- Bruggeman, Q., Garmier, M., de Bont, L., Soubigou-Taconnat, L., Mazubert, C., Benhamed, M., Raynaud, C., Bergounioux, C., & Delarue, M. (2014). The Polyadenylation Factor Subunit CLEAVAGE AND POLYADENYLATION SPECIFICITY FACTOR30: A Key Factor of Programmed Cell Death and a Regulator of Immunity in Arabidopsis. *Plant Physiology*, *165*(2), 732–746. <https://doi.org/10.1104/pp.114.236083>
- Busby, P. E., Peay, K. G., & Newcombe, G. (2016). Common foliar fungi of *Populus trichocarpa* modify *Melampsora* rust disease severity. *New Phytologist*, *209*(4), 1681–1692. <https://doi.org/10.1111/nph.13742>
- Carrión, V. J., Perez-Jaramillo, J., Cordovez, V., Tracanna, V., de Hollander, M., Ruiz-Buck, D., Mendes, L. W., van Ijcken, W. F. J., Gomez-Exposito, R., Elsayed, S. S., Mohanraju, P., Arifah, A., van der Oost, J., Paulson, J. N., Mendes, R., van Wezel, G. P., Medema, M. H., & Raaijmakers, J. M. (2019). Pathogen-induced activation of disease-suppressive functions in the endophytic root microbiome. *Science*, *366*(6465), 606–612.
<https://doi.org/10.1126/science.aaw9285>
- Cubero, O. F., Crespo, A., Fatehi, J., & Bridge, P. D. (1999). DNA extraction and PCR amplification method suitable for fresh, herbarium-stored, lichenized, and other fungi.

- Plant Systematics and Evolution*, 216(3–4), 243–249.
<https://doi.org/10.1007/BF01084401>
- Darker, G. (1932). *The Hypodermataceae of Conifers* (Vol. 1). Contributions from the Arnold Arboretum of Harvard University.
- Deckert, R. J., Hsiang, T., & Peterson, R. L. (2002). Genetic relationships of endophytic *Lophodermium nitens* isolates from needles of *Pinus strobus*. *Mycological Research*, 106(3), 305–313. <https://doi.org/10.1017/S0953756201005494>
- Eaton, C. J., Cox, M. P., & Scott, B. (2011). What triggers grass endophytes to switch from mutualism to pathogenism? *Plant Science*, 180(2), 190–195.
<https://doi.org/10.1016/j.plantsci.2010.10.002>
- Edgar, R. C., Haas, B. J., Clemente, J. C., Quince, C., & Knight, R. (2011). UCHIME improves sensitivity and speed of chimera detection. *Bioinformatics*, 27(16), 2194–2200.
<https://doi.org/10.1093/bioinformatics/btr381>
- Feau, N., & Hamelin, R. C. (2017). Say hello to my little friends: How microbiota can modulate tree health. *New Phytologist*, 215(2), 508–510. <https://doi.org/10.1111/nph.14649>
- Fox, J., & Weisberg, S. (2019). *An R Companion to Applied Regression* (Third edition) [Computer software]. <https://socialsciences.mcmaster.ca/jfox/Books/Companion/>
- Gao, F., Dai, C., & Liu, X. (2010). Mechanisms of fungal endophytes in plant protection against pathogens. *African Journal of Microbiology Research*, 4(13), 1346–1351.
- Grabherr, M. G., Haas, B. J., Yassour, M., Levin, J. Z., Thompson, D. A., Amit, I., Adiconis, X., Fan, L., Raychowdhury, R., Zeng, Q., Chen, Z., Mauceli, E., Hacohen, N., Gnirke, A., Rhind, N., di Palma, F., Birren, B. W., Nusbaum, C., Lindblad-Toh, K., ... Regev, A.

- (2011). Full-length transcriptome assembly from RNA-Seq data without a reference genome. *Nature Biotechnology*, 29(7), 644–652. <https://doi.org/10.1038/nbt.1883>
- Grigoriev, I. V., Nikitin, R., Haridas, S., Kuo, A., Ohm, R., Otiillar, R., Riley, R., Salamov, A., Zhao, X., Korzeniewski, F., Smirnova, T., Nordberg, H., Dubchak, I., & Shabalov, I. (2014). MycoCosm portal: Gearing up for 1000 fungal genomes. *Nucleic Acids Research*, 42(D1), D699–D704. <https://doi.org/10.1093/nar/gkt1183>
- Hayden, H. L., Savin, K. W., Wadeson, J., Gupta, V. V. S. R., & Mele, P. M. (2018). Comparative Metatranscriptomics of Wheat Rhizosphere Microbiomes in Disease Suppressive and Non-suppressive Soils for *Rhizoctonia solani* AG8. *Frontiers in Microbiology*, 9, 859. <https://doi.org/10.3389/fmicb.2018.00859>
- Hopkins, M. T., Lampi, Y., Wang, T.-W., Liu, Z., & Thompson, J. E. (2008). Eukaryotic Translation Initiation Factor 5A Is Involved in Pathogen-Induced Cell Death and Development of Disease Symptoms in Arabidopsis. *Plant Physiology*, 148(1), 479–489. <https://doi.org/10.1104/pp.108.118869>
- Howlett, B. J. (2006). Secondary metabolite toxins and nutrition of plant pathogenic fungi. *Current Opinion in Plant Biology*, 9(4), 371–375. <https://doi.org/10.1016/j.pbi.2006.05.004>
- Hunt, R. S., Ying, C. C., & Ashbee, D. (1987). Variation in damage among *Pinus contorta* provenances caused by the needle cast fungus *Lophodermella concolor*. *Canadian Journal of Forest Research*, 17, 594–597.
- Jagodzik, P., Tajdel-Zielinska, M., Ciesla, A., Marczak, M., & Ludwikow, A. (2018). Mitogen-Activated Protein Kinase Cascades in Plant Hormone Signaling. *Frontiers in Plant Science*, 9, 1387. <https://doi.org/10.3389/fpls.2018.01387>

- Jenior, M. L., Leslie, J. L., Young, V. B., & Schloss, P. D. (2018). *Clostridium difficile* Alters the Structure and Metabolism of Distinct Cecal Microbiomes during Initial Infection To Promote Sustained Colonization. *MSphere*, 3(3), e00261-18, /msphere/3/3/mSphere261-18.atom. <https://doi.org/10.1128/mSphere.00261-18>
- Jia, Q., Qu, J., Mu, H., Sun, H., & Wu, C. (2020). Foliar endophytic fungi: Diversity in species and functions in forest ecosystems. *Symbiosis*, 80(2), 103–132. <https://doi.org/10.1007/s13199-019-00663-x>
- Kanehisa, M., Furumichi, M., Sato, Y., Ishiguro-Watanabe, M., & Tanabe, M. (2021). KEGG: Integrating viruses and cellular organisms. *Nucleic Acids Research*, 49(D1), D545–D551. <https://doi.org/10.1093/nar/gkaa970>
- Kanehisa, M., Sato, Y., & Morishima, K. (2016). BlastKOALA and GhostKOALA: KEGG Tools for Functional Characterization of Genome and Metagenome Sequences. *Journal of Molecular Biology*, 428(4), 726–731. <https://doi.org/10.1016/j.jmb.2015.11.006>
- Kashyap, P. L., Rai, P., Kumar, S., Chakdar, H., & Srivastava, A. K. (2017). DNA Barcoding for Diagnosis and Monitoring of Fungal Plant Pathogens. In B. P. Singh & V. K. Gupta (Eds.), *Molecular Markers in Mycology* (pp. 87–122). Springer International Publishing. https://doi.org/10.1007/978-3-319-34106-4_5
- Kopylova, E., Noé, L., & Touzet, H. (2012). SortMeRNA: Fast and accurate filtering of ribosomal RNAs in metatranscriptomic data. *Bioinformatics*, 28(24), 3211–3217. <https://doi.org/10.1093/bioinformatics/bts611>
- Koskella, B., Meaden, S., Crowther, W. J., Leimu, R., & Metcalf, C. J. E. (2017). A signature of tree health? Shifts in the microbiome and the ecological drivers of horse chestnut

bleeding canker disease. *New Phytologist*, 215(2), 737–746.

<https://doi.org/10.1111/nph.14560>

Kovalchuk, A., Mukrimin, M., Zeng, Z., Raffaello, T., Liu, M., Kasanen, R., Sun, H., & Asiegbu, F. O. (2018). Mycobiome analysis of asymptomatic and symptomatic Norway spruce trees naturally infected by the conifer pathogens *Heterobasidion* spp.: Mycobiome of Norway spruce. *Environmental Microbiology Reports*, 10(5), 532–541.

<https://doi.org/10.1111/1758-2229.12654>

Kowalski, T., & Krygier, J. (1996). *Mycological study on symptomless and diseased needles in pine stand attacked by Lophodermella sulcigena (Rostr.) V. Höhn.* 11, 159–168.

Kozich, J. J., Westcott, S. L., Baxter, N. T., Highlander, S. K., & Schloss, P. D. (2013).

Development of a Dual-Index Sequencing Strategy and Curation Pipeline for Analyzing Amplicon Sequence Data on the MiSeq Illumina Sequencing Platform. *Applied and Environmental Microbiology*, 79(17), 5112–5120. <https://doi.org/10.1128/AEM.01043-13>

Krings, M., Taylor, T. N., Hass, H., Kerp, H., Dotzler, N., & Hermsen, E. J. (2007). Fungal endophytes in a 400-million-yr-old land plant: Infection pathways, spatial distribution, and host responses. *New Phytologist*, 174(3), 648–657. <https://doi.org/10.1111/j.1469-8137.2007.02008.x>

Lenth, R., Singmann, H., Love, J., Buerkner, P., & Herve, M. (2020). *Package “emmeans”:* *Estimated Marginal Means, aka Least-Squares Means* (1.4.6) [Computer software].

<https://github.com/rvlenth/emmeans>

Legendre, P. & Anderson, M.J. (1999). Distance-based redundancy analysis: testing multispecies responses in multifactorial ecological experiments. *Ecological Monographs*, 69, 1-24.

- Li, B., & Dewey, C. N. (2011). RSEM: Accurate transcript quantification from RNA-Seq data with or without a reference genome. *BMC Bioinformatics*, *12*(1), 323.
<https://doi.org/10.1186/1471-2105-12-323>
- Liu, H., Brettell, L. E., & Singh, B. (2020). Linking the Phyllosphere Microbiome to Plant Health. *Trends in Plant Science*, *25*(9), 841–844.
<https://doi.org/10.1016/j.tplants.2020.06.003>
- Magan, N., & Smith, M. K. (1996). Isolation of the endophytes *Lophodermium piceae* and *Rhizosphaera kalkhoffii* from Sitka spruce needles in poor and good growth sites and in vitro effects of environmental factors. *Phyton*, *36*(3), 103–110.
- Mahesh, S. K., Liu, H., & Qiu, D. (2012). The Role of Radical Burst in Plant Defense Responses to Necrotrophic Fungi. *Journal of Integrative Agriculture*, *11*(8), 1305–1312.
[https://doi.org/10.1016/S2095-3119\(12\)60127-0](https://doi.org/10.1016/S2095-3119(12)60127-0)
- Martí, J. M., Arias-Giraldo, L. F., Díaz-Villanueva, W., Arnau, V., Rodríguez-Franco, A., & Garay, C. P. (2020). Metatranscriptomic dynamics after *Verticillium dahliae* infection and root damage in *Olea europaea*. *BMC Plant Biology*, *20*(1), 79.
<https://doi.org/10.1186/s12870-019-2185-0>
- Martinez, K. B., Leone, V., & Chang, E. B. (2017). Microbial metabolites in health and disease: Navigating the unknown in search of function. *Journal of Biological Chemistry*, *292*(21), 8553–8559. <https://doi.org/10.1074/jbc.R116.752899>
- McMurdie, P. J., & Holmes, S. (2013). phyloseq: An R Package for Reproducible Interactive Analysis and Graphics of Microbiome Census Data. *PLoS ONE*, *8*(4), e61217.
<https://doi.org/10.1371/journal.pone.0061217>

- Millar, C. S. (1984). Lophodermella species on pines. *In: Recent Research on Conifer Needle Diseases*. Eds. Glenn W. Peterson. USDA Forest Service, General Technical Report GTR-WO 50., 45–55.
- Minic, Z. (2008). Physiological roles of plant glycoside hydrolases. *Planta*, 227(4), 723–740.
<https://doi.org/10.1007/s00425-007-0668-y>
- Minic, Z., & Jouanin, L. (2006). Plant glycoside hydrolases involved in cell wall polysaccharide degradation. *Plant Physiology and Biochemistry*, 44(7–9), 435–449.
<https://doi.org/10.1016/j.plaphy.2006.08.001>
- Mistry, J., Chuguransky, S., Williams, L., Qureshi, M., Salazar, G. A., Sonnhammer, E. L. L., Tosatto, S. C. E., Paladin, L., Raj, S., Richardson, L. J., Finn, R. D., & Bateman, A. (2021). Pfam: The protein families database in 2021. *Nucleic Acids Research*, 49(D1), D412–D419. <https://doi.org/10.1093/nar/gkaa913>
- Monack, D. M., Mueller, A., & Falkow, S. (2004). Persistent bacterial infections: The interface of the pathogen and the host immune system. *Nature Reviews Microbiology*, 2(9), 747–765. <https://doi.org/10.1038/nrmicro955>
- NCBI Resource Coordinators, Agarwala, R., Barrett, T., Beck, J., Benson, D. A., Bollin, C., Bolton, E., Bourexis, D., Brister, J. R., Bryant, S. H., Canese, K., Cavanaugh, M., Charowhas, C., Clark, K., Dondoshansky, I., Feolo, M., Fitzpatrick, L., Funk, K., Geer, L. Y., ... Zbicz, K. (2018). Database resources of the National Center for Biotechnology Information. *Nucleic Acids Research*, 46(D1), D8–D13.
<https://doi.org/10.1093/nar/gkx1095>

- Nixon, P. J. (2004). FtsH-mediated repair of the photosystem II complex in response to light stress. *Journal of Experimental Botany*, *56*(411), 357–363.
<https://doi.org/10.1093/jxb/eri021>
- O’Connell, R. J., Thon, M. R., Hacquard, S., Amyotte, S. G., Kleemann, J., Torres, M. F., Damm, U., Buiate, E. A., Epstein, L., Alkan, N., Altmüller, J., Alvarado-Balderrama, L., Bauser, C. A., Becker, C., Birren, B. W., Chen, Z., Choi, J., Crouch, J. A., Duvick, J. P., ... Vaillancourt, L. J. (2012). Lifestyle transitions in plant pathogenic *Colletotrichum* fungi deciphered by genome and transcriptome analyses. *Nature Genetics*, *44*(9), 1060–1065. <https://doi.org/10.1038/ng.2372>
- Oksanen, J., Blanchet, F. G., Friendly, M., Kindt, R., Legendre, P., McGlenn, D., Minchin, P. R., O’Hara, R. B., Simpson, G. L., Solymos, P., Stevens, M. H. M., Szoecs, E., & Wagner, H. (2020). *Package “vegan”: Community ecology package*. <https://cran.r-project.org>
- Oono, R., Lefèvre, E., Simha, A., & Lutzoni, F. (2015). A comparison of the community diversity of foliar fungal endophytes between seedling and adult loblolly pines (*Pinus taeda*). *Fungal Biology*, *119*(10), 917–928. <https://doi.org/10.1016/j.funbio.2015.07.003>
- Osuna-Cruz, C. M., Paytuví-Gallart, A., Di Donato, A., Sundesha, V., Andolfo, G., Aiese Cigliano, R., Sanseverino, W., & Ercolano, M. R. (2018). PRGdb 3.0: A comprehensive platform for prediction and analysis of plant disease resistance genes. *Nucleic Acids Research*, *46*(D1), D1197–D1201. <https://doi.org/10.1093/nar/gkx1119>
- País, S. M., Téllez-Iñón, M. T., & Capiati, D. A. (2009). Serine/Threonine Protein Phosphatases type 2A and their roles in stress signaling. *Plant Signaling & Behavior*, *4*(11), 1013–1015. <https://doi.org/10.4161/psb.4.11.9783>

- Paulson, J. N., Olson, N. D., Braccia, D. J., Wagner, J., Talukder, H., Pop, M., & Bravo, H. C. (2013). *metagenomeSeq: Statistical analysis for sparse high-throughput sequencing*. <http://www.cbcb.umd.edu/software/metagenomeSeq>
- Perlin, M. H., Andrews, J., & San Toh, S. (2014). Essential Letters in the Fungal Alphabet. In *Advances in Genetics* (Vol. 85, pp. 201–253). Elsevier. <https://doi.org/10.1016/B978-0-12-800271-1.00004-4>
- Peters, S., Dammeyer, B., & Schulz, B. (1998). Endophyte-host Interactions. I. Plant defense reactions to endophytic and pathogenic fungi. *Symbiosis*, *25*, 193–211.
- Petersen, C., & Round, J. L. (2014). Defining dysbiosis and its influence on host immunity and disease. *Cellular Microbiology*, *16*(7), 1024–1033. <https://doi.org/10.1111/cmi.12308>
- Pham, T. A. N., & Lawley, T. D. (2014). Emerging insights on intestinal dysbiosis during bacterial infections. *Current Opinion in Microbiology*, *17*, 67–74. <https://doi.org/10.1016/j.mib.2013.12.002>
- Pickard, J. M., Zeng, M. Y., Caruso, R., & Núñez, G. (2017). Gut microbiota: Role in pathogen colonization, immune responses, and inflammatory disease. *Immunological Reviews*, *279*(1), 70–89. <https://doi.org/10.1111/imr.12567>
- Précigout, P.-A., Claessen, D., Makowski, D., & Robert, C. (2020). Does the Latent Period of Leaf Fungal Pathogens Reflect Their Trophic Type? A Meta-Analysis of Biotrophs, Hemibiotrophs, and Necrotrophs. *Phytopathology*®, *110*(2), 345–361. <https://doi.org/10.1094/PHYTO-04-19-0144-R>
- Prihatini, I., Glen, M., Wardlaw, T. J., & Mohammed, C. L. (2015). *Lophodermium pinastri* and an unknown species of Teratosphaeriaceae are associated with needle cast in a *Pinus*

- radiata* selection trial. *Forest Pathology*, 45(4), 281–289.
<https://doi.org/10.1111/efp.12169>
- Rajala, T., Velmala, S. M., Tuomivirta, T., Haapanen, M., Müller, M., & Pennanen, T. (2013). Endophyte communities vary in the needles of Norway spruce clones. *Fungal Biology*, 117(3), 182–190. <https://doi.org/10.1016/j.funbio.2013.01.006>
- Ridout, M., & Newcombe, G. (2018). *Sydowia polyspora* is both a Foliar Endophyte and a Preemergent Seed Pathogen in *Pinus ponderosa*. *Plant Disease*, 102(3), 640–644.
<https://doi.org/10.1094/PDIS-07-17-1074-RE>
- Robinson, M. D., McCarthy, D. J., & Smyth, G. K. (2010). edgeR: A Bioconductor package for differential expression analysis of digital gene expression data. *Bioinformatics*, 26(1), 139–140. <https://doi.org/10.1093/bioinformatics/btp616>
- Rodriguez, R. J., White Jr, J. F., Arnold, A. E., & Redman, R. S. (2009). Fungal endophytes: Diversity and functional roles: *Tansley review*. *New Phytologist*, 182(2), 314–330.
<https://doi.org/10.1111/j.1469-8137.2009.02773.x>
- Ruan, B., Hua, Z., Zhao, J., Zhang, B., Ren, D., Liu, C., Yang, S., Zhang, A., Jiang, H., Yu, H., Hu, J., Zhu, L., Chen, G., Shen, L., Dong, G., Zhang, G., Zeng, D., Guo, L., Qian, Q., & Gao, Z. (2019). Os ACL -A2 negatively regulates cell death and disease resistance in rice. *Plant Biotechnology Journal*, 17(7), 1344–1356. <https://doi.org/10.1111/pbi.13058>
- Ryan, E. T. (2013). The Intestinal Pathobiome: Its Reality and Consequences Among Infants and Young Children in Resource-Limited Settings. *Journal of Infectious Diseases*, 208(11), 1732–1733. <https://doi.org/10.1093/infdis/jit509>
- Schloss, P. D., Westcott, S. L., Ryabin, T., Hall, J. R., Hartmann, M., Hollister, E. B., Lesniewski, R. A., Oakley, B. B., Parks, D. H., Robinson, C. J., Sahl, J. W., Stres, B.,

- Thallinger, G. G., Van Horn, D. J., & Weber, C. F. (2009). Introducing mothur: Open-Source, Platform-Independent, Community-Supported Software for Describing and Comparing Microbial Communities. *Applied and Environmental Microbiology*, *75*(23), 7537–7541. <https://doi.org/10.1128/AEM.01541-09>
- Schulz, B., & Boyle, C. (2005). The endophytic continuum. *Mycological Research*, *109*(6), 661–686. <https://doi.org/10.1017/S095375620500273X>
- Shetty, N. P., Mehrabi, R., Lütken, H., Haldrup, A., Kema, G. H. J., Collinge, D. B., & Jørgensen, H. J. L. (2007). Role of hydrogen peroxide during the interaction between the hemibiotrophic fungal pathogen *Septoria tritici* and wheat. *New Phytologist*, *174*(3), 637–647. <https://doi.org/10.1111/j.1469-8137.2007.02026.x>
- Sieber, T. N. (2007). Endophytic fungi in forest trees: Are they mutualists? *Fungal Biology Reviews*, *21*(2–3), 75–89. <https://doi.org/10.1016/j.fbr.2007.05.004>
- Singh, U., & Wurtele, E. S. (2021). orfipy: A fast and flexible tool for extracting ORFs. *Bioinformatics*, btab090. <https://doi.org/10.1093/bioinformatics/btab090>
- Slippers, B., & Wingfield, M. J. (2007). Botryosphaeriaceae as endophytes and latent pathogens of woody plants: Diversity, ecology and impact. *Fungal Biology Reviews*, *21*(2–3), 90–106. <https://doi.org/10.1016/j.fbr.2007.06.002>
- Smith-Unna, R., Boursnell, C., Patro, R., Hibberd, J. M., & Kelly, S. (2016). TransRate: Reference-free quality assessment of de novo transcriptome assemblies. *Genome Research*, *26*(8), 1134–1144. <https://doi.org/10.1101/gr.196469.115>
- Solomon, P. (2017). HaveI finally opened the door to understanding *Septoria tritici* blotch disease in wheat? *The New Phytologist*, *214*(2), 493–495.

- Sorbara, M. T., & Pamer, E. G. (2019). Interbacterial mechanisms of colonization resistance and the strategies pathogens use to overcome them. *Mucosal Immunology*, *12*(1), 1–9.
<https://doi.org/10.1038/s41385-018-0053-0>
- Sperschneider, J., Dodds, P. N., Gardiner, D. M., Singh, K. B., & Taylor, J. M. (2018). Improved prediction of fungal effector proteins from secretomes with EffectorP 2.0: Prediction of fungal effectors with EffectorP 2.0. *Molecular Plant Pathology*, *19*(9), 2094–2110.
<https://doi.org/10.1111/mpp.12682>
- Steinegger, M., & Söding, J. (2017). MMseqs2 enables sensitive protein sequence searching for the analysis of massive data sets. *Nature Biotechnology*, *35*(11), 1026–1028.
<https://doi.org/10.1038/nbt.3988>
- Stewart, J. E., Kim, M.-S., Lalande, B., & Klopfenstein, N. B. (2021). Pathobiome and microbial communities associated with forest tree root diseases. In *Forest Microbiology* (pp. 277–292). Elsevier. <https://doi.org/10.1016/B978-0-12-822542-4.00004-8>
- Stone, J. K. (1987). Initiation and development of latent infections by *Rhizoctonia parkeri* on Douglas-fir. *Canadian Journal of Botany*, *65*(12), 2614–2621.
<https://doi.org/10.1139/b87-352>
- Stone, J. K., Polishook, J. D., & White, J. F. (2004). ENDOPHYTIC FUNGI. In *Biodiversity of Fungi* (pp. 241–270). Elsevier. <https://doi.org/10.1016/B978-012509551-8/50015-5>
- Sun, X., Wang, F., Cai, H., Zhao, C., Ji, W., & Zhu, Y. (2013). Functional characterization of an Arabidopsis prolyl aminopeptidase AtPAP1 in response to salt and drought stresses. *Plant Cell, Tissue and Organ Culture (PCTOC)*, *114*(3), 325–338.
<https://doi.org/10.1007/s11240-013-0328-9>

- Szawłowska, U., Grabowska, A., Zdunek-Zastocka, E., & Bielawski, W. (2012). TsPAP1 encodes a novel plant prolyl aminopeptidase whose expression is induced in response to suboptimal growth conditions. *Biochemical and Biophysical Research Communications*, *419*(1), 104–109. <https://doi.org/10.1016/j.bbrc.2012.01.140>
- Tang, D., Wang, G., & Zhou, J.-M. (2017). Receptor Kinases in Plant-Pathogen Interactions: More Than Pattern Recognition. *The Plant Cell*, *29*(4), 618–637. <https://doi.org/10.1105/tpc.16.00891>
- Teixeira, P. J. P. L., Thomazella, D. P. de T., Reis, O., do Prado, P. F. V., do Rio, M. C. S., Fiorin, G. L., José, J., Costa, G. G. L., Negri, V. A., Mondego, J. M. C., Mieczkowski, P., & Pereira, G. A. G. (2014). High-Resolution Transcript Profiling of the Atypical Biotrophic Interaction between *Theobroma cacao* and the Fungal Pathogen *Moniliophthora perniciosa*. *The Plant Cell*, *26*(11), 4245–4269. <https://doi.org/10.1105/tpc.114.130807>
- Terhonen, E., Blumenstein, K., Kovalchuk, A., & Asiegbu, F. O. (2019). Forest Tree Microbiomes and Associated Fungal Endophytes: Functional Roles and Impact on Forest Health. *Forests*, *10*(1), 42. <https://doi.org/10.3390/f10010042>
- Urban, M., Cuzick, A., Seager, J., Wood, V., Rutherford, K., Venkatesh, S. Y., De Silva, N., Martinez, M. C., Pedro, H., Yates, A. D., Hassani-Pak, K., & Hammond-Kosack, K. E. (2019). PHI-base: The pathogen–host interactions database. *Nucleic Acids Research*, *gkz904*. <https://doi.org/10.1093/nar/gkz904>
- Vleeshouwers, V. G. A. A., & Oliver, R. P. (2014). Effectors as Tools in Disease Resistance Breeding Against Biotrophic, Hemibiotrophic, and Necrotrophic Plant Pathogens.

- Molecular Plant-Microbe Interactions*®, 27(3), 196–206. <https://doi.org/10.1094/MPMI-10-13-0313-IA>
- Wang, Q., Garrity, G. M., Tiedje, J. M., & Cole, J. R. (2007). Naïve Bayesian Classifier for Rapid Assignment of rRNA Sequences into the New Bacterial Taxonomy. *Applied and Environmental Microbiology*, 73(16), 5261–5267. <https://doi.org/10.1128/AEM.00062-07>
- Wang, Y., Hu, H., & Li, X. (2017). rRNAFilter: A Fast Approach for Ribosomal RNA Read Removal Without a Reference Database. *Journal of Computational Biology*, 24(4), 368–375. <https://doi.org/10.1089/cmb.2016.0113>
- Wang, Y., Liu, H., Wang, S., Li, H., & Xin, Q. (2015). Overexpressing of a novel wheat prolyl aminopeptidase gene enhances zinc stress tolerance in transgenic *Arabidopsis thaliana*. *Plant Cell, Tissue and Organ Culture (PCTOC)*, 121(2), 489–499. <https://doi.org/10.1007/s11240-015-0719-1>
- White, T. J., Bruns, T., Lee, S., & Taylor, J. (1990). Amplification and direct sequencing of fungal ribosomal RNA genes for phylogenetics. In *PCR Protocols: A Guide to Methods and Applications*. Edited by: Innis MA, Gelfand DH, Sninsky JJ, White TJ (pp. 315–322). Academic Press Inc.
- Worrall, J. J., Marchetti, S. B., & Mask, R. A. (2012). An Epidemic of Needle Cast on Lodgepole Pine in Colorado. In *Biological Evaluation R2-12-01* (p. 16). USDA Forest Service, Rocky Mountain Region, Forest Health Protection.
- Würth, D. G., Dahl, M. B., Trouillier, M., Wilmking, M., Unterseher, M., Scholler, M., Sørensen, S., Mortensen, M., & Schnittler, M. (2019). The needle mycobiome of *Picea*

- glauca – A dynamic system reflecting surrounding environment and tree phenological traits. *Fungal Ecology*, 41, 177–186. <https://doi.org/10.1016/j.funeco.2019.05.006>
- Xu, L., Dong, Z., Fang, L., Luo, Y., Wei, Z., Guo, H., Zhang, G., Gu, Y. Q., Coleman-Derr, D., Xia, Q., & Wang, Y. (2019). OrthoVenn2: A web server for whole-genome comparison and annotation of orthologous clusters across multiple species. *Nucleic Acids Research*, 47(W1), W52–W58. <https://doi.org/10.1093/nar/gkz333>
- Yang, F., Li, W., & Jørgensen, H. J. L. (2013). Transcriptional Reprogramming of Wheat and the Hemibiotrophic Pathogen *Septoria tritici* during Two Phases of the Compatible Interaction. *PLoS ONE*, 8(11), e81606. <https://doi.org/10.1371/journal.pone.0081606>
- Ye, W., Liu, T., Zhang, W., Li, S., Zhu, M., Li, H., Kong, Y., & Xu, L. (2019). Disclosure of the Molecular Mechanism of Wheat Leaf Spot Disease Caused by *Bipolaris sorokiniana* through Comparative Transcriptome and Metabolomics Analysis. *International Journal of Molecular Sciences*, 20(23), 6090. <https://doi.org/10.3390/ijms20236090>
- Zeng, Z., Raffaello, T., Liu, M.-X., & Asiegbu, F. O. (2018). Co-extraction of genomic DNA & total RNA from recalcitrant woody tissues for next-generation sequencing studies. *Future Science OA*, 4(6), FSO309. <https://doi.org/10.4155/fsoa-2018-0026>
- Zhang, H., Yohe, T., Huang, L., Entwistle, S., Wu, P., Yang, Z., Busk, P. K., Xu, Y., & Yin, Y. (2018). dbCAN2: A meta server for automated carbohydrate-active enzyme annotation. *Nucleic Acids Research*, 46(W1), W95–W101. <https://doi.org/10.1093/nar/gky418>
- Zhao, J. (2015). Phospholipase D and phosphatidic acid in plant defence response: From protein–protein and lipid–protein interactions to hormone signalling. *Journal of Experimental Botany*, 66(7), 1721–1736. <https://doi.org/10.1093/jxb/eru540>

Zwiers, L.-H., Stergiopoulos, I., Gielkens, M. M. C., Goodall, S. D., & De Waard, M. A. (2003).

ABC transporters of the wheat pathogen *Mycosphaerella graminicola* function as protectants against biotic and xenobiotic toxic compounds. *Molecular Genetics and Genomics*, 269(4), 499–507. <https://doi.org/10.1007/s00438-003-0855-x>

CHAPTER 4: DEVELOPMENT OF PCR-BASED MARKERS FOR THE IDENTIFICATION
AND DETECTION OF LOPHODERMELLA NEEDLE CAST PATHOGENS ON *PINUS*
CONTORTA AND *P. FLEXILIS*

Introduction

Recent increasing prevalence of needle diseases have been attributed to several factors such as the enhanced activity of needle pathogens brought about by regional warm rain events (Gray et al., 2013; Rodas et al., 2016; Welsh et al., 2014), the emergence of new needle pathogens that may be previously cryptic or latent (e.g., Dick et al., 2014; Durán et al., 2008), and the introduction and spread of needle pathogens in vulnerable ecosystems due to the expansion of international trade (EFSA Panel on Plant Health, 2013). While previous occurrences caused minor damage, the increasing severity of needle diseases leads to severe ecological and economic losses of ecosystem goods and services (EFSA Panel on Plant Health, 2013; Jansons et al., 2020), and to possible forest decline as they predispose stressed forest trees to other diseases (Wyka et al., 2018). However, efficient monitoring and control of diseases caused by these emerging forest pathogens are often undermined by our limited understanding of their disease mechanisms and lack of tools for accurate disease diagnosis.

Lophodermella needle cast is a common disease in natural *Pinus contorta* stands in the Rocky Mountain Region (RMR), USA (Rocky Mountain Region, Forest Health Protection, 2010). In 2008 to 2011, two *Lophodermella* needle cast epidemics in natural *P. contorta* stands in Colorado were recorded with small but heavily infected forest patches (Worrall et al., 2012). Symptoms include discoloration and defoliation of infected needles that could severely affect highly compromised trees (Darker, 1932; Worrall et al., 2012). The recent epidemics were caused

by *Lophodermella concolor* (Dearn.) Darker and *L. montivaga* Petrak (Rhytismataceae), which are characterized by their tanned or colorless subhypodermal hysterothecia, clavate ascospores with mucilaginous sheath, and asci wider than *Lophodermium* species (Darker, 1932). While both pathogens occur in *P. contorta* stands in RMR, they have been reported infecting other two-needle pines in western states and provenances of USA and Canada, respectively, including *P. banksiana* for *L. concolor* and *P. attenuata* for *L. montivaga* (Darker, 1932; Minter & Millar, 1993). Recently, metabarcoding analysis detected both pathogens on symptomatic and asymptomatic *P. contorta* needles, indicating that *Lophodermella* pathogens were either part of the ‘normal’ needle mycobiota or existed as persistent infections that have evaded plant immune response, as shown in Chapter 3. However, despite their presence, there was no pathogenic activity of the fungal community in asymptomatic needles which further suggested a latent phase of *Lophodermella* infection, a trait common on other needle pathogens, that was not previously observed for *Lophodermella* species. This also indicated that *Lophodermella* spp. may be needle endophytes that could transition to pathogenic necrotrophs when environmental perturbations (e.g., biotic and abiotic stresses; Bass et al., 2019; Sieber, 2007) and/or host adaptation and stress response persist (Précigout et al., 2020; Shetty et al., 2007).

Needle cast in *P. flexilis* stands in RMR is commonly caused by *Lophodermella arcuata* (Darker) Darker and *Bifusella linearis* (Peck) Höhn. While *B. linearis* has been recorded in *P. strobus* and *P. monticola* (Broders et al., 2015; Darker, 1932), *L. arcuata* occurs only on five-needle pines such as *P. flexilis* in Colorado and *P. monticola* along the western Rockies (Darker, 1932; Minter & Millar, 1993). This pathogen can be distinguished among other *Lophodermella* species through the size of ascomata and ascospores, and host occurrence (Darker, 1932). Unlike its *Lophodermella* relatives that caused epidemics in *P. contorta*, *L. arcuata* historically only

caused insignificant damage in natural stands (Minter & Millar, 1993). However, its increasing presence together with *B. linearis* on *P. flexilis*, although not quantified, has been recently observed in RMR. In addition, *B. linearis* has been attributed to white pine needle damage together with other needle pathogens such as *Lecanosticta acicola* and *Lophophacidium dooksii* (Broders et al., 2015).

Pathogen identification and detection are vital for early and accurate disease diagnosis and monitoring. It enables access to necessary information (e.g., host specificity, mating systems and lifestyles) in addressing their potential threats (Crous et al., 2016). However, among *Lophodermella* species, rapid and accurate identification are impaired by similarities in symptomology and morphological characteristics, varied features across developmental stages, and lack of asexual structures (Darker, 1932; Worrall et al., 2012). Due to their cryptic and fastidious or potentially obligate lifestyle, rapid detection is also hampered as *Lophodermella* pathogens could remain asymptomatic in their hosts and cannot be isolated in pure cultures. With the challenges in fungal systematics and phenotypic identification, gene-based technologies for accurate identification and rapid detection of phytopathogens need to be integrated in quarantine and management systems (Crous et al., 2016).

Modern approaches improve plant fungal disease diagnosis with genetic and genomic tools, which are regarded as reliable and precise methods for rapidly identifying plant pathogens. While a variety of assays are now used to detect pathogens in forestry and agriculture, assays for conifer needle diseases are limited to only a few pathogens such as *Dothistroma pini*, *D. septosporum* and *Lecanosticta acicola* (Aglietti et al., 2021; Barnes et al., 2008; Janoušek et al., 2014; Myrholm et al., 2021; Siziba et al., 2016). Thus, this study aimed to develop molecular assays to rapidly identify and detect *Lophodermella* needle pathogens on *P. contorta* and *P. flexilis*.

I developed specific PCR-based primers from the internal transcribed spacer (ITS) region for *L. arcuata*, *L. concolor* and *L. montivaga*, including *Bifusella linearis*. To enhance robust detection and discrimination of co-existing *L. concolor* and *L. montivaga* on *P. contorta*, I also searched and designed primers from single-copy gene regions with the aid of genome sequences of related rhytismataceous species.

Methodology

Sample Collection and DNA Extraction

I used DNA from hysterothecia of *L. concolor*, *L. montivaga* and *L. arcuata* samples obtained by Ata et al., (2021), including the non-target species *Lophophacidium dooksii* (Table 4.1). In addition, DNA of *B. linearis* and non-target species (Table 4.2) were extracted from hysterothecia or potato dextrose agar-grown mycelia out of *P. contorta* needles using similar methods described by Ata et al. (2021). Briefly, hysterothecia on symptomatic needles or mycelia were excised or scraped, respectively. These were then ground into powder by submerging in liquid nitrogen and grinding using FastPrep prior to the CTAB method (Cubero et al., 1999). Quality and quantity of all DNA samples were determined using NanoDrop™ spectrophotometer.

Amplification of the ITS region of all the target and non-target species was performed in a 25- μ L PCR reaction mixture of 1 \times standard Taq reaction buffer (New England BioLabs), 0.2 mM of each dNTP (GoldBio), 0.4 μ M of each universal primer ITS1 and ITS4 (White et al. 1990), 0.625 units Taq polymerase (New England BioLabs), and ca. 40 ng template DNA. Cycle parameters included initial denaturation at 94 °C for 2 mins, followed by 30 cycles of denaturation at 94 °C for 40 s, annealing at 55 - 57°C for 40 s, extension at 72 °C for 1 min, and final extension

Table 4.1. PCR amplification using specific primers designed from the internal transcribed spacer (ITS) and gene cluster 2175 on *Lophodermella* spp. and *Bifusella linearis* (Rhytismataceae) samples collected from *Pinus contorta* and *P. flexilis* stands in Colorado (CO) and in Maine (ME), USA. Plus (+) and minus (-) signs represent presence and absence of a single band with target amplicon size, respectively.

Sample ID	Host	Region	GenBank Accession	ITS				2175		
				LC ITS	LM ITS	LA ITS	BL ITS	RH 2175	LC 2175	LM 2175
<i>Lophodermella concolor</i> (Dearn.) Darker										
CS9C	<i>P. contorta</i>	CO	MN937612	+	-	-	-	+	+	-
FS8C	<i>P. contorta</i>	CO	MN937610	+	-	-	-	+	+	-
OBJ9C	<i>P. contorta</i>	CO	NA	+	-	NA	NA	+	+	-
SR3C	<i>P. contorta</i>	CO	MN937617	+	-	NA	NA	+	+	-
FS6C	<i>P. contorta</i>	CO	MN937618	+	NA	-	-	+	+	-
<i>Lophodermella montivaga</i> Petrak										
CU1M	<i>P. contorta</i>	CO	MN937633	-	+	-	-	+	-	+
NC2M	<i>P. contorta</i>	CO	MN937625	-	+	-	-	+	-	+
NC10M	<i>P. contorta</i>	CO	MN937637	-	+	-	-	+	-	+
NC6M	<i>P. contorta</i>	CO	MN937626	-	+	NA	NA	+	-	+
PT11M	<i>P. contorta</i>	CO	MN937630	-	+	NA	NA	+	-	+
<i>Lophodermella arcuata</i> (Darker) Darker										
RMNP_LU1	<i>P. flexilis</i>	CO	MN937644	NA	-	+	NA	+	-	+
RMNP_LU16	<i>P. flexilis</i>	CO	MT906333	-	-	+	-	+	-	+
RMNP_LU12	<i>P. flexilis</i>	CO	NA	-	-	+	-	-	NA	NA

<i>Bifusella linearis</i> (Peck) Höhn.										
BiTR	<i>P. flexilis</i>	CO	NA	–	–	–	+	+	–	–
BP20	<i>P. flexilis</i>	CO	NA	–	–	–	+	+	–	–
MB02	<i>P. strobilus</i>	ME	NA	–	–	–	+	+	–	–

Primers are designed for *L. concolor* (LC), *L. montivaga* (LM), *L. arcuata* (LA), *Bifusella linearis* (BL) and species within Rhytismataceae (RH)

Table 4.2. Non-target species used in the study to test specificity of primers for *Lophodermella concolor* and *L. montivaga* on *Pinus contorta*, and *Bifusella linearis* and *L. arcuata* on *P. flexilis*.

Sample ID	ITS BLAST ID	GenBank	% Identity (e-value)	Family	Host	Material
<i>DNA samples</i>						
InfNSA 1	<i>Alternaria alternata</i> YZU	MN615420.1	100 (0.0)	Pleosporaceae	<i>P. contorta</i>	Mycelium
EDSR1 9	<i>Davisomycella medusa</i> BPI842078	AY465525.1	94.86 (6e-105)	Rhytismataceae	<i>P. contorta</i>	Hysterothecia
PTKN9 AP	<i>Hendersonia pinicola</i> EBJul30-4	KT000192.1	100 (0.0)	Phaeosphaeriaceae	<i>P. contorta</i>	Mycelium
T2-WY	<i>Mycosphaerella</i> sp. sd3cN2b	AY465456.1	100 (0.0)	Mycosphaerellaceae	<i>P. contorta</i>	Hysterothecia
GLRC	<i>Lophodermium nitens</i> NB-283-2D	KY485136.1	100 (4e-173)	Rhytismataceae	<i>P. flexilis</i>	Mycelium
SD_B	<i>Lophodermium resinosum</i> LPiPres2_12_3	MW466468.1	95.60 (0.0)	Rhytismataceae	<i>P. contorta</i>	Mycelium
MB05	<i>Lophophacidium dooksii</i>	KF889693.1	98.94 (0.0)	Rhytismataceae	<i>P. strobilus</i>	Hysterothecia
InfNSA P2	<i>Thielavia</i> sp. SR-6	MK246011.1	99.78 (0.0)	Chaetomiaceae	<i>P. contorta</i>	Mycelium
WWFB B.1	<i>Sydowia polyspora</i> ENDO-PINE669-BOTTOMA	MK762617.1	100 (0.0)	Dothioraceae	<i>P. ponderosa</i>	Mycelium
ED- AZ2	<i>Epicoccum layuense</i> isolate 17	MT573479.1	100 (0.0)	Didymellaceae	<i>P. ponderosa</i>	Mycelium

<i>JGI Mycosm genome sequences</i>				
Species	Label/ID	Family	Assembly Length (bp)	Genes Count
<i>Elytroderma deformans</i>	CBS 183.68 v1.0	Rhytismataceae	50,483,512	12,886
<i>Lophodermium nitens</i>	PLMe3-1-3 v1.0	Rhytismataceae	74,665,558	19,985
<i>Pseudographis elatina</i>	Pseel1	Rhytismataceae	36,124,988	11,338
<i>Coccomyces strobi</i>	CBS 202.91 v1.0	Rhytismataceae	32,666,196	11,537
<i>Spathularia flavida</i>	Spaf11	Rhytismataceae	35,536,079	9,941
<i>Bulgaria inquinans</i>	CBS 118.31 v1.0	Bulgariaceae	26,108,822	9,864
<i>Rutstroemia firma</i>	CBS 116.86 v1.0	Rutstroemiaceae	44,266,318	13,359
<i>Thelebolus microsporus</i>	ATCC 90970 v1.0	Thelebolaceae	27,344,100	10,290

at 72 °C for 5 mins. Sterile molecular grade H₂O was used as negative control throughout the assays. All amplifications were carried out in Eppendorf Mastercycler ProS thermal cycler. PCR products were analyzed on 1.5% agarose gels in 0.5 × TBE and photographed using Azure™ gel imaging system. Enzymatic cleanup was performed among PCR amplicons using Affymetrix™ ExoSAP-IT. All amplicons were sequenced by Eurofins Genomics. The ITS sequences of *B. linearis* and non-target species were then matched to the National Center for Biotechnology Information (NCBI) database (NCBI Resource Coordinators et al., 2018) using NCBI BLAST to search for highly similar fungal sequences. Cloning of PCR products was performed using pGEM® T-Easy Vector Systems (Promega) among randomly selected samples to validate that the sequenced amplicon for each sample was that of a single species.

Primer Development and Assay from ITS Region

Specific primers for *L. concolor* (LC_ITS), *L. montivaga* (LM_ITS), *L. arcuata* (LA_ITS) and *B. linearis* (BL_ITS) were developed based on the ITS sequences of the target fungal samples (Table 4.3). Primers were designed and initially screened using the Primer 3 module (v2.3.4; Untergasser et al., 2012) in Geneious (v R9.05). Primer sets were tested across *Lophodermella* spp. and among non-target species. Direct PCR amplifications were performed with similar 25 µL-PCR reaction mixture as described above but using only ca. 10 ng template DNA. Cycle conditions were also similar as described above except for the annealing temperatures, as shown in Table 3.

Primer Development and Assay from Genomic Data

Genomic data of five Rhytismataceae species and three outgroup species from the Joint Genome Institute MycoCosm (Grigoriev et al., 2014) were used to explore primers from other genomic regions (Table 4.2). Multigene clusters among these genomes were identified from the

Table 4.3. Primers developed for *Lophodermella concolor*, *L. montivaga* and *Bifusella linearis* and their parameters for direct and nested PCR amplification.

Gene Region/ Cluster	Target Pathogen	Primer Name	Direction	Sequence	Annealing Temperature (°C)	Number of Cycles	Product Length (bp)
Direct PCR							
ITS	<i>L. concolor</i>	LC_ITS	Forward	TGAGCTTCTCACCCCTGTA	66	35	260
			Reverse	GAGCTTGAGGGCTGGTTGAT			
	<i>L. montivaga</i>	LM_ITS	Forward	CCTGGTAAACTCGCACCCCT	70	30	259
			Reverse	GCTTGAGGGTTGTAATGACGC			
	<i>B. linearis</i>	BL_ITS	Forward	TTGCAGTCTGAGTACCACAC	65	35	248
			Reverse	TACTGCGCTGGAGCTTAGAT			
	<i>L. arcuata</i>	LA_ITS	Forward	GCCTGGTAACTCACACCTC	58	30	338
			Reverse	GTACTACGCTTAGGGGGCA			
Nested PCR							
2175	Rhytismataceae	RH_2175	Forward	CTGCTATCGGAGAAGAAGAT	49	35	525
			Reverse	TTGATGTTTCCAAGAGCTTG			
	<i>L. concolor</i>	LC_2175	Forward	TCTCTGACGAGCGTGATATT	68	35	215
			Reverse	ATGAACCTCCAACCCTAATC			
	<i>L. montivaga</i>	LM_2175	Forward	CTGACCAGCTCGACATCAAA	65	30	212
			Reverse	ATGAGCCTCCGACCTTGATA			

Joint Genome Institute (JGI) MycoCosm (<https://mycocosm.jgi.doe.gov/clm/run/Elyde1-comparative.2723;gwnsxm?organism=Elyde1>). Amino acid sequences were extracted and aligned using MUSCLE. Codon alignments per cluster were generated using PAL2NAL with -nomismatch parameter (Suyama et al. 2006). Single copy orthologs were selected to limit sequence variations within a species. To further reduce the number of orthologs to be analyzed, only clusters with a gene length < 2000 bp were considered. Sequence alignments of candidate clusters were then randomly selected and manually inspected for variations between Rhytismataceae species and outgroups. Primer sets were then designed from eight candidate gene clusters using Primer 3 and screened for specificity to rhytismataceous target and non-target species. Of these, the primer set (exterior primer) of only one gene cluster (RH_2175) was selected due to its clear amplification among rhytismataceous species. This region was then used for designing nested PCR primers specifically for *L. concolor* and *L. montivaga*. PCR amplification of RH_2175 was carried out using a 25 μ L PCR reaction mixture described above with 10 ng of template DNA with cycle parameters shown in Table 3.

The amplified RH_2175 region of *L. concolor* and *L. montivaga* were then sequenced to identify nucleotide polymorphisms in both *Lophodermella* species. Species-specific primers (interior primers) LC_2175 and LM_2175 were then designed from polymorphic sites using Primer 3 (Table 4.3). PCR amplification using these specific primers was carried out using the previously described 25 μ L-PCR reaction mixture with 4 μ L of diluted PCR product (1:100) generated from the RH_2175 amplification and cycle parameters presented in Table 3. Cycle conditions, except for annealing temperature, for the nested PCR amplification assay was similar as described above.

In silico and In vitro Primer Testing

The designed ITS and 2175 primers were tested for specificity *in silico* using NCBI Primer BLAST with nr and Refseq representative genomes databases, respectively, prior to *in vitro* assays. I also tested the *Lophodermella* specific 2175 gene primers against the genome sequences of related species available at JGI Mycocosm using Primer 3. *In vitro* primer assays were performed on available non-target species (Table 4.4) following the PCR conditions for each specific primer set. Available ITS sequences of other *Lophodermella* spp. and closely related species, including RH_2175 amplicon sequences were aligned using the MUSCLE module in Geneious (v R9.05).

Detection of Lophodermella Pathogens on Environmental Samples

Given the endophytic lifestyle of some needle pathogens, we used whole symptomatic and asymptomatic needles of *P. contorta* and *P. flexilis* to assess the sensitivity of primers. Specifically, two sets of environmental samples were tested. The first set of samples (SET 1) were obtained from Chapter 3. These were DNA samples from asymptomatic (n=12) and symptomatic (n=8) *P. contorta* needles infected with either *L. concolor* or *L. montivaga* (Figure 4.1, Table 4.5) with estimates of *L. concolor* and/or *L. montivaga* contigs which were obtained through sequencing of the internal transcribed spacer (ITS) region [ITS3: (GCATCGATGAAGAACGCAGC) and ITS4: (TCCTCCGCTTATTGATATGC)] via Illumina MiSeq (NCBI SRA Bioproject PRJNA7531). The second set (SET 2) were asymptomatic needles of *P. contorta* and *P. flexilis* collected from Colorado and Wyoming, USA without associated metabarcoding data.

Needle cleaning and DNA extraction were performed prior to DNA extraction. Briefly, two to three needles per tree were pooled for each sample. Needles were washed by vortexing in

Table 4.4. Amplification using primers designed for *Lophodermella concolor* (LC) and *L. montivaga* (LM) on *Pinus contorta*, and *Bifusella linearis* (BL) and *L. arcuata* (LA) on *P. flexilis* on non-target species. RH represents primers designed for species within Rhytismataceae. Single asterisk (*) represents single band but not the target size, double asterisk (**) represents multiple bands. Plus (+) and minus (-) signs represent presence and absence of a single band with target amplicon size, respectively.

Sample (NCBI BLAST ID)	Location	ITS				2175		
		LC_ITS	LM_ITS	LA_ITS	BL_ITS	RH_2175	LC_2175	LM_2175
InfNSA1 (<i>Alternaria alternata</i>)	Wyoming	-	-	-	-	*	-	-
PTKN9AP (<i>Hendersonia pinicola</i>)	Colorado	-	-	-	-	-	-	-
GLRC (<i>Lophodermium nitens</i>)	Colorado	-	-	-	-	+	-	-
SD_B (<i>Lophodermium resinsum</i>)	South Dakota	-	-	-	-	+	-	-
InfNSAP2 (<i>Thielavia</i> sp.)	Wyoming	-	-	-	-	*	-	-
WWFB B.1 (<i>Sydowia polyspora</i>)	Colorado	-	-	-	-	**	-	-
ED-AZ2 (<i>Epicoccum layuense</i>)	Arizona	-	-	-	-	**	-	-
MB05 (<i>Lophophacidium dooksii</i>)	New Hampshire	-	-	-	+	+	-	+
ED-19 (<i>Davisomycella</i> sp.)	Colorado	-	-	-	-	+	-	-
T2-WY (<i>Mycosphaerella</i> sp.)	Wyoming	-	-	-	-	+	-	-



Figure 4.1. Needles of *Pinus contorta* that were asymptomatic and symptomatic of either *L. concolor* and *L. montivaga* (A), and asymptomatic needles of *P. flexilis* (B).

Table 4.5. Amplification using primers designed for *Lophodermella concolor* (LC) and *L. montivaga* (LM) on *Pinus contorta*, and *Bifusella linearis* (BL) and *L. arcuata* (LA) on *P. flexilis* on *P. contorta* needles asymptomatic and symptomatic of *L. concolor* and *L. montivaga* and asymptomatic *P. flexilis* needles. RH represents primers designed for species within Rhytismataceae. Asterisk (*) represents faint single band. Plus (+) and minus (-) signs represent presence and absence of a single band with target amplicon size, respectively. Pound sign (#) represents primer assay requiring high concentration of primer set. Number of contigs obtained from NCBI Bioproject PRJNA753461.

Sample ID	Host	DNA Amount (ng)	Number of Contigs		ITS				2175		
			LC	LM	LC_ITS	LM_ITS	BL_ITS	LA_ITS	RH_2175	LC_2175	LM_2175
<i>SET 1: Asymptomatic needles</i>											
CS02-19CN	<i>P. contorta</i>	150	271	0	-	-	NA	NA	-	-	-
LV01-19CN	<i>P. contorta</i>	148	34,489	0	+	-	NA	NA	+	+	-
LV02-18MN	<i>P. contorta</i>	146	22,078	18,744	+	+	NA	NA	-	+	+
LP02-19CN	<i>P. contorta</i>	150	4,260	336	+	-	NA	NA	-	-	-
MP02-19CN	<i>P. contorta</i>	150	18,629	33	+	-	NA	NA	-	+	-
NC02-19CN	<i>P. contorta</i>	150	859	6,300	-	-	NA	NA	-	-	-
NC11-19MN	<i>P. contorta</i>	150	14,933	2,360	+#	+#	NA	NA	-	+#	-
NC13-19MN	<i>P. contorta</i>	150	23,931	152	+	-	NA	NA	-	+	-
PT11-19CN	<i>P. contorta</i>	150	6,363	7,066	-	-	NA	NA	-	-	-
TC03-19MN	<i>P. contorta</i>	150	19,183	121	+	+	NA	NA	-	+	-
TC07-19CN	<i>P. contorta</i>	150	3,033	28	-	-	NA	NA	-	-	-

TC09-19CN	<i>P. contorta</i>	110	10,857	0	+#	-	NA	NA	-	+	-
<i>SET 1: Symptomatic needles</i>											
NC04-18MP	<i>P. contorta</i>	15	3	63,789	-	+	NA	NA	+	-	+
OBJ10-19CP	<i>P. contorta</i>	15	42,459	0	+	-	NA	NA	+	+	-
TC03-19CP	<i>P. contorta</i>	15	53,718	9	+	-	NA	NA	+	+	-
TC05-19CP	<i>P. contorta</i>	15	52,241	0	+	-	NA	NA	+	+	-
LP06-19CP	<i>P. contorta</i>	15	38,751	0	+	-	NA	NA	+	+	-
NC11-19CP	<i>P. contorta</i>	15	48,366	0	+	-	NA	NA	+	+	-
PT01-19CP	<i>P. contorta</i>	15	34,845	0	+	-	NA	NA	+	+	-
NC11-19MP	<i>P. contorta</i>	15	17	53,102	-	+	NA	NA	+	-	+
<i>SET 2</i>											
T1U	<i>P. contorta</i>	150	NA	NA	-	-	-	-	-	+	-
SA1U	<i>P. contorta</i>	150	NA	NA	-	-	-	-	-	-	-
SEED2U	<i>P. contorta</i>	150	NA	NA	-	-	-	-	-	-	-
PN22U	<i>P. flexilis</i>	50	NA	NA	-	-	+	-	-	-	-
BP20U	<i>P. flexilis</i>	50	NA	NA	-	-	-	-	-	-	-
BP17U	<i>P. flexilis</i>	50	NA	NA	-	-	+	-	-	+	-

a 0.2% Tween 20 solution and cleaned in 70% ethanol. To evaluate the removal of contamination, I followed Rajala et al. (2013) with modifications: randomly selected clean symptomatic and asymptomatic needles were washed with distilled water and vortexed for approximately 10 mins. The resulting rinse solution was used as template for ITS amplification with primers ITS1 and ITS4 (White et al., 1990). Amplification was only observed in symptomatic needles as spores can easily be dispersed with mature hysterothecia. Approximately 1 mm segment from the sheath-covered base was removed. Whole needle DNA was extracted using the CTAB method with similar modifications presented above. DNA samples were stored in -20°C prior to primer assays.

Direct and nested PCR amplifications were performed following the described assays for primers designed from regions ITS and cluster 2175, respectively. To determine the optimal DNA concentration, amplification was evaluated using the presence of *L. concolor* and/or *L. montivaga* on samples with associated metabarcoding data (Table 5). A prior test was performed that showed that 10ng and undiluted DNA with > 400ng amount did not yield any amplification. Thus, DNA concentration of asymptomatic needles was adjusted to be within the 110ng to 150ng range. A total of 15ng of DNA was used for symptomatic needle samples. Since no contigs of *L. arcuata* nor *B. linearis* were detected from the previous metabarcoding analysis, the SET 1 samples were only tested for the sensitivity of *L. concolor* and *L. montivaga* primers. All designed primers were tested among the SET 2 samples. To check the accuracy of amplification in only target species in asymptomatic needles, cleaned amplicons from direct and nested PCR assays were randomly selected for sequencing.

Results

Identification of Needle Pathogens and Non-Target Species

Amplification of the ITS region using the universal fungal primers ITS1 and 4 for *B. linearis* and non-target fungal species yielded quality sequences. All *B. linearis* samples matched to *B. linearis* sequence in NCBI (KT000195.1) with 99.02% to 99.55% identity (e-value 4e-152 to 0.0). Four out of the 10 non-target samples were identified as species within Rhytismataceae belonging to genera *Davisomycella* and *Lophodermium* with > 90% similarity to the NCBI sequences (Table 4.2). The other non-target samples belonged to six fungal families which include Pleosporaceae, Phaeosphaeraiaceae, Mycosphaerellaceae, Chaetomiaceae, Dothioraceae and Didymellaceae, with percent identities ranging from 99.78% to 100%.

Primer Specificity

In silico analyses showed no match of either the forward or reverse LC_ITS and the forward LM_ITS to the NCBI fungal database. However, the BL_ITS and LA_ITS matched the ITS sequences of *B. linearis* (GenBank accession numbers KT000195.1, KT000194.1, AY465527.1 and KT000193.1) and *L. arcuata* (AY465518.1) in the database, respectively. While exterior primer 2175 (RH_2175) had BLAST hits to other non-rhytismataceous genomes, none were predicted to produce the target amplicon length. Using JGI genome sequences of closely related species and three outgroups, RH_2175 only matched to *Elytroderma deformans*, *Lophodermium nitens*, *Pseudographis elatina*, *Coccomyces strobi* and *Spathularia flavida*, all within Rhytismataceae. The interior primers LC_2175 and LM_2175, however, had no match to any of the genome sequences.

For the *in vitro* assays, the PCR conditions were optimized for each primer to enhance specificity. The LM_ITS primer set had the highest annealing temperature at 70°C. Primers

designed from the ITS region amplified the expected sequence of the target species with amplicon lengths ranging from 248-338 bp (Tables 4.1 and 4.3), with a clear singular band in the electrophoresis gel (Supplementary Figures 8-14). There were no amplifications among the non-target samples using LC_ITS, LM_ITS and LA_ITS primer pairs based on the absence of a single band. While most of the non-target species did not yield any amplifications using the BL_ITS primer set, a single band was observed in *Lophophacidium dooksii* hysterothecia on *P. strobus* (MB05; Supplementary Figure 11), which may be due to *B. linearis* co-existing on the same *Pinus* host. After amplicon sequencing, the sequence matched to the *B. linearis* ITS sequences rather than to that of *L. dooksii*.

Out of the eight gene clusters screened for specificity, only the singleton gene region 2175 amplified the target size (409-527 bp) in most Rhytismataceae species. This gene was annotated as domain TCP-1/cpn60 chaperonin family for all the five rhytismataceous species and three outgroups. The tail end of this gene cluster in *Pseudographis elatina* and *Spathularia flavida* genomes was further annotated by JGI as cofilin/tropomyosin-type actin-binding protein domain. The low annealing temperature (49°C) for the exterior primer RH_2175 assay allowed the amplification of most target and non-target rhytismataceous species used in this study with an amplicon size of 525 bp, except for one sample of *L. arcuata* (RMNP_LU1) which contained only 1.2 ng DNA.

Most non-target species had either no amplification or had differently sized band/s using RH_2175 (Table 4.4, Supplementary Figure 12). A target amplicon size was produced in *Mycosphaerella* sp. (T2-WY) using RH_2175, but not with the species-specific primers LC_2175 and LM_2175. Assays for interior primers LC_2175 and LM_2175 showed clear amplification among *L. concolor* and *L. montivaga* samples, respectively, and discriminated these two coexisting

pathogens (Table 4.1, Supplementary Figures 13 and 14). Except for *L. arcuata* and *Lophophacidium dooksii*, other non-target species did not amplify using LC_2175 and LM_2175.

Primer Sensitivity

To test the sensitivity of primers, we utilized the DNA samples extracted from whole *P. contorta* and *P. flexilis* needles. Using the designed ITS and 2175 primers, amplifications were observed in most SET 1 DNA samples from *P. contorta* needles which were symptomatic and asymptomatic of *L. concolor* and *L. montivaga* (Table 4.5). Among symptomatic needles, the primers were able to detect the dominant pathogen despite the marginal presence of the other *Lophodermella* species. For example, LC_ITS and LC_2175 detected *L. concolor* in six symptomatic needle samples that contained more *L. concolor* contigs (<35,000) than *L. montivaga* contigs. Conversely, LM_ITS and LM_2175 detected *L. montivaga* in two *L. montivaga* dominated symptomatic needles.

Among SET 1 asymptomatic needles, LC_ITS and LM_ITS detected 58% of the 12 samples and 33% of the 9 samples that contained *L. concolor* and *L. montivaga*, respectively. Two samples (LV02-18MN and TC03-19MN) had an amplification for both LC_ITS and LM_ITS regions. Further, in sample TC03-19MN, LM_ITS detected *L. montivaga* despite low pathogen concentration (121 contigs). In contrast, despite a relatively heavy presence of *L. concolor* in TC09-19CN (10,857 contigs), a target size band was produced only after increasing the concentration of LC_ITS primer (100 μ M) although some faint bands were also observed.

Amplification of RH_2175 produced multiple faint bands among most *P. contorta* asymptomatic needles with no visible target size band (Supplementary Figure 12), which could suggest the presence of multiple non-target species as was observed in the metadata reported in Chapter 3. However, a clear target-sized band was observed in LV01-19CN and all symptomatic

needle samples, which may be due to the large number of rhytismataceous species (e.g., *L. concolor* and *L. montivaga*) relative to other asymptomatic needle samples. Interestingly, from the diluted amplicons produced in the first round of amplification, LC_2175 and LM_2175 detected both *L. concolor* and *L. montivaga*, respectively, in asymptomatic samples that had a relatively heavy pathogen presence (>11,000 and > 19,000 *L. concolor* and *L. montivaga* contigs; Table 4.5 and Supplementary Figures 13 and 14). While most of the amplifications were consistent between the specific ITS and 2175 primers, three asymptomatic samples (NC11-19MN, TC03-19MN and LP02-19CN) with relatively low *Lophodermella* contigs did not have a visible band using either LC_2175 or LM_2175 despite amplification using LC_ITS or LM_ITS. All sequenced amplicons from both specific ITS and 2175 primer assays matched to either *L. concolor* and/or *L. montivaga*.

Among SET 2 samples, BL_ITS amplification produced a band in two out of three asymptomatic *P. flexilis* samples, but none were produced with RH_2175 (Table 4.5, Supplementary Figures 11 and 12). *Lophodermella arcuata*, on the other hand, was not detected among *P. flexilis* asymptomatic needles. Interestingly, the DNA concentration of *P. flexilis* asymptomatic needles needed to be reduced from 150ng to 50ng to yield a band in the BL_ITS reaction. Sequencing of BL_ITS amplicons that showed a faint band across the two samples yielded only poor-quality sequences which is likely due to the low number of amplicons. Further, an LC_2175 band was observed in a 50ng asymptomatic sample of *P. flexilis* (BP17U). For SET 2 *P. contorta* asymptomatic needles, *L. concolor* was the only pathogen detected using LC_2175 in one sample (TIU). Amplicon sequence matched correspondingly to that of *L. concolor*.

Discussion

Here, I explored the use of multi-copy and single-copy gene regions to develop primers that would accurately identify and rapidly detect emerging needle cast pathogens, *Lophodermella*

spp. and *Bifusella linearis*, on *P. contorta* and *P. flexilis*, respectively. *In silico* and *in vitro* primer assays revealed the specificity and sensitivity of markers developed from ITS and 2175 gene regions, which will be useful in the early detection of the target pathogens for efficient forest disease monitoring. Further, through amplification of target regions using the designed primers, this study determined for the first time the latent lifestyle of obligate *Bifusella linearis* in *P. strobus* and *P. flexilis*.

Pathogen Identification and Detection using Specific ITS and RH_2175 Primers

The developed primers based on single nucleotide polymorphisms in the ITS and 2175 gene regions enabled delimitation of species and pathogen detection of asymptomatic needles, indicating the efficiency of multi- and single-copy gene regions in pathogen identification and disease diagnosis. The primers distinguished the target needle pathogens from the non-target fungal species, including foliar endophytes that are common members of the needle mycobiota (Deckert et al., 2002; Del Frari et al., 2019; Guo et al., 2004; Ridout & Newcombe, 2018; Soltani & Hosseini Moghaddam, 2015; Tanney & Seifert, 2017) and needle pathogens that occur on *P. contorta* in the RMR (Rocky Mountain Region Forest Health Protection, 2010).

However, one drawback was the amplification using LM_2175 in two non-target species that were closely related to *L. montivaga*, which could suggest insufficient polymorphic sites to allow further discrimination between close relatives. Phylogenetic analysis found that *L. arcuata*, *Lophophacidium dooksii* and *L. sulcigena* clustered together with *L. montivaga* in the *Lophodermella* (LOD) subclade, with 99.9 Bayesian posterior probability and 80.1 bootstrap support (Ata et al., 2021). Using the tools developed herein, while not specific to *L. montivaga*, LM_2175 could be used to discriminate *L. montivaga* from *L. concolor* coexisting within *P.*

contorta and to identify species within the LOD subclade, and then the presence of *L. montivaga* could be further confirmed through ITS-specific primer LM_ITS.

I detected both *Lophodermella* pathogens in some asymptomatic *P. contorta* needles using the designed primers (i.e., LC_ITS and LC_2175 for *L. concolor*, and LM_ITS and LM_2175 for *L. montivaga*), although a higher concentration of template DNA was needed. This further suggests primer efficiency using environmental DNA samples without potential interference from the fungal endophytes and *Pinus* hosts DNA. Interestingly, the ITS-based primers LC_ITS and LM_ITS had about 9% more positive detections than the 2175 primers, indicating a higher sensitivity of the ITS-based primers likely due to the multiple copies within the ITS region (Jurado et al., 2006; Salvioli et al., 2008; Tekpinar & Kalmer, 2019).

Despite primer specificity, with a low amount of target DNA, the detection efficacy of single copy gene-based primers is typically low (Kulik et al., 2020). This is likely why no amplification was observed in an *L. arcuata* sample with low DNA amount with RH_2175 despite this sample amplifying the ITS primers, and why no amplification occurred with LC_2175 and LM_2175 in some asymptomatic needles despite low pathogen contig counts obtained from previous metabarcoding data. While 2175-based primers can detect *Lophodermella* pathogens, my results indicate a larger pathogen load in asymptomatic needles is necessary for amplification with the LC_2175 and LM_2175 primer sets. However, the threshold range of pathogen load for such amplifications could not be determined due to the large gaps between *Lophodermella* contig counts across samples.

I further observed no amplification using LC_ITS in some asymptomatic needles despite pathogen presence or detection with LC_2175, which could be attributed to competition from mixed DNA templates for reaction reagents resulting in inefficient amplification of relatively low

abundant target DNA templates (Kalle et al., 2014). Thus, the increase in primer concentration that resulted in visible bands in TC09-19CN asymptomatic sample could have likely allocated primers for the relatively less abundant DNA templates including that of *L. concolor*. For these reasons, I recommend the use of both the ITS- and 2175-based primers to determine pathogen presence in asymptomatic needles.

With the aid of metabarcoding data, this study showed that the lack of amplification could suggest a low colonization of one or both pathogens. In contrast, the amplification/s of *L. concolor* and/or *L. montivaga* specific ITS and/or 2175 regions among asymptomatic samples could indicate the increasing presence and biomass changes of the *Lophodermella* pathogen/s which may influence disease occurrence. This enhanced abundance of latent needle pathogens, such as *Lophodermella* spp. in the microbiome, due to abiotic and biotic stresses is a common characteristic during pathogenic transitions from normal to a diseased state of the host (Bass et al., 2019; Sieber, 2007).

Genome Sequences of Related Species to Search for Markers

To search for single-copy gene regions among species with unavailable genome sequences (i.e., *L. concolor* and *L. montivaga*), this study demonstrated the use of genome sequences of non-target but closely related species to explore candidate gene regions with distinct polymorphisms to develop markers for non-model target species. Among the primers designed from eight candidate gene regions, only RH_2175 from gene cluster 2175 amplified samples that represented at least five rhytismataceous genera at a low optimal annealing temperature. Gene 2175 was annotated as TCP1/cpn60 chaperonin family (Grigoriev et al., 2014), a ubiquitous protein found in prokaryotes and eukaryotes. While essential in the assembly of actin and tubulin among fungi (Stoldt et al., 1996), the role of cytosolic chaperonin among eukaryotes in disease remains

unknown. Interestingly, chaperonin members among pathogenic bacteria are major antigenic proteins important in infection and immunity (Gupta, 1995; Ranford, 2002). However, in this present study, the relationship of amplifications using RH_2175 across target and non-target samples with the gene function was not further explored.

Detection of Lophodermella concolor on P. flexilis

My assays detected *L. concolor* in one of my three asymptomatic *P. flexilis* using LC_2175. This is a surprising finding since, on the basis of hysterothecia development, *L. concolor* has only been reported to occur on two-needle pines *P. banksiana* and *P. contorta* of subsection Contortae and *P. sylvestris* of subsection Pinus (Darker, 1932; Millar, 1984; Minter & Millar, 1993). As *P. flexilis* is present in *P. contorta* stands in the southern parts of Wyoming and northern Colorado (Steele, 1990), it is possible that *L. concolor* inoculum from infected *P. contorta* stands could infect, albeit rarely, nearby *P. flexilis* trees asymptotically. Thus, like other needle pathogens thriving as endophytes (Magan & Smith, 1996; Sieber et al., 1999; Stone et al., 2004), *L. concolor* may be endophytic in adjacent *P. flexilis* stands. Currently, there is no evidence to suggest pathogenicity of *L. concolor* in *P. flexilis*. Since there was no associated metabarcoding data for the SET2 asymptomatic needle samples, we cannot confirm the presence nor the amount of *L. concolor* within the samples. However, given the amplification observed in asymptomatic *P. contorta* needles, I surmise that a relatively heavy *L. concolor* load may have been present.

Detection of B. linearis on Environmental Samples

Using BL_ITS, I detected *B. linearis* present in *Lophophacidium dooksii* hysterothecia on *P. strobus* and asymptomatic *P. flexilis* needles, which likely indicates an endophytic or latent pathogen lifestyle of *B. linearis* and coinfection of both pathogens on *Pinus* hosts. Similar to *Lophodermella* spp., the inability of *B. linearis* to grow or have only ephemeral growth in culture

(Broders et al., 2015; Merrill et al., 1996) may have contributed to the lack of evidence on its latency in *Pinus* needles. Ganley et al. (2004) further reported that none of the media-grown endophytes of *P. monticola* were synonymous or closely related to the host's known foliar parasites such as *B. linearis* and *L. arcuata*. As *B. linearis* and *L. dooksii* were both attributed to *P. strobus* needle damage (Broders et al., 2015), the amplification using BL_ITS in *L. dooksii* from *P. strobus* could further indicate the ability of *B. linearis* to coexist asymptotically with other needle pathogens in an individual host. A cryptic lifestyle of *B. linearis* could pose a greater threat to pine forests as this species causes defoliation to multiple white pine hosts.

Challenges in using Primers for Accurate Latent Pathogen Identification and Detection

The detection of *B. linearis* in *L. dooksii* hysterothecia was further explored with ITS sequencing and ITS amplicon sequence matched *B. linearis* rather than *L. dooksii*, despite clear morphological and molecular characterization. Similarly, RH_2175 detected a rhytismataceous species on *Mycosphaerella* sp. hysterothecia. These amplifications may be caused by other rhytismataceous colonizers in a small piece of host tissue where hysterothecia were embedded. This type of contamination has also been observed in primers for specific arbuscular mycorrhizal fungi deeply embedded within plant roots (Redecker et al., 2003). Thus, hysterothecia immersed beneath the plant cuticle must be excised with care to avoid plant tissue that may contain target latent pathogens.

Primer development for closely-related taxa using environmental DNA assay could be confounded by unresolved taxonomy and intraspecific polymorphisms (Wilcox et al., 2015). As primer assays were performed among a limited set of foliar fungal endophytes from a small range of *P. contorta* stands, cross-amplification and interference may occur as more closely related endophytes that are rare and/or undescribed are tested. While target regions were successfully

amplified on asymptomatic needles despite the presence of a diverse endophytic community, more assays to test for false positives need to be conducted using asymptomatic needle samples or environmental DNA from a variety of populations and hosts.

As changes in climate that favors needle pathogens continue, molecular tools for needle pathogen identification and diagnosis are promising for efficient monitoring of needle disease outbreaks. While more sophisticated tools are available for a few needle pathogens, the PCR-based markers from single and multi-copy gene regions developed from this study can help diagnose needle diseases caused by emerging non-model fungal pathogens such as *Lophodermella* spp. and *Bifusella linearis*. Further, the ability of the primers to detect these pathogens on asymptomatic needles at a given pathogen abundance can help predict the onset of needle cast. With the taxon-specific primers, my study also demonstrates the use of environmental DNA for the early detection and surveillance of latent needle pathogens.

References

- Aglietti, C., Meinecke, C. D., Ghelardini, L., Barnes, I., van der Nest, A., & Villari, C. (2021). Rapid Detection of Pine Pathogens *Lecanosticta acicola*, *Dothistroma pini* and *D. septosporum* on Needles by Probe-Based LAMP Assays. *Forests*, *12*(4), 479. <https://doi.org/10.3390/f12040479>
- Arnold, A. E. (2007). Understanding the diversity of foliar endophytic fungi: Progress, challenges, and frontiers. *Fungal Biology Reviews*, *21*(2–3), 51–66. <https://doi.org/10.1016/j.fbr.2007.05.003>
- Ata, J. P., Burns, K. S., Marchetti, S., Munck, I. A., Beenken, L., Worrall, J. J., & Stewart, J. E. (2021). Molecular characterization and phylogenetic analyses of *Lophodermella* needle pathogens (Rhytismataceae) on *Pinus* species in the USA and Europe. *PeerJ*, *9*, e11435. <https://doi.org/10.7717/peerj.11435>
- Barnes, I., Cortinas, M. N., Wingfield, M. J., & Wingfield, B. D. (2008). Microsatellite markers for the red band needle blight pathogen, *Dothistroma septosporum*. *Molecular Ecology Resources*, *8*(5), 1026–1029. <https://doi.org/10.1111/j.1755-0998.2008.02142.x>
- Bass, D., Stentiford, G. D., Wang, H.-C., Koskella, B., & Tyler, C. R. (2019). The Pathobiome in Animal and Plant Diseases. *Trends in Ecology & Evolution*, *34*(11), 996–1008. <https://doi.org/10.1016/j.tree.2019.07.012>
- Broders, K., Munck, I., Wyka, S., Iriarte, G., & Beaudoin, E. (2015). Characterization of Fungal Pathogens Associated with White Pine Needle Damage (WPND) in Northeastern North America. *Forests*, *6*(12), 4088–4104. <https://doi.org/10.3390/f6114088>
- Crous, P. W., Groenewald, J. Z., Slippers, B., & Wingfield, M. J. (2016). Global food and fibre security threatened by current inefficiencies in fungal identification. *Philosophical*

- Transactions of the Royal Society B: Biological Sciences*, 371(1709), 20160024.
<https://doi.org/10.1098/rstb.2016.0024>
- Cubero, O. F., Crespo, A., Fatehi, J., & Bridge, P. D. (1999). DNA extraction and PCR amplification method suitable for fresh, herbarium-stored, lichenized, and other fungi. *Plant Systematics and Evolution*, 216(3–4), 243–249.
<https://doi.org/10.1007/BF01084401>
- Darker, G. (1932). *The Hypodermataceae of Conifers* (Vol. 1). Contributions from the Arnold Arboretum of Harvard University.
- Deckert, R. J., Hsiang, T., & Peterson, R. L. (2002). Genetic relationships of endophytic *Lophodermium nitens* isolates from needles of *Pinus strobus*. *Mycological Research*, 106(3), 305–313. <https://doi.org/10.1017/S0953756201005494>
- Del Frari, G., Cabral, A., Nascimento, T., Boavida Ferreira, R., & Oliveira, H. (2019). *Epicoccum layuense* a potential biological control agent of esca-associated fungi in grapevine. *PLOS ONE*, 14(3), e0213273. <https://doi.org/10.1371/journal.pone.0213273>
- Dick, M. A., Williams, N. M., Bader, M. K.-F., Gardner, J. F., & Bulman, L. S. (2014). Pathogenicity of *Phytophthora pluvialis* to *Pinus radiata* and its relation with red needle cast disease in New Zealand. *New Zealand Journal of Forestry Science*, 44(1), 6.
<https://doi.org/10.1186/s40490-014-0006-7>
- Durán, A., Gryzenhout, M., Slippers, B., Ahumada, R., Rotella, A., Flores, F., Wingfield, B. D., & Wingfield, M. J. (2008). *Phytophthora pinifolia* sp. Nov. Associated with a serious needle disease of *Pinus radiata* in Chile. *Plant Pathology*, 57(4), 715–727.
<https://doi.org/10.1111/j.1365-3059.2008.01893.x>

- EFSA Panel on Plant Health. (2013). Scientific Opinion on the risk to plant health posed by *Dothistroma septosporum* (Dorog.) M. Morelet (*Mycosphaerella pini* E. Rostrup, syn. *Scirrhia pini*) and *Dothistroma pini* Hulbary to the EU territory with the identification and evaluation of risk reduction options. *EFSA Journal*, 2013; 11(1):3026.
<https://doi.org/10.2903/j.efsa.2013.3026>
- Ganley, R. J., Brunfeld, S. J., & Newcombe, G. (2004). A community of unknown, endophytic fungi in western white pine. *Proceedings of the National Academy of Sciences*, 101(27), 10107–10112. <https://doi.org/10.1073/pnas.0401513101>
- Gray, L. K., Russell, J. H., Yanchuk, A. D., & Hawkins, B. J. (2013). Predicting the risk of cedar leaf blight (*Didymascella thujina*) in British Columbia under future climate change. *Agricultural and Forest Meteorology*, 180, 152–163.
<https://doi.org/10.1016/j.agrformet.2013.04.023>
- Grigoriev, I. V., Nikitin, R., Haridas, S., Kuo, A., Ohm, R., Otilar, R., Riley, R., Salamov, A., Zhao, X., Korzeniewski, F., Smirnova, T., Nordberg, H., Dubchak, I., & Shabalov, I. (2014). MycoCosm portal: Gearing up for 1000 fungal genomes. *Nucleic Acids Research*, 42(D1), D699–D704. <https://doi.org/10.1093/nar/gkt1183>
- Guo, L.-D., Xu, L., Zheng, W.-H., & Hyde, K. D. (2004). Genetic variation of *Alternaria alternata*, an endophytic fungus isolated from *Pinus tabulaeformis* as determined by random amplified microsatellites (RAMS). *Fungal Diversity*, 16, 53–65.
- Gupta, R. (1995). Evolution of chaperonin families (Hsp60, Hsp10 and Tcp-1) of proteins and the origin of eukaryotic cells. *Molecular Microbiology*, 15(1), 1–11.
- Janoušek, J., Krumböck, S., Kirisits, T., Bradshaw, R. E., Barnes, I., Jankovský, L., & Stauffer, C. (2014). Development of microsatellite and mating type markers for the pine needle

- pathogen *Lecanosticta acicola*. *Australasian Plant Pathology*, 43(2), 161–165.
<https://doi.org/10.1007/s13313-013-0256-5>
- Jansons, Ā., Zeltiņš, P., Donis, J., & Neimane, U. (2020). Long-Term Effect of *Lophodermium* Needle Cast on The Growth of Scots Pine and Implications for Financial Outcomes. *Forests*, 11(7), 718. <https://doi.org/10.3390/f11070718>
- Jurado, M., Vázquez, C., Marín, S., Sanchis, V., & Teresa González-Jaén, M. (2006). PCR-based strategy to detect contamination with mycotoxigenic *Fusarium* species in maize. *Systematic and Applied Microbiology*, 29(8), 681–689.
<https://doi.org/10.1016/j.syapm.2006.01.014>
- Kalle, E., Kubista, M., & Rensing, C. (2014). Multi-template polymerase chain reaction. *Biomolecular Detection and Quantification*, 2, 11–29.
<https://doi.org/10.1016/j.bdq.2014.11.002>
- Kulik, T., Biliska, K., & Źelechowski, M. (2020). Promising Perspectives for Detection, Identification, and Quantification of Plant Pathogenic Fungi and Oomycetes through Targeting Mitochondrial DNA. *International Journal of Molecular Sciences*, 21(7), 2645.
<https://doi.org/10.3390/ijms21072645>
- Magan, N., & Smith, M. K. (1996). Isolation of the endophytes *Lophodermium piceae* and *Rhizosphaera kalkhoffii* from Sitka spruce needles in poor and good growth sites and in vitro effects of environmental factors. *Phyton*, 36(3), 103–110.
- Merrill, W., Wenner, N. G., & Dreisbach, T. A. (1996). *Canavirgella banfieldii* gen. And sp. Nov.: A needle-cast fungus on pine. *Canadian Journal of Botany*, 74, 1476–1481.

- Millar, C. S. (1984). Lophodermella species on pines. *In: Recent Research on Conifer Needle Diseases*. Eds. Glenn W. Peterson. USDA Forest Service, General Technical Report GTR-WO 50., 45–55.
- Minter, D. W., & Millar, C. S. (1993). IMI Descriptions of Fungi and Bacteria. Lophodermella arcuata. *Mycopathologia*, 121(1), 49–50.
- Myrholm, C. L., Tomm, B. D., Heinzlmann, R., Feau, N., Hamelin, R. C., McDougal, R., Winkworth, R. C., & Ramsfield, T. D. (2021). Development of a Rapid Loop-Mediated Isothermal Amplification Assay for the Detection of Dothistroma septosporum. *Forests*, 12(3), 362. <https://doi.org/10.3390/f12030362>
- NCBI Resource Coordinators, Agarwala, R., Barrett, T., Beck, J., Benson, D. A., Bollin, C., Bolton, E., Bourexis, D., Brister, J. R., Bryant, S. H., Canese, K., Cavanaugh, M., Charowhas, C., Clark, K., Dondoshansky, I., Feolo, M., Fitzpatrick, L., Funk, K., Geer, L. Y., ... Zbicz, K. (2018). Database resources of the National Center for Biotechnology Information. *Nucleic Acids Research*, 46(D1), D8–D13. <https://doi.org/10.1093/nar/gkx1095>
- Précigout, P.-A., Claessen, D., Makowski, D., & Robert, C. (2020). Does the Latent Period of Leaf Fungal Pathogens Reflect Their Trophic Type? A Meta-Analysis of Biotrophs, Hemibiotrophs, and Necrotrophs. *Phytopathology*®, 110(2), 345–361. <https://doi.org/10.1094/PHTO-04-19-0144-R>
- Rajala, T., Velmala, S. M., Tuomivirta, T., Haapanen, M., Müller, M., & Pennanen, T. (2013). Endophyte communities vary in the needles of Norway spruce clones. *Fungal Biology*, 117(3), 182–190. <https://doi.org/10.1016/j.funbio.2013.01.006>

- Ranford, J. C. (2002). Chaperonins in disease: Mechanisms, models, and treatments. *Molecular Pathology*, 55(4), 209–213. <https://doi.org/10.1136/mp.55.4.209>
- Redecker, D., Hijri, I., & Weimken, A. (2003). Molecular identification of arbuscular mycorrhizal fungi in roots: Perspectives and problems. *Folia Geobotanica*, 38, 113–124.
- Ridout, M., & Newcombe, G. (2018). *Sydowia polyspora* is both a Foliar Endophyte and a Preemergent Seed Pathogen in *Pinus ponderosa*. *Plant Disease*, 102(3), 640–644. <https://doi.org/10.1094/PDIS-07-17-1074-RE>
- Rocky Mountain Region, Forest Health Protection. (2010). *Field guide to diseases & insects of the Rocky Mountain Region* (Gen. Tech. Rep. RMRS-GTR-241). Department of Agriculture, Forest Service, Rocky Mountain Research Station.
- Rodas, C. A., Wingfield, M. J., Granados, G. M., & Barnes, I. (2016). Dothistroma needle blight: An emerging epidemic caused by *Dothistroma septosporum* in Colombia. *Plant Pathology*, 65(1), 53–63. <https://doi.org/10.1111/ppa.12389>
- Salvioli, A., Lumini, E., Anca, I. A., Bianciotto, V., & Bonfante, P. (2008). Simultaneous detection and quantification of the unculturable microbe *Candidatus Glomeribacter gigasporarum* inside its fungal host *Gigaspora margarita*. *New Phytologist*, 180(1), 248–257. <https://doi.org/10.1111/j.1469-8137.2008.02541.x>
- Shetty, N. P., Mehrabi, R., Lütken, H., Haldrup, A., Kema, G. H. J., Collinge, D. B., & Jørgensen, H. J. L. (2007). Role of hydrogen peroxide during the interaction between the hemibiotrophic fungal pathogen *Septoria tritici* and wheat. *New Phytologist*, 174(3), 637–647. <https://doi.org/10.1111/j.1469-8137.2007.02026.x>
- Sieber, T. N. (2007). Endophytic fungi in forest trees: Are they mutualists? *Fungal Biology Reviews*, 21(2–3), 75–89. <https://doi.org/10.1016/j.fbr.2007.05.004>

- Sieber, T. N., Rys, J., & Holdenrieder, O. (1999). Mycobiota in symptomless needles of *Pinus mugo* ssp. *Uncinata*. *Mycological Research*, *103*(3), 306–310.
<https://doi.org/10.1017/S0953756298007229>
- Siziba, V. I., Wingfield, M. J., Sadiković, D., Mullett, M. S., Piškur, B., & Barnes, I. (2016). Development of microsatellite markers for the pine needle blight pathogen, *Dothistroma pini*. *Forest Pathology*, *46*(5), 497–506. <https://doi.org/10.1111/efp.12282>
- Soltani, J., & Hosseyni Moghaddam, M. S. (2015). Fungal Endophyte Diversity and Bioactivity in the Mediterranean Cypress *Cupressus sempervirens*. *Current Microbiology*, *70*(4), 580–586. <https://doi.org/10.1007/s00284-014-0753-y>
- Steele, R. (1990). *Pinus flexilis* James. In *Silvics of North America* (Vol. 1, pp. 348–354). U.S. Department of Agriculture.
- Stoldt, V., Rademacher, F., Kehren, V., Ernst, J. M., Pearce, D. A., & Sherman, F. (1996). Review: The Cct eukaryotic chaperonin subunits of *Saccharomyces cerevisiae* and other yeasts. *Yeast*, *12*, 523–529.
- Stone, J. K., Polishook, J. D., & White, J. F. (2004). ENDOPHYTIC FUNGI. In *Biodiversity of Fungi* (pp. 241–270). Elsevier. <https://doi.org/10.1016/B978-012509551-8/50015-5>
- Tanney, J. B., & Seifert, K. A. (2017). *Lophodermium resinosum* sp. Nov. From red pine (*Pinus resinosa*) in Eastern Canada. *Botany*, *95*(8), 773–784. <https://doi.org/10.1139/cjb-2017-0012>
- Tekpinar, A. D., & Kalmer, A. (2019). Utility of various molecular markers in fungal identification and phylogeny. *Nova Hedwigia*, *109*(1–2), 187–224.

- Untergasser, A., Cutcutache, I., Koressaar, T., Ye, J., Faircloth, B. C., Remm, M., & Rozen, S. G. (2012). Primer3—New capabilities and interfaces. *Nucleic Acids Research*, *40*(15), e115–e115. <https://doi.org/10.1093/nar/gks596>
- Welsh, C., Lewis, K. J., & Woods, A. J. (2014). Regional outbreak dynamics of *Dothistroma* needle blight linked to weather patterns in British Columbia, Canada. *Canadian Journal of Forest Research*, *44*(3), 212–219. <https://doi.org/10.1139/cjfr-2013-0387>
- White, T. J., Bruns, T., Lee, S., & Taylor, J. (1990). Amplification and direct sequencing of fungal ribosomal RNA genes for phylogenetics. In *PCR Protocols: A Guide to Methods and Applications*. Edited by: Innis MA, Gelfand DH, Sninsky JJ, White TJ (pp. 315–322). Academic Press Inc.
- Wilcox, T. M., Carim, K. J., McKelvey, K. S., Young, M. K., & Schwartz, M. K. (2015). The Dual Challenges of Generality and Specificity When Developing Environmental DNA Markers for Species and Subspecies of *Oncorhynchus*. *PLOS ONE*, *10*(11), e0142008. <https://doi.org/10.1371/journal.pone.0142008>
- Worrall, J. J., Marchetti, S. B., & Mask, R. A. (2012). An Epidemic of Needle Cast on Lodgepole Pine in Colorado. In *Biological Evaluation R2-12-01* (p. 16). USDA Forest Service, Rocky Mountain Region, Forest Health Protection.
- Wyka, S. A., Munck, I. A., Brazee, N. J., & Broders, K. D. (2018). Response of eastern white pine and associated foliar, blister rust, canker and root rot pathogens to climate change. *Forest Ecology and Management*, *423*, 18–26. <https://doi.org/10.1016/j.foreco.2018.03.011>

CHAPTER 5: SUMMARY AND CONCLUSIONS

Research Synthesis

Lophodermella needle cast is an emerging disease on *Pinus* attributed to the increasing frequency of warm rain events. It causes needle discoloration and defoliation that could lead to mortality among highly susceptible trees and could predispose host trees to other diseases. Recent Lophodermella needle cast epidemics severely affected a small but increasing number of patches of *P. contorta* stands in the Rocky Mountain Region (Worrall et al., 2012). Despite the need to control the disease, the knowledge on *Lophodermella* pathogens is limited which makes efficient disease management and phytosanitary measures difficult. Their unique lifestyles, particularly the lack of asexual spores (Darker, 1932; Minter & Millar, 1993) and the inability to grow in artificial culture media (Darker, 1932; Millar, 1984), also make it challenging to perform classical techniques to understand their pathogenic mechanisms. Adding to that is the difficulty in disease diagnosis due to the challenges in taxonomic identification and differentiation of *Lophodermella* species with other needle pathogens (Worrall et al., 2012). Thus, to fill in the gaps in our understanding of emerging *Lophodermella* needle pathogens, I made use of molecular genetic tools to (1) determine the phylogenetic relationship of *Lophodermella* spp. with its Rhytismataceae relatives using three gene regions, (2) analyze the structural and functional changes of the mycobiome in healthy vs. diseased *P. contorta* needles through next generation sequencing, and (3) develop primers from the multi- and single copy gene regions to efficiently identify and rapidly detect *Lophodermella* pathogens.

Understanding the phylogeny of emerging forest fungal pathogens is important in identifying patterns of shared and unique pathogenicity traits and in predicting new pathogen

outbreaks (Berbee, 2001; Gilbert & Parker, 2016). Thus, I analyzed the phylogeny of five *Lophodermella* needle cast pathogens on *Pinus* in North America and Europe (*L. arcuata*, *L. concolor*, *L. conjuncta*, *L. montivaga* and *L. sulcigena*) using three gene regions (i.e., internal transcribed spacer, large subunit ribosomal nucleic acid, and translation elongation factor), and compared their morphological characters from the resulting phylogeny to identify shared derived characters. The results highlighted a distinct clade composed of *Lophodermella* species and *Lophophacidium dooksii* within Rhytismataceae. Similar key morphological traits such as subhypodermal ascomata and ascospore shape for species delimitation within the clade could also indicate synapomorphy and could provide insights on their evolution. Further, I also observed a *Lophodermella* species on *P. flexilis* that is morphologically similar yet genetically distinct from *L. arcuata*, which suggests the presence of undescribed cryptic *Lophodermella* species. More investigations of *Lophodermella* species using advanced molecular tools can also help answer genetic, evolutionary and ecological inquiries such as on population structure, pathogenicity, host specialization, hybridization, and other biological inferences.

Profiling the composition and activity of fungal endophytes and pathogens in healthy vs. diseased forest ecosystems helps us understand their pathogenicity mechanisms and community interactions that could impact forest health (Anal et al., 2020; Terhonen et al., 2019). Here, I analyzed the structural and functional changes of the mycobiota in the *Lophodermella* needle cast caused by *L. concolor* and *L. montivaga* on *P. contorta* through next generation sequencing of DNA and RNA from asymptomatic and symptomatic needles. When needles transitioned from asymptomatic to symptomatic, a highly diverse mycobiome community was significantly reduced but with a remarkable enrichment of *Lophodermella* pathogens at the symptomatic state. In addition, a variety of pathogenicity-related genes that included carbohydrate and protein degrading

enzymes, effectors, and secondary metabolites was highly expressed by the mycobiome at the necrotrophic phase of the disease, indicating an active pathogen response in symptomatic needles that may be low or absent in asymptomatic needles. For the first time, this study also revealed that *Lophodermella* spp. are members of the *P. contorta* needle mycobiome in both asymptomatic and symptomatic needles. However, despite their significant presence, pathogenic activities were not detected in asymptomatic needles which suggests a period of dormant lifestyle of *Lophodermella* pathogens.

This study also revealed the response of the *P. contorta* host to the pathogenic activity of the mycobiota dominated by *L. concolor* and *L. montivaga*. Infected hosts upregulate various defense genes in healthy needles, indicating response to fungal recognition while a variety of genes related to biotic and abiotic stresses were activated in diseased needles. While triggers of pathogenic transition remain unknown, this study provided important insights into the host-microbial interactions in non-model pathosystems which can contribute to the development of new forest management strategies against emerging latent pathogens. Moreover, as expressed non-rhytismataceous and non-fungal genes were found in asymptomatic needles, this study recommends further investigation to elucidate the possible antagonistic interplay of other biotic members leading to disease progression and/or suppression.

Key to efficient forest disease management are accurate disease diagnosis and early detection despite morphological similarities and fastidious development of fungal needle pathogens (Luchi et al., 2020; McCartney et al., 2003). Thus, I developed and determined the specificity and sensitivity of PCR-based markers for *L. concolor* and *L. montivaga* co-occurring on *P. contorta*, and *L. arcuata* and *Bifusella linearis* on *P. flexilis* through ITS and rhytismataceous genome sequences. The specific ITS and 2175 primers successfully differentiated the needle

pathogens, although LM_2175 specific for *L. montivaga* also detected closely related needle pathogens of white pines. These primers also detected the target needle pathogens in environmental samples without the masking of DNA from plant host and other needle fungal endophytes. Caveats on the use of *Lophodermella* primers for accurate identification and detection were also discussed. While more sophisticated tools are available for a few needle pathogens, the PCR-based markers from this study can help diagnose needle diseases caused by emerging non-model fungal pathogens such as *Lophodermella* spp. and *Bifusella linearis*. Further, the ability of the primers to detect these latent pathogens on asymptomatic needles at certain levels of pathogen abundance can help predict the onset of needle cast.

Our little understanding of the disease mechanisms including the taxonomy, biology, and ecology of emerging non-model plant pathogens undermines their impact in forest ecosystem health and socioeconomic development. Thus, as forest diseases increasingly emerge with global change, there is a need to improve awareness on understudied yet emerging disease agents through available modern molecular approaches in forest pathology. This research unravels the evolutionary relationships and new cryptic relatives, unique lifestyles, interactions with host and mycobiota, and molecular diagnosis of the least known *Lophodermella* needle cast pathogens. The findings imply a vast occurrence of needle pathogens that could remain undetected and overlooked during disease surveys and/or quarantines until their rapid emergence to cause disease on stressed hosts. Dysbiosis in the needle mycobiota during disease also reveals a huge yet often underestimated impact of emerging needle diseases in the diversity and maintenance of ecologically important endophytes. Overall, it provided basic and applied molecular information about needle cast pathosystem dynamics, which serve as resources that will leverage forest management and policy on emerging forest diseases.

This research also unlocks exciting new questions and possible future research directions on conifer needle pathosystems. What are the mechanisms underpinning the dominance of one of two or more needle pathogens coexisting in *Pinus* hosts? How do environmental factors trigger molecular signatures between host and latent pathogen leading to pathogenic transitions? How do natural endophytes modify the activities of *Lophodermella* pathogens in resistant and susceptible host genotypes? Answers to these questions will further contribute to our understanding of conifer foliar pathosystems as a complex and dynamic biological system interacting with ever-changing environments.

Research Outlook

As omics technology becomes even more accessible, more scientific discoveries on non-model fungal pathogens will advance our understanding of unique and understudied forest pathosystems in rapidly changing environments. Currently, the lack of pure cultures and asexual structures of *Lophodermella* spp. challenges us to obtain standard DNA and RNA quality and quantity for an affordable and exclusive nucleotide sequencing of the target pathogen. These factors also contribute to the difficulty in conducting controlled experiments to further elucidate gene expressions of the pathogen at defined environmental conditions. Nonetheless, while relatively costly at present, cultivation-free single cell approach in omics-based research is a promising tool to expand our knowledge on the biology of many uncultured fungal lineages (Ahrendt et al., 2018).

Fungal genome research has contributed tremendously in establishing solid foundational knowledge about ecologically and economically important fungal pathogens (Aylward et al., 2017; Xu et al., 2006). Comparative and functional genome analyses help further explore genes that may be attributed to their trophic and endophytic lifestyles, and other traits that could provide

phylogenetic and evolutionary inferences that are especially relevant to pathogenicity. Genomic information on many rhytismataceous needle pathogens is still generally lacking. Currently, of the 44 genera within Rhytismataceae, only five represent the genome database which include *Lophodermium*, *Elytroderma*, *Spathularia*, *Coccomyces* and *Pseudographis* (JGI Mycosm; Grigoriev et al., 2011). Of these, none were used yet for comparative analyses to explore genes that may be attributed to their trophic lifestyles and interactions, and other traits that could provide phylogenetic and evolutionary inference. However, their availability coupled with the expansion of the genome sequence database to many needle pathogens, including *Lophodermella* species, greatly presents an opportunity to investigate the biology and mechanisms, genomic patterns, and diversification of pathogenicity-related genes of these latent pathogens. Exploring the *Lophodermella* genomes could also lead to the discovery of unique genes related to their latent lifestyles, sexual mating systems, host specificity, etc., and *Lophodermella* genome sequences could further parse out genes differentially expressed by *L. concolor* and *L. montivaga* from the *Lophodermella* needle cast metatranscriptome obtained from our current research.

Proteomics and metabolomics are another growing omics-based research in forest pathology to investigate the proteins and/or metabolites that trigger pathogenic transitions. This is especially relevant as an imbalance of the secondary metabolites exchanged between host and microbes had been found to result in disease development (Schulz & Boyle, 2005). In the present research, I found differences in plant and fungal metabolic pathways in asymptomatic and symptomatic *P. contorta* needles that indicate a unique communication between disease players in healthy vs. diseased states. As many needle pathogens could remain latent until a certain set of conditions are met, it is then crucial to understand the metabolic transitions between host plant-pathogen interactions at ever-changing complex environments. However, many investigations on

the metabolome of latent pathogens and host plants are focused on agricultural crops. For example, distinct metabolites produced during infection by latent pathogen *Botrytis cinerea* in strawberries signaled early stage of disease development (Hu et al., 2019). Also noteworthy are changes in the metabolome of the host plants. Latent phase infection of some Botryosphaeriaceae species, that cause decay in grapevine, activated about 20 candidate genes in its host plant (Czemmel et al., 2015) and resulted in differentially expressed genes, suggesting a complex plant defense mechanism (Zhang et al., 2019). While information on metabolites of endophytes in conifer needles is available (McMullin et al., 2018; Miller, 1986), most are focused on control of disease and herbivory. None have yet to consider metabolomic characterization specifically in needle diseases caused by latent pathogens. These research investigations will complement genomics and transcriptomics for more robust analyses of conifer needle pathosystems.

Omics-based research could also upgrade plant disease diagnosis, as this can lead to the discovery of potential biomarkers and early indicators of plant health (Gomez-Casati et al., 2013; Kasote et al., 2020; Maia et al., 2020). Apart from the deep insights on interaction mechanisms, gene expression and metabolic variations in lifestyle transitions and environmental responses of latent forest pathogens such as *Lophodermella* spp. could be used as early indicators of pathogen transition from latent to pathogenic state. This further facilitates adequate forest disease monitoring amidst varying environmental conditions, allowing us to predict the transition of a seemingly harmless endophyte to becoming severely pathogenic and virulent.

Another research area that has garnered a growing interest in forest disease management is on disease modification and resistance through endophytes. Gearing away from the conventional reactive solutions to forest health problems, understanding more about tree-associated microbiomes has become an attractive proactive ecosystem-based approach to protect perennials

that are slow evolving than insect pests and pathogens (Witzell & Martín, 2018). The biological control potential of the endophytes stems from their modes of action which could be classified as plant growth promotion, pathogen and herbivore competition, and induction of host resistance (Terhonen et al., 2018). However, the highly variable and context-dependent roles of endophytes make it necessary to study more wild plant pathosystems to grasp the ecological functions of endophytes across various host-pathogen associations (Busby et al., 2016). While my current research has not explicitly explored the specific endophytes that play a role in disease control, results from my research showed a set of bacterial proteins possibly antagonistic to the pathogenic fungal community. To convert these information into endophyte technologies for crop protection, carefully designed *in vitro* and *in vivo* assays including field experiments and additional observational studies would be required to fully understand plant genotype-microbiome-environment interactions (Busby et al., 2016; Terhonen et al., 2018).

References

- Ahrendt, S. R., Quandt, C. A., Ciobanu, D., Clum, A., Salamov, A., Andreopoulos, B., Cheng, J.-F., Woyke, T., Pelin, A., Henrissat, B., Reynolds, N. K., Benny, G. L., Smith, M. E., James, T. Y., & Grigoriev, I. V. (2018). Leveraging single-cell genomics to expand the fungal tree of life. *Nature Microbiology*, *3*(12), 1417–1428.
<https://doi.org/10.1038/s41564-018-0261-0>
- Anal, A. K. D., Rai, S., Singh, M., & Solanki, M. K. (2020). Plant Mycobiome: Current Research and Applications. In M. K. Solanki, P. L. Kashyap, & B. Kumari (Eds.), *Phytobiomes: Current Insights and Future Vistas* (pp. 81–104). Springer Singapore.
https://doi.org/10.1007/978-981-15-3151-4_4
- Aylward, J., Steenkamp, E. T., Dreyer, L. L., Roets, F., Wingfield, B. D., & Wingfield, M. J. (2017). A plant pathology perspective of fungal genome sequencing. *IMA Fungus*, *8*(1), 1–15. <https://doi.org/10.5598/imafungus.2017.08.01.01>
- Berbee, M. L. (2001). The phylogeny of plant and animal pathogens in the Ascomycota. *Physiological and Molecular Plant Pathology*, *59*(4), 165–187.
<https://doi.org/10.1006/pmpp.2001.0355>
- Busby, P. E., Ridout, M., & Newcombe, G. (2016). Fungal endophytes: Modifiers of plant disease. *Plant Molecular Biology*, *90*(6), 645–655. <https://doi.org/10.1007/s11103-015-0412-0>
- Czemmel, S., Galarneau, E. R., Travadon, R., McElrone, A. J., Cramer, G. R., & Baumgartner, K. (2015). Genes Expressed in Grapevine Leaves Reveal Latent Wood Infection by the Fungal Pathogen *Neofusicoccum parvum*. *PLOS ONE*, *10*(3), e0121828.
<https://doi.org/10.1371/journal.pone.0121828>

- Darker, G. (1932). *The Hypodermataceae of Conifers* (Vol. 1). Contributions from the Arnold Arboretum of Harvard University.
- Gilbert, G. S., & Parker, I. M. (2016). The Evolutionary Ecology of Plant Disease: A Phylogenetic Perspective. *Annual Review of Phytopathology*, *54*(1), 549–578.
<https://doi.org/10.1146/annurev-phyto-102313-045959>
- Gomez-Casati, D. F., Zanol, M. I., & Busi, M. V. (2013). Metabolomics in Plants and Humans: Applications in the Prevention and Diagnosis of Diseases. *BioMed Research International*, *2013*, 1–11. <https://doi.org/10.1155/2013/792527>
- Grigoriev, I. V., Cullen, D., Goodwin, S. B., Hibbett, D., Jeffries, T. W., Kubicek, C. P., Kuske, C., Magnuson, J. K., Martin, F., Spatafora, J. W., Tsang, A., & Baker, S. E. (2011). Fueling the future with fungal genomics. *Mycology*, *2*(3), 192–209.
<https://doi.org/10.1080/21501203.2011.584577>
- Hu, Z., Chang, X., Dai, T., Li, L., Liu, P., Wang, G., Liu, P., Huang, Z., & Liu, X. (2019). Metabolic Profiling to Identify the Latent Infection of Strawberry by *Botrytis cinerea*. *Evolutionary Bioinformatics*, *15*, 117693431983851.
<https://doi.org/10.1177/1176934319838518>
- Kasote, D. M., Jayaprakasha, G. K., Singh, J., Ong, K., Crosby, K. M., & Patil, B. S. (2020). Metabolomics-based biomarkers of Fusarium wilt disease in watermelon plants. *Journal of Plant Diseases and Protection*, *127*(4), 591–596. <https://doi.org/10.1007/s41348-020-00314-0>
- Luchi, N., Ioos, R., & Santini, A. (2020). Fast and reliable molecular methods to detect fungal pathogens in woody plants. *Applied Microbiology and Biotechnology*, *104*(6), 2453–2468. <https://doi.org/10.1007/s00253-020-10395-4>

- Maia, M., Ferreira, A. E. N., Nascimento, R., Monteiro, F., Traquete, F., Marques, A. P., Cunha, J., Eiras-Dias, J. E., Cordeiro, C., Figueiredo, A., & Sousa Silva, M. (2020). Integrating metabolomics and targeted gene expression to uncover potential biomarkers of fungal/oomycetes-associated disease susceptibility in grapevine. *Scientific Reports*, *10*(1), 15688. <https://doi.org/10.1038/s41598-020-72781-2>
- McCartney, H. A., Foster, S. J., Fraaije, B. A., & Ward, E. (2003). Molecular diagnostics for fungal plant pathogens. *Pest Management Science*, *59*(2), 129–142. <https://doi.org/10.1002/ps.575>
- McMullin, D. R., Nguyen, H. D. T., Daly, G. J., Menard, B. S., & Miller, J. D. (2018). Detection of foliar endophytes and their metabolites in *Picea* and *Pinus* seedling needles. *Fungal Ecology*, *31*, 1–8. <https://doi.org/10.1016/j.funeco.2017.09.003>
- Millar, C. S. (1984). *Lophodermella* species on pines. In: *Recent Research on Conifer Needle Diseases*. Eds. Glenn W. Peterson. USDA Forest Service, General Technical Report GTR-WO 50., 45–55.
- Miller, J. D. (1986). Toxic metabolites of epiphytic and endophytic fungi of conifer needles. In *Microbiology of the Phyllosphere*. Fokkema, N.J. and van den Heuvel, J. (editors). (pp. 221–231). Cambridge University Press.
- Minter, D. W., & Millar, C. S. (1993). IMI Descriptions of Fungi and Bacteria. *Mycopathologia*, *121*(1), 53–56.
- Schulz, B., & Boyle, C. (2005). The endophytic continuum. *Mycological Research*, *109*(6), 661–686. <https://doi.org/10.1017/S095375620500273X>

- Terhonen, E., Blumenstein, K., Kovalchuk, A., & Asiegbu, F. O. (2019). Forest Tree Microbiomes and Associated Fungal Endophytes: Functional Roles and Impact on Forest Health. *Forests*, *10*(1), 42. <https://doi.org/10.3390/f10010042>
- Terhonen, E., Kovalchuk, A., Zarsav, A., & Asiegbu, F. O. (2018). Biocontrol Potential of Forest Tree Endophytes. In A. M. Pirttilä & A. C. Frank (Eds.), *Endophytes of Forest Trees* (Vol. 86, pp. 283–318). Springer International Publishing. https://doi.org/10.1007/978-3-319-89833-9_13
- Witzell, J., & Martín, J. A. (2018). Endophytes and Forest Health. In A. M. Pirttilä & A. C. Frank (Eds.), *Endophytes of Forest Trees* (Vol. 86, pp. 261–282). Springer International Publishing. https://doi.org/10.1007/978-3-319-89833-9_12
- Worrall, J. J., Marchetti, S. B., & Mask, R. A. (2012). An Epidemic of Needle Cast on Lodgepole Pine in Colorado. In *Biological Evaluation R2-12-01* (p. 16). USDA Forest Service, Rocky Mountain Region, Forest Health Protection.
- Xu, J.-R., Peng, Y.-L., Dickman, M. B., & Sharon, A. (2006). The Dawn of Fungal Pathogen Genomics. *Annual Review of Phytopathology*, *44*(1), 337–366. <https://doi.org/10.1146/annurev.phyto.44.070505.143412>
- Zhang, W., Yan, J., Li, X., Xing, Q., Chethana, K. W. T., & Zhao, W. (2019). Transcriptional response of grapevine to infection with the fungal pathogen *Lasiodiplodia theobromae*. *Scientific Reports*, *9*(1), 5387. <https://doi.org/10.1038/s41598-019-41796-9>

APPENDICES

Supplementary Table 1. Sequences downloaded from NCBI GenBank and used in phylogenies.

Species	Gene Region	Isolate/Strain/Voucher ID	GenBank Accession Number
<i>Bifusella camelliae</i>	LSU	HOU561	KF797450.1
<i>Bifusella linearis</i>	ITS	BPI843543	AY465527.1
<i>Bifusella linearis</i>	ITS	EBJul30-15	KT000195.1
<i>Chalara</i> sp.	ITS	MFLU 18-1812	MK584986.1
<i>Chalara</i> sp.	LSU	MFLU-18-1812	MK592006.1
<i>Chalara</i> sp.	ITS	MFLU 15-3167	MK584995.1
<i>Chalara</i> sp.	LSU	MFLU 15-3167	MK591953.1
<i>Chalara</i> sp.	TEF1 α	MFLU 15-3167	MK348529.1
<i>Coccomyces mucronatus</i>	ITS	R73	GU138732.1
<i>Coccomyces strobil</i>	LSU	DAOMC251589	MH457157.1
<i>Coccomyces strobil</i>	TEF1 α	AFTOL-ID1250	DQ471099.2
<i>Colpoma quercinum</i>	ITS	--	U92306.1
<i>Colpoma quercinum</i>	LSU	Lantz 368 (UPS)	HM140513.1
<i>Cudonia confusa</i>	TEF1 α	C315	KC833384.1
<i>Cudonia sichuanensis</i>	ITS	C328	KC833122.1
<i>Cudonia sichuanensis</i>	LSU	C328	KC833220.1
<i>Cudonia sichuanensis</i>	TEF1 α	C328	KC833386.1
<i>Elytroderma deformans</i>	ITS	--	AF203469.1
Fungal Endophyte	ITS	3277	DQ979552.1
Fungal Endophyte	LSU	3277	DQ79426.1
Fungal Endophyte	ITS	5744	DQ979779.1
<i>Hypoderma campanulatum</i>	LSU	ICMP: 17383	HM140517.1
<i>Hypoderma hederiae</i>	LSU	Lantz & Minter 421 (UPS)	HM140522.1
<i>Hypoderma minterii</i>	ITS	275B/ BJTC201203	JX232416.1
<i>Hypoderma rubi</i>	ITS	PRJ R902	JF683416.1
<i>Lirula macrospora</i>	ITS	LM-CASTCBS	AF462441.1
<i>Lirula macrospora</i>	LSU	13	HQ902152.1
<i>Lophodermella arcuata</i>	ITS	BPI842080	AY465518.1
<i>Lophodermium australe</i>	ITS	1	EU934074.1
<i>Lophodermium conigenum</i>	ITS	A08	LC033959.1
<i>Lophodermium culmigenum</i>	LSU	Lantz 442 (UPS)	HM140540.1
<i>Lophodermium molitoris</i>	ITS	CV1_3a	KM106803.1
<i>Lophodermium nitidum</i>	LSU	Lantz 435 (UPS)	HM140547.1
<i>Lophodermium sphaeroides</i>	LSU	Lantz 382 (UPS)	HM140556.1
<i>Lophodermium picea</i>	ITS	P1	KX009045.1
<i>Lophodermium pinastri</i>	ITS	Yinggao	AY422490.1
<i>Lophodermium</i> sp. (<i>Lophodermium resinosum</i>)	ITS	JBT-2017a	KY485127.1
<i>Lophodermium</i> sp. (<i>Lophodermium resinosum</i>)	LSU	JBT-2017a/ NB-770-1/ DAOMC 251482	KY485135.1/ NG_060349.1
<i>Lophodermium resinosum</i>	TEF1 α	DAOMC 251482	KY702582.1

<i>Lophophacidium dooksii</i>	ITS	737873	KF889651.1
<i>Lophophacidium dooksii</i>	ITS	B13N3	KF889704.1
<i>Meloderma desmazieresii</i>	ITS	--	AF203470.1
<i>Rhytisma acerinum</i>	ITS	Hou et al. 203	GQ253100.1
<i>Rhytisma punctatum</i>	ITS	WA-1	MH507272.1
<i>Rhytisma salicinum</i>	ITS	BPI843550	AY465516.1
<i>Spathularia flavida</i> subsp. <i>rufa</i>	ITS	H336	KC833071.1
<i>Spathularia flavida</i> subsp. <i>rufa</i>	LSU	H336	KC833228.1
<i>Spathularia flavida</i> subsp. <i>rufa</i>	TEF1 α	H336	KC833395.1
<i>Spatularia velutipes</i>	TEF1 α	S3/ JC32	KC833431.1
<i>Terriera minor</i>	LSU	Lantz & Minter 418 (UPS)	HM140569.1
<i>Therrya fuckelii</i>	ITS	CBS 377.58	JF683416.1
<i>Therrya pini</i>	ITS	CBS 177.56	MH857568.1
<i>Therrya pini</i>	LSU	CBS 177.56	MH869111.1
<i>Tryblidiopsis pinastri</i>	ITS	CBS 445.71	JF793678.1
<i>Tryblidiopsis pinastri</i>	LSU	CBS 445.71	MH871979.1
<i>Tryblidiopsis pinastri</i>	TEF1 α	AFTOL-ID 1319	DQ471106.1

Supplementary Table 2. Identity and the range of similarity and e-value of $\geq 50\%$ of the sequences of each *Lophodermella* spp. and *Lophophacidium dooksii* generated from this study at the three loci as inferred from NCBI Basic Local Alignment Search Tool (BLAST).

Sample Species	Sequences used for BLAST search (%)	Top BLAST ID hit	GenBank Accession	Similarity (%)	e-value
ITS					
<i>L. arcuata</i>	100	<i>L. arcuata</i> BPI842080	AY465518.1	98.60 – 98.64	0.0
<i>L. concolor</i>	100	Fungal Endophyte 5744	DQ79779.1	85.78 – 87.89	8e-130 – 5e-122
<i>L. conjuncta</i>	100	<i>Lophodermium pinastri</i> US2-2-2i	KY742594.1	84.42 – 84.72	7e-146 – 9e-140
<i>L. montivaga</i>	100	<i>Lophophacidium dookisii</i> QFB14721N4	KF889694.1	95.35 – 96.26	3e-158 – 0.0
<i>L. sulcigena</i>	100	<i>L. dooksii</i> B13N3	KF889704.1	95.4	0.0
<i>Lophodermella</i> sp.	100	<i>L. dooksii</i> QFB14721N3	KF889693.1	98.38	0.0
<i>L. dooksii</i>	100	<i>L. dooksii</i> DAOM183323	KF889652.1	98.94	0.0
LSU					
<i>L. arcuata</i>	100	<i>Coccomyces pinicola</i> HOU486A	KP322585.1	93.16 – 93.32	0.0
<i>L. concolor</i>	50	<i>Lophodermium piceae</i> voucher Lantz 317 (UPS)	HM140551.1	92.28 – 93.14	0.0
<i>L. conjuncta</i>	67	<i>Pseudographis elatina</i> voucher GJO:0090016	MK781803.1	95.27	0.0
<i>L. montivaga</i>	93	<i>Lophodermium nitidum</i> Lantz 435 (UPS)	HM140547.1	93.04 – 93.40	0.0
<i>L. sulcigena</i>	100	<i>Lophodermium arundinaceum</i> Lantz 323 (UPS)	HM140535.1	94.16	0.0
<i>Lophodermella</i> sp.	100	<i>Lophodermium nitidum</i> Lantz 435 (UPS)	HM140547.1	93.43	0.0
<i>L. dooksii</i>	100	<i>Lophodermium nitidum</i> Lantz 435 (UPS)	HM140547.1	93.08	0.0

TEF1 α					
<i>L. arcuata</i>	100	<i>Lophodermium resinosum</i> DAOMC 251482	KY702582.1	94.24 – 94.25	0.0
<i>L. concolor</i>	100	<i>Lophodermium resinosum</i> DAOMC 251482	KY702582.1	94.18 - 94.30	0.0
<i>L. conjuncta</i>	100	<i>Tryblidiopsis pinastri</i> AFTOL- ID 1319	DQ471106.1	90.99-91.11	0.0
<i>L. montivaga</i>	82	<i>Lophodermium resinosum</i> DAOMC 251482	KY702582.1	94.99-95.15	0.0
<i>L. sulcigena</i>	100	<i>Lophodermium resinosum</i> DAOMC 251482	KY702582.1	95.03	0.0
<i>Lophodermella</i> sp.	100	<i>Lophodermium resinosum</i> DAOMC 251482	KY702582.1	94.99	0.0
<i>L. dooksii</i>	100	<i>Lophodermium resinosum</i> DAOMC 251482	KY702582.1	94.71	0.0

Supplementary Table 3. Maximum likelihood distance of *Lophodermella* spp. with *Lophodermium* spp. and *Elytroderma deformans* in the concatenated dataset.

	<i>Lophodermella_montivaga_Gen1</i>	<i>Lophodermella_montivaga_Gen2</i>	<i>Lophodermella_montivaga_Gen3</i>	<i>Lophodermella_sulcigena</i>	<i>Lophophacidium_dooksii_737873</i>	<i>Lophophacidium_dooksii_B13N3</i>	<i>Lophophacidium_dooksii</i>	<i>Lophodermella_sp.</i>	<i>Lophodermella_arcuata_RMNP_LU16</i>	<i>Lophodermella_arcuata_BPI842080</i>	<i>Lophodermella_arcuata_RMNP_LU1</i>	<i>Lophodermella_concolor_Gen3</i>	<i>Lophodermella_concolor_Gen4</i>	<i>Lophodermella_concolor_Gen1</i>	<i>Lophodermella_concolor_Gen2</i>	<i>Elytroderma_deformans</i>	<i>Lophodermella_conjuncta_PHP19_0986</i>	<i>Lophodermella_conjuncta_PHP18_0655</i>	<i>Lophodermella_conjuncta_PHP19_0987</i>	<i>Lophodermium_culmigenum</i>	<i>Lophodermium_mitidum</i>	<i>Lophodermium_mollens</i>	<i>Lophodermium_rasinissum_JBT-2017a</i>
<i>Lophodermella_montivaga_Gen1</i>	0	0.002	0.018	0.023	0.023	0.026	0.019	0.03	0.032	0.03	0.086	0.085	0.085	0.086	0.426	0.439	0.439	0.439	0.387	0.386	0.417	0.384	
<i>Lophodermella_montivaga_Gen2</i>	0	0.002	0.018	0.023	0.023	0.026	0.019	0.03	0.032	0.03	0.086	0.085	0.085	0.086	0.426	0.439	0.439	0.439	0.387	0.386	0.417	0.384	
<i>Lophodermella_montivaga_Gen3</i>	0.002	0.002	0.016	0.021	0.021	0.025	0.017	0.029	0.031	0.028	0.084	0.083	0.083	0.084	0.424	0.437	0.437	0.438	0.385	0.384	0.415	0.382	
<i>Lophodermella_sulcigena</i>	0.018	0.018	0.016	0.021	0.021	0.024	0.017	0.029	0.031	0.028	0.084	0.083	0.083	0.084	0.424	0.437	0.437	0.437	0.385	0.384	0.415	0.382	
<i>Lophophacidium_dooksii_737873</i>	0.023	0.023	0.021	0.021	0	0.003	0.004	0.016	0.018	0.016	0.071	0.071	0.071	0.071	0.411	0.424	0.424	0.425	0.373	0.372	0.403	0.369	
<i>Lophophacidium_dooksii_B13N3</i>	0.023	0.023	0.021	0.021	0	0.003	0.004	0.016	0.018	0.016	0.071	0.071	0.071	0.071	0.412	0.425	0.425	0.425	0.373	0.372	0.403	0.37	
<i>Lophophacidium_dooksii</i>	0.026	0.026	0.025	0.024	0.003	0.003	0.008	0.019	0.021	0.019	0.075	0.074	0.074	0.075	0.415	0.428	0.428	0.428	0.376	0.375	0.406	0.373	
<i>Lophodermella_sp.</i>	0.019	0.019	0.017	0.017	0.004	0.004	0.008	0.012	0.014	0.011	0.067	0.066	0.066	0.067	0.407	0.42	0.42	0.42	0.368	0.367	0.398	0.365	
<i>Lophodermella_arcuata_RMNP_LU16</i>	0.03	0.03	0.029	0.029	0.016	0.016	0.019	0.012	0.002	0.001	0.079	0.078	0.078	0.079	0.419	0.432	0.432	0.432	0.38	0.379	0.41	0.377	
<i>Lophodermella_arcuata_BPI842080</i>	0.032	0.032	0.031	0.031	0.018	0.018	0.021	0.014	0.002	0.003	0.081	0.08	0.08	0.081	0.421	0.434	0.434	0.434	0.382	0.381	0.412	0.379	
<i>Lophodermella_arcuata_RMNP_LU1</i>	0.03	0.03	0.028	0.028	0.016	0.016	0.019	0.011	0.001	0.003	0.078	0.078	0.078	0.078	0.418	0.431	0.431	0.432	0.38	0.379	0.41	0.376	
<i>Lophodermella_concolor_Gen3</i>	0.086	0.086	0.084	0.084	0.071	0.071	0.075	0.067	0.079	0.081	0.078	0.001	0.001	0.001	0.442	0.455	0.455	0.455	0.403	0.402	0.433	0.4	
<i>Lophodermella_concolor_Gen4</i>	0.085	0.085	0.083	0.083	0.071	0.071	0.074	0.066	0.078	0.08	0.078	0.001	0	0.001	0.441	0.454	0.454	0.455	0.403	0.402	0.433	0.399	
<i>Lophodermella_concolor_Gen1</i>	0.085	0.085	0.083	0.083	0.071	0.071	0.074	0.066	0.078	0.08	0.078	0.001	0	0.001	0.441	0.454	0.454	0.455	0.403	0.402	0.433	0.399	
<i>Lophodermella_concolor_Gen2</i>	0.086	0.086	0.084	0.084	0.071	0.071	0.075	0.067	0.079	0.081	0.078	0.001	0.001	0.001	0.442	0.455	0.455	0.455	0.403	0.402	0.433	0.4	

<i>Elytroderma deformans</i>	0.426	0.426	0.424	0.424	0.411	0.412	0.415	0.407	0.419	0.421	0.418	0.442	0.441	0.441	0.442	0.44	0.44	0.441	0.388	0.387	0.418	0.385
<i>Lophodermella conjuncta_PHP19_0986</i>	0.439	0.439	0.437	0.437	0.424	0.425	0.428	0.42	0.432	0.434	0.431	0.455	0.454	0.454	0.455	0.44	0	0.001	0.401	0.401	0.431	0.398
<i>Lophodermella conjuncta_PH18_0655</i>	0.439	0.439	0.437	0.437	0.424	0.425	0.428	0.42	0.432	0.434	0.431	0.455	0.454	0.454	0.455	0.44	0	0	0.401	0.4	0.431	0.398
<i>Lophodermella conjuncta_PHP19_0987</i>	0.439	0.439	0.438	0.437	0.425	0.425	0.428	0.42	0.432	0.434	0.432	0.455	0.455	0.455	0.455	0.441	0.001	0	0.402	0.401	0.432	0.399
<i>Lophodermium culmigenum</i>	0.387	0.387	0.385	0.385	0.373	0.373	0.376	0.368	0.38	0.382	0.38	0.403	0.403	0.403	0.403	0.388	0.401	0.401	0.402	0.005	0.38	0.347
<i>Lophodermium nitidum</i>	0.386	0.386	0.384	0.384	0.372	0.372	0.375	0.367	0.379	0.381	0.379	0.402	0.402	0.402	0.402	0.387	0.401	0.4	0.401	0.005	0.379	0.346
<i>Lophodermium molitoris</i>	0.417	0.417	0.415	0.415	0.403	0.403	0.406	0.398	0.41	0.412	0.41	0.433	0.433	0.433	0.433	0.418	0.431	0.431	0.432	0.38	0.379	0.056
<i>Lophodermium resinosum_JBT-2017a</i>	0.384	0.384	0.382	0.382	0.369	0.37	0.373	0.365	0.377	0.379	0.376	0.4	0.399	0.399	0.4	0.385	0.398	0.398	0.399	0.347	0.346	0.056

Supplementary Table 4. Morphological characters and character states of the *Lophodermella* and non-*Lophodermella* species.

	1	2	3	4	5
	Ascocarps	Ascocarps	Asci shape	Ascospores	Host
	0 non-linear or -elliptical, 1 mostly linear, nervisequious, dark brown to black, 2 mostly elliptical, concolorous to black	external/superficial 0,subcuticular 1,intraepidermal 2,supepidermal 3, subhypodermal 4	0 more or less broadly saccate to clavate, 1 narrowly clavate or cylindrical	Acicular 0,Filiform 1,Clavate 2,Cylindrical 3, fusiform to oval 4, rod-shaped 5, double-spindle shaped 6, ellipsoid to fusoid 7	Non-pine 0, Pine 1
<i>Lophodermella montivaga</i>	2	4	0	2	1
<i>Lophophacidium dooksii</i>	1	4	0	4	1
<i>Lophodermella arcuata</i>	2	4	0	2	1
<i>Lophodermella sp.</i>	2	4	0	2	1
<i>Lophodermella concolor</i>	2	4	1	2	1
<i>Lophodermium pinastri</i>	2	3	0	1	1

<i>Lophodermium australe</i>	1	3	1	1	1
<i>Lophodermium conigenum</i>	2	3	1	1	1
<i>Elytroderma deformans</i>	2	3	0	3	1
<i>Meloderma desmazieresii</i>	2	?	1	5	1
<i>Bifusella linearis</i>	2	1	0	6	1
<i>Lophodermium resinosum</i>	2	3	1	1	1
<i>Lophodermium molitoris</i>	?	?	?	?	?
<i>Therrya pini</i>	0	3	0	1	1
<i>Therrya fockelii</i>	0	3	0	3	1
<i>Coccomyces mucronatus</i>	0	2,3	1	1	0
<i>Cudonia sichuanensis</i>	0	0	0	0	0
<i>Spathularia flavida</i>	0	0	1	?	?
<i>Colpoma quercinum</i>	2	?	1	1	0
<i>Rhytisma acerinum</i>	2	1	1	3	0
<i>Rhytisma punctatum</i>	?	?	?	?	?
<i>Hypoderma rubi</i>	2	1	1	2,3	0
<i>Hypoderma minterii</i>	?	?	?	?	?
<i>Rhytisma salicinum</i>	?	?	?	?	?
<i>Lirula macrospora</i>	2	2	1	1,3	1
<i>Lophodermium piceae</i>	2	2	1	1	0
<i>Tryblidiopsis pinastri</i>	0	?	1	2	0,1
<i>Chalara sp.</i>	0	1	1	7	?
<i>Lophodermella sulcigena</i>	2	4	0	2	1
<i>Lophodermella conjuncta</i>	2	4	1	2	1
<i>Fungal endophyte 3277</i>	?	?	?	?	?
<i>Fungal endophyte 5744</i>	?	?	?	?	?

Supplementary Table 5. Morphological characters and character states of *Lophodermella* species, including *Elytroderma deformans* and *Chalara* sp. as outgroups.

	1	2	3	4	5	6
	Ascomata	Ascomata	Ascomata	Ascospores	Asci	Host Needles
	hysterothecia ≥1 mm light 0, hysterothecia short 1	hysterothecia brown 0, hysterothecia concolorous 1	hysterothecia not fused 0, hysterothecia fused 1	short (23-60u) clavate 0, elongate (98- 90u) clavate 1, fusiform to oval 2, cylindrical 3, ellipsoid to fusoid 4	4 spores 4, 8 spores 8	2-needle pine 2, 3-needle pine 3, 5-needle pine 5
<i>Lophodermella montivaga</i>	0	0	0	0	8	2,3,5
<i>Lophophacidium dooksii</i>	0	0	0	2	8	5
<i>Lophodermella arcuata</i>	0	0,1	0	0	8	5
<i>Lophodermella</i> sp.	0	0	0	0	8	5
<i>Lophodermella concolor</i>	1	1	0	0	8	2
<i>Lophodermella sulcigena</i>	0	0	0	0	4,8	2
<i>Lophodermella conjuncta</i>	0	0	1	1	8	2
<i>Elytroderma deformans</i>	0	0	0	3	8	2,3
<i>Chalara</i> sp.	?	?	?	4	?	?

Supplementary File 1. Genomic DNA and RNA extraction protocol developed following methods by Cubero et al., (1999) and Zeng et al., (2018) to extract DNA and RNA of *Pinus contorta* needles from Colorado, USA that were asymptomatic and symptomatic of *Lophodermella concolor* and *L. montivaga*. Volumes were adjusted for small amount of sample.

DAY 1

1. In 2mL tubes, add clean metal and glass beads with the samples. Grind samples in FastPrep after submerging in liquid nitrogen. Repeat until samples are in powder form. Samples must be stored in -80°C prior to grinding.
2. Add 500µL of warm extraction buffer with 2% polyvinyl pyrrolidone (PVP) and 10µL dithiothreitol (DTT) to the samples. Run in FastPrep once then incubate the samples for 20mins at 65°C.
3. Add equal volume of chloroform:isoamyl alcohol 24:1, and mix with the extraction buffer by inversion. Centrifuge the samples to 10,000g for 15mins and transfer the aqueous phase (~400µL) into new tubes.
4. Add a quarter volume (~100µL) of 10 M lithium chloride (LiCl) and mix the solution by inversion. Precipitate the total RNA overnight at 4°C.

DAY 2

5. Centrifuge samples at 10,000g for 30mins at 4°C. Pour out supernatant (gDNA) and transfer to new 1.5mL tubes. Leave the pellet to dry (totRNA).

Genomic DNA extraction

6. Add 3 M NaAc (1/10 volume of supernatant) and isopropanol (1 volume of supernatant) to the supernatant (gDNA from step 5). Mix the solution by inversion and incubate for 5mins at room temperature. Centrifuge the samples at 10,000g for 30mins at 4°C.
7. Remove supernatant in the gDNA sample and resuspend pellet in 350µL of 1.2 M NaCl. Add 2µL of RNase A to the samples and incubate for 30mins at 37°C.
8. Add 1 volume of chloroform and mix the solution well. Centrifuge for 5mins at 10,000g and transfer the upper phase of the solution to new tubes.
9. Add 0.6 volume of ice-cold isopropanol and mix well. Incubate the sample at -20°C for at least 15 mins (or overnight).
10. Centrifuge the sample for 20mins at 13,000g at 4°C. Decant supernatant and add 1mL of 70% cold ethanol.
11. Centrifuge the samples for 3mins at 13,000g at 4°C. Carefully decant the solution using pipette avoiding pellet. Leave the pellet to dry.
12. Resuspend pellet in TE buffer or molecular grade water. Store DNA sample in -20°C.

Total RNA extraction

13. Dissolve the pellet (from step 5, totRNA) in 400µL of SSTE buffer (preheated at 65°C). Add same volume of chloroform and mix well. Centrifuge for 15mins at 10,000g.
14. Transfer aqueous phase in 2mL tubes. Add 100% ethanol (three times the volume of the aqueous phase) and mix well. Precipitate overnight at -80°C.

DAY3

15. Centrifuge sample from step 13 at 10,000g at 4°C for 30mins. Pipette out the supernatant and leave the pellet to dry. Dissolve the pellet in molecular grade or nuclease free water. Store in -80°C.

References

Cubero, O. F., Crespo, A., Fatehi, J., & Bridge, P. D. (1999). DNA extraction and PCR

amplification method suitable for fresh, herbarium-stored, lichenized, and other fungi.

Plant Systematics and Evolution, 216(3–4), 243–249.

<https://doi.org/10.1007/BF01084401>

Zeng, Z., Raffaello, T., Liu, M.-X., & Asiegbu, F. O. (2018). Co-extraction of genomic DNA &

total RNA from recalcitrant woody tissues for next-generation sequencing studies. *Future*

Science OA, 4(6), FSO309. <https://doi.org/10.4155/fsoa-2018-0026>

Supplementary Table 6. Analysis of Variance (ANOVA) and permutational analysis of variance (PERMANOVA) of alpha and beta diversity in *Pinus contorta* needles asymptomatic and symptomatic of *Lophodermella* needle cast pathogens, *Lophodermella concolor* and *L. montivaga*

A. ANOVA for alpha diversity						
Treatment	<i>Richness</i>		<i>Shannon Index</i>		<i>Inverse Simpson Index</i>	
	F value	P value	F value	P value	F value	P value
Disease symptoms	86.86	< 9.93e-15	160.41	< 2.2e-16	153.55	< 2.2e-16
Pathogen	6.73	0.011	15.49	0.0002	6.84	0.01
Site	2.53	0.03	1.42	0.23	1.33	0.26
Disease symptoms × pathogen	8.08	0.006	18.24	4.96e-05	12.63	0.0006
B. PERMANOVA for beta diversity						
Treatment	R ²		F value		P value	
Disease symptoms × pathogen	0.15		24.386		0.001	
Residual	0.57					

Supplementary Table 7. Analysis of Variance (ANOVA) and permutational analysis of variance (PERMANOVA) of alpha and beta diversity in *Pinus contorta* needles asymptomatic and symptomatic of *Lophodermella* needle cast pathogens, *Lophodermella concolor* and *L. montivaga* using the data without contigs assigned as ‘Fungi unclassified.’ Results of the ANOVA post-hoc analysis are shown in Table C.

A. ANOVA for alpha diversity						
Treatment	<i>Richness</i>		<i>Shannon Index</i>		<i>Inverse Simpson Index</i>	
	F value	P value	F value	P value	F value	P value
Disease symptoms	69.96	8.96e-13	147.75	< 2.2e-16	139.16	< 2.2e-16
Pathogen	4.04	0.05	13	0.0005	7.15	0.009
Site	2	0.09	1.52	0.19	1.36	0.25
Disease symptoms × pathogen	19.62	2.73e-05	8.74	0.004	3.52	0.06
B. PERMANOVA for beta diversity						
Treatment	R ²		F value		P value	
Disease symptoms × pathogen	0.16		25.68		0.001	
Residual	0.56					
C. Contrasts						
Treatment	Pathogen	Predicted means (se)	t-ratio		p-value	
			<i>Richness</i>			
Asymptomatic	<i>L. concolor</i>	51.9 (3.33)	-1.649		0.1028	
	<i>L. montivaga</i>	61.2 (4.61)				

Symptomatic	<i>L. concolor</i>	36.4 (3.33)	4.53	<0.0001
	<i>L. montivaga</i>	10.8 (4.61)		
<i>Shannon</i>				
Asymptomatic	<i>L. concolor</i>	2.21 (0.11)	0.522	0.6028
	<i>L. montivaga</i>	2.12 (0.15)		
Symptomatic	<i>L. concolor</i>	1.03 (0.11)	4.645	<0.0001
	<i>L. montivaga</i>	0.18 (0.15)		
<i>Inverse Simpson</i>				
Asymptomatic	<i>L. concolor</i>	0.74 (0.04)	6.09e-01	0.5444
	<i>L. montivaga</i>	0.69 (0.06)		
Symptomatic	<i>L. concolor</i>	0.25 (0.04)	3.224	0.002
	<i>L. montivaga</i>	0.03 (0.06)		

Supplementary Table 8. Number of fungal reads per sample from DNA and RNA sequencing of *Pinus contorta* needles that were asymptomatic and symptomatic of *Lophodermella concolor* (LC) and *L. montivaga* (LM).

Sample		Treatment	Number of reads				
			Metabarcoding			Metatranscriptome	
			Total OTUs	LC	LM	Total transcripts	Rhytismataceae
1	CS02-18CN	LC_ASYM	71,391	1014	173	1462	192
2	TC01-19CN	LC_ASYM	36,424	2,386	3,706	426	8
3	CS02-18CP	LC_SYM	28,586	26,149	84	966,767	1,983
4	SR10-19CP	LC_SYM	26,273	22,791	0	484,636	1,804
5	LV02-18MN	LM_ASYM	73,470	22,078	18,744	3,728	362
6	LV03-18MN	LM_ASYM	142,417	522	4,785	4,886	296
7	SR09-18MN	LM_ASYM	63,454	26,245	1,422	836	25
8	LV02-18MP	LM_SYM	20,353	0	20,353	3,660,546	4,275
9	SR09-18MP	LM_SYM	48,207	0	43,121	5,381,920	4,291

Supplementary Table 9. Taxonomic fungal identities represented with at least 10 differentially expressed transcripts found between *Pinus contorta* needles that asymptomatic (ASYM) and symptomatic (SYM) of *Lophodermella concolor* (LC) and *L. montivaga* (LM). Fungal identities were inferred from NCBIInr and JGI databases.

Family	Species	count	
		LC_ASYM	LC_SYM
Rhytismataceae	<i>Lophodermium piceae</i>	0	925
Tribliaceae	<i>Pseudographis elatina</i>	0	449
Rhytismataceae	<i>Elytroderma deformans</i>	0	417
Rhytismataceae	<i>Coccomyces strobi</i>	0	390
Rhytismataceae	<i>Lophodermium nitens</i>	0	257
Cudoniaceae	<i>Spathularia flavida</i>	0	209
Myxotrichaceae	<i>Amorphotheca resinae</i> ATCC 22711	0	41
Helotiales incertae sedis	<i>Cadophora sp.</i> DSE1049	0	38
Dermateaceae	<i>Coleophoma cylindrospora</i>	0	29
Lachnaceae	<i>Lachnellula arida</i>	0	27
Lachnaceae	<i>Lachnellula suecica</i>	0	27
Helotiaceae	<i>Glarea lozoyensis</i> ATCC 20868	0	26
Hyaloscyphaceae	<i>Hyphodiscus hymeniophilus</i>	0	26
Mollisiaceae	<i>Phialocephala subalpina</i>	0	26
Hyaloscyphaceae	<i>Hyaloscypha bicolor</i> E	0	25
Helotiaceae	<i>Cudoniella acicularis</i>	0	24
Hyaloscyphaceae	<i>Hyaloscypha hepaticicola</i>	0	22
Dermateaceae	<i>Coleophoma crateriformis</i>	0	21
Hyaloscyphaceae	<i>Hyaloscypha variabilis</i> F	0	21
Drepanopezizaceae	<i>Diplocarpon rosae</i>	0	19
Leotiomyces incertae sedis	<i>Scytalidium lignicola</i>	0	19
Chlorociboriaceae	<i>Chlorociboria aeruginascens</i>	0	18
Pleuroascaceae	<i>Venustampulla echinocandica</i>	0	18

Mollisiaceae	<i>Phialocephala scopiformis</i>	0	17
Rutstroemiaceae	<i>Rutstroemia</i> sp. NJR-2017a WRK4	0	17
Lachnaceae	<i>Lachnellula cervina</i>	0	16
Mollisiaceae	<i>Acephala macrosclerotiorum</i>	0	16
unclassified Helotiales	<i>Helotiales</i> sp. DMI_Dod_QoI	0	16
Helotiales incertae sedis	<i>Rhynchosporium agropyri</i>	0	15
Rutstroemiaceae	<i>Rutstroemia</i> sp. NJR-2017a BBW	0	15
Sclerotiniaceae	<i>Monilinia fructicola</i>	0	15
Botryosphaeriaceae	<i>Botryosphaeria dothidea</i>	0	14
Gloniaceae	<i>Glonium stellatum</i>	0	14
Rutstroemiaceae	<i>Rutstroemia</i> sp. NJR-2017a BVV2	0	14
Lachnaceae	<i>Lachnellula hyalina</i>	0	13
Lachnaceae	<i>Lachnellula occidentalis</i>	0	13
Lachnaceae	<i>Lachnellula subtilissima</i>	0	13
Dermateaceae	<i>Marssonina brunnea</i> f. sp. 'multigermtubi' MB m1	0	11
Helotiales incertae sedis	<i>Chalara longipes</i> BDJ	0	11
Myxotrichaceae	<i>Oidiodendron maius</i> Zn	0	11
Sclerotiniaceae	<i>Sclerotium cepivorum</i>	0	11
Helotiales incertae sedis	<i>Rhynchosporium secalis</i>	0	10
Dothideomycetes incertae sedis	<i>Cryomyces minteri</i>	0	10
Gelatinodiscaceae	<i>Ascocoryne sarcoides</i>	0	10

Supplementary Table 9 (cont'd). Taxonomic fungal identities represented with at least 10 differentially expressed (FDR < 0.05) transcripts found between *Pinus contorta* needles that asymptomatic (ASYM) and symptomatic (SYM) of *Lophodermella concolor* (LC) and *L. montivaga* (LM). Fungal identities were inferred from NCBI nr and JGI databases.

Family	Species	count	
		LM ASYM	LM SYM
Rhytismataceae	<i>Lophodermium piceae</i>	0	1992
Triblidiaceae	<i>Pseudographis elatina</i>	0	1076
Rhytismataceae	<i>Elytroderma deformans</i>	0	974
Rhytismataceae	<i>Coccomyces strobi</i>	0	836
Rhytismataceae	<i>Lophodermium nitens</i>	0	617
Cudoniaceae	<i>Spathularia flavida</i>	0	504
Lachnaceae	<i>Lachnellula suecica</i>	0	70
Mollisiaceae	<i>Acephala macrosclerotiorum</i>	0	68
Myxotrichaceae	<i>Oidiodendron maius</i> Zn	0	67
Leotiomyces incertae sedis	<i>Scytalidium lignicola</i>	0	59
Chlorociboriaceae	<i>Chlorociboria aeruginascens</i>	0	57
Dermateaceae	<i>Coleophoma crateriformis</i>	0	57
Mollisiaceae	<i>Phialocephala subalpina</i>	0	56
Mollisiaceae	<i>Phialocephala scopiformis</i>	0	52
Hyaloscyphaceae	<i>Hyaloscypha bicolor</i> E	0	51
Myxotrichaceae	<i>Amorphotheca resinae</i> ATCC 22711	0	49
Dermateaceae	<i>Coleophoma cylindrospora</i>	0	49
Helotiaceae	<i>Cudoniella acicularis</i>	0	49
Hyaloscyphaceae	<i>Hyaloscypha variabilis</i> F	0	47
Helotiales incertae sedis	<i>Cadophora</i> sp. DSE1049	0	40
Hyaloscyphaceae	<i>Hyaloscypha hepaticicola</i>	0	39
unclassified Helotiales	<i>Helotiales</i> sp. DMI_Dod_QoI	0	38
Helotiales incertae sedis	<i>Chalara longipes</i> BDJ	0	36

Lachnaceae	<i>Lachnellula arida</i>	0	29
Lachnaceae	<i>Lachnellula cervina</i>	0	29
Hyaloscyphaceae	<i>Hyphodiscus hymeniophilus</i>	0	28
Umbilicariaceae	<i>Lasallia pustulata</i>	0	26
Pleuroascaceae	<i>Venustampulla echinocandica</i>	0	26
Drepanopezizaceae	<i>Diplocarpon rosae</i>	0	25
Helotiaceae	<i>Glarea lozoyensis</i> ATCC 20868	0	25
Sclerotiniaceae	<i>Monilinia fructigena</i>	0	25
Lachnaceae	<i>Lachnellula occidentalis</i>	0	24
Dermateaceae	<i>Marssonina brunnea</i> f. sp. 'multigermtubi' MB_m1	0	24
Rutstroemiaceae	<i>Rutstroemia</i> sp. NJR-2017a BVV2	0	24
Rutstroemiaceae	<i>Rutstroemia</i> sp. NJR-2017a WRK4	0	23
Helotiales incertae sedis	<i>Rhynchosporium agropyri</i>	0	21
Sclerotiniaceae	<i>Botrytis cinerea</i> B05.10	0	20
Aspergillaceae	<i>Aspergillus subnutans</i>	0	19
Gloniaceae	<i>Glonium stellatum</i>	0	19
Sacotheciaceae	<i>Aureobasidium pullulans</i>	0	18
Rutstroemiaceae	<i>Rutstroemia</i> sp. NJR-2017a BBW	0	18
Sclerotiniaceae	<i>Sclerotinia borealis</i> F-4128	0	18
Dermateaceae	<i>Marssonina coronariae</i>	0	17
Saccharataceae	<i>Saccharata proteae</i> CBS 121410	0	17
Magnaporthaceae	<i>Gaeumannomyces tritici</i> R3-111a-1	0	16
Sclerotiniaceae	<i>Sclerotinia sclerotiorum</i> 1980 UF-70	0	16
Lachnaceae	<i>Lachnellula willkommii</i>	0	15
Sordariales incertae sedis	<i>Madurella mycetomatis</i>	0	15
Pseudeurotiaceae	<i>Pseudogymnoascus</i> sp. WSF 3629	0	15
Lachnaceae	<i>Lachnellula subtilissima</i>	0	14
Helotiales incertae sedis	<i>Rhynchosporium secalis</i>	0	14

Sclerotiniaceae	<i>Monilinia laxa</i>	0	13
Ceratobasidiaceae	<i>Rhizoctonia solani</i> AG-3 Rhs1AP	0	13
Sclerotiniaceae	<i>Sclerotinia trifoliorum</i>	0	13
Erysiphaceae	<i>Blumeria graminis f. sp. tritici</i>	0	12
Argynnaceae	<i>Lepidopterella palustris</i> CBS 459.81	0	12
Sclerotiniaceae	<i>Monilinia fructicola</i>	0	12
Rhizodiscinaceae	<i>Rhizodiscina lignyota</i>	0	12
Trichocomaceae	<i>Talaromyces cellulolyticus</i>	0	12
Hypocreaceae	<i>Trichoderma virens</i> Gv29-8	0	12
Pseudeurotiaceae	<i>Pseudogymnoascus</i> sp. 23342-1-I1	0	11
Sclerotiniaceae	<i>Sclerotium cepivorum</i>	0	11
Sclerotiniaceae	<i>Botrytis elliptica</i>	0	10
Coniochaetaceae	<i>Coniochaeta</i> sp. 2T2.1	0	10
Dothideomycetes incertae sedis	<i>Coniosporium apollinis</i> CBS 100218	0	10
Pseudeurotiaceae	<i>Pseudogymnoascus</i> sp. VKM F-3775	0	10
Microascaceae	<i>Scedosporium apiospermum</i>	0	10
Plectosphaerellaceae	<i>Verticillium dahliae</i>	0	10

Supplementary Table 10. PFAM and DBCAN annotations of significantly differentially expressed (FDR < 0.05) fungal transcripts in *Pinus contorta* needles that were asymptomatic (ASYM) and symptomatic (SYM) of *L. concolor* (LC) and *L. montivaga* (LM)

LC_ASYM vs. LC_SYM	
LC_SYM	
Enzyme	count
Auxilliary Activities	14
Carbohydrate Binding Module	9
Carbohydrate Esterase	4
Glycosyl Hydrolase	97
Glycosyl Transferase	53
PF00450:Serine carboxypeptidase	2
PF00561:alpha/beta hydrolase fold;PF12146:Serine aminopeptidase, S33	1
PF00675:Insulinase (Peptidase family M16)	1
PF00930:Dipeptidyl peptidase IV (DPP IV) N-terminal region;PF00326:Prolyl oligopeptidase family	2
PF01432:Peptidase family M3	1
PF01546:Peptidase family M20/M25/M40	2
PF01828:Peptidase A4 family	3
PF02127:Aminopeptidase I zinc metalloprotease (M18)	3
PF02190:ATP-dependent protease La (LON) substrate-binding domain	3
PF02338:OTU-like cysteine protease	1
PF03051:Peptidase C1-like family	3
PF03571:Peptidase family M49	2
PF04573:Signal peptidase subunit	1
PF05193:Peptidase M16 inactive domain	5
PF05362:Lon protease (S16) C-terminal proteolytic domain	1
PF05388:Carboxypeptidase Y pro-peptide;PF00450:Serine carboxypeptidase	1
PF05576:PS-10 peptidase S37	2
PF05576:PS-10 peptidase S37;PF05577:Serine carboxypeptidase S28	2

PF05903:PPPDE putative peptidase domain	1
PF05903:PPPDE putative peptidase domain;PF08324:PUL domain	1
PF07910:Peptidase family C78	1
PF08367:Peptidase M16C associated	2
PF11838:ERAP1-like C-terminal domain;PF01433:Peptidase family M1 domain	3
PF12146:Serine aminopeptidase, S33	1
PF12436:ICP0-binding domain of Ubiquitin-specific protease 7;PF14533:Ubiquitin-specific protease C-terminal	1
PF16491:CAAX prenyl protease N-terminal, five membrane helices;PF01435:Peptidase family M48	2
PF17771:ADAM cysteine-rich domain;PF13688:Metallo-peptidase family M12;PF13574:Metallo-peptidase family M12B Reprolysin-like;PF13583:Metallo-peptidase family M12B Reprolysin-like;PF01421:Reprolysin (M12B) family zinc metalloprotease	1

Supplementary Table 10 (cont'd). PFAM and DBCAN annotations of significantly differentially expressed (FDR < 0.05) fungal transcripts in *Pinus contorta* needles that were asymptomatic (ASYM) and symptomatic (SYM) of *L. concolor* (LC) and *L. montivaga* (LM).

LM ASYM vs. LM SYM	
<i>LM SYM</i>	
Enzyme	count
Auxilliary Activities	36
Carbohydrate Binding Module	32
Carbohydrate Esterase	1
Glycosyl Hydrolase	166
Glycosyl Transferase	83
PF00026:Eukaryotic aspartyl protease	2
PF00026:Eukaryotic aspartyl protease;PF14541:Xylanase inhibitor C-terminal	1
PF00026:Eukaryotic aspartyl protease;PF14543:Xylanase inhibitor N-terminal	1
PF00557:Metallopeptidase family M24	2

PF00561:alpha/beta hydrolase fold;PF12146:Serine aminopeptidase, S33	2
PF00574:Clp protease	2
PF00675:Insulinase (Peptidase family M16)	1
PF00814:Glycoprotease family	2
PF01019:Gamma-glutamyltranspeptidase	3
PF01433:Peptidase family M1 domain;PF17900:Peptidase M1 N-terminal domain	1
PF01434:Peptidase family M41	3
PF01470:Pyroglutamyl peptidase	1
PF01546:Peptidase family M20/M25/M40	1
PF01828:Peptidase A4 family	1
PF02338:OTU-like cysteine protease	1
PF02517:CPBP intramembrane metalloprotease	1
PF03051:Peptidase C1-like family	1
PF03572:Peptidase family S41	2
PF04389:Peptidase family M28	3
PF04389:Peptidase family M28;PF04253:Transferrin receptor-like dimerisation domain	2
PF04450:Peptidase of plants and bacteria	5
PF05362:Lon protease (S16) C-terminal proteolytic domain	2
PF05577:Serine carboxypeptidase S28	1
PF05903:PPPDE putative peptidase domain;PF08324:PUL domain	1
PF05903:PPPDE putative peptidase domain;PF08324:PUL domain;PF00085:Thioredoxin	1
PF06703:Microsomal signal peptidase 25 kDa subunit (SPC25)	1
PF07728:AAA domain (dynein-related subfamily);PF07726:ATPase family associated with various cellular activities (AAA);PF05362:Lon protease (S16) C-terminal proteolytic domain	2
PF07910:Peptidase family C78	1
PF08367:Peptidase M16C associated	1
PF09768:Peptidase M76 family	1

PF11838:ERAP1-like C-terminal domain;PF01433:Peptidase family M1 domain;PF17900:Peptidase M1 N-terminal domain	1
PF11838:ERAP1-like C-terminal domain;PF17900:Peptidase M1 N-terminal domain	1
PF12436:ICP0-binding domain of Ubiquitin-specific protease 7;PF00443:Ubiquitin carboxyl-terminal hydrolase	1
PF12436:ICP0-binding domain of Ubiquitin-specific protease 7;PF00443:Ubiquitin carboxyl-terminal hydrolase;PF14533:Ubiquitin-specific protease C-terminal	1
PF12770:CHAT domain;PF03568:Peptidase family C50	1
PF13365:Trypsin-like peptidase domain	1
PF13650:Aspartate protease;PF09668:Aspartyl protease;PF13975:gag-polyprotein putative aspartyl protease	2
PF16188:C-terminal region of peptidase_M24	1
PF16188:C-terminal region of peptidase_M24;PF16189:Creatinase/Prolidase N-terminal domain	3
PF16491:CAAX prenyl protease N-terminal, five membrane helices	1
PF16491:CAAX prenyl protease N-terminal, five membrane helices;PF01435:Peptidase family M48	1
PF17771:ADAM cysteine-rich domain;PF00200:Disintegrin;PF13688:Metallo-peptidase family M12;PF13574:Metallo-peptidase family M12B Reprolysin-like;PF13583:Metallo-peptidase family M12B Reprolysin-like;PF01421:Reprolysin (M12B) family zinc metalloprotease	4
PF17900:Peptidase M1 N-terminal domain	2
PF18323:Cop9 signalosome subunit 5 C-terminal domain;PF01398:JAB1/Mov34/MPN/PAD-1 ubiquitin protease	1

Supplementary Table 11. KEGG annotations of differentially expressed (FDR < 0.05) fungal transcripts between *Pinus contorta* needles that were asymptomatic (ASYM) and symptomatic (SYM) of *Lophodermella concolor* (LC) and *L. montivaga* (LM).

LC_ASYM vs. LC_SYM					
LC_ASYM			LC_SYM		
KEGG annotations	KO_count	Transcript	KEGG annotations	KO_count	Transcript
None	0	0	01110 Biosynthesis of secondary metabolites	136	254
			<i>Metabolism of terpenoids and polyketides</i>		
			00900 Terpenoid backbone biosynthesis	6	10
			00909 Sesquiterpenoid and triterpenoid biosynthesis	1	1
			00906 Carotenoid biosynthesis	2	4
			00981 Insect hormone biosynthesis	1	3
			00903 Limonene and pinene degradation	1	3
			00281 Geraniol degradation	1	1
			<i>Biosynthesis of other secondary metabolites</i>		
			00940 Phenylpropanoid biosynthesis	3	11
			00950 Isoquinoline alkaloid biosynthesis	3	10
			00960 Tropane, piperidine and pyridine alkaloid biosynthesis	3	10
			00232 Caffeine metabolism	1	2
			00965 Betalain biosynthesis	1	2
			00966 Glucosinolate biosynthesis	1	4
			0032 Carbapenem biosynthesis	2	2
			00261 Monobactam biosynthesis	2	2
			00521 Streptomycin biosynthesis	2	5
			00524 Neomycin, kanamycin and gentamicin biosynthesis	1	2
			00401 Novobiocin biosynthesis	1	2

		00333 Prodigiosin biosynthesis	2	5
		00254 Aflatoxin biosynthesis	1	1
		<i>Xenobiotics biodegradation and metabolism</i>		
		00362 Benzoate degradation	2	2
		00627 Aminobenzoate degradation	4	13
		00364 Fluorobenzoate degradation	2	2
		00625 Chloroalkane and chloroalkene degradation	4	9
		00361 Chlorocyclohexane and chlorobenzene degradation	3	3
		00623 Toluene degradation	3	4
		00643 Styrene degradation	4	16
		00930 Caprolactam degradation	3	6
		00621 Dioxin degradation	1	7
		00626 Naphthalene degradation	2	10
		00624 Polycyclic aromatic hydrocarbon degradation	1	7
		00980 Metabolism of xenobiotics by cytochrome P450	3	11
		00982 Drug metabolism - cytochrome P450	2	10
		00983 Drug metabolism - other enzymes	5	15

Supplementary Table 11 (cont'd). KEGG annotations of differentially expressed (FDR < 0.05) fungal transcripts between *Pinus contorta* needles that were asymptomatic (ASYM) and symptomatic (SYM) of *Lophodermella concolor* (LC) and *L. montivaga* (LM).

LM_ASYM vs. LM_SYM					
LM_ASYM			LM_SYM		
KEGG annotations	KO_count	Transcript	KEGG annotations	KO_count	Transcript
None	0	0	01110 Biosynthesis of secondary metabolites	148	468
			<i>Metabolism of terpenoids and polyketides</i>		
			00900 Terpenoid backbone biosynthesis	10	23
			00906 Carotenoid biosynthesis	2	4
			00981 Insect hormone biosynthesis	1	2
			00903 Limonene and pinene degradation	1	2
			00281 Geraniol degradation	1	3
			<i>Biosynthesis of other secondary metabolites</i>		
			00940 Phenylpropanoid biosynthesis	4	26
			00901 Indole alkaloid biosynthesis	1	4
			00950 Isoquinoline alkaloid biosynthesis	6	29
			00960 Tropane, piperidine and pyridine alkaloid biosynthesis	3	18
			00232 Caffeine metabolism	2	4
			00965 Betalain biosynthesis	2	10
			00311 Penicillin and cephalosporin biosynthesis	1	1
			00261 Monobactam biosynthesis	2	12
			00521 Streptomycin biosynthesis	2	25
			00524 Neomycin, kanamycin and gentamicin biosynthesis	1	13
			00401 Novobiocin biosynthesis	1	12

			00405 Phenazine biosynthesis	1	1
			00333 Prodigiosin biosynthesis	1	4
			00254 Aflatoxin biosynthesis	1	1
			<i>Xenobiotics biodegradation and metabolism</i>		
			00362 Benzoate degradation	3	7
			00627 Aminobenzoate degradation	6	23
			00625 Chloroalkane and chloroalkene degradation	4	9
			00361 Chlorocyclohexane and chlorobenzene degradation	2	4
			00623 Toluene degradation	1	2
			00643 Styrene degradation	3	25
			Atrazine degradation	1	6
			00930 Caprolactam degradation	3	17
			00621 Dioxin degradation	1	6
			00626 Naphthalene degradation	2	8
			00624 Polycyclic aromatic hydrocarbon degradation	1	6
			00980 Metabolism of xenobiotics by cytochrome P450	3	10
			00982 Drug metabolism - cytochrome P450	5	16
			00983 Drug metabolism - other enzymes	7	22

Supplementary Table 12. PRGdb annotations of differentially expressed plant transcripts between *Pinus contorta* needles that were asymptomatic (ASYM) and symptomatic (SYM) of *Lophodermella concolor* (LC) and *L. montivaga* (LM).

LC_ASYM vs. LC_SYM			
LC_ASYM			
Trinity_isoform	PRGdb Gene Name	Domain	Class
TRINITY_DN295056_c4_g1_i1	295167_OPUNC05G25400.1	TM, Kinase	KIN
TRINITY_DN297892_c1_g1_i7	2143973_Thecc1EG026703t1	NBS, CC, TM	CN
TRINITY_DN311910_c0_g1_i8	220042_Bo01390s020.1	TM, Kinase	KIN
TRINITY_DN312007_c0_g1_i8	2101569_37796	NBS, TM	N
TRINITY_DN312711_c3_g1_i5	252315_Kalax.0019s0068.2.p	TM, Kinase	KIN
TRINITY_DN316284_c3_g2_i6	271508_Migut.I00566.1.p	Kinase	KIN
TRINITY_DN316314_c0_g2_i1	2174318_DCAR_025158	CC, NBS, TM	CN
TRINITY_DN318496_c6_g1_i14	2141987_Thecc1EG030191t1	TM, LRR	RLP
TRINITY_DN319429_c3_g3_i1	2174056_DCAR_029810	TM, Kinase	KIN
TRINITY_DN322828_c4_g2_i1	258725_MDP0000312874	LRR, TM	RLP
TRINITY_DN326218_c4_g1_i1	283491_BGIOSGA033602-PA	LRR, TM	RLP
TRINITY_DN327185_c2_g5_i2	292065_ONIVA06G08300.1	TM, Kinase	KIN
TRINITY_DN327568_c11_g1_i5	2156952_Traes_6DL_7662129AC.1	CC, TM, Kinase	CK
TRINITY_DN328994_c2_g1_i11	291397_ONIVA09G01460.4	LRR, Kinase, TM	RLK
TRINITY_DN332422_c2_g1_i1	24380_evm_27.model.AmTr_v1.0_scaffold00013.263	TM, Kinase	KIN
LC_SYM			
TRINITY_DN287985_c7_g1_i7	2121971_29982.m000218	TM, Kinase	KIN
TRINITY_DN318993_c0_g1_i13	2165672_VIT_13s0067g02030.t01	LRR, Kinase, TM	RLK
TRINITY_DN317341_c1_g1_i8	2169374_AC230011.2_FGP002	NBS, LRR, TM	NL
TRINITY_DN300060_c3_g6_i4	161449_Xa5	None	Others
TRINITY_DN302437_c0_g2_i6	23957_evm_27.model.AmTr_v1.0_scaffold00002.359	NBS, TM	N
TRINITY_DN312711_c3_g1_i10	252315_Kalax.0019s0068.2.p	TM, Kinase	KIN
TRINITY_DN327784_c0_g4_i1	270574_99058	TM, LRR	RLP

Supplementary Table 12 (cont'd). PRGdb annotations of differentially expressed plant transcripts between *Pinus contorta* needles that were asymptomatic (ASYM) and symptomatic (SYM) of *Lophodermella concolor* (LC) and *L. montivaga* (LM).

LM_ASYM vs. LM_SYM			
LM_ASYM			
Trinity_isoform	PRGdb Gene Name	Domain	Class
TRINITY_DN327718_c1_g1_i9	2110801_Pp3c4_23480V3.5.p	TM, Kinase	KIN
TRINITY_DN312841_c0_g1_i3	211298_AT1G33250.1	TM, LRR	RLP
TRINITY_DN332135_c2_g2_i8	2113160_Pp3c9_3020V3.3.p	TM	TRAN
TRINITY_DN317104_c1_g1_i11	2118666_Prupe.6G141700.1.p	Kinase	KIN
TRINITY_DN326067_c0_g1_i1	2126077_SapurV1A.1546s0040.1.p	NBS, CC, LRR, TM	CNL
TRINITY_DN316497_c1_g1_i14	2126539_EFJ26072	CC, TM, Kinase	CK
TRINITY_DN314186_c0_g1_i11	2141379_Spipo7G0007500	TM, Kinase	KIN
TRINITY_DN318496_c6_g1_i5	2141987_Thecc1EG030191t1	TM, LRR	RLP
TRINITY_DN314457_c2_g1_i4	2142312_Thecc1EG036312t1	TM, Kinase	KIN
TRINITY_DN297892_c1_g1_i4	2143973_Thecc1EG026703t1	NBS, CC, TM	CN
TRINITY_DN330350_c2_g1_i17	2157536_Traes_2BS_47E2D6444.3	TM, Kinase	KIN
TRINITY_DN300137_c5_g2_i2	2158771_Traes_5DL_B89CD8432.2	NBS, TM	N
TRINITY_DN318083_c1_g1_i10	2167379_GRMZM2G311328_P01	TM, Kinase	KIN
TRINITY_DN316547_c2_g2_i3	228716_Eucgr.I00321.3.p	NBS	N
TRINITY_DN302690_c0_g1_i1	236145_mrna13099.1-v1.0-hybrid	NBS, CC, LRR, TM	CNL
TRINITY_DN332213_c5_g3_i19	236248_mrna26650.1-v1.0-hybrid	CC, LRR	CL
TRINITY_DN332213_c5_g3_i3	236248_mrna26650.1-v1.0-hybrid	CC, LRR	CL
TRINITY_DN305565_c0_g1_i11	23975_evm_27.model.AmTr_v1.0_scaffold00159.5	TM, LRR	RLP
TRINITY_DN325875_c1_g1_i3	24194_evm_27.model.AmTr_v1.0_scaffold00175.16	TM, Kinase	KIN
TRINITY_DN327923_c0_g1_i5	24225_evm_27.model.AmTr_v1.0_scaffold00036.71	Kinase	KIN
TRINITY_DN309777_c0_g1_i14	244043_Gorai.002G080700.4	TM, Kinase	KIN
TRINITY_DN324089_c0_g2_i5	24429_evm_27.model.AmTr_v1.0_scaffold00004.128	CC, TM, Kinase	CK
TRINITY_DN319984_c0_g2_i11	24954_Aco001151.1	NBS, TM	N
TRINITY_DN295279_c0_g1_i6	255571_LPERR09G04070.2	NBS, CC, LRR, TM	CNL
TRINITY_DN323057_c0_g2_i3	256133_Lus10018308	NBS, TM, LRR	NL
TRINITY_DN329373_c2_g6_i5	256554_Lus10002966	TM, Kinase	KIN
TRINITY_DN326870_c0_g1_i7	25675_Aco003435.1	LRR, Kinase, TM	RLK

TRINITY DN316713 c5 g1 i4	258909 MDP0000256746	TM, LRR	RLP
TRINITY DN328953 c5 g1 i1	259084 MDP0000280399	LRR, TM	RLP
TRINITY DN297053 c0 g2 i2	259545 MDP0000267318	TM, Kinase, LRR	RLK
TRINITY DN314713 c5 g3 i1	260167 MDP0000265371	TM, Kinase	KIN
TRINITY DN309109 c4 g1 i12	262008 MDP0000275440	TM, Kinase	KIN
TRINITY DN279301 c0 g1 i1	269964 Medtr6g015455.1	NBS, CC, TM, TIR, LRR	CTNL
TRINITY DN312056 c2 g1 i8	273634 GSMUA_Achr4P15370_001	Kinase	KIN
TRINITY DN329776 c1 g2 i5	283707 BGIOSGA022935-PA	CC, TM, Kinase	CK
TRINITY DN296991 c0 g3 i1	284416 BGIOSGA018486-PA	TM, Kinase	KIN
TRINITY DN317547 c0 g1 i16	285234 BGIOSGA035510-PA	CC, NBS, TM	CN
TRINITY DN311910 c0 g2 i5	2855 EMT14464	TM, Kinase	KIN
TRINITY DN327124 c1 g1 i5	286320 KN539463.1_FGP012	TM, Kinase	KIN
TRINITY DN321631 c1 g3 i6	289407 OMERI09G04140.1	TM, Kinase	KIN
<i>LM_SYM</i>			
TRINITY DN300060 c3 g9 i7	161449 Xa5	None	Others
TRINITY DN322920 c2 g3 i2	2111550 Pp3c1_23810V3.5.p	TM, Kinase	KIN
TRINITY DN322920 c2 g3 i3	2111550 Pp3c1_23810V3.5.p	TM, Kinase	KIN
TRINITY DN289035 c0 g1 i4	21403 EMT03839	CC, TM, Kinase	CK
TRINITY DN321104 c0 g2 i8	2144461 Traes_3DL_D3A6BBA9A.1	LRR	L
TRINITY DN314105 c0 g2 i2	2173701 DCAR_006660	CC, Kinase	CK
TRINITY DN280246 c3 g1 i1	2175807 maker_scaffold23795_snap_gene_0_12_mRNA_1	TM, Kinase	KIN
TRINITY DN321699 c3 g1 i2	260037 MDP0000282499	TM, Kinase	KIN
TRINITY DN322404 c7 g4 i8	260088 MDP0000302027	CC, TM, Kinase	CK
TRINITY DN322462 c1 g2 i3	266982 Medtr8g023445.1	LRR, TM	RLP
TRINITY DN325045 c6 g1 i1	270829_50694	LRR	L
TRINITY DN325045 c6 g1 i10	270829_50694	LRR	L
TRINITY DN325045 c6 g1 i11	270829_50694	LRR	L
TRINITY DN325045 c6 g1 i14	270829_50694	LRR	L
TRINITY DN312915 c0 g1 i8	288863 OMERI03G01250.1	TM, Kinase	KIN
TRINITY DN323472 c5 g2 i3	295167 OPUNC05G25400.1	TM, Kinase	KIN

Supplementary Table 13. KEGG annotations of differentially expressed plant transcripts between *Pinus contorta* needles that were asymptomatic (ASYM) and symptomatic (SYM) of *Lophodermella concolor* (LC) and *L. montivaga* (LM).

LC_ASYM vs. LC_SYM		
<i>LC_ASYM</i>		
KEGG annotations	KO_count	Transcript
Biosynthesis of secondary metabolites	11	11
Metabolism of terpenoids and polyketides	1	1
<i>Biosynthesis of other secondary metabolites</i>		
Phenylpropanoid biosynthesis	1	1
Monobactam biosynthesis	1	1
Streptomycin biosynthesis	1	1
<i>Plant-pathogen interaction</i>	1	1
<i>Signal transduction</i>		
Phospholipase D signaling pathway	1	1
Plant hormone signal transduction	2	2
MAPK signaling pathway	3	3
Ras signaling pathway	1	1
cAMP signaling pathway	1	1
Sphingolipid signaling pathway	1	1
<i>LC_SYM</i>		
Biosynthesis of secondary metabolites	5	11
<i>Biosynthesis of other secondary metabolites</i>		
Phenylpropanoid biosynthesis	1	1
Stilbenoid, diarylheptanoid and gingerol biosynthesis	1	1
Flavonoid biosynthesis	1	1
<i>Xenobiotics biodegradation and metabolism</i>		
Metabolism of xenobiotics by cytochrome P450	1	1
Drug metabolism - cytochrome P450	1	1
Drug metabolism - other enzymes	2	2
<i>Plant-pathogen interaction</i>	1	1
<i>Signal transduction</i>		
Hippo signaling pathway	1	2

Plant hormone signal transduction	1	1
MAPK signaling pathway	1	1
PI3K-Akt signaling pathway	1	2
AMPK signaling pathway	1	2
Sphingolipid signaling pathway	1	2

Supplementary Table 13 (cont'd). KEGG annotations of differentially expressed plant transcripts between *Pinus contorta* needles that were asymptomatic (ASYM) and symptomatic (SYM) of *Lophodermella concolor* (LC) and *L. montivaga* (LM).

LM_ASYM vs. LM_SYM		
LM_ASYM		
KEGG annotations	KO_count	Transcript
Biosynthesis of secondary metabolites	18	19
<i>Biosynthesis of other secondary metabolites</i>		
Isoquinoline alkaloid biosynthesis	1	1
Flavonoid biosynthesis	1	1
Indole alkaloid biosynthesis	1	1
Betalain biosynthesis	1	1
<i>Xenobiotics biodegradation and metabolism</i>		
Chloroalkane and chloroalkene degradation	1	1
Naphthalene degradation	1	1
Metabolism of xenobiotics by cytochrome P450	1	1
Drug metabolism - cytochrome P450	1	1
<i>Signal transduction</i>		
Two-component system	1	2
MAPK signaling pathway	4	4
Plant hormone signal transduction	5	6
PI3K-Akt signaling pathway	1	1
AMPK signaling pathway	1	1
Sphingolipid signaling pathway	1	1
Phospholipase D signaling pathway	1	1

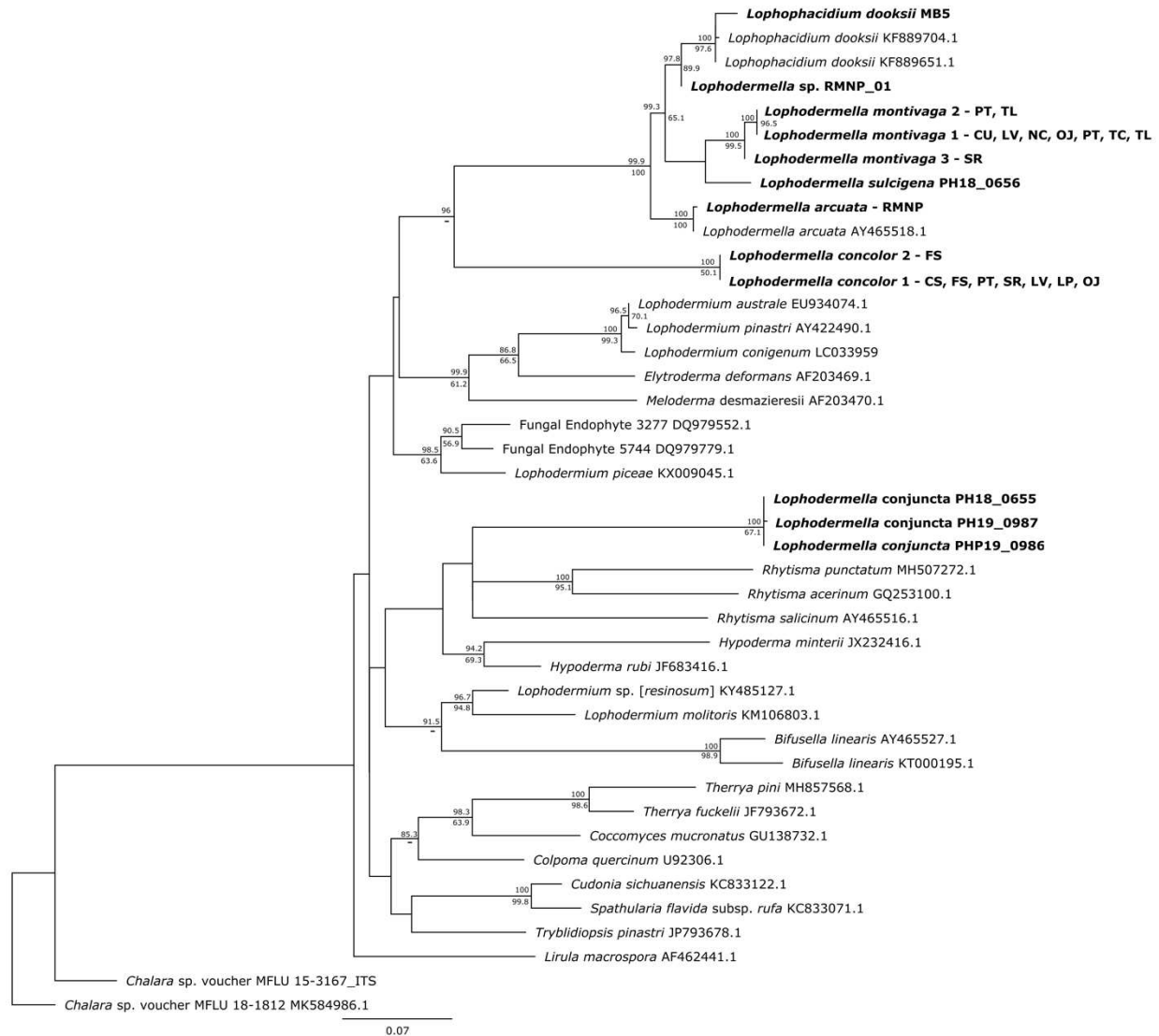
<i>LM_SYM</i>		
Biosynthesis of secondary metabolites	5	8
<i>ABC transporters</i>	1	1
<i>Signal transduction</i>		
Hippo signaling pathway	1	1
Phosphatidylinositol signaling pathway	1	1
Sphingolipid signaling pathway	1	4
PI3K-Akt signaling pathway	1	4
AMPK signaling pathway	1	4

Supplementary Table 14. NCBI protein annotations represented with at least 10 differentially expressed (FDR < 0.05) bacterial transcripts found between *Pinus contorta* needles that asymptomatic (ASYM) and symptomatic (SYM) of *Lophodermella concolor* (LC) and *L. montivaga* (LM).

LC ASYM vs. LC_SYM			
LC_ASYM		LC_SYM	
Protein	count	Protein	count
hypothetical protein	2	hypothetical protein	472
		MFS transporter	20
		alpha/beta hydrolase	17
		GNAT family N-acetyltransferase	17
		ATP-binding cassette domain-containing protein	16
		ABC transporter ATP-binding protein	13
		Uncharacterised protein	11
		TetR/AcrR family transcriptional regulator	10
LM ASYM vs. LM_SYM			
None		hypothetical protein	983
		MFS transporter	35
		ABC transporter ATP-binding protein	32

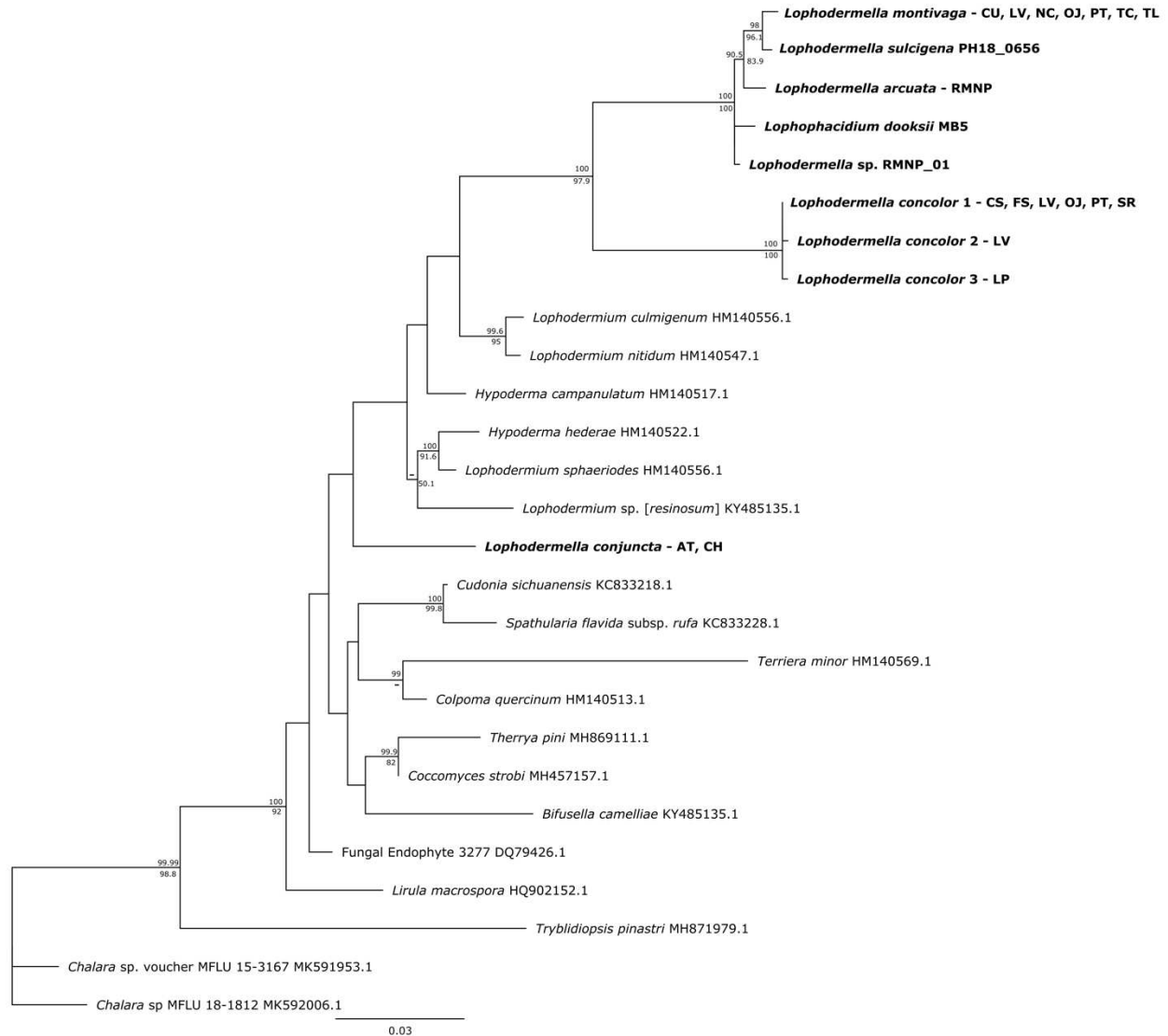
	glycoside hydrolase	27
	ATP-binding cassette domain-containing protein	25
	glycosyltransferase family 4 protein	25
	alpha/beta hydrolase	23
	DUF1223 domain-containing protein	19
	glycosyltransferase	19
	MULTISPECIES: hypothetical protein	19
	DUF3987 domain-containing protein	18
	LysR family transcriptional regulator	18
	GNAT family N-acetyltransferase	17
	ABC transporter permease	16
	sigma 54-interacting transcriptional regulator	16
	response regulator	15
	RNA polymerase sigma-70 factor, ECF subfamily	15
	ATP-dependent zinc metalloprotease FtsH	14
	leucyl/phenylalanyl-tRNA--protein transferase	14
	PE-PPE domain-containing protein	14
	porin	14
	TMEM165/GDT1 family protein	14
	ABC transporter substrate-binding protein	13
	ankyrin repeat domain-containing protein	13
	AraC family transcriptional regulator	13
	helix-turn-helix transcriptional regulator	13
	polysaccharide biosynthesis protein	13
	TonB-dependent receptor	13
	apolipoprotein N-acyltransferase	12
	DASS family sodium-coupled anion symporter	12
	DHA2 family efflux MFS transporter permease subunit	12

		efflux transporter outer membrane subunit	12
		Gfo/Idh/MocA family oxidoreductase	12
		HNH endonuclease	12
		uroporphyrinogen-III synthase	12
		alpha/beta fold hydrolase	11
		amidohydrolase	11
		ribose-5-phosphate isomerase RpiA	11
		ATP-binding protein	10
		DUF2087 domain-containing protein	10
		EAL domain-containing protein	10
		MULTISPECIES: 2-methylcitrate synthase	10
		MULTISPECIES: Gldg family protein	10
		putative hydro-lyase	10
		response regulator transcription factor	10
		SAM-dependent methyltransferase	10
		serine/threonine protein kinase	10
		TetR/AcrR family transcriptional regulator	10
		transcriptional regulator	10
		universal stress protein	10
		xanthine dehydrogenase family protein molybdopterin-binding subunit	10

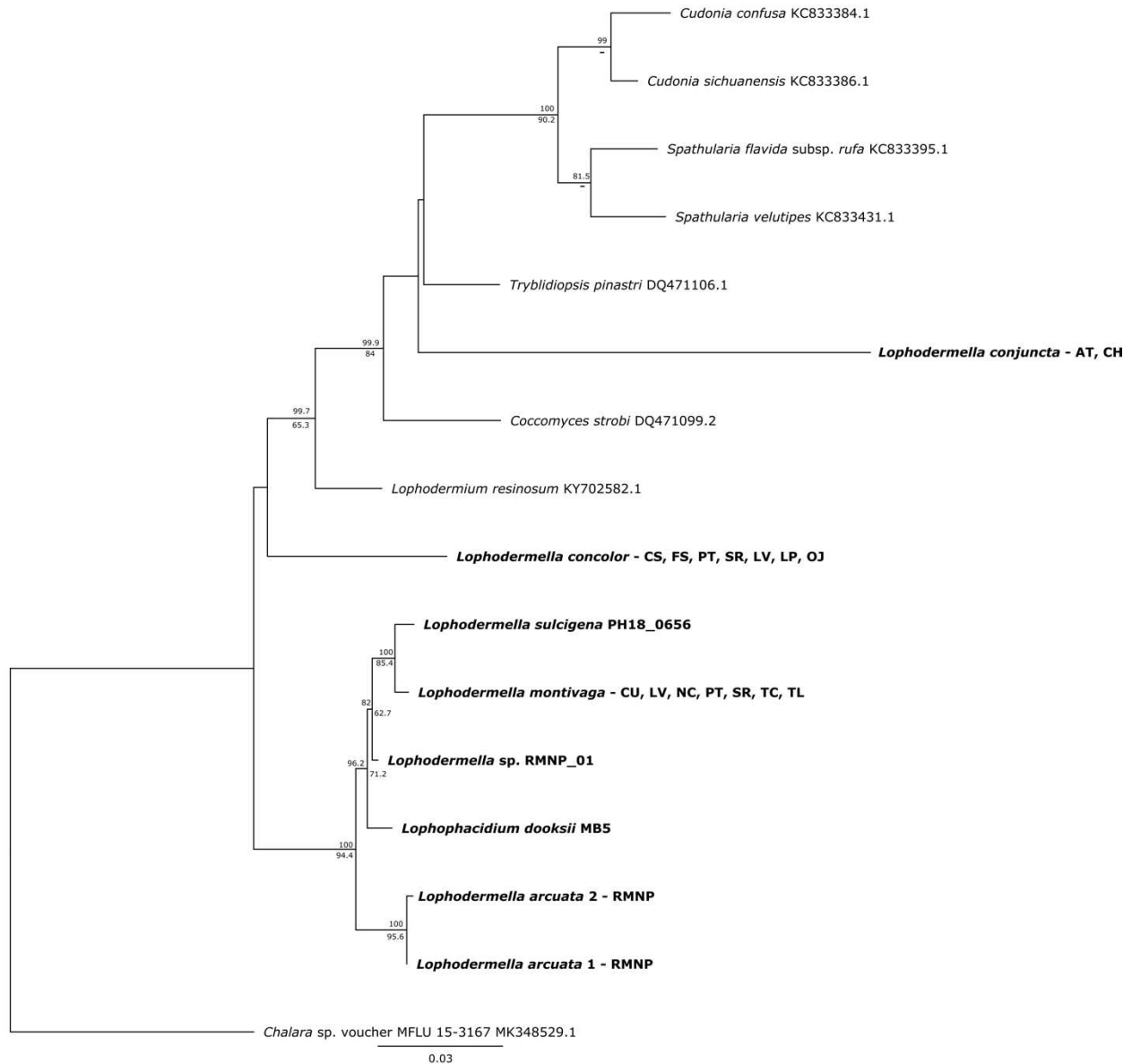


Supplementary Figure 1. Maximum likelihood phylogeny depicting phylogenetic relationships of *Lophodermella montivaga* and *L. concolor* within the *Lophodermella* clade based at the internal transcribed spacer (ITS). Bayesian posterior probabilities (PP) greater than 0.80 and bootstrap (BS) support values from maximum likelihood analysis greater than 50 are shown above and below node, respectively. Species in bold are samples derived from this study.

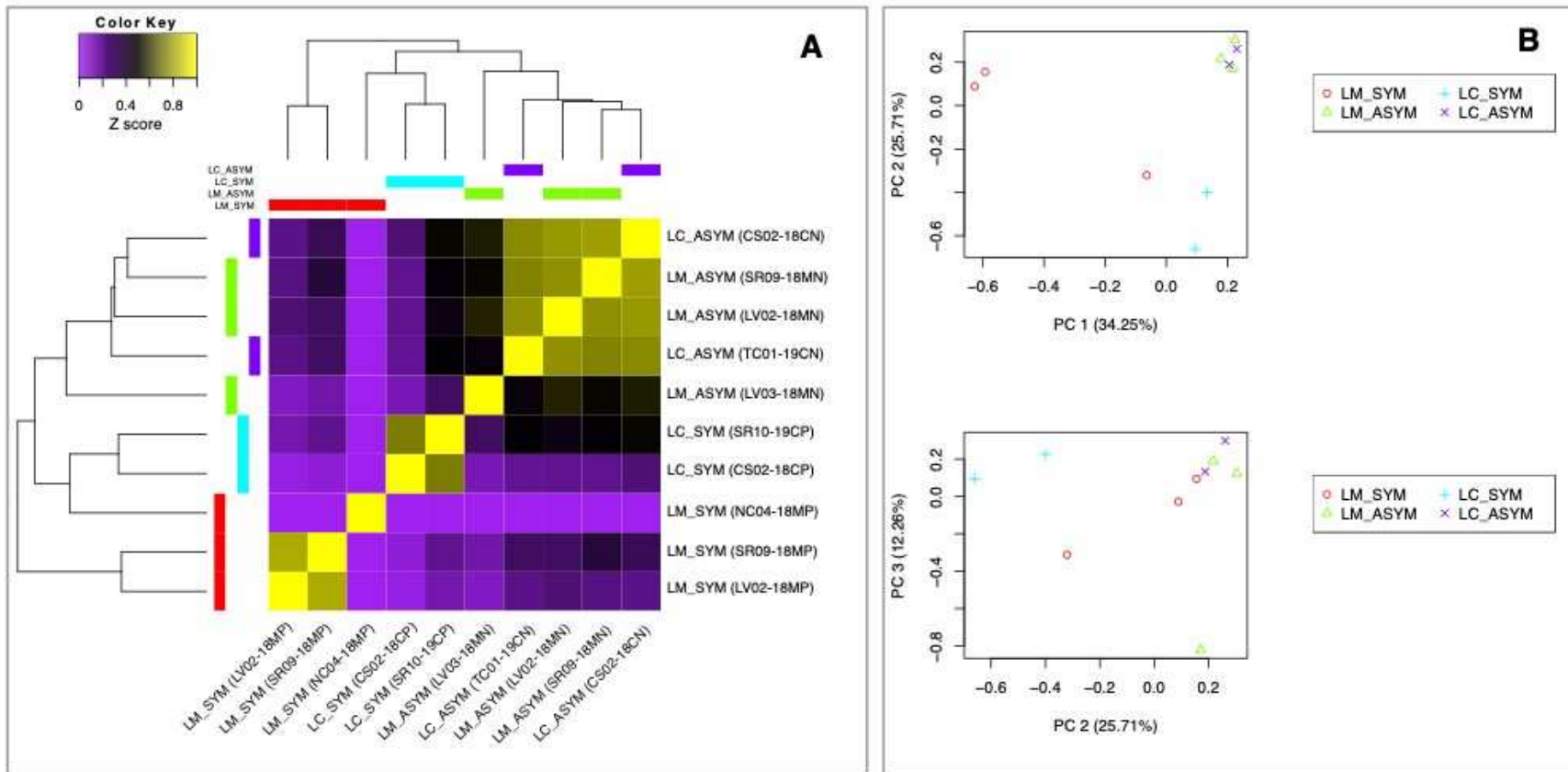
Lophodermella concolor and *L. montivaga* are distinguished per site within Gunnison National Park, CO, USA: CS – Cold Springs, FS – Fisherman Trail, LP – Lodgepole Campground, LV – Lakeview Campground, OJ – Oh Be Joyful, PT – Pitkin, SR – Slate River, TC – Tincup, TL – Taylor. Other *Lophodermella* species: RMNP – Rocky Mountain National Park, Colorado. Numbers correspond to genotype.



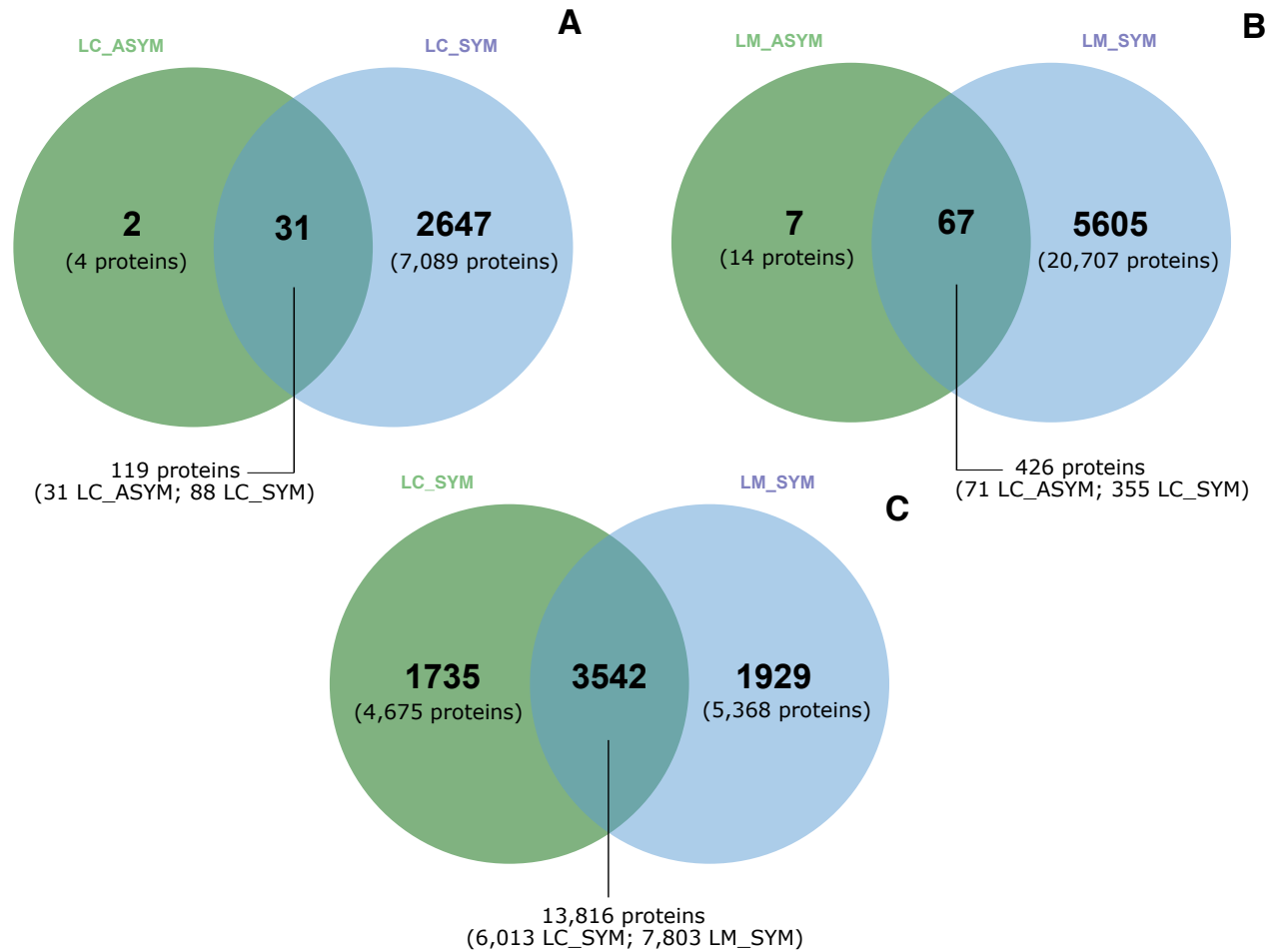
Supplementary Figure 2. Maximum likelihood phylogeny depicting phylogenetic relationships of *Lophodermella montivaga* and *L. concolor* within the *Lophodermella* clade based at the large ribosomal subunit (LSU). Bayesian posterior probabilities (PP) greater than 0.80 and bootstrap (BS) support values from maximum likelihood analysis greater than 50 are shown above and below node, respectively. Species in bold are samples derived from this study. *Lophodermella concolor* and *L. montivaga* are distinguished per site within Gunnison National Park, CO, USA: CS – Cold Springs, FS – Fisherman Trail, LP – Lodgepole Campground, LV – Lakeview Campground, OJ – Oh Be Joyful, PT – Pitkin, SR – Slate River, TC – Tincup, TL - Taylor. Other *Lophodermella* species: RMNP – Rocky Mountain National Park, Colorado, AT – Austria and CH – Switzerland. Numbers correspond to genotype.



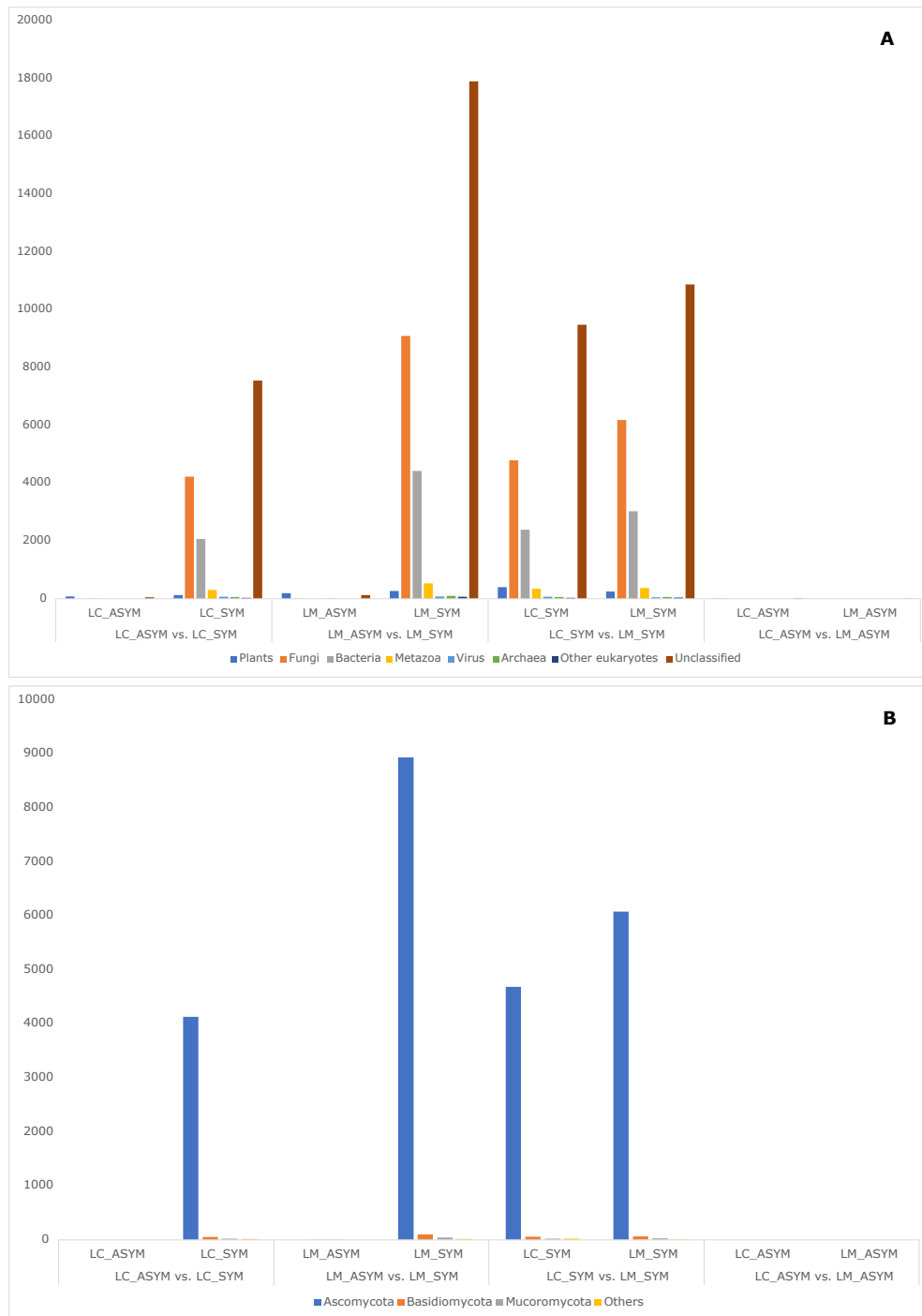
Supplementary Figure 3. Bayesian phylogeny depicting phylogenetic relationships of *Lophodermella montivaga* and *L. concolor* within the *Lophodermella* clade based at the translation elongation factor 1-alpha (*TEF1 α*). Bayesian posterior probabilities (PP) greater than 0.80 and bootstrap (BS) support values from maximum likelihood analysis greater than 50 are shown above and below node, respectively. Species in bold are samples derived from this study. *Lophodermella concolor* and *L. montivaga* are distinguished per site within Gunnison National Park, CO, USA: CS – Cold Springs, FS – Fisherman Trail, LP – Lodgepole Campground, LV – Lakeview Campground, OJ – Oh Be Joyful, PT – Pitkin, SR – Slate River, TC – Tincup, TL – Taylor. Other *Lophodermella* species: RMNP – Rocky Mountain National Park, Colorado, AT – Austria and CH – Switzerland. Numbers correspond to genotype.



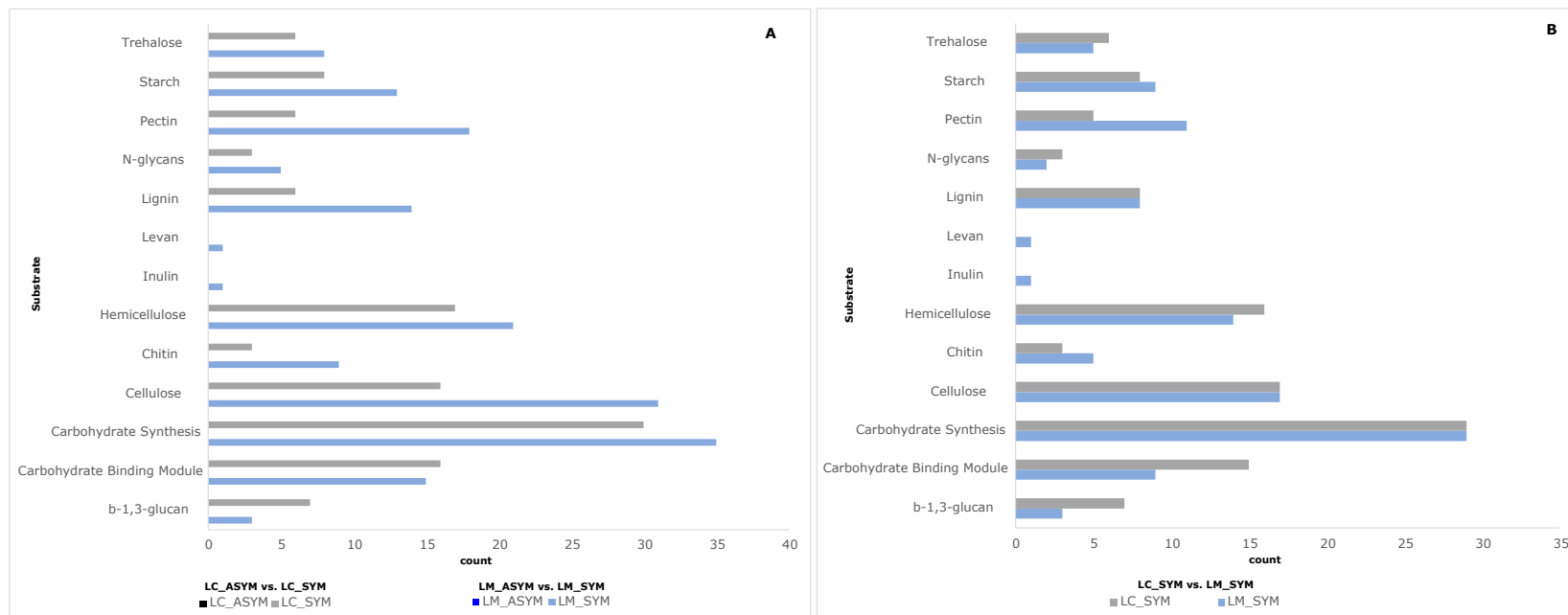
Supplementary Figure 4. Heatmap of the isoform correlation and Principal Component Analysis between *Pinus contorta* needle samples that were asymptomatic (ASYM) and symptomatic (SYM) of *Lophodermella concolor* (LC) and *L. montivaga* (LM).



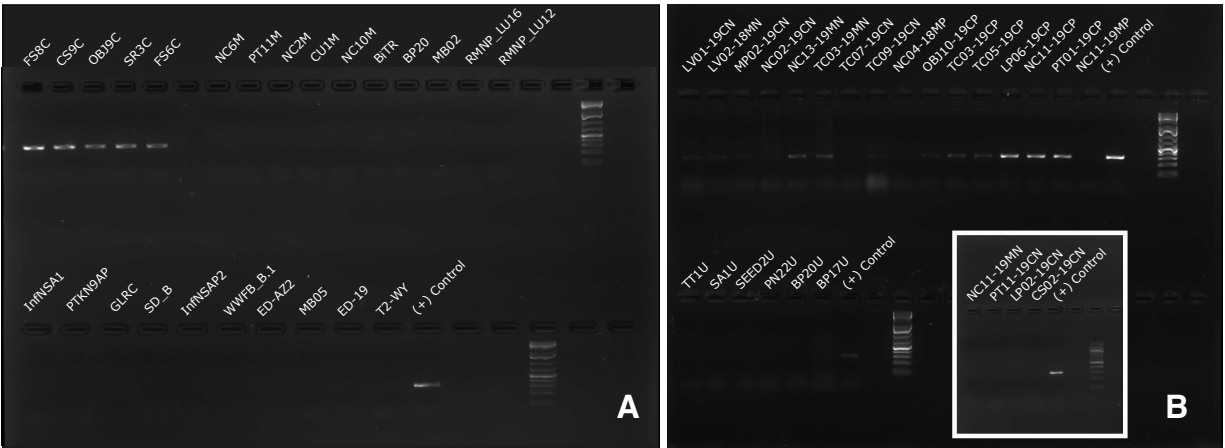
Supplementary Figure 5. Number of shared and unique orthologous protein clusters between (A) *Pinus contorta* needles symptomatic and asymptomatic of *Lophodermella concolor* (LC_ASYM vs. LC_SYM) and (B) *L. montivaga* (LM_ASYM vs. LM_SYM), and (C) between symptomatic needles of *L. concolor* and *L. montivaga* (LC_SYM vs. LM_SYM) inferred from Orthovenn2. Bold numbers correspond to the number of protein clusters.



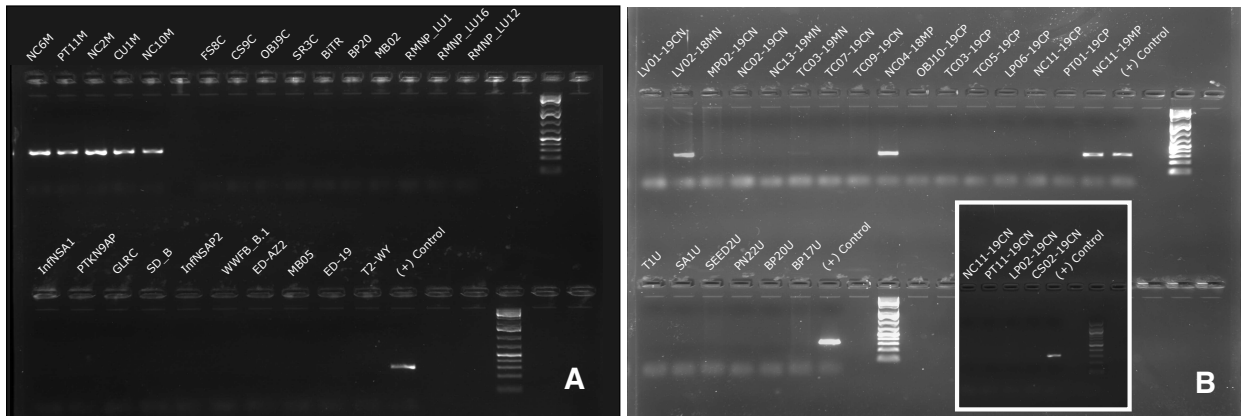
Supplementary Figure 6. Taxonomic lineage (A) and fungal phyla (B) of the significantly differentially expressed transcripts (FDR < 0.05, p-value < 0.05) across all comparisons determined through mmseqs2 search in the concatenated databases of NCBI-nr and JGI Mycocosm. Number of transcripts in LC_ASYNC vs. LM_ASYNC comparison is too low.



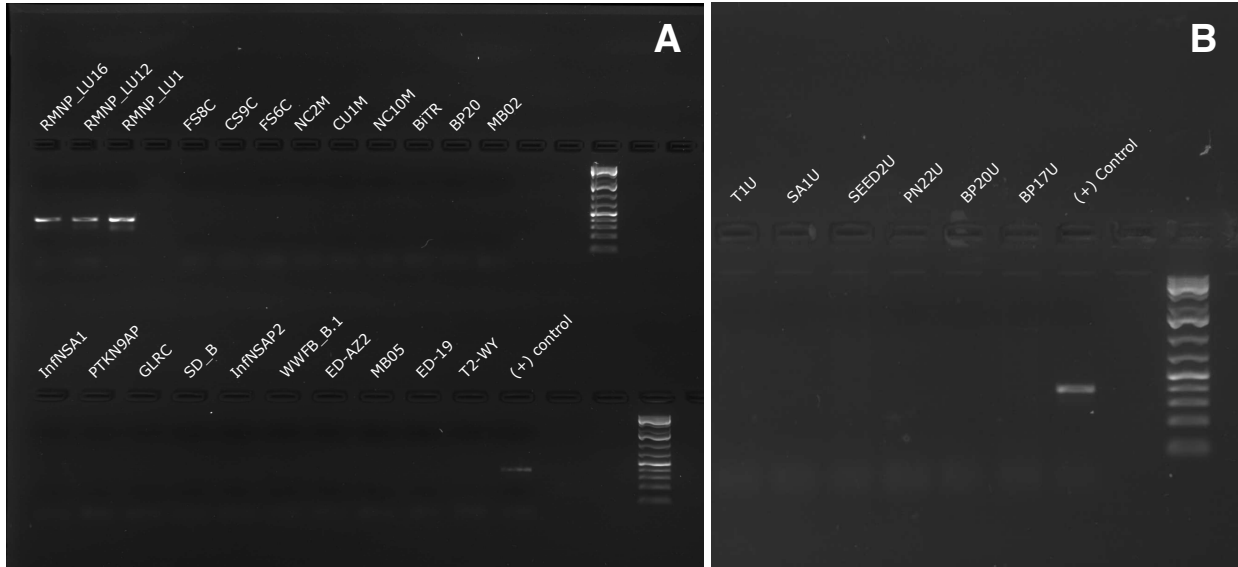
Supplementary Figure 7. Number of bacterial enzymes that degrade various substrates that were differentially expressed between (A) *Pinus contorta* needles symptomatic and asymptomatic of *Lophodermella concolor* (LC_ASYM vs. LC_SYM) and *L. montivaga* (LM_ASYM vs. LM_SYM)



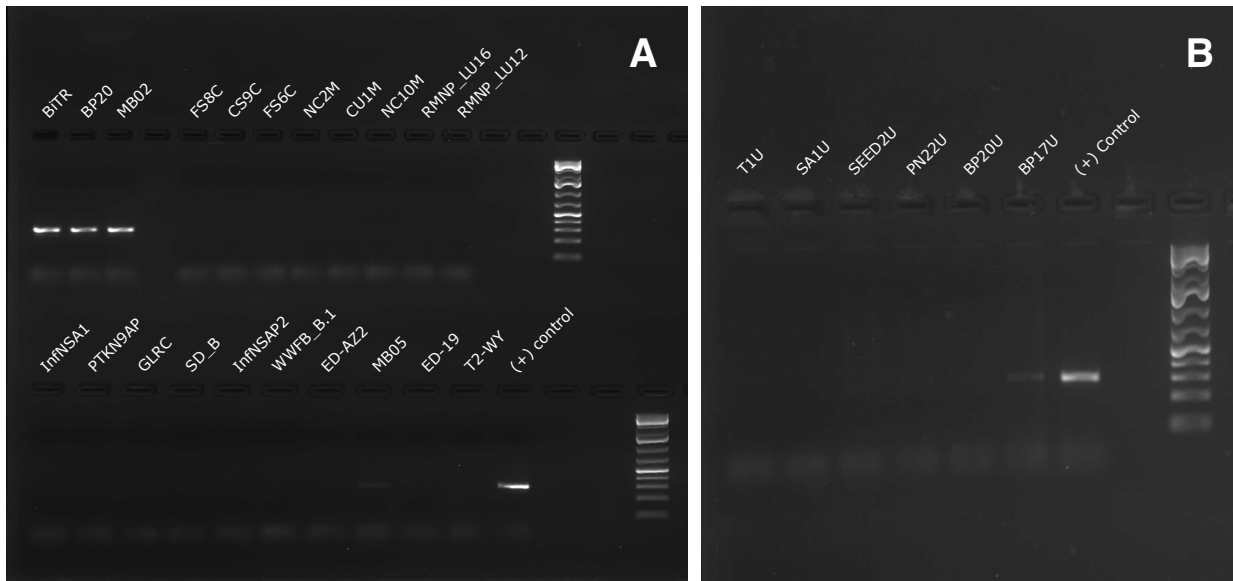
Supplementary Figure 8. LC_ITS primer assay across target (*Lophodermella concolor*) and non-target species (A) and across asymptomatic and symptomatic needles (B). Gel photographs were taken using using Azure™ gel imaging system.



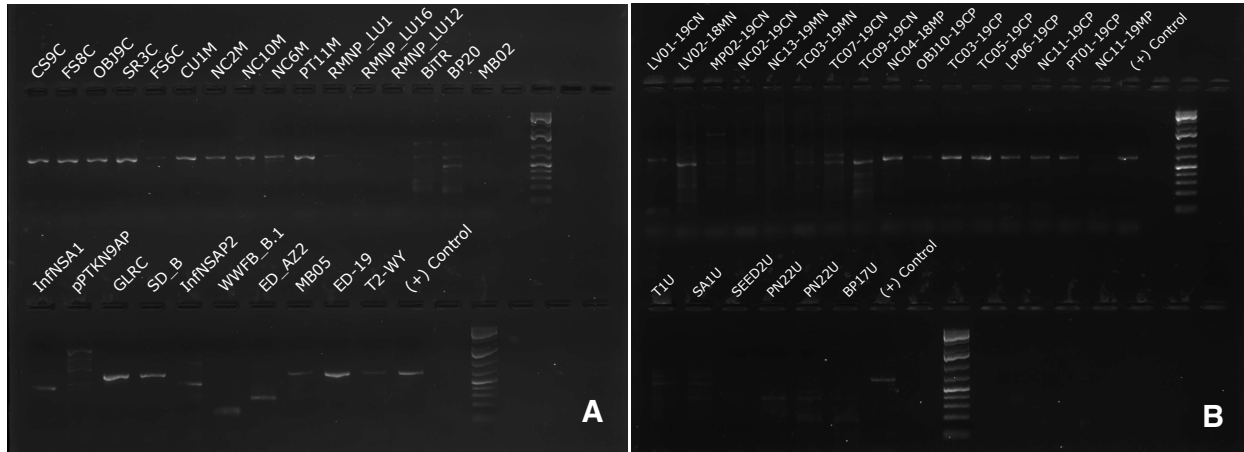
Supplementary Figure 9. LM_ITS primer assay across target (*Lophodermella montivaga*) and non-target species (A) and across asymptomatic and symptomatic needles (B). Gel photographs were taken using using Azure™ gel imaging system.



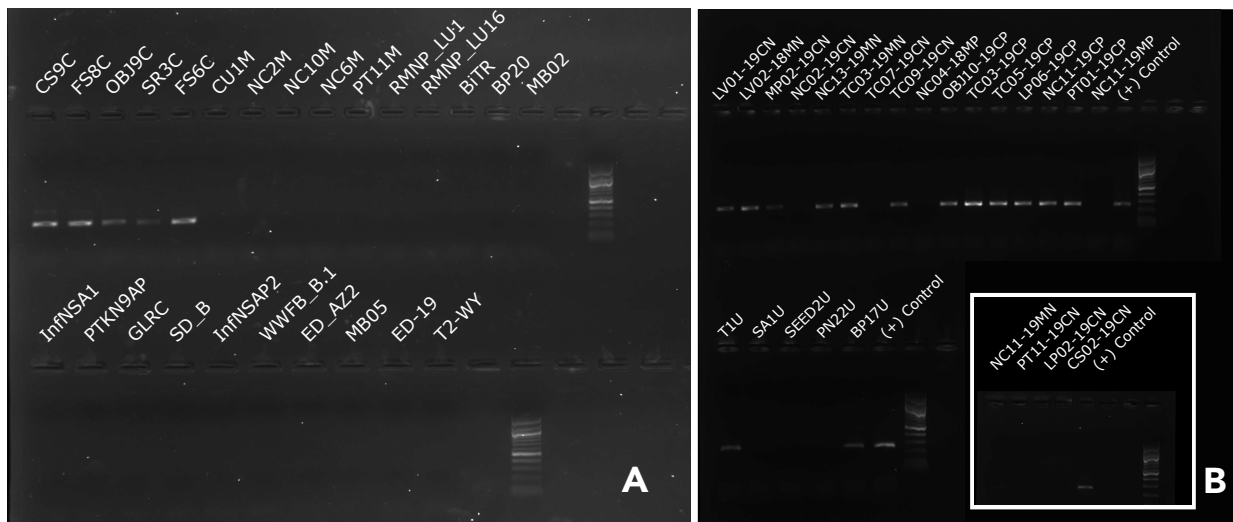
Supplementary Figure 10. LA ITS primer assay across target (*Lophodermella arcuata*) and non-target species (A) and across asymptomatic and symptomatic needles (B). Gel photographs were taken using using Azure™ gel imaging system.



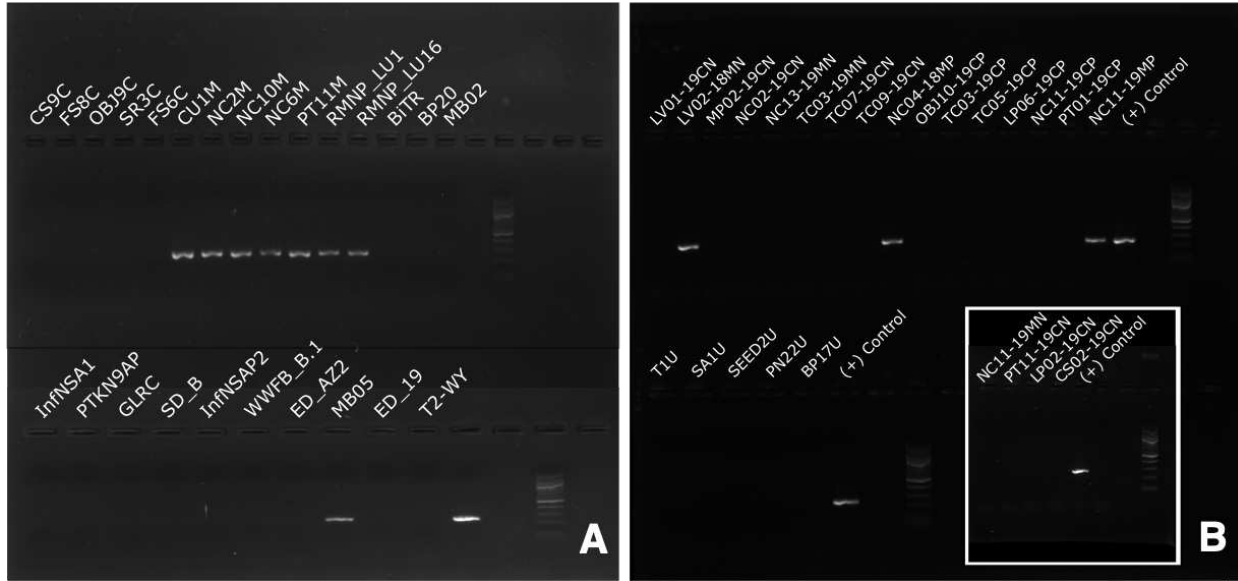
Supplementary Figure 11. BL ITS primer assay across target (*Bifusella linearis*) and non-target species (A) and across asymptomatic and symptomatic needles (B). Gel photographs were taken using using Azure™ gel imaging system.



Supplementary Figure 12. RH_2175 primer assay across target (Rhytismataceae) and non-target species (A) and across asymptomatic and symptomatic needles (B). Gel photographs were taken using using Azure™ gel imaging system.



Supplementary Figure 13. LC_2175 primer assay across target (*Lophodermella concolor*) and non-target species (A) and across asymptomatic and symptomatic needles (B). Gel photographs were taken using using Azure™ gel imaging system.



Supplementary Figure 14. LM_2175 primer assay across target (*Lophodermella montivaga*) and non-target species (A) and across asymptomatic and symptomatic needles (B). Gel photographs were taken using using Azure™ gel imaging system.